

# Characterization of Dwarf Novae Using SDSS Colors

Taichi KATO

*Department of Astronomy, Kyoto University, Sakyo-ku, Kyoto 606-8502*  
*tkato@kusastro.kyoto-u.ac.jp*

Hiroyuki MAEHARA

*Kwasan and Hida Observatories, Kyoto University, Yamashina, Kyoto 607-8471*  
and

Makoto UEMURA

*Astrophysical Science Center, Hiroshima University, Kagamiyama, 1-3-1 Higashi-Hiroshima 739-8526*

(Received 2011 0; accepted 2011 0)

## Abstract

We have developed a method for estimating the orbital periods of dwarf novae from the Sloan Digital Sky Survey (SDSS) colors in quiescence using an artificial neural network. For typical objects below the period gap with sufficient photometric accuracy, we were able to estimate the orbital periods with an accuracy to a  $1\sigma$  error of 22 %. The error of estimation is worse for systems with longer orbital periods. We have also developed a neural-network-based method for categorical classification. This method has proven to be efficient in classifying objects into three categories (WZ Sge type, SU UMa type and SS Cyg/Z Cam type) and works for very faint objects to a limit of  $g=21$ . Using this method, we have investigated the distribution of the orbital periods of dwarf novae from a modern transient survey (Catalina Real-Time Survey). Using Bayesian analysis developed by Uemura et al. (2010), we have found that the present sample tends to give a flatter distribution toward the shortest period and a shorter estimate of the period minimum, which may have resulted from the uncertainties in the neural network analysis and photometric errors. We also provide estimated orbital periods, estimated classifications and supplementary information on known dwarf novae with quiescent SDSS photometry.

**Key words:** methods: statistical — stars: novae, cataclysmic variables — stars: dwarf novae — stars: evolution — surveys

## 1. Introduction

Cataclysmic variables (CVs) are close binary systems consisting of a white dwarf (WD) and a red-dwarf secondary transferring matter via the Roche-lobe overflow [for reviews, see Warner (1995); Hellier (2001)]. Dwarf novae (DNe) are a class of CVs characterized by the presence of outbursts, which are generally believed to be a result of thermal instabilities in the accretion disk. Dwarf novae are classified into three major classes: SS Cyg-type, Z Cam-type and SU UMa-type dwarf novae. Among them SU UMa-type dwarf novae show superhumps during their long-lasting superoutbursts. The superhumps are generally believed to arise from the precessing eccentric accretion disk whose eccentricity is excited by the 3:1 resonance (Osaki 1989).

According to the standard scenario of CV evolution, CVs with orbital periods ( $P_{\text{orb}}$ ) longer than  $\sim 3$  hr evolve towards shorter  $P_{\text{orb}}$  through the loss of angular momentum by magnetic braking (Verbunt, Zwaan 1981; Rappaport et al. 1983) and gravitational wave radiation. When the systems reach certain periods around  $P_{\text{orb}} \sim 3$  hr, the secondary becomes fully convective and the effect of the magnetic braking is believed to decrease dramatically, followed by the shrinkage of the secondary and reduction of the CV activity. This state lasts till the sec-

ondary again fills the Roche lobe at around  $P_{\text{orb}} \sim 2$  hr and forms the famous “period gap” in the  $P_{\text{orb}}$  distribution of CVs. After crossing the period gap,  $P_{\text{orb}}$  further decreases mainly through the loss of angular momentum by gravitational wave radiation until the secondary becomes degenerate. Around the time when this point is reached, the  $P_{\text{orb}}$  increases due to two reasons: the thermal time-scale of the secondary exceeds the mass-transfer time-scale and the mass-radius relation is reversed for degenerate dwarfs. This mechanism leads to the existence of the minimum period for ordinary CVs (Paczynski, Sienkiewicz 1981).<sup>1</sup> Those systems whose periods go past the period minimum are usually called period bouncers.

The early model calculations yielded the minimum period of 60–80 min (Paczynski, Sienkiewicz 1981; Rappaport et al. 1982; Paczynski, Sienkiewicz 1983). Later refined models yielded short periods of 65–70 min (Kolb, Baraffe 1999; Howell et al. 2001), which is significantly shorter than the observed value (e.g. Kolb 1993). This disagreement is called “period minimum problem”. Furthermore, population synthesis studies expect that most systems have already reached the period minimum

<sup>1</sup> We only showed the outline for the reason of the existence of the period minimum. Modern works have suggested that the mechanism is more complex than this simplified picture (cf. Kolb, Baraffe 1999; Knigge et al. 2011; Araujo-Betancor et al. 2005).

and that there is a heavy accumulation of systems around the period minimum (period spike). Since such a spike was not observationally evident until very recently, this disagreement was called “period spike problem” (Kolb, Baraffe 1999; Renvoizé et al. 2002). The observational evidence for the period spike has only recently been shown (cf. Gänsicke et al. 2009; Uemura et al. 2010).

Some of non-magnetic CVs above the period gap and most of CVs below the period gap exhibit dwarf nova-type outbursts. In addition to color-based surveys such as Palomar Green (PG) survey (Green et al. 1986) and Hamburg Quasar Survey (HQS; Hagen et al. 1995), and color-selected spectroscopic survey such as Sloan Digital Sky Survey (SDSS; York et al. 2000), dwarf nova-type outbursts have been both traditionally, and in modern times, playing an important role in discovering CVs.

In variability-based surveys of CVs, SU UMa-type dwarf novae are a particularly important group for two reasons: (1) SU UMa-type dwarf novae show superhumps and we can estimate the orbital periods using only photometric observations. (2) Most of dwarf novae below the period gap are SU UMa-type dwarf novae, and WZ Sge-type dwarf novae (a subgroup of SU UMa-type dwarf novae; cf. Bailey 1979; O’Donoghue et al. 1991; Kato et al. 2001) are considered to occupy the terminal stage of the CV evolution. Indeed, the recent increase in discoveries of new SU UMa-type dwarf novae, helped by massive transient surveys such as Catalina Real-Time Survey (CRTS, Drake et al. 2009)<sup>2</sup>, the All Sky Automated Survey-3 (ASAS-3, Pojmański 2002) and by amateur observers (notably K. Itagaki), have a significant impact on the distribution of orbital periods in CVs (Gänsicke et al. 2009; Uemura et al. 2010). Both works have indicated that the period minimum spike, which has only become observationally apparent, are heavily composed of newly identified SU UMa-type dwarf novae or faint SDSS CVs. Using Bayesian statistical analysis, Uemura et al. (2010) suggested a possibility that the true period minimum is even shorter than what is observed, considering the effect of low detectability of very low mass-transfer systems.

These surveys and statistics, however, unavoidably suffer from various kinds of biases. There are a bias because essentially all surveys are magnitude-limited, with bias being introduced by color selection criteria, and bias resulting from follow-up strategies. The first two biases are more serious in color and spectroscopy-selected searches. The last bias is more important in variability-based searches, because long- $P_{\text{orb}}$  SS Cyg and Z Cam-type dwarf novae do not show superhumps, and short- $P_{\text{orb}}$  SU UMa-type ones show such  $P_{\text{orb}}$  as are more easily determined. Furthermore, it is known that large-amplitude dwarf novae tend to receive popular attention, potentially leading to a bias toward detecting a larger number of shorter- $P_{\text{orb}}$  systems.

Estimating  $P_{\text{orb}}$  from colors of dwarf novae in quiescence, if it is feasible, could reduce the effect of the last

bias. There has been a long history of using colors in classifying CVs: Bruch (1984) compiled  $UBV$  colors of CVs and tried to classify them on the color-color diagram and Bruch, Engel (1994) extended this work. Szkody (1987) used  $UBVJHK$  photometry and spectroscopy to characterize quiescent dwarf novae. Szkody (1987) showed that  $(V - J)$  and  $(U - B)$  colors become bluer in shorter- $P_{\text{orb}}$ . Sproats et al. (1996) used  $(J - K)$  color to characterize the secondary and CV type. Hoard et al. (2002) compiled 2MASS colors of CVs and extended the results by Sproats et al. (1996). Imada et al. (2006) closely examined 2MASS color to characterize dwarf novae. Ak et al. (2007) further used 2MASS color to estimate absolute magnitudes of CVs and derived space distributions (Ak et al. 2008). Wils et al. (2010) used SDSS color cuts, UV color and variability for detecting new dwarf novae.

In this study, we used the SDSS photometric catalog for exploring a new way to estimate  $P_{\text{orb}}$ , and we discuss the implication of the resultant period distribution.

## 2. The Sample

The sample we used are the known dwarf novae in the General Catalog of Variable Stars (GCVS, Samus et al. 2011), Downes CV Catalog, Archival Edition (Downes et al. 2001), the online version of RKCcat [Ritter, Kolb 2003, (update RKCcat7.15, 2011)], SDSS CVs (Szkody et al. 2002; Szkody et al. 2003; Szkody et al. 2004; Szkody et al. 2005; Szkody et al. 2006; Szkody et al. 2007; Szkody et al. 2009), newly recognized dwarf novae by CRTS, CRTS Mount Lemmon Survey (MLS)<sup>3</sup>, CRTS Siding Spring Survey (SSS)<sup>4</sup>, candidate dwarf novae selected by color and variability (Wils et al. 2010), and newly discovered dwarf novae whose properties have been investigated in Kato et al. (2009), Kato et al. (2010) and Kato et al. (2012). For CRTS objects, most of dwarf novae were easily recognized based on their light curves (typical dwarf nova-type light curve and existence of past outbursts). Some CRTS dwarf novae were selected based on single outburst detections and typical CV colors in quiescence. For SDSS CVs, we selected objects that are recognized as dwarf novae based on the presence of outbursts and objects that have dwarf nova-type spectra.

We selected the objects whose magnitudes are present in the SDSS Photometric Catalog, Releases 8 (DR8). Since some objects or measurements are missing in SDSS DR8, we used SDSS DR7 instead.

We rejected SDSS magnitudes measured during outbursts or standstills (in Z Cam-type dwarf novae) by comparing with other photometric catalogs, known ranges of variability and typical quiescent magnitudes in the CRTS data. If there are two or measurements in SDSS and their magnitudes differ by more than 1 mag, we rejected the measurements whose magnitudes are brighter by more than 1 mag than the faintest one in order to minimize the contamination of outbursts. Even if multiple SDSS

<sup>2</sup> <<http://nesssi.cacr.caltech.edu/catalina/>>. For the information of the individual Catalina CVs, see <<http://nesssi.cacr.caltech.edu/catalina/AllCV.html>>.

<sup>3</sup> <<http://nesssi.cacr.caltech.edu/MLS/AllCV.html>>.

<sup>4</sup> <<http://nesssi.cacr.caltech.edu/SSS/AllCV.html>>.

entries are present for the same object, we used the measurements individually and did not use an averaged value of each object before analysis. We rejected measurements that have saturated pixels (shown as blanks in table 3).

For estimating Galactic extinction, we used Schlegel et al. (1998) for a through-the-Galaxy estimate, and obtained the extinction at the distance of the object using Bahcall, Soneira (1980) assuming a scale height of  $H = 100$  pc for the interstellar dust (Spitzer 1978; Bahcall, Soneira 1980). We employed an iterative process to obtain self-consistent estimates of distance and extinction. We examined the dependence of the results on the assumption of  $H$ , using extreme set of  $H = 70$  pc (typical value for molecular clouds) and  $H = 200$  pc (typical value for cold neutral medium). The resultant periods of neural network analysis (section 4) varied within 5 % of the  $H = 100$  pc result for 68 % of objects.

We used distance estimates tabulated in Patterson (2011) and those of Roelofs et al. (2007) for GP Com, Slavin et al. (1995) for GK Per and (Unda-Sanzana et al. 2008) for GD 552. For estimating the distance of the rest of the objects, we used Warner’s relations (Warner 1987; Warner 1995). If apparent magnitudes of maximum are available we estimated the distances by assuming the absolute magnitudes ( $M_V(\text{max})$ ) using the updated Warner’s relation (Patterson 2011) for objects with  $P_{\text{orb}} < 0.5$  d, and our own calibration based on GK Per [the interstellar extinction correction of  $E(B - V) = 0.3$  was taken from Wu et al. 1989] for longer  $P_{\text{orb}}$ :

$$M_V(\text{max}) = \begin{cases} 5.70 - 17.2P_{\text{orb}}, & (P_{\text{orb}} < 0.5) \\ 2.79 - 1.05P_{\text{orb}}, & (P_{\text{orb}} \geq 0.5) \end{cases} \quad (1)$$

If the apparent magnitudes of maximum were unavailable, we used the following equation (corresponding to equation 3.3 in Warner 1995):

$$M_V(\text{min}) = 7.1 + 1.64 \log T_n(\text{d}) - 6.24P_{\text{orb}}, \quad (2)$$

assuming  $\log T_n = 2.5$  to estimate minimum  $M_V$  and estimated observed apparent magnitudes of minimum to the distances. When the orbital periods were not available, we used the results of a neural network analysis (section 4). We used a mean maximum  $M_V = 4.95$  for objects without measured and estimated orbital periods.

Since Warner’s relation for the maximum is not very sensitive to the orbital period, the uncertainty introduced by the uncertainty of the orbital period is estimated to be sufficiently small. We used the coefficients in Schlegel et al. (1998) to convert  $V$ -band absorption  $A(V)$  to extinctions in SDSS passbands. Since the application of Warner’s relation requires orbital periods, the estimation of Galactic extinction is dependent on the results of the neural network analysis for objects without known orbital periods. We therefore repeated this process three times, using the results of the neural network analysis for estimating the distances, to obtain self-consistent estimates of distances and orbital periods from de-reddened colors. These values and the methods of estimation are placed in a later table (table 4) in order to save space.

**Table 1.** Samples in this paper.

Sample type	Objects
All samples	Sample described in section 2. Identical with objects in table 3.
WZ Sge-type DNe (subsection 3.1)	UZ Boo, EG Cnc, V592 Her, RZ Leo, UW Tri, BC UMa, HV Vir, SDSS J080434.20+510349.2, SDSS J133941.11+484727.5, SDSS J160501.35+203056.9, OT J012059.6+325545, OT J074727.6+065050, OT J090239.7+052501, OT J104411.4+211307, SDSS J161027.61+090738.4
Systems below the period minimum (subsection 3.4)	EI Psc, SDSS J150722.30+523039.8, OT J112253.3–111037
Training set (subsection 4.1)	Sample used for training the neural network. Objects in table 3 with $P_{\text{orb}}$ entries, excluding two AM CVn stars (GP Com and SDSS J012940.05+384210.4), AR Cnc, GZ Cet, MT Com, EI Psc, QZ Ser and OT J231308.1+233702.
DNe used for study of period distribution (section 5)	CRTS transients with known SDSS colors and $70 < P_{\text{orb}}(\text{min}) < 130$ . Listed in table 5.

Since there are different kinds of samples in this paper, we summarized the samples in table 1 for the convenience of readers.

### 3. Color Analysis

#### 3.1. Location of WZ Sge-Type Dwarf Novae on Color-Color Diagrams

We attempted to separate WZ Sge-type dwarf novae based on locations on color-color diagrams. We selected WZ Sge-type dwarf novae using the criteria described in Kato et al. (2009). The selected WZ Sge-type dwarf novae were UZ Boo, EG Cnc, V592 Her, RZ Leo, UW Tri, BC UMa, HV Vir, SDSS J080434.20+510349.2, SDSS J133941.11+484727.5, SDSS J160501.35+203056.9, OT J012059.6+325545, OT J074727.6+065050, OT J090239.7+052501, OT J104411.4+211307, and the CV selected by Wils et al. (2010) SDSS J161027.61+090738.4. Among them, RZ Leo and BC UMa are “borderline” WZ Sge-type dwarf novae with relatively frequent (super)outbursts, but with well-defined early superhumps. Most of other objects are more extreme WZ Sge-type dwarf novae with very infrequent (super)outbursts or with multiple rebrightenings.

In figure 1, WZ Sge-type dwarf novae and dwarf novae of other classes without known outburst properties are superimposed on the diagram. It seems that WZ Sge-type dwarf novae tend to cluster on the  $(u - g, g - r)$  color-color

diagram. This trend can be interpreted as the smaller contribution of the Balmer continuum, arising from the accretion disk, to the  $u$  light; in WZ Sge-type dwarf novae, this spectral range is usually dominated by the white dwarf and the level of disk-originated  $u$  light is smaller. The  $(g-r, r-i)$  diagram is less diagnostic. The  $(r-i, i-z)$  diagram again shows some degree of clustering of WZ Sge-type dwarf novae. This trend can be interpreted as the contribution of the secondary to the  $z$  light in longer- $P_{\text{orb}}$  objects. The two WZ Sge-type objects with large  $i-z$  colors are RZ Leo and OT J090239.7+052501. The former has a long  $P_{\text{orb}}$  and the secondary significantly contributes to the  $z$  band. The unusual position of the latter was caused by large photometric errors in SDSS due to its faintness ( $g=23.2$ ). The locations of WZ Sge-type dwarf novae, excluding these two objects, can be used to discriminate WZ Sge-type candidates in the color-color space. The average values and standard deviations for  $u-g$ ,  $g-r$ ,  $r-i$  and  $i-z$  colors for these samples are 0.03(0.17),  $-0.04(0.07)$ ,  $-0.12(0.18)$ ,  $0.04(0.22)$ , respectively.

### 3.2. Dependence of Colors on Orbital Period

We studied the dependence of colors on the orbital period. Whenever available, we used well-determined orbital periods from radial-velocity studies or photometric observations of eclipses.<sup>5</sup> For some WZ Sge-type dwarf novae,

<sup>5</sup> The values of orbital periods are taken from tables in our compilations (Kato et al. 2009, Kato et al. 2010 and Kato et al. 2012; references are listed therein), and supplemented for RX And (Kaitchuck 1989), UU Aql (Ritter, Kolb 2003, J. R. Thorstensen, private communication), VZ Aqr, V516 Cyg, V478 Her, VZ Sex, HS 1055+0939 (Thorstensen et al. 2010), CR Boo (Provencal et al. 1997), AM Cas (Taylor, Thorstensen 1996), V630 Cas (Orosz et al. 2001), WW Cet (Tappert et al. 1997), EN Cet, SDSS J090103.93+480911.1, SDSS J124426.26+613514.6, SDSS J171145.08+301320.0 (Dillon et al. 2008), GY Cet, SDSS J005050.88+000912.6, SDSS J155531.99-001055.0, SDSS J205914.87-061220.5, SDSS J233325.92+152222.2 (Southworth et al. 2007b), HP Cet, SDSS J091127.36+084140.7, SDSS J121607.03+052013.9 (Southworth et al. 2006), AR Cnc (Howell et al. 1990), GY Cnc, IR Com (Feline et al. 2005), GP Com (Marsh 1999), MT Com (Patterson et al. 2005), AB Dra (Thorstensen, Freed 1985), DO Dra (Haswell et al. 1997), ES Dra (Ringwald, Velasco 2011), BF Eri, BI Ori, FO Per (Sheets et al. 2007), LT Eri (Ak et al. 2005), AH Her (Horne et al. 1986), X Leo (Shafter, Harkness 1986), DO Leo (Abbott et al. 1990), HM Leo (Thorstensen, Taylor 2001), CW Mon (Kato et al. 2003), HX Peg (Ringwald 1994), IP Peg (Copperwheat et al. 2010), V367 Peg (Woudt et al. 2005b), V405 Peg (Thorstensen et al. 2009), GK Per (Crampton et al. 1986), KT Per (Thorstensen, Ringwald 1997), AY Psc (Diaz, Steiner 1990), X Ser (Thorstensen, Taylor 2000), RY Ser, SDSSp J081321.91+452809.4 (Thorstensen et al. 2004), QZ Ser (Thorstensen et al. 2002), V386 Ser (Woudt et al. 2004), EL UMa (Ritter, Kolb 2003, derived from Kato et al. 2010), VW Vul (Thorstensen et al. 1998), GD 552 (Hessman, Hopp 1990), 1RXS J171456.2+585130 (Wils 2011), HS 1016+3412, HS 1340+1524 (Aungwerojwit et al. 2006), HS 2205+0201 (Ritter, Kolb 2003, A. Aungwerojwit, Ph.D. thesis, Univ. of Warwick), HS 2219+1824 (Rodríguez-Gil et al. 2005), RX J1715.6+6856, RX J1831.7+6511 (Pretorius et al. 2007), SDSS J003941.06+005427.5, SDSS J075059.97+141150.1 (Southworth et al. 2010), SDSS J004335.14-003729.8, SDSS J165837.70+184727.4,

we could use the periods of early superhumps when spectroscopic orbital periods are not available. We could estimate orbital periods fairly well for SU UMa-type dwarf novae with known superhump periods ( $P_{\text{SH}}$ ). For systems with  $P_{\text{SH}} < 0.084$  d (stage B superhumps, see Kato et al. 2009 for definition of stages) or  $P_{\text{SH}} < 0.076$  d (stage C superhumps), we employed the newly calibrated relations in Kato et al. (2012) for deriving estimated  $P_{\text{orb}}$ . The  $1\sigma$  error for the estimated  $P_{\text{orb}}$  is 0.0003 d. For systems with longer  $P_{\text{SH}}$ , we used the relation in Stolz, Schoembs (1984).

The result is shown figure 2. The figure includes unusual short- $P_{\text{orb}}$  systems EI Psc, and OT J112253.3-111037 but does not include AM CVn-type objects (for a review of AM CVn-type stars, see Solheim 2010) which show dwarf-nova outbursts or which are similar to dwarf novae in quiescence (GP Com and SDSS J012940.05+384210.4 in the present sample). The only SDSS CV having  $P_{\text{orb}}$  longer than 1 d (SDSS J204448.92-045928.8) is outside this figure.

Excepting  $u-g$ , the colors of dwarf novae in quiescence become redder in longer  $P_{\text{orb}}$ . The  $u-g$  color is practically constant for  $\log P_{\text{orb}} > -1.2$ . In shorter  $P_{\text{orb}}$ , the  $u-g$  color becomes noticeably redder, reflecting the increasing contribution of the white dwarf in systems with very low mass-transfer rates.

It is particularly noteworthy that all colors have significant dependence on  $P_{\text{orb}}$  even below the period gap. This dependence is expected to provide a way to estimate  $P_{\text{orb}}$  only from SDSS photometric data. The  $i-z$  color tends to become bluer in very short- $P_{\text{orb}}$  systems.

### 3.3. Period Bouncers and SDSS Fiber Exclusion Boxes

SDSS spectroscopic follow-up observations used exclusion boxes to locate the fibers in order to reduce the contamination from white dwarfs, A-type stars and white dwarf-main sequence binaries (cf. figure 1 and figure 6 in Gänsicke et al. 2009). There has been a concern that SDSS-selected CVs may have a bias resulting from these exclusion policies.

As we have seen, there appears to be a tendency that the  $i-z$  color sharply becomes bluer according as the

SDSS J220553.98+115553.7 (Southworth et al. 2008), SDSS J074531.92+453829.6, SDSS J155656.92+352336.6 (Szkody et al. 2006), SDSS J075507.70+143547.6, SDSS J080534.49+072029.1, SDSS J143544.02+233638.7 (Szkody et al. 2007), SDSS J080303.90+251627.0, SDSS J142955.86+414516.8 (Szkody et al. 2005), SDSS J080846.19+313106.0, SDSS J153817.35+512338.0, SDSS J223439.93+004127.2, SDSSp J230351.64+010651.0 (Gänsicke et al. 2009, Dillon et al. in prep.), SDSS J084400.10+023919.3, SDSS J091945.11+085710.1 (Gänsicke et al. 2009, Thorstensen et al. in prep.), SDSS J090016.56+430118.2 (Szkody et al. 2004), SDSS J090403.48+035501.2 (Woudt et al. 2005a), SDSS J100658.40+233724.4 (Southworth et al. 2009), SDSS J103533.02+055158.3, SDSS J143317.78+101123.3, SDSS J150137.22+550123.4, SDSS J150722.30+523039.8 (Littlefair et al. 2008), SDSS J123813.73-033933.0 (Zharikov et al. 2006), SDSS J124058.03-015919.2 (Roelofs et al. 2005), SDSS J145758.21+514807.9 (Uthas 2011), SDSS J154453.60+255348.8 (Skinner et al. 2011), SDSS J204448.92-045928.8 (Peters, Thorstensen 2005).



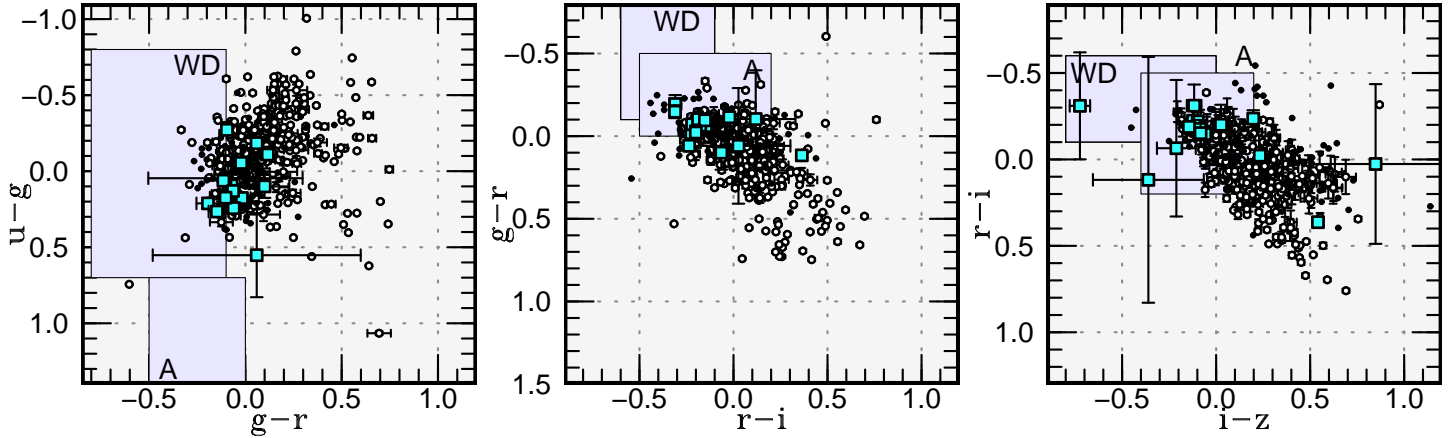


Fig. 1. Location of WZ Sge-type dwarf novae on color-color diagrams. Lightly filled squares represent well-characterized WZ Sge-type dwarf novae. The other open circles represent other classifications or objects without known outburst properties. For better visualization, the plots of object other than WZ Sge-type dwarf novae are limited to those having errors smaller than 0.1 mag in all ( $u-g$ ,  $g-r$ ,  $r-i$ ,  $i-z$ ) colors. The small dots represents objects other than WZ Sge-type dwarf novae with larger (up to 0.3 mag) photometric errors. Two boxes in the figures are white dwarf (WD) exclusion box and A-type star (A) exclusion one in the spectroscopic follow-up of SDSS quasar candidates.

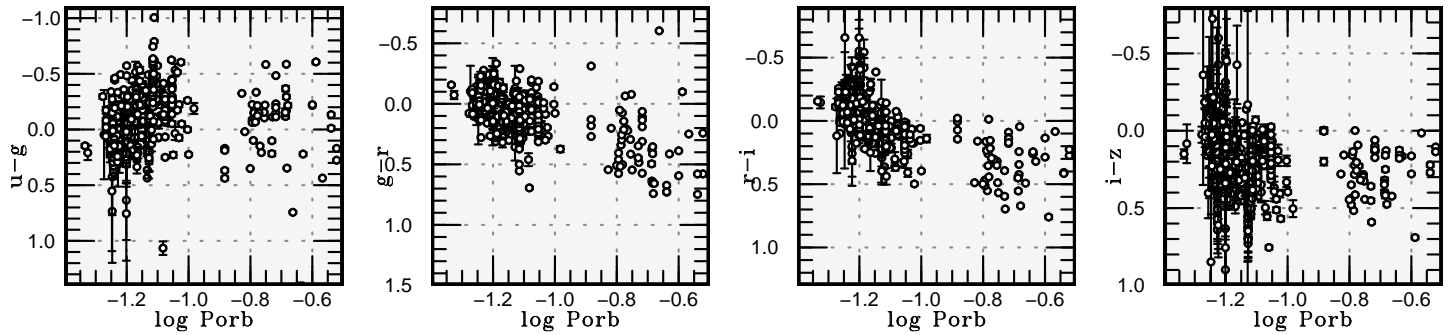


Fig. 2. Dependence of SDSS colors of dwarf novae on orbital period.

$P_{\text{orb}}$  shortens (figure 2). Most of the shortest- $P_{\text{orb}}$  objects  $i-z$  bluer than 0, and the spectroscopic detections these objects and potential period bouncers are expected to be limited by the exclusion criterion of  $i-z \leq -0.1$ . This might explain the too small number of candidates for period bouncers in known and SDSS-selected CVs compared to predictions by population models (Gänsicke et al. 2009).

Among CRTS and other transients, OT J010329.0+331822, OT J010550.1+190317, OT J012059.6+325545, OT J020056.0+195727, OT J035003.4+370052, OT J074419.7+325448, OT J074727.6+065050, OT J091453.6+113402, OT J151037.4+084104, OT J164748.0+433845 and OT J213122.4-003937 were inside the WD exclusion box. Two objects (OT J010329.0+331822 and OT J035003.4+370052) were brighter than the limit ( $i = 19.1$ ) of the quasar target selection algorithm up to SDSS DR7 (Richards et al. 2002) and one object (OT J151037.4+084104) was brighter than the limit

( $i = 19.9$ ) for SDSS DR8 (Eisenstein et al. 2011),<sup>6</sup> and there seems to have been a possibility that by this exclusion criterion significant fraction of CVs have escaped detection by SDSS. Notably, OT J074727.6+065050 is one of the renowned candidate for a period bouncer with multiple rebrightenings (Kato et al. 2009). OT J012059.6+325545 is also a WZ Sge-type dwarf nova with multiple rebrightenings (Kato et al. 2012). Although the latter two objects were below the limit of the target selection algorithm of SDSS, these results suggest that the fraction of shortest- $P_{\text{orb}}$  objects and period bouncers was significantly biased in the SDSS CVs.

### 3.4. Systems Below the Period Minimum

There are three objects (EI Psc, SDSS J150722.30+523039.8, OT J112253.3-111037) having  $0.04 < P_{\text{orb}} < 0.05$  (d) in our sample. SDSS

<sup>6</sup> Although SDSS did not obtain spectra for the objects in the Sloan Extension for Galactic Understanding and Exploration (SEGUE) imaging footprint, none of the objects within the WD exclusion box are within the SEGUE field.

J150722.30+523039.8 is an unusual hydrogen-rich CV with a very short  $P_{\text{orb}}$  (Littlefair et al. 2007; Patterson et al. 2008). It has been well-known that the region of this  $P_{\text{orb}}$  contains objects with unusually massive and luminous secondaries: EI Psc and V485 Cen (Augusteijn et al. 1993; Augusteijn et al. 1996). The remaining one object, OT J112253.3-111037, has a blue  $g - z$  color (+0.01) unlike EI Psc (+0.74). The color is more similar to SDSS J150722.30+523039.8 (−0.13). A low resolution spectrum of OT J112253.3-111037 in quiescence shows a stronger signature of helium lines (vsnet-alert 12026). The object might supply an important missing link between the enigmatic object SDSS J150722.30+523039.8, whose population and evolutionary status are not yet unclear, and EI Psc-like objects, and detailed follow-up observations are indispensable.

## 4. Neural-Network Analysis

### 4.1. Method and Training Set

In order to estimate orbital periods from SDSS colors, we employed a single-hidden-layer artificial neural network, a kind of multiple-layer perceptrons (Bishop 1995 and references therein), using  $\log P_{\text{orb}}$  as the response, and colors as inputs.<sup>7</sup> The procedure is practically the same as in photometric redshift estimations (see Collister, Lahav 2004 for the definition of the activation function and numerical method for the training). We used samples with known orbital periods in training the neurons. The samples were restricted with photometric errors (in each SDSS band) smaller than upper 90% quantiles. GZ Cet = SDSS J013701.06−091234.9 was rejected from the sample because this object has an unusually evolved massive secondary (Imada et al. 2006; Ishioka et al. 2007). OT J231308.1+233702 was not included due to its unusually red color, suggesting the possibility of similarity to GZ Cet. AR Cnc was also rejected because this object is deeply eclipsing (Howell et al. 1990), and the SDSS observation was likely obtained during its eclipse. We also rejected EI Psc (subsection 3.2), QZ Ser (system with an unusually luminous secondary, Thorstensen et al. 2002) and MT Com [suggested to be a WZ Sge-like object (Patterson et al. 2005), but the true nature and the period are still poorly known].

When there are multiple measurements for the same object, we used weights reversely proportional to the number of measurements in training the neural network.

### 4.2. Optimization and Uncertainties

We have optimized the number of units in the hidden layer ( $N_{\text{hid}}$ ) by the following cross-validation method. We first randomly selected 70 % of sample for the training data; the remaining samples were used for estimating the prediction error. The residuals for the training data were used for estimating the training error. We used 100 different sets of randomly selected samples and randomly

created and trained neural networks for each  $N_{\text{hid}}$  and averaged resultant errors for each  $N_{\text{hid}}$ . Although the training error decreased as  $N_{\text{hid}}$  increases, the decrease becomes slower for  $N_{\text{hid}} > 3$ . The prediction error slowly increases as  $N_{\text{hid}}$  increases, especially  $N_{\text{hid}} > 5$ . We therefore adopted  $N_{\text{hid}} = 3$ . This adoption of  $N_{\text{hid}}$  was also supported by the following analysis of estimated uncertainties and analysis of resultant correlation coefficients.

We estimated uncertainties of period estimations using the following process. For each object (with a known orbital period), a subsample excluding the target object was created and estimated the orbital period of the target object using the parameters of the neural network resulting from the subsample.

The maximum correlation coefficient excluding outliers reached a maximum for  $N_{\text{hid}} = 3$ . The number of outliers suggests that  $\sim 2$  % of ordinary objects will give totally unreliable  $P_{\text{orb}}$  in this method.<sup>8</sup> In a model with  $N_{\text{hid}} = 1$ , there remained a strong tendency of departure of estimated  $P_{\text{orb}}$  for long- $P_{\text{orb}}$  systems, and thus we did not adopt this model. For  $N_{\text{hid}} \geq 5$ , correlation coefficient tends to decrease. The correlation for objects below the period gap, however, was almost always equally good regardless of  $N_{\text{hid}}$  tested. The correlation was generally worse in long- $P_{\text{orb}}$  systems than in systems below the period gap. This can be naturally explained by the large spread of mass-transfer rate above the period gap (cf. Warner 1987).

Diagrams of the estimated orbital periods versus the true ones using this  $N_{\text{hid}}$  are shown in figure 3. The  $1 \sigma$  error for estimating  $P_{\text{orb}}$  for systems below the gap (excluding outliers) was 22 %. For systems with  $0.12 < P_{\text{orb}} < 0.4$  (d) (excluding outliers), the  $1 \sigma$  error was 57 %.

### 4.3. Estimation of Orbital Period

In order to reflect the uncertainties of the neural network and the photometric ones, we used different neural networks using all subsamples described in subsection 4.2. We also added random errors to the observed data according to error estimates of the SDSS photometry. After adopting 90% quantiles of the results, the mean estimates (mean in its logarithmic value) of the resultant  $P_{\text{orb}}$  and their standard deviations are given in table 3.

The columns of estimated orbital periods were left blank if the estimated periods were shorter than 0.04 d or longer than 1 d. The object with large estimated errors (larger than 0.4 times the estimated orbital periods) were also rejected.

There are objects with a multiplicity of up to 31 SDSS scans. For objects with more than four measurements, we have obtained standard deviations of estimated  $P_{\text{orb}}$

<sup>7</sup> We used **nnet** package in R software (The R Foundation for Statistical Computing: <<http://cran.r-project.org/>>).

<sup>8</sup> Since our primary aim is to qualify dwarf novae, e.g. whether they are likely candidates for objects below the period gap, we used “totally unreliable” here for objects whose estimated periods are below the period gap while the true  $P_{\text{orb}}$  are well above the period gap, or in the reverse cases. Since the members of these outliers are not fixed, but dependent on the neural networks, only the statistical description in fraction of outliers is meaningful. Some of these outliers can be properly characterized in the category analysis (subsection 4.4).

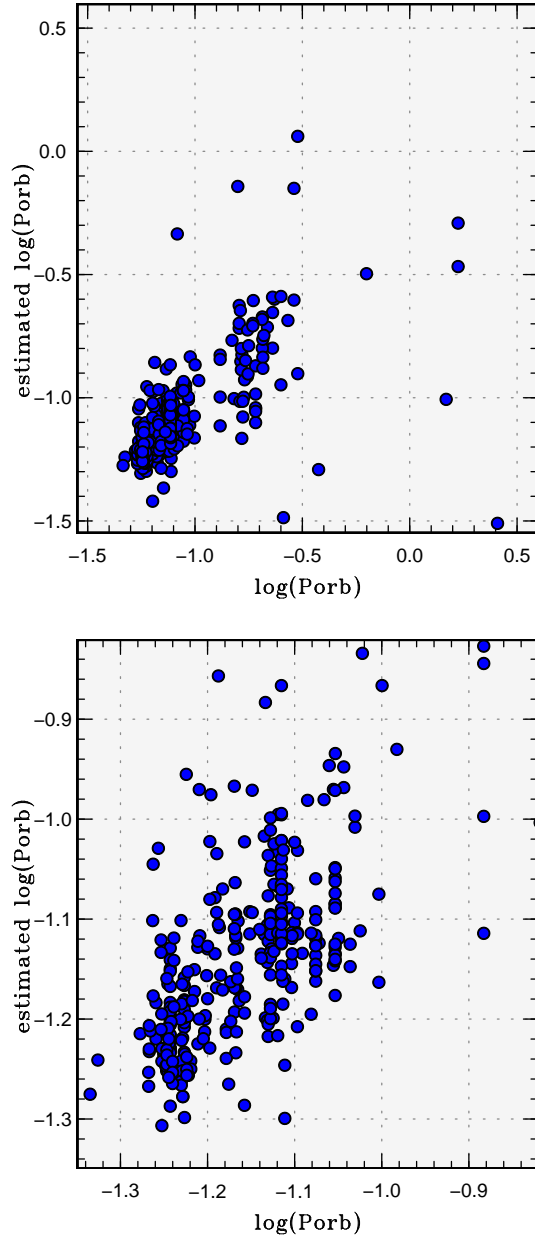


**Fig. 3.** Estimated versus true orbital periods. (Upper): All samples. (Lower): Estimations for objects below the period gap. The upper object situated outside this panel is GZ Cet.

**Table 2.** Averaged  $P_{\text{orb}}$  estimates for objects with more than four SDSS scans.

Object	$N^*$	mean $P_{\text{est}}$	error of $P_{\text{est}}$
V496 Aur	4	0.077(20)	0.023
EN Cet	13	0.067(4)	0.003
GS Cet	15	0.062(14)	0.007
BI Ori	6	0.103(29)	0.002
QZ Ser	4	0.210(7)	0.055
FSV J1722+2723	4	0.081(5)	0.003
OT J032839.9−010240	31	0.062(13)	0.007
OT J043829.1+004016	13	0.077(7)	0.002
OT J051419.9+011121	4	0.077(6)	0.003
OT J052033.9−000530	6	0.325(83)	0.035
OT J055842.8+000626	4	0.263(77)	0.016
OT J074222.5+172807	4	0.092(16)	0.004
OT J074419.7+325448	4	0.054(9)	0.010
OT J081418.9−005022	5	0.076(12)	0.001
OT J082123.7+454135	6	0.109(14)	0.004
OT J092839.3+005944	4	0.119(15)	0.018
OT J171223.1+362516	4	0.236(46)	0.078
OT J211550.9−000716	11	0.124(59)	0.081
OT J213122.4−003937	12	0.100(72)	0.055
OT J221128.7−030516	5	0.065(7)	0.002
OT J234440.5−001206	22	0.081(10)	0.004
ROTSE3 J221519.8−003257.2	16	0.080(7)	0.005
SDSS J003941.06+005427.5	14	0.051(4)	0.004
SDSS J004335.14−003729.8	21	0.064(6)	0.002
SDSS J053659.12+002215.1	6	0.042(2)	0.004
SDSS J075507.70+143547.6	4	0.056(1)	0.001
SDSS J075939.79+191417.3	4	0.114(22)	0.004
SDSS J085623.00+310834.0	4	0.055(2)	0.002
SDSS J091001.63+164820.0	4	0.078(6)	0.002
SDSS J094325.90+520128.8	4	0.081(5)	0.006
SDSS J113215.50+624900.4	4	0.076(8)	0.002
SDSS J155644.24−000950.2	4	0.075(6)	0.001
SDSS J155644.24−000950.2	4	0.075(6)	0.001
SDSS J160501.35+203056.9	4	0.057(2)	0.002
SDSS J204720.76+000007.7	10	0.073(7)	0.004
SDSS J210014.12+004446.0	13	0.076(6)	0.001
SDSS J210449.94+010545.8	13	0.074(8)	0.006
SDSS J211605.43+113407.5	4	0.087(52)	0.038
SDSS J223439.93+004127.2	17	0.082(8)	0.002
SDSSp J230351.64+010651.0	25	0.087(13)	0.002
SDSS J081408.42+090759.1 <sup>†</sup>	4	0.122(10)	0.006

\*Number of SDSS scans.

<sup>†</sup>Dwarf nova proposed by Wils et al. (2010).

in order to assess the quality of estimated errors of the neural-network analysis. Although these estimates were generally well-correlated ( $r^2 = 0.86$ , figure 4 and table 2), the estimated errors tend to be smaller than the standard deviations of estimated  $P_{\text{orb}}$ . The ratio of the standard deviations of estimated  $P_{\text{orb}}$  to the estimated errors was 1.8 (median). This difference may be partly interpreted as the intrinsic variation of the objects.

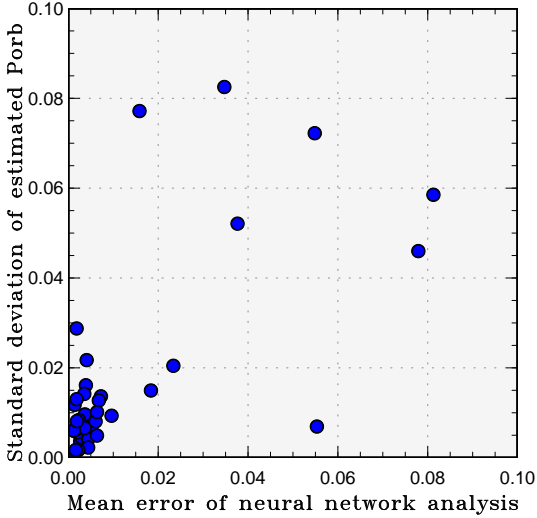


**Fig. 4.** Standard deviations of estimated  $P_{\text{orb}}$  and mean errors of the neural-network analysis for objects with more than four SDSS measurements. The standard deviation of estimated  $P_{\text{orb}}$  tends to be larger than the estimated errors by a factor of two.

#### 4.4. Category Classification by Neural Network

Since a direct estimation of  $P_{\text{orb}}$  is sometimes difficult, especially if the object is too faint (large photometric errors), or if the object has an unusually red color (due to the relatively small number of training samples for long- $P_{\text{orb}}$  objects), we provide an alternative way for distinguishing dwarf novae into three categories: *ultrashort* ( $P_{\text{orb}} < 0.06$ ), *short* ( $0.06 \leq P_{\text{orb}} < 0.10$ ) and *long* ( $P_{\text{orb}} \geq 0.10$ ), approximately corresponding to WZ Sge type, SU UMa type and SS Cyg/Z Cam type. We applied neural-network analysis to these categories, and estimated the probability belonging to each category (table 4).

Except for some objects with unusually bright and luminous secondaries, and, and except for the objects that are unusual for dwarf novae (see appendix 1 for individual notes), this classification appears to be very effective, and can be applied to very faint objects. We can obtain reasonable classifications for ordinary dwarf novae of  $g = 21$ , and even  $g = 22$  if the objects are dominated by the secondary. In particular, objects with probabilities for *ultrashort* category exceed 0.4 can be considered to be very likely candidates for WZ Sge-type dwarf novae or related objects. We infer that this probability index can be used to identify new WZ Sge-type dwarf novae or potential period bouncers.

## 5. Distribution of Orbital Periods

The present study provides a sample of DNe whose quiescent states were recorded by SDSS and whose outbursts were detected with CRTS. Since most of non-magnetic CVs below the period gap are DNe, this sample can be used to explore the distribution of orbital periods of CVs toward the shortest end. This sample has an advantage of being uniformly sampled, and less biased than any known

previous samples, including SDSS CVs, which were selected initially by colors and then by spectroscopy. Since there is a chance that on the SDSS color criterion might have missed a significant part of CVs, particularly WZ Sge-type dwarf novae, inside the color exclusion zones (cf. subsection 3.3), the present outburst-selected sample would be an excellent alternative.<sup>9</sup>

In discussing the parent population of an outburst-selected sample, we need to incorporate the effect of the detection probability. Uemura et al. (2010) proposed a method to estimate the intrinsic  $P_{\text{orb}}$ -distribution of DNe using a Bayesian approach. In this subsection, we applied this method to the present sample of the CRTS transients.

The CRTS-SDSS sample was selected in the following way: first, we selected DNe having  $P_{\text{est}} = 70\text{--}130$  min, since by the Bayesian model we used objects only in this region; second, we excluded objects whose  $P_{\text{est}}$  had a large error of  $> 40\%$  of  $P_{\text{est}}$ . We obtained the remaining 123 SDSS objects whose outbursts were detected by CRTS. We used weighted mean  $P_{\text{est}}$  in the case that multiple SDSS observations provided multiple  $P_{\text{est}}$  for the same object. Table 5 lists their names,  $P_{\text{est}}$ , their errors, and the number of recorded outbursts in the CRTS data. Most of them are new sources discovered by CRTS (namely “OT” sources), while CRTS detected outbursts of several known sources, which are also included in the table. The inclusion of these already-known sources in the sample is important for avoiding a bias resulting from exclusion of already-known, i.e. frequently outbursting, relatively long- $P_{\text{orb}}$  objects.

Uemura et al. (2010) assumed that the detection probability ( $= 1/T_s$ , where  $T_s$  is the typical recurrence time of superoutbursts) is independent of  $P_{\text{orb}}$  in a long  $P_{\text{orb}}$  region of  $P_{\text{orb}} \gtrsim 85$  min, while it is lower in a shorter  $P_{\text{orb}}$  region at  $P_{\text{orb}} \lesssim 85$  min. This assumption can be tested with the present CRTS-SDSS sample. Figure 5 shows the relation between the number of recorded outbursts and  $P_{\text{est}}$  of the sample. As can be seen in the figure, the CRTS-SDSS sample follows the trend assumed in Uemura et al. (2010): the number of high activity sources is small in a short period region of  $P_{\text{est}} \lesssim 85$  min.

The  $P_{\text{est}}$  distribution of our CRTS-SDSS sample is shown in figure 6. In Uemura et al. (2010), two samples, the “ASAS” and “mixed” samples, were analyzed. The ASAS sample included 42 DNe, whose outbursts were detected with the ASAS survey from 2003 to 2007. The mixed sample included 146 DNe, whose outbursts were reported to VSNET. We applied the Kolmogorov-Smirnov (KS) test to evaluate whether the CRTS-SDSS sample differs from those samples. The KS probabilities were calculated to be 0.18 and 0.08 for the ASAS and mixed samples, respectively. Hence, this test indicates that the

<sup>9</sup> It would be worth noting that both OT J074727.6+065050 and OT J012059.6+325545 mentioned in subsection 3.3 were discovered by amateur observers and not by the CRTS. There might have been a difference in detection policies between the CRTS and amateur observers, and it might affect the homogeneity of the CRTS transients. This aspect needs to be investigated further.



**Table 3.** List of dwarf novae

Object	<i>u</i>	<i>g</i>	<i>r</i>	<i>i</i>	<i>z</i>	$P_{\text{orb}}$	$P_{\text{est}}^*$
RX And	13.996(4)	14.082(4)	13.741(3)	—	13.108(5)	0.2099	—
BV And	16.893(7)	16.366(4)	16.319(5)	16.222(5)	16.115(7)	—	0.072(1)
FN And	18.718(21)	18.719(8)	18.473(9)	18.140(9)	17.664(17)	—	0.105(3)
IZ And	19.402(30)	19.621(13)	19.312(13)	18.878(13)	18.361(27)	—	0.108(5)
LL And	20.182(47)	20.073(17)	19.993(20)	20.079(28)	20.165(105)	0.0551	0.066(2)
LL And	20.209(70)	20.152(21)	20.163(30)	20.349(49)	20.523(211)	0.0551	0.057(2)
LT And	19.767(31)	19.505(11)	19.281(12)	19.214(15)	19.041(45)	—	0.099(3)
V402 And	20.584(55)	20.390(20)	20.276(26)	20.210(35)	20.072(98)	0.0618 <sup>†</sup>	0.077(3)
UU Aql	16.759(8)	16.851(5)	16.443(4)	15.848(5)	15.292(5)	0.1635	0.149(5)
KX Aql	18.169(14)	18.381(7)	18.007(7)	18.087(9)	17.676(18)	0.0604	0.058(5)
V725 Aql	18.526(19)	18.914(9)	18.554(9)	18.273(9)	17.770(23)	0.0945 <sup>†</sup>	0.078(1)
V1047 Aql	18.136(15)	18.275(7)	17.357(21)	17.868(8)	17.666(21)	—	—
VY Aqr	16.853(8)	16.949(4)	16.855(5)	16.731(5)	16.392(9)	0.0631	0.073(1)
VZ Aqr	17.435(11)	17.605(5)	16.988(4)	16.494(4)	16.120(8)	0.1606	0.221(7)
VZ Aqr	17.934(14)	17.967(6)	17.520(6)	16.981(6)	16.520(9)	0.1606	0.173(7)
VZ Aqr	17.944(13)	17.953(6)	17.451(5)	16.950(5)	16.447(9)	0.1606	0.191(7)
EG Aqr	19.040(29)	19.102(11)	18.934(13)	18.664(13)	18.140(29)	0.0763 <sup>†</sup>	0.089(3)
BG Ari	19.983(37)	20.280(21)	19.980(23)	19.569(22)	19.128(63)	0.0822 <sup>†</sup>	0.105(4)
V496 Aur	21.554(148)	21.452(46)	21.575(86)	21.324(97)	21.049(316)	0.0597 <sup>†</sup>	0.093(9)
V496 Aur	21.909(274)	21.724(76)	21.737(119)	21.440(139)	21.831(688)	0.0597 <sup>†</sup>	0.105(24)
V496 Aur	21.530(165)	21.451(45)	21.573(83)	21.334(100)	21.897(1414)	0.0597 <sup>†</sup>	0.074(26)
V496 Aur	21.912(225)	21.820(71)	21.876(131)	21.523(150)	22.430(861)	0.0597 <sup>†</sup>	—
TT Boo	19.340(23)	19.322(11)	19.309(13)	19.147(16)	18.767(33)	0.0755 <sup>†</sup>	0.079(2)
UZ Boo	19.916(43)	19.704(14)	19.695(17)	19.902(26)	20.009(108)	0.0604 <sup>†</sup>	0.057(1)
V391 Cam	16.154(6)	16.346(5)	16.234(5)	16.365(6)	16.249(8)	0.0562	0.058(3)
AM Cas	15.488(5)	15.281(3)	14.917(4)	14.744(3)	14.576(4)	0.1652	0.071(1)
KZ Cas	18.786(22)	18.719(10)	18.235(8)	17.611(7)	17.092(12)	—	0.125(8)
KZ Cas	19.064(21)	19.153(11)	18.359(8)	17.763(7)	17.239(14)	—	0.141(6)
LM Cas	19.477(29)	19.472(13)	19.073(12)	19.040(15)	18.865(45)	—	0.059(1)
V630 Cas	17.678(11)	17.099(4)	16.339(4)	16.508(5)	15.505(6)	2.5639	2.256(96)
WW Cet	14.598(3)	14.678(3)	14.244(3)	13.913(4)	13.619(4)	0.1758	0.173(7)
EN Cet	20.247(55)	20.168(25)	20.312(38)	20.307(52)	20.178(155)	0.0593	0.069(3)
EN Cet	20.472(64)	20.575(30)	20.565(38)	20.528(49)	20.048(123)	0.0593	0.067(2)
EN Cet	20.646(75)	20.690(34)	20.633(39)	20.525(56)	20.246(154)	0.0593	0.076(4)
EN Cet	20.673(63)	20.689(28)	20.635(37)	20.585(53)	20.067(114)	0.0593	0.068(2)
EN Cet	20.697(66)	20.698(29)	20.598(33)	20.570(42)	20.142(105)	0.0593	0.069(2)
EN Cet	20.708(66)	20.672(29)	20.558(35)	20.680(58)	20.483(193)	0.0593	0.064(2)
EN Cet	20.720(63)	20.684(28)	20.583(40)	20.662(62)	20.007(138)	0.0593	0.066(4)
EN Cet	20.742(67)	20.623(31)	20.548(35)	20.638(51)	20.232(136)	0.0593	0.064(2)
EN Cet	20.743(69)	20.775(31)	20.768(44)	20.787(62)	20.218(147)	0.0593	0.064(3)
EN Cet	20.758(78)	20.627(31)	20.604(39)	20.653(58)	20.042(121)	0.0593	0.065(3)
EN Cet	20.928(69)	20.733(27)	20.733(37)	20.729(51)	20.206(105)	0.0593	0.066(2)
EN Cet	20.935(62)	20.735(26)	20.794(35)	20.823(48)	20.569(134)	0.0593	0.064(2)
EN Cet	20.936(65)	20.813(28)	20.790(34)	20.857(52)	20.272(117)	0.0593	0.063(3)
FI Cet	21.589(158)	21.554(55)	21.724(123)	21.680(152)	21.419(405)	—	0.075(8)
GS Cet	20.035(47)	19.943(19)	19.963(26)	20.208(42)	20.440(215)	—	0.054(2)
GS Cet	20.199(44)	20.118(21)	20.202(36)	20.356(58)	20.606(270)	—	0.059(3)
GS Cet	20.306(66)	20.319(26)	20.305(33)	20.466(54)	20.915(316)	—	0.059(4)
GS Cet	20.393(63)	20.287(24)	20.280(30)	20.475(47)	20.371(178)	—	0.056(2)
GS Cet	20.473(55)	20.410(21)	20.455(30)	20.528(44)	21.187(335)	—	0.065(8)
GS Cet	20.514(62)	20.471(23)	20.493(33)	20.646(46)	20.612(183)	—	0.058(2)
GS Cet	20.515(64)	20.358(23)	20.539(33)	20.537(48)	21.490(437)	—	0.066(20)
GS Cet	20.531(51)	20.381(19)	20.492(26)	20.656(39)	20.470(133)	—	0.056(1)
GS Cet	20.543(61)	20.446(23)	20.423(29)	20.594(44)	21.169(299)	—	0.058(7)
GS Cet	20.571(55)	20.338(20)	20.408(25)	20.618(40)	20.674(165)	—	0.054(1)

\*Orbital period estimated with neural network.

<sup>†</sup>Determined from superhump period.<sup>‡</sup>Dwarf novae proposed by Wils et al. (2010).

**Table 3.** List of dwarf novae (continued)

Object	<i>u</i>	<i>g</i>	<i>r</i>	<i>i</i>	<i>z</i>	$P_{\text{orb}}$	$P_{\text{est}}^*$
GS Cet	20.578(68)	20.395(23)	20.412(36)	20.543(55)	20.434(206)	–	0.060(2)
GS Cet	20.600(65)	20.427(22)	20.412(27)	20.489(40)	20.768(217)	–	0.070(5)
GS Cet	20.610(61)	20.381(20)	20.369(31)	20.477(50)	20.739(261)	–	0.066(4)
GS Cet	20.847(80)	20.508(26)	20.563(34)	20.662(54)	20.977(330)	–	0.065(5)
GS Cet	21.237(242)	20.455(53)	20.411(51)	20.594(67)	21.001(283)	–	0.114(45)
GY Cet	18.267(16)	18.294(7)	18.329(8)	18.525(12)	18.458(33)	0.0566	0.056(1)
GY Cet	18.276(15)	18.296(7)	18.414(9)	18.586(14)	18.433(38)	0.0566	0.058(2)
GZ Cet	18.993(28)	18.710(9)	18.446(9)	18.058(9)	17.788(25)	0.0553	0.166(13)
HP Cet	19.815(42)	19.858(16)	19.726(18)	19.914(30)	19.809(85)	0.0667	0.060(1)
EU CMa	21.248(152)	21.069(42)	20.656(48)	19.951(33)	19.308(71)	–	0.132(8)
AK Cnc	18.896(20)	18.797(8)	18.737(9)	18.587(10)	18.237(24)	0.0651	0.079(1)
AR Cnc	18.245(14)	18.520(7)	18.085(7)	17.843(7)	17.455(15)	0.2146	0.117(3)
CC Cnc	16.363(6)	15.873(3)	15.914(4)	16.011(4)	16.126(7)	0.0735	0.068(2)
CC Cnc	17.188(9)	16.769(4)	16.566(5)	16.483(5)	16.431(9)	0.0735	0.136(5)
DE Cnc	20.088(39)	18.465(7)	17.771(7)	17.482(7)	17.287(14)	–	0.202(12)
DE Cnc	20.216(40)	18.458(7)	17.766(7)	17.459(7)	17.314(14)	–	0.211(32)
EG Cnc	18.990(21)	18.839(9)	18.867(10)	19.059(14)	19.131(50)	0.0600	0.055(1)
GY Cnc	15.924(6)	16.029(4)	15.697(5)	15.322(5)	15.002(5)	0.1754	0.133(4)
GZ Cnc	15.424(5)	14.736(3)	–	–	14.689(5)	0.0882	–
HH Cnc	18.938(20)	19.158(10)	18.523(8)	18.189(9)	17.891(16)	–	0.251(11)
FU Com	20.015(36)	18.847(8)	18.485(8)	18.341(10)	18.293(25)	–	–
GO Com	17.923(12)	17.936(6)	17.891(7)	17.866(8)	17.677(16)	0.0615 <sup>†</sup>	0.070(1)
GP Com	15.844(6)	15.908(4)	16.152(4)	16.301(4)	16.521(9)	0.0323	0.061(2)
GP Com	15.854(6)	15.919(4)	16.136(4)	16.324(4)	16.454(9)	0.0323	0.058(2)
IM Com	18.782(17)	17.721(5)	17.536(6)	17.465(7)	17.460(16)	–	0.373(108)
IM Com	19.094(23)	17.776(6)	17.553(6)	17.495(7)	17.501(17)	–	–
IR Com	18.240(14)	18.317(7)	18.412(7)	18.042(8)	17.264(11)	0.0870	0.099(3)
MT Com	19.272(25)	19.125(10)	19.186(12)	19.340(18)	19.440(61)	0.0829	0.059(1)
VW CrB	19.744(37)	19.636(16)	19.541(16)	19.450(22)	19.312(65)	0.0706 <sup>†</sup>	0.082(2)
VW CrB	19.874(41)	19.887(15)	19.864(18)	19.663(24)	19.222(51)	0.0706 <sup>†</sup>	0.082(2)
V516 Cyg	14.945(4)	14.416(3)	–	14.565(3)	14.528(5)	0.1712	–
V1081 Cyg	17.724(29)	17.749(10)	–	16.374(7)	16.159(17)	–	–
V1089 Cyg	19.059(28)	18.587(8)	17.641(6)	17.106(6)	16.777(11)	–	0.183(10)
V1153 Cyg	19.824(263)	18.781(10)	17.434(28)	17.652(7)	17.352(17)	–	–
V1251 Cyg	20.532(79)	20.474(28)	20.263(32)	19.940(32)	19.358(81)	0.0743	0.084(3)
V1363 Cyg	18.171(16)	17.861(6)	16.922(5)	16.343(5)	15.873(7)	–	0.440(167)
V1449 Cyg	19.193(540)	19.049(19)	16.810(40)	17.819(14)	16.214(89)	–	–
HO Del	18.705(18)	18.892(9)	18.854(11)	18.880(15)	18.540(38)	0.0627	0.063(2)
AB Dra	15.617(5)	15.530(4)	15.277(4)	15.084(4)	14.897(5)	0.152	0.109(2)
DM Dra	20.425(59)	20.296(23)	20.118(23)	19.913(26)	19.499(61)	0.0733 <sup>†</sup>	0.098(4)
DM Dra	20.517(70)	20.325(22)	20.273(26)	20.173(34)	19.839(114)	0.0733 <sup>†</sup>	0.079(3)
DO Dra	15.234(4)	15.557(4)	15.046(4)	14.598(4)	14.179(5)	0.1654	0.166(6)
AQ Eri	17.161(8)	17.411(5)	17.429(6)	17.361(6)	17.165(11)	0.0609	0.073(1)
BF Eri	15.119(4)	14.599(3)	14.286(3)	14.161(3)	14.109(4)	0.2709	0.214(12)
LT Eri	18.024(12)	17.748(5)	17.445(5)	17.079(6)	16.795(11)	0.1702	0.142(6)
HQ Gem	21.111(100)	20.386(21)	19.385(15)	18.978(16)	18.572(33)	–	0.277(32)
IR Gem	15.502(6)	15.996(5)	15.729(5)	15.609(5)	15.496(6)	0.0684	0.074(1)
KZ Gem	19.940(36)	18.666(8)	18.149(7)	17.965(8)	17.898(19)	–	–
AH Her	14.247(6)	–	–	–	13.415(7)	0.2581	–
AH Her	14.412(6)	14.975(10)	15.041(11)	14.260(10)	13.550(7)	0.2581	0.187(17)
V478 Her	18.403(15)	17.741(6)	17.320(6)	17.194(6)	17.007(11)	0.6290	0.445(49)
V544 Her	20.408(59)	19.744(15)	19.043(12)	18.599(11)	18.421(32)	–	0.258(47)
V589 Her	18.070(14)	18.305(7)	18.200(8)	18.006(8)	17.704(20)	–	0.081(1)
V589 Her	18.434(17)	18.631(8)	18.153(7)	18.199(9)	17.995(21)	–	0.108(5)
V589 Her	18.959(19)	19.105(10)	18.803(10)	18.646(11)	18.323(22)	–	0.086(3)
V592 Her	21.612(117)	21.459(53)	21.319(54)	21.358(88)	21.546(385)	0.0558 <sup>‡</sup>	0.079(8)

\*Orbital period estimated with neural network.

<sup>†</sup>Determined from superhump period.<sup>‡</sup>Dwarf novae proposed by Wils et al. (2010).

**Table 3.** List of dwarf novae (continued)

Object	<i>u</i>	<i>g</i>	<i>r</i>	<i>i</i>	<i>z</i>	$P_{\text{orb}}$	$P_{\text{est}}^*$
V592 Her	21.648(115)	21.421(36)	21.413(48)	21.541(82)	21.426(335)	0.0558 <sup>†</sup>	0.062(4)
V592 Her	21.483(114)	21.301(35)	21.272(45)	21.387(73)	21.402(334)	0.0558 <sup>†</sup>	0.062(3)
V610 Her	21.552(101)	21.222(39)	20.918(38)	20.630(44)	20.438(145)	–	0.176(19)
V610 Her	21.564(161)	21.421(57)	21.136(54)	20.862(59)	20.716(223)	–	0.137(14)
V610 Her	21.649(241)	21.582(79)	21.262(86)	20.827(84)	20.578(296)	–	0.152(17)
V611 Her	20.311(45)	20.584(22)	20.534(27)	20.387(39)	19.847(93)	–	0.076(3)
V611 Her	20.510(53)	20.659(25)	20.687(35)	20.595(47)	20.058(108)	–	0.072(3)
V660 Her	19.754(39)	19.696(15)	19.468(15)	19.260(16)	18.864(42)	0.0782 <sup>†</sup>	0.082(2)
V844 Her	17.084(9)	17.193(5)	17.095(5)	16.991(5)	16.831(12)	0.0546	0.080(1)
V844 Her	17.590(10)	17.742(5)	17.719(6)	17.726(7)	17.613(16)	0.0546	0.068(1)
V849 Her	15.215(4)	15.002(3)	15.179(4)	15.302(4)	15.417(5)	–	0.059(1)
V849 Her	15.498(5)	15.210(4)	15.341(4)	15.457(4)	15.553(6)	–	0.059(1)
CT Hya	18.588(18)	18.733(9)	18.700(11)	18.571(13)	18.370(39)	0.0646 <sup>†</sup>	0.079(1)
CT Hya	18.695(17)	18.774(8)	18.855(10)	18.832(12)	18.597(38)	0.0646 <sup>†</sup>	0.069(1)
X Leo	15.787(5)	15.832(3)	15.515(3)	15.242(4)	15.008(5)	0.1644	0.134(3)
X Leo	16.295(6)	16.337(3)	16.061(4)	15.694(3)	15.400(5)	0.1644	0.136(4)
RZ Leo	18.639(19)	18.716(9)	18.575(9)	18.196(9)	17.640(18)	0.0760	0.103(5)
DO Leo	18.230(16)	17.970(6)	17.526(6)	17.187(6)	17.005(12)	0.2345	0.258(21)
HM Leo	18.266(14)	18.320(7)	17.791(6)	17.066(6)	16.449(9)	0.1868	0.176(13)
SS LMi	22.007(327)	21.556(107)	21.586(160)	22.231(439)	20.626(392)	0.0566	–
SS LMi	22.911(452)	22.150(96)	22.190(136)	22.442(243)	22.627(696)	0.0566	–
SX LMi	16.288(6)	16.740(4)	16.461(4)	16.386(5)	16.428(8)	0.0672	0.078(1)
CW Mon	15.900(5)	15.913(4)	15.834(4)	15.245(4)	14.828(5)	0.1766	0.146(8)
V982 Oph	20.333(55)	20.251(20)	19.660(16)	19.179(15)	18.784(36)	–	0.181(8)
V1032 Oph	17.910(13)	17.647(5)	17.385(5)	17.193(6)	16.973(11)	0.0811	0.071(1)
V2335 Oph	22.629(305)	22.507(124)	21.978(107)	20.806(68)	19.771(93)	–	0.158(59)
BI Ori	16.288(6)	16.290(4)	16.094(4)	15.948(4)	15.797(6)	0.1915	0.082(1)
BI Ori	16.563(6)	16.596(3)	16.319(4)	16.131(4)	15.947(7)	0.1915	0.092(1)
BI Ori	16.590(6)	16.705(4)	16.307(4)	16.106(4)	15.925(7)	0.1915	0.106(1)
BI Ori	16.607(7)	16.689(4)	16.538(5)	16.304(5)	16.079(7)	0.1915	0.089(1)
BI Ori	16.726(7)	16.725(4)	16.503(4)	16.307(4)	16.133(7)	0.1915	0.091(1)
BI Ori	16.729(6)	17.098(4)	16.437(4)	16.209(5)	16.097(7)	0.1915	0.157(5)
GR Ori	23.836(1024)	22.405(144)	21.301(96)	20.791(104)	20.919(403)	–	–
GR Ori	24.007(1233)	22.358(136)	21.190(75)	20.597(68)	20.440(211)	–	–
HX Peg	14.243(6)	–	–	–	13.990(6)	0.2008	–
IP Peg	15.683(5)	15.287(4)	14.743(4)	14.223(4)	13.757(4)	0.1582	0.293(32)
V367 Peg	17.551(11)	17.348(5)	17.216(5)	17.002(6)	16.797(10)	0.1619	0.096(2)
V369 Peg	19.957(60)	18.762(10)	17.969(8)	17.537(8)	17.254(21)	0.0827 <sup>†</sup>	0.132(17)
V405 Peg	15.783(5)	16.100(3)	15.351(3)	14.653(3)	14.091(4)	0.1776	0.156(8)
V405 Peg	17.001(9)	16.792(5)	15.914(5)	–	14.196(5)	0.1776	–
FO Per	17.116(7)	16.859(4)	16.600(4)	16.272(4)	15.932(6)	0.1719	0.147(8)
GK Per	15.171(5)	–	–	–	12.419(4)	1.9968	–
KT Per	15.309(4)	15.316(3)	14.690(3)	14.386(3)	14.187(4)	0.1627	0.226(8)
QY Per	20.381(46)	20.313(21)	20.153(25)	19.914(25)	19.600(64)	0.0760 <sup>†</sup>	0.086(3)
V336 Per	20.013(41)	19.703(15)	18.883(11)	18.400(10)	18.056(23)	–	0.379(40)
V336 Per	20.389(44)	20.021(15)	19.103(11)	18.597(10)	18.241(20)	–	0.419(102)
V336 Per	20.571(57)	19.996(18)	19.019(11)	18.506(10)	18.213(25)	–	–
V372 Per	21.831(186)	21.629(53)	21.048(51)	20.233(38)	19.515(68)	–	0.173(22)
TY Psc	16.952(9)	17.167(5)	16.895(5)	16.816(5)	16.608(10)	0.0683	0.076(2)
TY Psc	17.049(11)	17.078(4)	17.082(5)	17.036(6)	16.799(12)	0.0683	0.069(1)
XY Psc	21.057(130)	20.943(38)	20.854(50)	20.895(86)	20.406(211)	–	0.069(4)
XY Psc	21.237(102)	21.130(33)	21.133(45)	21.119(74)	21.013(251)	–	0.072(5)
XY Psc	21.246(113)	21.136(35)	21.105(49)	20.977(72)	20.522(165)	–	0.077(4)
AS Psc	22.107(394)	22.015(113)	21.568(135)	22.391(386)	21.791(870)	–	–
AY Psc	17.414(10)	16.590(4)	17.132(5)	16.601(5)	16.142(8)	0.2173	0.168(9)
EI Psc	17.093(8)	16.331(4)	15.939(4)	15.760(4)	15.592(6)	0.0446	0.473(50)

\*Orbital period estimated with neural network.

<sup>†</sup>Determined from superhump period.<sup>‡</sup>Dwarf novae proposed by Wils et al. (2010).

**Table 3.** List of dwarf novae (continued)

Object	<i>u</i>	<i>g</i>	<i>r</i>	<i>i</i>	<i>z</i>	$P_{\text{orb}}$	$P_{\text{est}}^*$
GV Psc	20.501(55)	20.409(21)	20.192(23)	19.903(24)	19.511(67)	0.0904 <sup>†</sup>	0.108(5)
GV Psc	20.032(49)	20.508(27)	20.200(25)	19.764(23)	19.346(59)	0.0904 <sup>†</sup>	0.111(5)
X Ser	17.388(10)	17.298(5)	16.821(5)	16.604(5)	16.523(8)	1.478	0.110(3)
RY Ser	16.759(8)	16.091(3)	15.470(3)	14.953(3)	14.626(4)	0.3009	0.159(10)
RY Ser	17.372(11)	16.598(4)	15.640(4)	15.171(4)	14.813(4)	0.3009	0.505(34)
QW Ser	17.795(11)	17.805(6)	17.823(7)	17.717(7)	17.408(14)	0.0745	0.074(1)
QZ Ser	17.822(12)	16.275(3)	15.721(3)	15.516(4)	15.427(5)	0.0832	0.180(56)
QZ Ser	17.846(11)	16.291(4)	15.728(4)	15.530(4)	15.444(5)	0.0832	0.180(58)
QZ Ser	17.848(11)	16.302(4)	15.724(4)	15.518(4)	15.439(5)	0.0832	0.173(50)
QZ Ser	17.855(15)	16.304(4)	15.720(4)	15.530(4)	15.436(6)	0.0832	0.184(59)
V386 Ser	19.123(25)	19.049(10)	18.975(11)	19.176(16)	19.314(58)	0.0559	0.054(1)
V386 Ser	19.217(22)	19.012(10)	19.006(11)	19.149(17)	19.083(54)	0.0559	0.055(1)
V386 Ser	19.218(27)	19.024(12)	19.053(13)	19.141(18)	19.229(64)	0.0559	0.060(1)
VZ Sex	16.494(6)	16.762(4)	16.175(4)	15.659(4)	15.354(5)	0.1487	0.192(11)
TX Tri	17.772(14)	17.490(5)	16.771(5)	16.447(5)	16.271(9)	–	0.447(41)
UW Tri	22.543(386)	22.370(107)	22.377(182)	22.197(232)	22.501(672)	0.0533	0.083(21)
UZ Tri	20.592(76)	19.525(13)	19.095(13)	18.896(17)	18.946(54)	–	–
SW UMa	16.900(8)	16.866(4)	16.890(5)	17.006(6)	16.828(13)	0.0568	0.058(1)
SW UMa	16.932(8)	16.862(4)	16.936(4)	16.975(5)	16.817(14)	0.0568	0.064(1)
BC UMa	18.607(16)	18.514(7)	18.605(9)	18.612(11)	18.366(25)	0.0626	0.065(1)
BZ UMa	15.410(4)	15.877(3)	15.862(3)	15.772(4)	15.481(6)	0.0680	0.076(1)
BZ UMa	15.972(5)	16.371(3)	16.045(4)	16.069(4)	15.882(7)	0.0680	0.067(2)
BZ UMa	16.297(6)	16.468(4)	16.301(4)	16.504(5)	16.232(8)	0.0680	0.058(2)
CY UMa	17.483(9)	17.768(5)	17.520(5)	17.335(6)	17.182(12)	0.0696	0.094(1)
DI UMa	17.757(10)	17.912(6)	17.794(6)	17.771(7)	17.779(17)	0.0546	0.075(2)
DV UMa	19.326(24)	19.372(11)	19.146(11)	18.805(12)	18.247(22)	0.0859	0.106(4)
EL UMa	20.384(45)	20.274(19)	20.340(26)	20.620(49)	20.641(166)	0.0594	0.052(2)
ER UMa	15.641(4)	15.415(3)	15.236(3)	15.247(3)	15.262(5)	0.0637	0.104(1)
IY UMa	17.765(11)	17.537(5)	17.635(6)	17.623(7)	17.189(12)	0.0739	0.064(1)
IY UMa	17.770(13)	17.561(5)	17.541(6)	17.478(6)	17.202(14)	0.0739	0.075(1)
IY UMa	17.871(12)	17.637(5)	17.740(6)	17.626(7)	17.278(15)	0.0739	0.076(1)
KS UMa	17.174(8)	17.354(4)	17.191(5)	17.149(5)	16.956(11)	0.0680	0.073(1)
KS UMa	17.293(9)	17.418(5)	17.180(5)	17.139(6)	16.942(12)	0.0680	0.083(3)
HV Vir	19.467(31)	19.181(11)	19.209(14)	19.335(19)	19.374(71)	0.0571	0.060(1)
OU Vir	18.435(14)	18.564(7)	18.424(8)	18.401(9)	18.355(23)	0.0727	0.072(2)
QZ Vir	14.693(4)	14.864(3)	15.128(3)	15.055(4)	14.817(5)	0.0588	0.078(2)
VW Vul	15.788(5)	15.772(3)	15.711(3)	15.336(3)	15.170(5)	0.1687	0.112(7)
1502+09	18.535(18)	18.995(9)	19.047(12)	19.015(14)	18.697(35)	–	0.075(3)
1502+09	18.578(17)	19.111(10)	19.174(13)	19.128(15)	18.796(37)	–	0.077(3)
1H1025+220	17.678(11)	17.402(5)	17.235(5)	17.092(5)	16.980(11)	–	0.117(4)
1RXS J003828.7+250920	18.595(18)	18.741(8)	18.548(9)	18.306(10)	17.884(23)	–	0.087(3)
1RXS J003828.7+250920	18.654(20)	18.849(8)	18.707(10)	18.427(10)	17.927(24)	–	0.088(2)
1RXS J012750.5+380830	16.781(7)	17.177(4)	17.058(5)	17.130(6)	17.165(12)	–	0.063(1)
1RXS J171456.2+585130	15.940(5)	15.021(3)	14.206(3)	–	13.641(4)	0.8380	–
2QZ J112555.7–001639	19.450(36)	19.601(18)	19.566(22)	19.791(40)	19.421(125)	–	0.056(3)
2QZ J112555.7–001639	19.480(29)	19.555(16)	19.470(18)	19.631(30)	19.575(84)	–	0.058(1)
2QZ J112555.7–001639	19.592(35)	19.511(13)	19.505(15)	–	19.316(56)	–	–
2QZ J121005.3–025543	21.092(86)	20.866(32)	21.001(49)	21.282(91)	20.631(202)	–	0.060(6)
2QZ J130441.7+010330	20.018(38)	20.187(19)	20.267(28)	20.338(40)	20.029(113)	–	0.064(2)
2QZ J130441.7+010330	20.542(57)	20.690(27)	20.586(35)	20.607(57)	20.587(215)	–	0.069(3)
2QZ J142701.6–012310	19.736(36)	19.985(17)	20.180(27)	20.242(39)	20.446(160)	–	0.063(6)
ASAS J224349+0809.5	19.297(26)	19.549(14)	19.329(14)	19.246(18)	18.699(41)	0.0678 <sup>‡</sup>	0.067(2)
ASAS J224349+0809.5	19.620(33)	19.707(15)	19.445(14)	19.413(18)	18.959(45)	0.0678 <sup>‡</sup>	0.066(2)
FSV J1722+2723	19.466(28)	19.950(16)	19.909(20)	19.737(24)	19.574(85)	–	0.081(2)
FSV J1722+2723	20.170(46)	20.664(32)	20.350(27)	20.189(37)	20.170(128)	–	0.084(4)
FSV J1722+2723	20.284(42)	20.599(23)	20.565(31)	20.457(39)	20.274(122)	–	0.076(2)

\*Orbital period estimated with neural network.

†Determined from superhump period.

‡Dwarf novae proposed by Wils et al. (2010).



**Table 3.** List of dwarf novae (continued)

Object	<i>u</i>	<i>g</i>	<i>r</i>	<i>i</i>	<i>z</i>	$P_{\text{orb}}$	$P_{\text{est}}^*$
FSV J1722+2723	20.340(46)	20.902(28)	20.605(29)	20.410(35)	20.320(117)	–	0.084(4)
GD 552	16.427(7)	16.398(4)	16.197(4)	16.533(5)	16.539(10)	0.0713	0.057(3)
GSC 847.1021	16.639(6)	15.138(3)	14.620(3)	14.412(3)	14.349(4)	–	0.170(55)
GUVV J090904.4+091714.4	21.049(92)	21.447(57)	21.092(50)	20.724(52)	20.459(154)	–	0.102(7)
GUVV J090904.4+091714.4	22.028(170)	22.360(91)	22.514(169)	21.656(135)	21.265(227)	–	0.151(39)
GUVV J090904.4+091714.4	22.316(192)	22.467(110)	22.103(108)	21.572(88)	21.221(228)	–	0.148(16)
HS 1016+3412	17.845(12)	18.391(7)	18.202(7)	18.072(8)	17.904(19)	0.0794	0.077(1)
HS 1055+0939	16.536(7)	15.876(3)	15.206(4)	14.914(4)	14.759(5)	0.3763	0.324(18)
HS 1340+1524	17.011(8)	17.316(5)	17.156(5)	17.119(6)	17.060(11)	0.0644	0.072(1)
HS 1340+1524	17.729(10)	17.960(6)	17.619(6)	17.701(7)	17.564(14)	0.0644	0.077(3)
HS 2205+0201	17.630(11)	17.224(5)	16.438(5)	16.363(6)	16.208(8)	0.208	0.406(134)
HS 2219+1824	17.560(10)	17.524(5)	17.518(6)	17.487(7)	17.248(14)	0.0599	0.067(1)
HS 2219+1824	17.642(13)	17.555(5)	17.510(6)	17.503(7)	17.248(15)	0.0599	0.065(1)
MASTER J013241.20+343809.1	23.204(1040)	21.483(79)	21.485(142)	21.614(253)	21.783(954)	–	–
MASTER J071948.9+405332	21.698(175)	21.831(97)	21.539(116)	21.538(187)	21.877(811)	–	0.080(17)
MASTER J071948.9+405332	21.968(129)	21.739(47)	21.856(75)	21.698(101)	21.608(231)	–	0.085(8)
NSV 02026	17.594(11)	17.549(5)	17.176(5)	16.930(6)	16.788(11)	–	0.080(1)
NSV 04394	22.388(385)	21.853(102)	22.520(274)	22.719(466)	21.990(708)	–	–
NSV 04838	18.234(13)	18.617(8)	18.327(8)	18.293(10)	18.342(28)	0.0679 <sup>†</sup>	0.080(2)
NSV 04838	18.531(15)	18.851(9)	18.697(9)	18.586(11)	18.510(27)	0.0679 <sup>†</sup>	0.080(1)
NSV 05031	18.788(27)	19.232(11)	18.914(11)	18.779(12)	18.414(29)	–	0.072(1)
NSV 05285	19.588(31)	19.623(15)	19.497(15)	19.359(19)	18.845(39)	0.0847 <sup>†</sup>	0.074(1)
NSV 14652	17.914(17)	17.918(6)	17.581(6)	17.432(7)	17.199(15)	0.0788 <sup>†</sup>	0.070(1)
NSV 14652	18.341(18)	18.545(7)	18.053(7)	17.904(9)	17.849(24)	0.0788 <sup>†</sup>	0.076(2)
NSV 14681	20.250(41)	20.179(18)	19.894(18)	19.599(19)	19.195(47)	–	0.091(2)
NSV 18230	19.627(30)	20.141(22)	19.971(22)	19.963(30)	19.715(77)	–	0.067(1)
NSV 18230	19.968(43)	20.429(22)	20.144(27)	20.123(40)	19.961(108)	–	0.071(2)
NSV 19466	18.000(13)	18.290(7)	18.081(7)	18.068(9)	17.941(22)	–	0.069(1)
NSV 19466	17.225(10)	17.686(6)	17.570(6)	17.436(7)	17.345(10)	–	0.078(2)
NSV 20657	21.179(96)	21.200(38)	21.183(55)	21.119(89)	21.034(386)	–	0.077(6)
OT J000024.7+332543	20.697(71)	20.760(31)	20.530(34)	20.401(43)	20.039(104)	–	0.080(4)
OT J000130.5+050624	20.845(95)	20.967(34)	20.757(39)	20.327(41)	19.950(121)	–	0.125(8)
OT J000659.6+192818	20.946(93)	21.231(56)	21.017(64)	20.898(82)	21.060(328)	–	0.085(8)
OT J000659.6+192818	21.184(141)	21.363(53)	21.013(62)	21.023(88)	20.632(247)	–	0.085(7)
OT J001158.3+315544	21.740(160)	21.869(65)	21.578(80)	21.565(114)	21.326(335)	–	0.084(9)
OT J001340.0+332124	22.290(329)	21.911(69)	21.783(112)	21.853(189)	21.195(371)	–	0.108(32)
OT J001340.0+332124	23.097(720)	22.021(95)	21.830(124)	21.916(176)	20.802(261)	–	–
OT J001538.3+263657	17.495(12)	17.894(6)	17.425(6)	17.395(6)	17.069(13)	–	0.091(4)
OT J001538.3+263657	17.726(13)	17.802(6)	17.690(6)	17.624(8)	17.249(20)	–	0.069(1)
OT J002500.2+073349	19.247(25)	19.677(13)	19.213(12)	18.934(12)	18.725(32)	–	0.122(3)
OT J002500.2+073349	19.768(63)	19.989(22)	19.426(21)	19.176(22)	18.952(67)	–	0.198(13)
OT J002500.2+073349	20.252(61)	20.218(20)	19.742(19)	19.414(19)	19.185(67)	–	0.220(15)
OT J002656.6+284933	21.393(105)	21.592(49)	21.464(68)	20.789(57)	20.251(121)	–	0.165(13)
OT J003203.6+314510	18.707(21)	19.070(10)	18.787(11)	18.494(11)	18.115(24)	–	0.090(2)
OT J003304.0+380106	20.332(74)	20.437(29)	20.409(36)	20.204(44)	19.691(96)	–	0.080(3)
OT J003304.0+380106	20.848(65)	20.726(31)	20.733(40)	20.579(51)	19.845(101)	–	0.073(2)
OT J003500.0+273620	21.469(186)	21.118(42)	22.445(221)	21.503(129)	21.186(389)	–	–
OT J004500.3+222708	20.197(72)	20.447(29)	20.214(33)	20.134(45)	19.655(94)	–	0.072(2)
OT J004518.4+185350	21.770(234)	21.049(54)	20.602(45)	20.455(50)	20.262(147)	–	0.467(117)
OT J004606.7+052100	22.613(579)	21.596(101)	21.238(122)	20.951(110)	20.721(399)	–	–
OT J004807.2+264621	21.156(181)	21.703(100)	21.697(143)	21.722(194)	21.229(433)	–	0.075(13)
OT J004807.2+264621	21.329(143)	21.571(58)	21.307(78)	21.452(133)	22.289(821)	–	–
OT J004902.0+074726	21.742(197)	21.520(59)	21.492(85)	21.795(164)	22.136(855)	–	0.052(10)
OT J005152.9+204017	18.957(28)	19.059(11)	18.369(8)	17.936(8)	17.554(17)	–	0.298(21)
OT J005824.6+283304	19.071(22)	19.217(10)	18.978(11)	19.150(15)	18.917(38)	–	0.060(2)
OT J010329.0+331822	18.484(18)	17.982(6)	18.123(8)	18.267(10)	18.335(28)	–	0.056(1)

\*Orbital period estimated with neural network.

†Determined from superhump period.

‡Dwarf novae proposed by Wils et al. (2010).

**Table 3.** List of dwarf novae (continued)

Object	<i>u</i>	<i>g</i>	<i>r</i>	<i>i</i>	<i>z</i>	$P_{\text{orb}}$	$P_{\text{est}}^*$
OT J010411.6–031341	19.017(24)	19.516(13)	19.140(13)	18.829(13)	18.898(42)	–	0.124(14)
OT J010522.2+110253	20.640(58)	20.712(23)	20.563(32)	20.283(33)	20.084(87)	–	0.105(4)
OT J010522.2+110253	20.833(77)	20.850(33)	20.680(40)	20.451(43)	19.978(102)	–	0.086(3)
OT J010522.2+110253	21.001(95)	20.914(34)	20.756(42)	20.548(52)	20.215(150)	–	0.092(5)
OT J010550.1+190317	19.421(36)	19.644(16)	19.818(21)	19.958(30)	19.984(99)	–	0.060(4)
OT J011134.5+275922	25.312(1930)	22.292(169)	21.642(144)	21.750(207)	22.566(933)	–	–
OT J011516.5+245530	20.759(59)	20.933(29)	20.876(36)	20.786(49)	20.436(127)	–	0.072(2)
OT J011516.5+245530	20.903(90)	21.076(42)	20.922(49)	20.927(79)	20.557(183)	–	0.065(3)
OT J011516.5+245530	21.452(99)	21.240(35)	21.240(46)	21.155(59)	20.636(161)	–	0.070(3)
OT J011543.2+333724	20.388(73)	20.558(31)	20.289(41)	20.107(47)	19.539(106)	–	0.078(3)
OT J011613.8+092216	19.036(27)	19.131(11)	19.034(13)	18.817(14)	18.619(40)	–	0.091(2)
OT J012059.6+325545	20.359(57)	20.088(18)	20.237(27)	20.518(47)	21.216(306)	0.0572	0.047(7)
OT J014150.4+090822	19.919(50)	20.061(21)	19.975(26)	19.966(34)	19.926(129)	0.0610 <sup>†</sup>	0.068(2)
OT J020056.0+195727	20.007(68)	19.280(15)	19.369(23)	19.448(33)	19.774(139)	–	0.067(7)
OT J021110.2+171624	19.442(32)	19.405(12)	19.181(14)	19.017(16)	18.707(37)	0.0789 <sup>†</sup>	0.078(2)
OT J021308.0+184416	21.177(107)	20.798(29)	19.998(21)	19.526(19)	19.163(43)	–	0.417(86)
OT J023211.7+303636	21.066(99)	20.825(28)	20.365(30)	19.830(26)	19.399(72)	–	0.183(14)
OT J025615.0+191611	25.406(753)	23.895(343)	22.847(232)	22.739(336)	23.366(595)	–	–
OT J032651.7+011513	22.630(452)	22.746(198)	21.164(70)	20.539(60)	20.127(147)	–	–
OT J032651.7+011513	22.646(393)	22.251(105)	20.956(72)	20.427(72)	19.989(168)	–	–
OT J032651.7+011513	22.676(510)	22.091(122)	21.034(78)	20.455(65)	20.019(144)	–	–
OT J032651.7+011513	22.939(572)	22.407(123)	21.320(70)	20.527(66)	20.150(136)	–	–
OT J032651.7+011513	22.966(406)	22.350(95)	21.249(58)	20.582(52)	20.205(136)	–	–
OT J032651.7+011513	22.996(495)	22.397(126)	21.213(70)	20.443(62)	20.093(184)	–	–
OT J032651.7+011513	23.208(451)	22.495(108)	21.196(61)	20.470(53)	20.148(142)	–	–
OT J032651.7+011513	23.477(738)	22.235(98)	21.147(57)	20.495(51)	20.095(138)	–	–
OT J032651.7+011513	23.556(543)	22.486(98)	21.286(59)	20.541(52)	20.019(117)	–	–
OT J032651.7+011513	23.639(709)	22.335(103)	21.167(54)	20.549(52)	20.000(117)	–	–
OT J032651.7+011513	23.703(994)	22.365(138)	21.132(83)	20.491(75)	20.157(195)	–	–
OT J032651.7+011513	23.757(675)	22.545(113)	21.258(55)	20.527(43)	20.130(108)	–	–
OT J032651.7+011513	23.872(671)	22.419(101)	21.229(58)	20.584(54)	20.002(114)	–	–
OT J032651.7+011513	23.928(832)	22.459(116)	21.150(57)	20.592(54)	20.026(110)	–	–
OT J032651.7+011513	23.959(1109)	22.387(128)	21.164(81)	20.495(75)	20.088(186)	–	–
OT J032651.7+011513	24.090(912)	22.664(137)	21.183(52)	20.588(47)	20.323(145)	–	–
OT J032651.7+011513	24.106(1138)	22.418(133)	21.238(73)	20.690(72)	20.235(183)	–	–
OT J032651.7+011513	24.210(844)	22.549(122)	21.167(56)	20.501(52)	19.952(120)	–	–
OT J032651.7+011513	24.268(881)	22.517(115)	21.176(53)	20.560(50)	20.170(136)	–	–
OT J032651.7+011513	24.395(800)	22.669(115)	21.258(52)	20.584(47)	20.076(109)	–	–
OT J032651.7+011513	24.670(895)	22.559(115)	21.153(54)	20.575(51)	19.862(106)	–	–
OT J032651.7+011513	24.676(963)	22.471(103)	21.309(67)	20.527(53)	20.070(126)	–	–
OT J032651.7+011513	25.357(770)	22.580(130)	21.149(61)	20.562(61)	20.354(203)	–	–
OT J032651.7+011513	25.723(635)	22.336(100)	21.152(61)	20.487(57)	20.143(160)	–	–
OT J032651.7+011513	25.800(591)	22.270(97)	21.235(68)	20.526(63)	20.080(112)	–	–
OT J032839.9–010240	20.552(63)	20.714(30)	20.776(45)	20.666(60)	20.439(202)	–	0.075(4)
OT J032839.9–010240	20.645(61)	20.759(29)	20.703(37)	20.777(59)	20.866(215)	–	0.061(3)
OT J032839.9–010240	20.673(59)	20.830(28)	20.693(40)	20.770(58)	21.056(272)	–	0.061(3)
OT J032839.9–010240	20.746(60)	20.785(28)	20.754(31)	20.862(48)	20.511(126)	–	0.059(3)
OT J032839.9–010240	20.857(143)	21.074(75)	20.939(73)	21.024(107)	20.652(280)	–	0.064(4)
OT J032839.9–010240	20.949(102)	21.033(48)	20.794(46)	20.949(77)	21.123(327)	–	0.060(3)
OT J032839.9–010240	20.950(104)	21.205(55)	21.087(59)	21.136(84)	20.952(265)	–	0.063(3)
OT J032839.9–010240	20.964(68)	21.134(36)	20.927(37)	21.058(60)	20.684(164)	–	0.059(3)
OT J032839.9–010240	20.987(82)	21.060(34)	20.974(46)	20.926(63)	20.711(187)	–	0.067(3)
OT J032839.9–010240	21.024(83)	21.199(49)	21.039(57)	21.200(84)	20.896(262)	–	0.059(3)
OT J032839.9–010240	21.047(80)	21.111(37)	20.835(36)	21.064(66)	21.318(312)	–	0.058(4)
OT J032839.9–010240	21.057(84)	21.328(46)	21.059(61)	21.261(107)	21.417(434)	–	0.058(5)
OT J032839.9–010240	21.178(101)	21.321(58)	21.156(61)	21.179(89)	21.077(307)	–	0.064(3)

\*Orbital period estimated with neural network.

<sup>†</sup>Determined from superhump period.<sup>‡</sup>Dwarf novae proposed by Wils et al. (2010).

**Table 3.** List of dwarf novae (continued)

Object	<i>u</i>	<i>g</i>	<i>r</i>	<i>i</i>	<i>z</i>	$P_{\text{orb}}$	$P_{\text{est}}^*$
OT J032839.9–010240	21.362(158)	21.220(64)	21.079(77)	21.173(115)	20.947(340)	–	0.063(5)
OT J032839.9–010240	21.380(83)	21.391(42)	21.145(46)	21.291(72)	21.213(232)	–	0.062(3)
OT J032839.9–010240	21.394(96)	21.518(49)	21.201(49)	21.423(94)	21.248(328)	–	0.064(5)
OT J032839.9–010240	21.498(145)	21.563(67)	21.402(74)	21.406(104)	21.534(390)	–	0.068(5)
OT J032839.9–010240	21.515(132)	21.550(67)	21.246(75)	21.590(134)	21.185(328)	–	0.072(13)
OT J032839.9–010240	21.554(112)	21.396(47)	21.341(75)	21.526(141)	21.965(681)	–	0.055(7)
OT J032839.9–010240	21.583(151)	21.305(56)	21.229(83)	21.619(156)	20.863(253)	–	0.075(21)
OT J032839.9–010240	21.587(165)	21.662(83)	21.606(120)	21.354(164)	20.526(311)	–	0.089(10)
OT J032839.9–010240	21.601(133)	21.507(51)	21.291(59)	21.513(110)	21.473(408)	–	0.060(5)
OT J032839.9–010240	21.602(122)	21.634(63)	21.430(73)	21.755(145)	21.836(449)	–	0.057(5)
OT J032839.9–010240	21.632(150)	21.544(64)	21.429(80)	21.388(117)	21.468(471)	–	0.073(8)
OT J032839.9–010240	21.658(129)	21.507(47)	21.437(59)	21.485(87)	21.272(247)	–	0.062(3)
OT J032839.9–010240	21.688(126)	21.598(64)	21.326(61)	21.348(99)	21.229(310)	–	0.076(7)
OT J032839.9–010240	21.735(159)	21.536(65)	21.536(99)	21.831(182)	21.585(486)	–	0.058(7)
OT J032839.9–010240	21.773(180)	21.774(82)	21.748(132)	21.758(229)	22.741(1076)	–	–
OT J032839.9–010240	21.790(143)	21.525(60)	21.400(65)	21.592(120)	21.991(518)	–	0.057(7)
OT J032839.9–010240	21.967(167)	21.584(55)	21.283(56)	21.601(119)	21.434(382)	–	0.107(26)
OT J032839.9–010240	22.020(190)	21.448(50)	21.398(67)	21.566(128)	21.116(348)	–	0.068(9)
OT J032902.0+060047	22.042(211)	21.625(64)	20.998(53)	20.652(62)	19.908(123)	–	0.095(11)
OT J032902.0+060047	22.050(187)	21.274(42)	20.897(46)	20.491(42)	19.931(98)	–	0.095(6)
OT J032902.0+060047	22.895(376)	22.037(72)	21.584(72)	21.112(63)	20.530(159)	–	0.124(18)
OT J033104.4+172540	19.979(39)	19.862(15)	19.324(13)	18.878(13)	18.467(32)	–	0.172(7)
OT J035003.4+370052	19.391(22)	18.938(9)	18.818(9)	18.869(12)	18.838(31)	–	0.055(1)
OT J035003.4+370052	19.883(37)	19.297(11)	19.157(13)	19.147(16)	19.144(50)	–	0.057(1)
OT J040659.8+005244	17.712(10)	17.844(5)	17.461(5)	17.165(6)	16.792(10)	0.0774 <sup>†</sup>	0.075(2)
OT J040659.8+005244	18.067(12)	18.584(7)	17.895(6)	17.535(7)	17.348(15)	0.0774 <sup>†</sup>	0.077(5)
OT J040659.8+005244	18.084(12)	18.386(7)	17.752(6)	17.524(6)	17.302(13)	0.0774 <sup>†</sup>	0.066(2)
OT J041636.9+292806	22.276(211)	22.252(89)	21.365(63)	20.788(58)	20.320(113)	–	0.086(6)
OT J041734.6–061357	22.259(337)	22.732(243)	22.993(437)	21.606(185)	24.654(430)	–	–
OT J042142.1+340329	22.547(192)	22.427(96)	21.897(83)	21.445(80)	20.841(164)	–	0.096(7)
OT J042229.3+161430	22.847(404)	21.958(80)	21.441(79)	20.916(64)	20.352(130)	–	0.096(10)
OT J042434.2+001419	24.219(769)	23.098(196)	22.871(212)	24.050(651)	22.299(459)	–	–
OT J043020.0+095318	20.747(70)	20.377(20)	19.639(17)	19.091(15)	18.650(31)	–	0.127(5)
OT J043517.8+002941	21.317(115)	21.124(40)	21.060(52)	21.077(76)	21.024(267)	–	0.067(4)
OT J043517.8+002941	21.563(131)	21.744(67)	22.105(142)	21.877(183)	21.374(416)	–	0.079(18)
OT J043517.8+002941	21.892(128)	21.957(65)	22.144(125)	22.708(302)	22.087(518)	–	–
OT J043546.9+090837	21.938(144)	21.827(52)	21.416(65)	21.212(76)	20.730(193)	–	0.073(4)
OT J043742.1+003048	20.474(57)	20.368(23)	20.146(26)	20.067(35)	19.694(81)	–	0.079(3)
OT J043829.1+004016	18.884(20)	19.218(12)	19.182(15)	18.996(20)	18.824(57)	–	0.082(2)
OT J043829.1+004016	19.041(24)	19.080(11)	19.014(14)	19.009(21)	18.877(56)	–	0.067(2)
OT J043829.1+004016	19.066(21)	19.226(11)	18.898(10)	18.912(14)	19.061(46)	–	0.084(5)
OT J043829.1+004016	19.223(22)	19.540(12)	19.082(12)	19.135(19)	19.165(64)	–	0.086(6)
OT J043829.1+004016	19.224(23)	19.489(13)	19.213(13)	19.184(18)	19.148(50)	–	0.072(2)
OT J043829.1+004016	19.319(25)	19.375(12)	19.278(14)	19.166(18)	18.973(51)	–	0.076(2)
OT J043829.1+004016	19.339(26)	19.306(11)	19.291(15)	19.235(20)	18.996(47)	–	0.069(2)
OT J043829.1+004016	19.373(28)	19.571(14)	19.387(15)	19.342(20)	19.223(63)	–	0.070(2)
OT J043829.1+004016	19.391(25)	19.677(14)	19.424(17)	19.325(21)	19.340(66)	–	0.079(2)
OT J043829.1+004016	19.415(29)	19.618(14)	19.256(13)	19.193(17)	19.021(45)	–	0.083(3)
OT J043829.1+004016	19.430(26)	19.492(12)	19.402(13)	19.281(17)	19.044(41)	–	0.076(2)
OT J043829.1+004016	19.447(24)	19.639(13)	19.439(13)	19.383(18)	19.159(49)	–	0.069(2)
OT J043829.1+004016	19.558(37)	19.714(16)	19.361(19)	19.348(29)	19.260(92)	–	0.083(4)
OT J044216.0–002334	21.967(160)	21.927(76)	21.527(82)	21.380(117)	21.054(327)	0.0743 <sup>‡</sup>	0.149(24)
OT J044216.0–002334	22.103(222)	22.266(115)	22.350(147)	22.051(159)	20.887(244)	0.0743 <sup>‡</sup>	0.101(15)
OT J044216.0–002334	22.230(185)	21.931(70)	21.725(90)	21.847(151)	21.990(586)	0.0743 <sup>‡</sup>	0.101(26)
OT J051419.9+011121	19.453(32)	19.799(15)	19.318(14)	19.201(19)	19.164(60)	–	0.083(3)
OT J051419.9+011121	19.736(48)	19.844(20)	19.748(28)	19.605(35)	19.215(100)	–	0.073(2)

\*Orbital period estimated with neural network.

†Determined from superhump period.

‡Dwarf novae proposed by Wils et al. (2010).

**Table 3.** List of dwarf novae (continued)

Object	<i>u</i>	<i>g</i>	<i>r</i>	<i>i</i>	<i>z</i>	$P_{\text{orb}}$	$P_{\text{est}}^*$
OT J051419.9+011121	19.744(35)	20.214(21)	20.209(34)	19.978(45)	19.613(106)	—	0.082(4)
OT J051419.9+011121	20.249(43)	20.509(22)	20.258(25)	20.135(35)	19.850(101)	—	0.070(2)
OT J052033.9−000530	19.785(36)	19.566(13)	19.060(12)	18.710(11)	18.466(28)	—	0.181(9)
OT J052033.9−000530	20.338(71)	20.195(24)	19.505(23)	19.131(24)	18.854(65)	—	0.286(20)
OT J052033.9−000530	20.579(54)	20.561(24)	19.724(18)	19.304(19)	18.855(52)	—	0.363(50)
OT J052033.9−000530	20.712(71)	20.473(24)	19.626(17)	19.158(17)	18.826(36)	—	0.409(66)
OT J052033.9−000530	20.754(71)	20.553(30)	19.714(21)	19.282(23)	18.885(62)	—	0.433(72)
OT J052033.9−000530	20.760(54)	20.521(21)	19.738(16)	19.269(16)	18.866(39)	—	0.374(50)
OT J055730.1+001514	25.009(653)	22.920(137)	22.074(101)	21.869(136)	22.033(579)	—	—
OT J055842.8+000626	20.624(62)	20.329(20)	18.975(11)	18.432(10)	17.929(21)	—	0.374(28)
OT J055842.8+000626	20.799(86)	19.803(15)	18.856(11)	18.164(9)	17.602(18)	—	0.259(22)
OT J055842.8+000626	20.846(64)	20.434(22)	19.383(14)	18.635(12)	18.011(25)	—	0.174(8)
OT J055842.8+000626	21.202(94)	20.732(29)	19.518(17)	18.697(12)	18.059(27)	—	0.255(13)
OT J073055.5+425636	22.388(289)	22.761(150)	23.017(273)	23.297(437)	21.779(413)	—	—
OT J073339.3+212201	20.832(81)	20.447(27)	19.618(18)	19.110(17)	18.781(39)	—	—
OT J073559.9+220132	20.260(50)	20.198(22)	20.177(31)	20.233(41)	20.325(132)	—	0.066(3)
OT J073758.5+205545	20.100(41)	19.984(18)	20.032(23)	20.278(44)	20.001(111)	—	0.053(2)
OT J073921.2+222454	22.783(316)	22.698(136)	22.380(158)	22.128(159)	22.526(636)	—	0.132(48)
OT J074222.5+172807	19.902(36)	19.942(15)	19.768(18)	19.765(25)	19.598(68)	—	0.071(2)
OT J074222.5+172807	19.925(38)	19.861(17)	19.871(20)	19.706(24)	19.661(83)	—	0.091(3)
OT J074222.5+172807	20.079(44)	19.897(18)	19.923(22)	19.656(26)	19.549(75)	—	0.111(6)
OT J074222.5+172807	20.431(50)	20.227(19)	20.047(21)	19.898(24)	19.806(85)	—	0.106(5)
OT J074419.7+325448	20.732(57)	20.763(24)	20.699(29)	20.827(41)	21.022(154)	—	0.061(3)
OT J074419.7+325448	21.208(81)	21.310(46)	21.574(79)	21.827(162)	22.229(638)	—	0.053(12)
OT J074419.7+325448	21.359(94)	21.441(48)	21.785(86)	22.053(166)	21.564(357)	—	0.070(15)
OT J074419.7+325448	21.372(99)	21.460(61)	21.699(105)	21.656(147)	21.902(533)	—	0.070(10)
OT J074727.6+065050	19.692(41)	19.402(13)	19.531(22)	19.830(32)	19.936(118)	0.0594 <sup>†</sup>	0.050(1)
OT J074820.0+245759	22.194(217)	22.523(134)	22.931(257)	22.768(336)	23.184(604)	—	—
OT J074820.0+245759	22.439(264)	22.366(128)	22.963(293)	24.386(848)	22.055(518)	—	—
OT J074820.0+245759	22.611(301)	22.514(114)	22.903(216)	22.358(179)	22.255(392)	—	0.107(31)
OT J074928.0+190452	20.444(64)	20.794(33)	20.516(36)	20.460(50)	20.065(115)	—	0.069(2)
OT J074928.0+190452	20.551(59)	21.115(42)	20.892(44)	20.828(61)	20.324(171)	—	0.070(4)
OT J074928.0+190452	20.769(79)	20.748(31)	20.500(34)	20.461(48)	20.337(142)	—	0.086(5)
OT J075332.0+375801	21.048(76)	21.289(46)	21.161(52)	21.124(75)	20.660(208)	—	0.068(3)
OT J075332.0+375801	21.258(101)	21.191(45)	21.358(96)	20.850(75)	21.106(355)	—	0.153(24)
OT J075332.0+375801	21.270(87)	21.333(46)	21.301(57)	21.195(78)	20.589(204)	—	0.072(4)
OT J075414.5+313216	19.906(37)	19.651(14)	19.644(17)	19.739(23)	19.618(63)	0.0615 <sup>†</sup>	0.059(1)
OT J075414.5+313216	20.167(59)	20.018(20)	19.976(32)	20.017(42)	20.129(154)	0.0615 <sup>†</sup>	0.070(3)
OT J075648.0+305805	20.957(107)	21.077(46)	20.980(72)	21.056(101)	21.132(402)	—	0.066(5)
OT J075648.0+305805	20.997(81)	20.859(33)	20.930(45)	20.872(59)	20.882(175)	—	0.075(5)
OT J080428.4+363104	22.228(190)	22.113(70)	21.881(77)	21.449(79)	21.239(231)	—	0.147(15)
OT J080428.4+363104	22.982(526)	22.948(175)	22.432(176)	21.866(145)	21.399(340)	—	0.197(51)
OT J080714.2+113812	20.691(65)	20.537(24)	20.652(34)	21.066(67)	20.444(139)	0.0596 <sup>†</sup>	0.062(9)
OT J080714.2+113812	21.020(78)	20.909(28)	20.961(41)	21.175(77)	21.145(248)	0.0596 <sup>†</sup>	0.056(2)
OT J080729.7+153442	22.193(193)	22.483(95)	22.061(107)	22.050(173)	22.202(617)	—	0.101(22)
OT J080729.7+153442	22.476(344)	22.367(119)	22.236(160)	21.732(156)	21.561(494)	—	0.153(26)
OT J080729.7+153442	22.913(665)	22.628(202)	22.095(168)	22.255(409)	22.525(1267)	—	—
OT J080853.7+355053	19.549(31)	19.656(13)	19.614(16)	19.516(17)	19.298(55)	—	0.074(2)
OT J081030.6+002429	21.402(105)	21.358(46)	21.315(61)	20.874(61)	19.994(122)	—	0.102(7)
OT J081414.9+080450	21.466(139)	21.337(48)	21.442(89)	20.967(98)	21.010(274)	—	0.150(20)
OT J081414.9+080450	21.593(109)	21.700(57)	21.415(64)	21.238(78)	20.979(176)	—	0.105(8)
OT J081414.9+080450	21.967(163)	22.232(100)	22.055(89)	21.587(90)	21.089(217)	—	0.122(13)
OT J081418.9−005022	18.302(13)	18.567(7)	18.462(9)	18.187(10)	17.833(24)	0.0741 <sup>†</sup>	0.092(2)
OT J081418.9−005022	18.480(15)	18.921(9)	18.676(9)	18.714(11)	18.406(29)	0.0741 <sup>†</sup>	0.062(1)
OT J081418.9−005022	18.926(18)	19.116(10)	18.973(11)	18.795(12)	18.507(29)	0.0741 <sup>†</sup>	0.082(1)
OT J081418.9−005022	18.970(22)	19.101(10)	18.939(12)	18.809(15)	18.484(44)	0.0741 <sup>†</sup>	0.076(2)

\*Orbital period estimated with neural network.

†Determined from superhump period.

‡Dwarf novae proposed by Wils et al. (2010).



**Table 3.** List of dwarf novae (continued)

Object	<i>u</i>	<i>g</i>	<i>r</i>	<i>i</i>	<i>z</i>	$P_{\text{orb}}$	$P_{\text{est}}^*$
OT J081418.9−005022	19.084(21)	19.193(11)	19.034(12)	19.015(15)	18.568(34)	0.0741 <sup>†</sup>	0.066(2)
OT J081712.3+055208	21.840(190)	21.387(55)	20.857(56)	20.612(67)	20.195(192)	—	0.488(123)
OT J081712.3+055208	22.024(241)	21.462(60)	20.903(55)	20.971(105)	20.634(266)	—	—
OT J081936.1+191540	20.876(83)	20.364(24)	19.938(22)	19.755(28)	19.907(116)	—	0.264(80)
OT J081936.1+191540	21.482(137)	20.479(24)	19.968(24)	19.796(27)	19.696(95)	—	0.403(149)
OT J082019.4+474732	21.267(94)	21.361(50)	21.305(58)	21.302(84)	20.894(205)	—	0.066(3)
OT J082123.7+454135	19.232(23)	19.472(12)	19.004(10)	18.822(12)	18.653(33)	—	0.126(3)
OT J082123.7+454135	19.488(32)	19.923(19)	19.500(18)	19.164(19)	18.922(47)	—	0.113(5)
OT J082123.7+454135	19.668(36)	19.987(20)	19.675(18)	19.416(23)	19.075(64)	—	0.092(2)
OT J082123.7+454135	19.781(35)	19.891(18)	19.674(18)	19.412(20)	19.014(48)	—	0.093(3)
OT J082123.7+454135	19.951(36)	20.090(20)	19.782(17)	19.480(19)	19.219(52)	—	0.115(4)
OT J082123.7+454135	20.217(44)	20.605(27)	20.219(30)	19.770(28)	19.371(62)	—	0.121(6)
OT J082603.7+113821	20.489(57)	20.630(26)	20.542(31)	20.444(39)	19.992(93)	—	0.071(2)
OT J082603.7+113821	20.680(67)	20.459(23)	20.421(30)	20.250(34)	19.649(67)	—	0.077(2)
OT J082603.7+113821	20.922(86)	20.687(30)	20.553(42)	20.260(50)	19.861(121)	—	0.108(7)
OT J082654.7−000733	19.659(37)	19.460(13)	19.203(14)	19.200(20)	19.333(78)	—	0.108(7)
OT J082654.7−000733	19.854(32)	19.523(12)	19.497(14)	19.644(20)	19.613(74)	—	0.059(1)
OT J082821.8+105344	22.113(242)	22.291(111)	22.075(149)	22.225(277)	22.128(795)	—	0.083(24)
OT J082908.4+482639	21.464(116)	21.433(63)	21.617(88)	21.605(121)	22.803(753)	—	—
OT J084041.5+000520	20.509(48)	20.590(23)	20.867(42)	21.050(82)	20.662(269)	—	0.067(8)
OT J084041.5+000520	20.544(50)	20.793(28)	20.803(39)	21.008(70)	20.641(222)	—	0.060(5)
OT J084041.5+000520	20.695(59)	20.777(29)	20.985(47)	21.087(72)	20.513(185)	—	0.069(5)
OT J084127.4+210053	20.421(53)	20.498(26)	20.264(28)	20.030(33)	19.704(91)	—	0.097(4)
OT J084127.4+210053	20.595(59)	20.610(25)	20.403(27)	20.077(32)	19.644(82)	—	0.105(5)
OT J084358.1+425037	19.598(33)	19.913(16)	19.877(19)	19.689(21)	19.302(55)	—	0.082(2)
OT J084413.7−012807	20.219(56)	20.349(25)	20.505(39)	20.446(47)	20.299(175)	—	0.074(3)
OT J084413.7−012807	20.309(62)	20.112(18)	20.126(28)	20.168(44)	20.177(160)	—	0.068(3)
OT J084413.7−012807	20.579(65)	20.522(26)	20.863(45)	21.155(91)	20.873(300)	—	0.062(9)
OT J084555.1+033930	20.566(56)	20.592(22)	20.595(30)	20.856(49)	21.032(161)	0.0591 <sup>†</sup>	0.054(2)
OT J084555.1+033930	20.760(71)	20.885(36)	20.891(47)	21.029(75)	21.264(300)	0.0591 <sup>†</sup>	0.061(3)
OT J084555.1+033930	21.172(192)	20.810(52)	20.816(80)	21.040(177)	21.182(472)	0.0591 <sup>†</sup>	0.064(9)
OT J085113.4+344449	20.244(51)	20.108(21)	20.038(26)	19.807(31)	19.147(66)	—	0.083(3)
OT J085113.4+344449	20.550(55)	20.445(21)	20.501(29)	20.034(27)	19.341(53)	—	0.117(6)
OT J085409.4+201339	20.313(49)	20.910(30)	20.477(30)	20.325(34)	20.106(114)	—	0.083(3)
OT J085603.8+322109	19.502(28)	19.638(13)	19.738(18)	19.774(23)	19.620(81)	—	0.067(1)
OT J085822.9−003729	21.822(174)	21.710(57)	21.378(74)	21.270(97)	21.204(343)	—	0.144(25)
OT J085822.9−003729	22.532(374)	22.343(158)	22.042(166)	21.977(224)	21.597(585)	—	—
OT J085822.9−003729	23.053(661)	22.785(211)	22.796(296)	22.517(316)	20.843(290)	—	—
OT J090016.7+343928	20.835(73)	20.467(24)	20.097(26)	19.913(31)	19.695(109)	—	0.257(23)
OT J090016.7+343928	21.281(95)	20.615(24)	20.315(25)	20.066(29)	19.731(83)	—	0.319(45)
OT J090239.7+052501	23.774(510)	23.161(177)	23.056(212)	23.000(278)	22.125(369)	0.0565	—
OT J090516.1+120451	19.326(32)	19.796(17)	19.563(19)	19.520(25)	19.629(106)	—	0.074(2)
OT J090516.1+120451	19.499(29)	19.754(14)	19.721(18)	19.592(19)	19.679(72)	—	0.085(4)
OT J090852.2+071640	20.548(56)	20.130(19)	20.279(28)	20.258(42)	20.203(137)	—	0.071(4)
OT J090852.2+071640	20.963(73)	20.987(36)	21.034(55)	20.836(65)	20.488(182)	—	0.084(5)
OT J091453.6+113402	21.231(93)	20.971(33)	21.051(47)	21.192(74)	21.315(250)	—	0.059(3)
OT J091453.6+113402	21.241(119)	20.962(39)	21.093(59)	21.141(90)	21.073(283)	—	0.066(5)
OT J091534.9+081356	22.249(225)	22.802(162)	23.094(279)	22.711(273)	21.760(376)	—	0.102(38)
OT J091534.9+081356	23.553(591)	23.028(169)	22.856(313)	23.138(584)	21.624(592)	—	—
OT J091634.6+130358	20.932(89)	21.453(61)	21.364(77)	21.129(94)	21.243(334)	—	0.091(12)
OT J091634.6+130358	21.376(99)	21.894(76)	21.549(88)	21.921(155)	21.627(320)	—	0.069(10)
OT J091634.6+130358	21.690(156)	21.834(87)	21.677(134)	21.700(182)	22.075(641)	—	0.075(16)
OT J092839.3+005944	21.558(321)	21.236(136)	21.096(168)	20.810(165)	20.451(476)	—	0.126(23)
OT J092839.3+005944	21.692(149)	21.775(76)	21.740(111)	21.350(120)	21.386(504)	—	0.117(20)
OT J092839.3+005944	21.698(168)	21.800(79)	21.691(99)	21.180(82)	21.047(317)	—	0.140(19)
OT J092839.3+005944	21.938(156)	21.901(71)	21.822(95)	21.375(101)	20.580(190)	—	0.108(12)

\*Orbital period estimated with neural network.

†Determined from superhump period.

‡Dwarf novae proposed by Wils et al. (2010).

**Table 3.** List of dwarf novae (continued)

Object	<i>u</i>	<i>g</i>	<i>r</i>	<i>i</i>	<i>z</i>	$P_{\text{orb}}$	$P_{\text{est}}^*$
OT J101035.5+140239	18.457(16)	17.196(4)	17.277(5)	17.359(6)	17.407(15)	—	0.153(32)
OT J101035.5+140239	19.224(22)	18.051(6)	17.854(6)	17.775(7)	17.713(16)	—	0.439(146)
OT J103704.6+100224	23.476(623)	23.421(274)	22.812(229)	22.693(296)	22.565(656)	—	—
OT J103704.6+100224	24.717(895)	22.857(180)	22.509(211)	22.275(274)	22.686(846)	—	—
OT J101545.9+033312	19.811(35)	20.168(19)	20.137(24)	20.130(33)	19.864(82)	—	0.068(2)
OT J102146.4+234926	20.847(64)	20.725(26)	20.628(31)	20.853(58)	20.436(151)	0.0554 <sup>†</sup>	0.063(3)
OT J102616.0+192045	20.108(40)	20.126(18)	20.082(22)	19.853(23)	19.509(54)	0.0800 <sup>†</sup>	0.090(3)
OT J102637.0+475426	20.160(41)	19.929(17)	20.097(24)	20.139(35)	19.987(112)	0.0663 <sup>†</sup>	0.064(2)
OT J102637.0+475426	20.245(46)	20.127(23)	20.177(29)	20.316(45)	20.026(130)	0.0663 <sup>†</sup>	0.057(1)
OT J102937.7+414046	22.212(213)	22.269(86)	22.317(116)	23.091(309)	22.012(524)	—	—
OT J102937.7+414046	22.547(274)	22.401(100)	22.426(167)	22.632(266)	22.972(756)	—	0.068(16)
OT J102937.7+414046	22.595(310)	22.137(89)	22.181(158)	22.350(275)	23.662(843)	—	—
OT J103317.3+072119	19.942(36)	19.893(16)	19.806(18)	19.751(23)	19.478(54)	—	0.072(2)
OT J103738.7+124250	22.114(168)	21.903(77)	21.775(91)	21.628(134)	20.933(269)	—	0.102(15)
OT J103738.7+124250	22.212(307)	22.064(130)	21.911(141)	21.625(170)	21.241(435)	—	0.127(21)
OT J104411.4+211307	19.198(23)	19.347(11)	19.262(12)	19.481(18)	19.268(45)	0.0591	0.056(2)
OT J105550.1+095621	19.026(21)	19.153(11)	18.505(8)	17.879(8)	17.399(13)	—	0.211(12)
OT J105835.1+054706	20.107(45)	20.299(24)	20.148(27)	20.188(40)	20.104(128)	—	0.066(2)
OT J105835.1+054706	20.141(42)	20.401(23)	20.237(25)	20.148(30)	19.939(87)	—	0.075(2)
OT J112112.0−130843	19.844(42)	19.851(18)	19.453(18)	19.263(22)	19.193(68)	—	0.137(6)
OT J112253.3−111037	20.712(62)	20.438(21)	20.461(26)	20.575(39)	20.462(119)	0.0472 <sup>†</sup>	0.058(1)
OT J112332.0+431718	19.427(27)	19.912(16)	19.753(19)	19.640(22)	19.474(61)	—	0.075(2)
OT J112509.7+231036	20.571(60)	20.988(36)	21.059(51)	21.296(88)	20.461(153)	—	0.073(14)
OT J112509.7+231036	20.960(82)	20.964(34)	21.111(53)	21.022(76)	20.933(228)	—	0.079(5)
OT J112634.0−100210	18.811(22)	18.809(9)	18.619(10)	18.375(11)	18.131(28)	—	0.102(2)
OT J115330.2+315836	20.690(67)	20.113(18)	19.945(21)	19.897(30)	19.971(124)	—	0.168(18)
OT J122756.8+622935	22.157(208)	21.572(55)	20.977(50)	20.402(44)	20.058(150)	—	0.245(83)
OT J122756.8+622935	22.584(321)	21.813(69)	21.383(73)	20.794(63)	20.792(283)	—	—
OT J122756.8+622935	23.119(579)	21.811(74)	21.351(71)	20.698(64)	20.535(262)	—	—
OT J123833.7+031854	22.258(269)	21.560(65)	21.327(82)	21.140(110)	21.360(452)	—	—
OT J124027.4−150558	21.328(134)	21.021(39)	20.766(44)	20.604(55)	20.327(145)	—	0.128(15)
OT J124417.9+300401	19.380(30)	19.571(12)	19.494(15)	19.490(20)	19.080(49)	—	0.065(1)
OT J124819.4+072050	21.663(141)	21.326(46)	21.401(70)	21.385(89)	21.285(330)	—	0.073(6)
OT J124819.4+072050	21.786(208)	21.371(59)	21.533(94)	21.329(116)	21.611(545)	—	0.094(16)
OT J130030.3+115101	19.891(45)	19.783(16)	19.802(21)	19.840(25)	19.421(53)	0.0627 <sup>†</sup>	0.061(1)
OT J132536.0+210037	22.132(223)	—	20.376(25)	20.637(41)	20.568(166)	—	—
OT J134052.1+151341	19.843(34)	18.623(8)	17.913(6)	17.653(7)	17.504(13)	—	0.149(38)
OT J134052.1+151341	20.259(42)	18.731(8)	17.988(7)	17.721(7)	17.572(15)	—	0.207(10)
OT J135219.0+280917	20.702(79)	20.669(26)	19.927(22)	19.584(24)	19.219(66)	—	0.479(96)
OT J135336.0−022043	21.838(197)	21.711(72)	21.069(53)	20.742(55)	20.395(170)	—	0.358(54)
OT J135716.8−093239	23.000(525)	22.761(157)	21.991(142)	21.609(149)	20.715(218)	—	—
OT J141002.2−124809	19.230(29)	19.160(11)	19.282(14)	19.366(21)	19.296(59)	—	0.062(1)
OT J141712.0−180328	20.437(69)	20.616(28)	20.274(26)	20.056(31)	19.519(81)	—	0.082(3)
OT J142548.1+151502	22.168(211)	21.802(61)	21.616(76)	21.324(75)	21.088(237)	—	0.151(22)
OT J144011.0+494734	21.253(137)	21.161(51)	21.006(67)	21.501(132)	22.608(946)	0.0631 <sup>†</sup>	—
OT J144316.5−010222	21.708(140)	22.185(88)	21.931(102)	21.913(141)	21.818(415)	—	0.073(6)
OT J144316.5−010222	22.069(176)	22.417(106)	22.120(149)	22.674(381)	22.196(800)	—	—
OT J144316.5−010222	22.110(149)	22.236(87)	22.116(117)	21.814(144)	21.858(491)	—	0.112(20)
OT J145502.2+143815	19.862(42)	20.117(21)	19.620(18)	19.250(18)	18.996(46)	—	0.158(6)
OT J145502.2+143815	20.240(43)	20.485(22)	19.944(20)	19.483(22)	19.124(57)	—	0.177(7)
OT J145502.2+143815	20.266(54)	20.282(23)	19.813(22)	19.447(24)	19.155(55)	—	0.188(11)
OT J145921.8+354806	21.257(66)	21.544(39)	21.070(36)	20.760(42)	20.403(94)	0.0822 <sup>†</sup>	0.145(8)
OT J151020.7+182303	21.458(124)	21.424(43)	20.688(32)	20.490(38)	20.245(108)	—	0.494(77)
OT J151037.4+084104	19.356(27)	19.120(10)	19.411(14)	19.579(19)	19.922(70)	—	0.059(3)
OT J152037.9+040948	21.703(139)	22.495(143)	22.121(118)	21.920(149)	21.332(302)	—	0.086(8)
OT J152501.8−013021	23.105(524)	22.679(138)	22.613(188)	23.824(641)	22.412(755)	—	—

\*Orbital period estimated with neural network.

†Determined from superhump period.

‡Dwarf novae proposed by Wils et al. (2010).

**Table 3.** List of dwarf novae (continued)

Object	<i>u</i>	<i>g</i>	<i>r</i>	<i>i</i>	<i>z</i>	$P_{\text{orb}}$	$P_{\text{est}}^*$
OT J153150.8+152447	22.975(332)	23.130(157)	22.686(156)	22.552(190)	22.077(429)	—	0.156(51)
OT J153317.6+273428	22.338(224)	21.932(76)	21.461(74)	21.146(91)	21.477(417)	—	—
OT J153645.2−142543	22.984(507)	22.879(150)	22.913(262)	22.558(300)	22.593(785)	—	0.092(28)
OT J154354.1−143745	21.219(128)	21.404(51)	21.090(55)	21.001(79)	20.527(215)	—	0.070(3)
OT J154428.1+335725	22.361(276)	22.108(90)	21.850(109)	22.280(251)	21.613(565)	—	—
OT J154544.9+442830	20.850(64)	20.943(26)	20.850(34)	20.718(41)	20.328(127)	0.0747 <sup>†</sup>	0.076(3)
OT J155325.7+114437	22.867(448)	22.646(142)	23.474(432)	22.730(437)	23.415(863)	—	—
OT J155325.7+114437	23.172(449)	23.235(186)	23.886(434)	22.931(335)	23.022(627)	—	—
OT J155430.6+365043	21.408(139)	21.608(59)	21.664(92)	21.774(161)	22.810(799)	—	0.049(17)
OT J155430.6+365043	21.782(191)	21.703(80)	21.521(90)	21.559(146)	22.089(694)	—	0.076(22)
OT J155748.0+070543	22.620(288)	22.813(149)	22.938(231)	23.480(467)	21.855(458)	—	—
OT J155748.0+070543	22.921(827)	22.740(202)	22.652(301)	23.516(871)	22.342(905)	—	—
OT J160204.8+031632	22.530(342)	22.653(178)	22.825(265)	22.731(370)	21.167(348)	—	—
OT J160204.8+031632	23.405(450)	23.223(200)	22.839(186)	22.492(216)	22.192(563)	—	0.139(37)
OT J160232.2+161733	22.543(262)	21.905(63)	21.779(75)	21.837(126)	21.326(354)	—	0.152(50)
OT J160524.1+060816	22.565(299)	22.839(150)	22.511(160)	22.027(167)	22.574(655)	—	0.138(41)
OT J160524.1+060816	23.676(859)	22.678(181)	22.640(189)	21.828(138)	22.296(575)	—	—
OT J160844.8+220610	20.842(80)	21.048(32)	20.991(41)	20.822(50)	20.683(156)	—	0.079(4)
OT J160844.8+220610	21.000(227)	20.890(91)	20.954(98)	21.012(137)	20.518(243)	—	0.068(5)
OT J160844.8+220610	21.170(74)	21.638(45)	20.973(37)	20.998(49)	20.895(166)	—	0.110(13)
OT J162012.0+115257	22.615(373)	22.211(83)	22.240(139)	22.215(204)	22.890(827)	—	0.077(24)
OT J162235.7+035247	22.356(332)	22.240(125)	21.728(108)	20.997(82)	20.294(160)	—	0.180(26)
OT J162605.7+225044	22.291(176)	22.681(98)	22.248(95)	22.092(142)	21.536(317)	—	0.099(13)
OT J162605.7+225044	23.575(600)	22.998(166)	22.617(152)	22.437(196)	21.854(383)	—	—
OT J162656.8−002549	22.221(238)	22.610(146)	22.352(187)	21.785(177)	21.687(550)	—	0.137(28)
OT J162806.2+065316	20.645(71)	20.544(27)	20.419(33)	20.420(38)	19.976(95)	0.0671 <sup>†</sup>	0.066(2)
OT J162806.2+065316	20.800(70)	20.649(26)	20.578(33)	20.494(49)	20.135(117)	0.0671 <sup>†</sup>	0.071(3)
OT J162619.8−125557	21.826(192)	21.601(61)	21.131(55)	20.898(68)	20.564(209)	—	0.071(4)
OT J163120.9+103134	19.039(25)	19.061(10)	19.094(12)	19.164(17)	18.793(42)	0.0624 <sup>†</sup>	0.061(2)
OT J163239.3+351108	23.160(369)	22.697(118)	23.073(253)	24.110(571)	22.247(577)	—	—
OT J163311.3−011132	21.174(80)	21.356(43)	21.086(47)	21.150(72)	20.758(190)	—	0.061(3)
OT J163942.7+122414	19.373(29)	19.481(12)	19.212(12)	19.068(14)	18.962(39)	—	0.094(2)
OT J163942.7+122414	20.398(59)	20.457(25)	20.307(28)	20.215(38)	19.832(100)	—	0.072(2)
OT J164146.8+121026	20.999(92)	21.333(48)	21.048(50)	20.702(55)	20.363(156)	—	0.104(6)
OT J164146.8+121026	21.219(95)	21.363(43)	21.125(49)	20.586(46)	20.721(208)	—	0.170(25)
OT J164146.8+121026	21.788(168)	21.488(46)	21.286(49)	21.084(60)	20.637(161)	—	0.109(11)
OT J164624.8+180808	23.167(411)	22.351(84)	22.177(91)	22.036(122)	21.221(230)	—	—
OT J164748.0+433845	21.389(180)	21.650(80)	21.760(135)	22.295(246)	22.787(973)	—	0.044(14)
OT J164748.0+433845	21.398(98)	21.535(46)	21.819(87)	22.271(194)	21.766(432)	—	0.065(17)
OT J164950.4+035835	18.861(38)	18.548(12)	18.587(12)	18.525(17)	18.343(45)	—	0.070(1)
OT J165002.8+435616	22.333(242)	22.758(164)	22.336(168)	21.868(189)	21.299(409)	—	0.152(27)
OT J165002.8+435616	22.649(381)	22.376(113)	22.671(203)	22.163(217)	22.694(740)	—	0.107(40)
OT J165002.8+435616	23.206(523)	22.855(161)	22.666(171)	22.592(248)	22.252(578)	—	0.164(66)
OT J170115.8−024159	24.055(1164)	22.977(203)	22.250(154)	22.288(271)	22.844(973)	—	—
OT J170151.6+132131	21.789(239)	21.317(76)	20.837(56)	20.475(63)	20.218(194)	—	0.285(51)
OT J170606.1+255153	21.227(166)	21.479(66)	21.308(82)	21.205(118)	21.043(436)	—	0.080(8)
OT J170609.7+143452	17.733(11)	18.231(7)	17.897(7)	17.709(7)	17.712(16)	—	0.076(5)
OT J170609.7+143452	18.004(15)	18.453(8)	18.240(8)	18.056(10)	17.959(28)	—	0.075(4)
OT J170702.5+165339	21.200(92)	21.593(51)	21.232(56)	21.034(66)	20.516(155)	—	0.077(3)
OT J171223.1+362516	20.781(68)	20.885(32)	19.904(19)	19.443(18)	19.257(54)	—	—
OT J171223.1+362516	20.847(87)	20.770(33)	19.910(22)	19.396(23)	19.138(61)	—	—
OT J171223.1+362516	20.851(91)	20.533(29)	19.805(21)	19.307(20)	19.018(51)	—	0.347(115)
OT J171223.1+362516	20.888(100)	20.652(33)	19.802(26)	19.355(23)	19.102(58)	—	—
OT J172515.5+073249	20.482(65)	20.656(30)	20.611(35)	20.732(57)	22.379(652)	—	—
OT J173307.9+300635	22.707(328)	22.535(106)	22.350(128)	21.943(121)	21.005(248)	—	0.118(17)
OT J175901.1+395551	22.559(369)	22.030(98)	22.519(236)	22.048(218)	21.865(662)	—	0.115(34)

\*Orbital period estimated with neural network.

†Determined from superhump period.

‡Dwarf novae proposed by Wils et al. (2010).

**Table 3.** List of dwarf novae (continued)

Object	<i>u</i>	<i>g</i>	<i>r</i>	<i>i</i>	<i>z</i>	$P_{\text{orb}}$	$P_{\text{est}}^*$
OT J182142.8+212154	20.195(53)	20.260(21)	20.198(25)	19.895(27)	19.438(62)	0.0794 <sup>†</sup>	0.089(3)
OT J202857.1−061803	20.767(77)	20.606(30)	20.557(36)	20.597(49)	20.145(126)	—	0.062(2)
OT J204001.4−144909	20.401(66)	20.563(25)	20.488(30)	20.443(38)	20.301(140)	—	0.071(2)
OT J204739.4+000840	23.154(715)	22.213(131)	21.997(153)	21.569(150)	21.322(512)	—	—
OT J210034.4+055436	21.970(189)	22.113(72)	22.024(121)	21.830(141)	20.948(226)	—	0.083(7)
OT J210034.4+055436	22.402(297)	22.248(90)	22.160(116)	21.852(119)	20.958(198)	—	0.094(9)
OT J210043.9−005212	21.178(131)	21.301(65)	20.759(52)	20.643(70)	20.381(233)	—	0.142(18)
OT J210043.9−005212	21.261(83)	21.613(51)	21.508(70)	21.056(70)	21.008(256)	—	0.122(17)
OT J210043.9−005212	21.366(138)	21.461(60)	21.322(86)	20.949(97)	20.670(259)	—	0.108(13)
OT J210043.9−005212	21.384(132)	21.183(52)	21.009(58)	20.820(73)	20.447(207)	—	0.089(6)
OT J210043.9−005212	21.402(122)	21.466(57)	21.407(80)	21.031(83)	20.718(269)	—	0.108(9)
OT J210043.9−005212	21.510(191)	21.596(93)	21.308(99)	21.017(110)	20.366(215)	—	0.098(9)
OT J210043.9−005212	21.520(135)	21.536(65)	21.130(64)	20.930(84)	20.885(314)	—	0.123(13)
OT J210043.9−005212	21.587(172)	21.344(67)	21.094(73)	20.790(80)	20.581(233)	—	0.128(14)
OT J210043.9−005212	21.593(520)	22.237(498)	21.115(154)	21.354(218)	20.458(272)	—	—
OT J210043.9−005212	21.713(152)	21.525(59)	21.120(58)	20.930(73)	20.763(246)	—	0.152(20)
OT J210043.9−005212	21.964(263)	21.662(93)	21.204(95)	21.332(181)	21.335(640)	—	—
OT J210043.9−005212	21.998(372)	21.506(102)	21.288(119)	21.270(166)	20.972(488)	—	0.118(34)
OT J210043.9−005212	22.027(400)	22.284(317)	21.393(124)	21.135(121)	20.968(374)	—	0.236(90)
OT J210205.7+025834	21.744(161)	21.483(47)	21.398(62)	20.860(54)	20.393(153)	—	0.137(9)
OT J210650.6+110250	19.779(37)	20.242(21)	20.163(25)	20.136(37)	19.795(101)	—	0.072(5)
OT J210650.6+110250	19.917(39)	20.501(25)	20.315(29)	20.154(35)	19.838(97)	—	0.078(3)
OT J210704.5+014416	23.380(485)	23.890(267)	23.091(198)	23.669(403)	23.537(435)	—	—
OT J210846.4−035031	18.084(17)	17.881(6)	17.677(6)	17.380(7)	17.025(14)	—	0.099(2)
OT J210846.4−035031	18.705(23)	18.615(9)	17.982(7)	17.552(7)	17.173(14)	—	0.248(12)
OT J210954.1+163052	19.133(21)	19.521(12)	19.315(13)	19.191(16)	19.093(54)	—	0.071(3)
OT J211550.9−000716	21.936(271)	22.533(169)	22.591(285)	22.261(331)	21.126(458)	—	0.112(33)
OT J211550.9−000716	22.330(306)	22.973(200)	23.082(386)	23.524(689)	22.561(748)	—	—
OT J211550.9−000716	22.374(487)	22.873(397)	23.289(514)	22.088(193)	22.370(617)	—	—
OT J211550.9−000716	22.431(217)	22.664(121)	22.494(155)	22.556(233)	23.210(687)	—	0.058(13)
OT J211550.9−000716	22.509(385)	23.277(221)	23.091(298)	22.229(229)	21.291(362)	—	0.151(38)
OT J211550.9−000716	22.729(401)	22.938(226)	22.377(191)	22.399(246)	21.684(440)	—	—
OT J211550.9−000716	23.019(538)	22.245(110)	22.689(299)	22.191(295)	22.265(935)	—	—
OT J211550.9−000716	23.147(446)	22.424(119)	22.350(170)	22.009(184)	20.867(279)	—	—
OT J211550.9−000716	23.296(1920)	22.795(566)	21.791(226)	21.454(176)	21.976(789)	—	—
OT J211550.9−000716	24.024(571)	23.313(183)	23.202(249)	22.756(257)	21.530(361)	—	—
OT J211550.9−000716	24.118(876)	23.120(198)	23.961(618)	22.603(322)	22.295(704)	—	—
OT J212025.1+194157	21.817(180)	21.819(64)	21.812(92)	21.643(114)	22.728(665)	—	—
OT J212555.1−032406	22.199(333)	21.977(88)	22.090(147)	22.863(395)	21.384(426)	—	—
OT J212555.1−032406	22.401(653)	22.000(179)	22.132(294)	23.485(1509)	21.139(720)	—	—
OT J212633.3+085459	20.495(57)	20.757(26)	20.742(35)	20.548(43)	20.247(126)	—	0.083(3)
OT J213122.4−003937	21.060(217)	20.894(74)	21.051(157)	21.210(276)	21.381(1063)	0.0629 <sup>†</sup>	0.064(17)
OT J213122.4−003937	21.528(115)	21.550(48)	21.555(62)	21.727(108)	22.169(499)	0.0629 <sup>†</sup>	0.058(6)
OT J213122.4−003937	21.585(162)	21.210(49)	21.370(91)	21.329(140)	21.615(626)	0.0629 <sup>†</sup>	0.075(13)
OT J213122.4−003937	21.615(195)	21.492(61)	21.381(88)	21.872(187)	21.755(586)	0.0629 <sup>†</sup>	0.061(17)
OT J213122.4−003937	21.628(145)	21.380(49)	21.444(67)	21.632(107)	21.280(343)	0.0629 <sup>†</sup>	0.059(4)
OT J213122.4−003937	21.660(137)	21.605(54)	21.470(64)	21.693(111)	22.169(528)	0.0629 <sup>†</sup>	0.059(7)
OT J213122.4−003937	21.761(233)	21.481(71)	21.468(99)	21.691(166)	21.030(377)	0.0629 <sup>†</sup>	0.073(12)
OT J213122.4−003937	21.762(178)	21.398(42)	21.076(55)	21.040(87)	21.014(268)	0.0629 <sup>†</sup>	0.169(34)
OT J213122.4−003937	21.863(196)	21.489(55)	21.343(62)	21.664(128)	21.370(346)	0.0629 <sup>†</sup>	0.087(18)
OT J213122.4−003937	21.864(199)	21.526(60)	21.689(81)	21.727(125)	21.938(560)	0.0629 <sup>†</sup>	0.068(8)
OT J213122.4−003937	22.170(355)	21.472(48)	21.502(79)	22.023(234)	21.096(352)	0.0629 <sup>†</sup>	—
OT J213122.4−003937	22.201(416)	21.382(74)	21.366(115)	21.992(303)	21.208(545)	0.0629 <sup>†</sup>	—
OT J213432.3−012040	23.613(766)	23.255(215)	23.311(331)	23.511(509)	23.247(730)	—	—
OT J213309.4+155004	22.377(293)	22.075(91)	21.927(106)	21.407(101)	21.203(292)	—	0.148(19)
OT J213701.8+071446	19.001(21)	19.017(9)	18.724(9)	18.209(9)	17.625(15)	0.0950 <sup>†</sup>	0.137(5)

\*Orbital period estimated with neural network.

<sup>†</sup>Determined from superhump period.<sup>‡</sup>Dwarf novae proposed by Wils et al. (2010).



**Table 3.** List of dwarf novae (continued)

Object	<i>u</i>	<i>g</i>	<i>r</i>	<i>i</i>	<i>z</i>	$P_{\text{orb}}$	$P_{\text{est}}^*$
OT J213829.5–001742	23.814(723)	23.531(362)	22.552(156)	22.606(245)	22.941(671)	–	–
OT J213937.6–023913	20.145(60)	20.138(26)	20.006(31)	19.791(38)	19.111(74)	–	0.079(2)
OT J213937.6–023913	20.201(68)	20.010(19)	19.866(25)	19.644(31)	19.206(72)	–	0.091(3)
OT J213937.6–023913	20.291(67)	20.069(19)	20.019(28)	19.677(28)	19.145(61)	–	0.099(4)
OT J214426.4+222024	18.909(26)	17.644(5)	17.131(5)	16.984(6)	16.911(14)	–	–
OT J214639.9+092119	22.173(312)	21.829(71)	21.710(89)	21.887(144)	22.327(740)	–	0.065(16)
OT J214804.4+080951	20.543(61)	20.957(30)	20.879(38)	20.686(42)	20.431(139)	–	0.081(3)
OT J214842.5–000723	22.496(255)	22.776(150)	22.410(179)	22.363(246)	21.835(568)	–	0.094(18)
OT J214842.5–000723	22.731(348)	22.854(158)	22.651(173)	22.778(337)	21.354(376)	–	–
OT J214842.5–000723	22.732(366)	22.722(182)	22.634(214)	22.877(380)	22.030(622)	–	0.097(37)
OT J214842.5–000723	22.857(313)	23.050(192)	23.077(285)	23.443(518)	22.696(776)	–	–
OT J214842.5–000723	22.896(365)	22.546(153)	22.413(148)	23.584(486)	22.326(740)	–	–
OT J214842.5–000723	22.930(462)	22.899(160)	22.946(250)	22.399(215)	22.590(638)	–	0.105(30)
OT J214842.5–000723	23.223(570)	22.760(154)	22.987(303)	23.381(610)	21.593(556)	–	–
OT J214842.5–000723	23.405(465)	22.677(120)	22.968(243)	23.317(436)	22.392(613)	–	–
OT J214842.5–000723	23.632(738)	23.006(205)	22.330(169)	22.436(265)	22.788(839)	–	–
OT J214842.5–000723	24.390(929)	22.853(162)	22.969(269)	23.441(526)	21.528(449)	–	–
OT J214959.9+124529	22.245(240)	21.928(80)	22.039(124)	21.886(179)	22.140(685)	–	0.081(14)
OT J215344.7+123524	21.925(434)	21.494(98)	21.118(101)	20.827(106)	20.220(249)	–	0.171(57)
OT J215344.7+123524	22.019(189)	22.107(92)	21.828(97)	21.272(97)	20.459(167)	–	0.118(11)
OT J215344.7+123524	22.712(495)	21.924(122)	21.341(100)	20.954(105)	20.095(167)	–	–
OT J215630.5–031957	21.710(272)	22.142(125)	21.800(133)	22.108(323)	22.021(791)	–	0.073(21)
OT J215630.5–031957	22.291(320)	22.169(111)	21.898(137)	22.156(245)	21.665(503)	–	0.098(28)
OT J215636.3+193242	18.915(22)	18.783(9)	18.488(9)	18.346(10)	18.074(23)	–	0.095(2)
OT J215636.3+193242	19.376(32)	19.339(12)	19.107(13)	18.921(15)	18.522(34)	–	0.082(2)
OT J215636.3+193242	19.631(38)	19.553(13)	19.108(13)	19.013(18)	18.685(50)	–	0.128(7)
OT J215815.3+094709	17.592(12)	17.478(5)	17.613(6)	17.552(7)	17.150(13)	0.0750 <sup>†</sup>	0.070(1)
OT J220031.2+033431	18.551(18)	18.664(8)	18.404(9)	18.127(9)	17.941(22)	–	0.110(3)
OT J220449.7+054852	20.236(50)	20.035(19)	19.838(20)	19.501(21)	19.059(52)	–	0.107(4)
OT J220449.7+054852	21.203(106)	20.940(32)	20.722(36)	20.139(34)	19.653(82)	–	0.150(10)
OT J221128.7–030516	19.654(34)	19.555(13)	19.459(15)	19.456(19)	19.132(51)	–	0.062(1)
OT J221128.7–030516	19.678(49)	19.718(17)	19.552(20)	19.513(26)	19.228(68)	–	0.066(1)
OT J221128.7–030516	20.019(59)	19.864(17)	19.762(22)	19.694(30)	19.225(67)	–	0.066(1)
OT J221128.7–030516	19.637(49)	20.177(24)	19.749(23)	19.660(28)	19.805(103)	–	0.076(3)
OT J221128.7–030516	20.069(54)	20.597(25)	20.367(33)	20.482(52)	20.400(179)	–	0.059(4)
OT J221232.0+160140	19.048(25)	19.112(10)	18.860(11)	18.588(12)	18.286(30)	–	0.101(2)
OT J221232.0+160140	19.110(25)	19.247(11)	18.924(11)	18.676(12)	18.380(30)	–	0.101(2)
OT J221344.0+173252	19.104(31)	19.261(11)	19.208(14)	19.156(18)	18.872(54)	–	0.069(1)
OT J222002.3+113825	20.557(75)	20.653(26)	20.059(27)	19.847(33)	19.579(76)	–	0.197(16)
OT J222002.3+113825	21.119(88)	21.372(40)	20.637(33)	20.310(40)	20.093(128)	–	0.259(23)
OT J222548.1+252511	20.138(63)	20.196(21)	19.958(31)	19.255(28)	18.754(58)	–	0.166(10)
OT J222724.5+284404	18.226(15)	18.563(8)	17.994(7)	18.003(8)	17.795(19)	–	0.110(5)
OT J222824.1+134944	22.698(235)	22.345(81)	22.435(111)	22.603(207)	22.429(469)	–	0.065(8)
OT J222824.1+134944	22.721(316)	22.310(101)	22.195(120)	22.552(263)	22.501(673)	–	0.079(25)
OT J222853.7+295115	23.314(434)	23.489(194)	23.605(370)	22.666(294)	22.310(587)	–	0.146(53)
OT J223018.8+292849	23.596(789)	22.481(127)	22.258(173)	22.892(435)	22.263(767)	–	–
OT J223058.3+210147	20.693(105)	20.788(37)	20.679(48)	20.789(85)	20.249(187)	–	0.063(4)
OT J223136.0+180747	21.234(119)	21.663(56)	21.407(71)	21.496(112)	21.773(528)	–	0.061(6)
OT J223235.4+304105	22.426(273)	22.473(99)	22.408(156)	22.052(195)	21.754(547)	–	0.105(17)
OT J223418.5–035530	20.422(58)	20.502(25)	20.195(29)	19.911(30)	19.594(73)	0.0884 <sup>‡</sup>	0.112(4)
OT J223606.3+050517	22.413(273)	22.304(94)	22.381(145)	22.566(259)	22.292(503)	–	0.064(11)
OT J223909.8+250331	19.164(28)	19.158(10)	19.047(13)	18.894(16)	18.802(55)	–	0.089(2)
OT J223958.2+231837	22.321(320)	22.167(131)	22.149(145)	22.045(197)	21.408(585)	–	0.099(20)
OT J223958.2+231837	22.728(298)	22.144(64)	21.923(89)	21.858(120)	22.939(664)	–	–
OT J223958.4+342306	25.451(703)	22.395(87)	22.510(153)	22.788(288)	22.279(639)	–	–
OT J224253.4+172538	20.462(75)	20.439(25)	20.274(30)	20.106(37)	19.801(110)	–	0.086(3)

\*Orbital period estimated with neural network.

<sup>†</sup>Determined from superhump period.<sup>‡</sup>Dwarf novae proposed by Wils et al. (2010).

**Table 3.** List of dwarf novae (continued)

Object	<i>u</i>	<i>g</i>	<i>r</i>	<i>i</i>	<i>z</i>	$P_{\text{orb}}$	$P_{\text{est}}^*$
OT J224505.4+011547	21.211(135)	21.463(68)	21.379(94)	21.551(182)	21.406(499)	—	0.061(7)
OT J224505.4+011547	21.313(125)	21.502(62)	21.554(99)	21.629(189)	20.790(333)	—	0.073(10)
OT J224505.4+011547	21.438(130)	21.553(57)	21.537(72)	21.665(117)	21.225(288)	—	0.063(5)
OT J224753.9+235522	21.101(142)	21.188(68)	20.781(83)	20.758(130)	20.278(271)	—	0.089(12)
OT J224753.9+235522	21.658(142)	21.500(52)	21.282(66)	21.399(114)	21.103(305)	—	0.068(5)
OT J224814.5+331224	19.390(30)	19.625(13)	19.002(12)	19.105(16)	19.346(73)	—	0.114(20)
OT J224814.5+331224	21.050(86)	20.938(28)	20.867(36)	20.793(52)	20.583(151)	—	0.070(3)
OT J224823.7−092059	21.128(131)	21.128(48)	21.156(59)	21.071(76)	20.769(223)	—	0.075(4)
OT J225749.6−082228	20.466(103)	20.181(30)	20.146(42)	20.239(63)	22.027(921)	—	—
OT J225749.6−082228	20.567(75)	20.137(21)	20.081(26)	20.400(55)	20.310(179)	—	0.066(5)
OT J230115.4+224111	23.706(839)	22.109(104)	22.041(149)	21.744(184)	22.095(938)	—	—
OT J230131.1+040417	23.736(686)	21.951(69)	21.415(63)	21.624(112)	21.462(336)	—	—
OT J230425.8+062546	21.119(120)	20.962(34)	20.640(40)	21.141(91)	20.895(259)	0.0653 <sup>†</sup>	0.126(40)
OT J230425.8+062546	21.337(101)	21.090(34)	20.985(36)	21.363(67)	21.106(199)	0.0653 <sup>†</sup>	0.061(6)
OT J230711.3+294011	22.205(214)	21.496(40)	20.682(33)	19.934(28)	19.411(57)	—	—
OT J231110.9+013003	22.346(298)	21.620(61)	21.572(80)	21.755(129)	21.047(259)	—	—
OT J231142.8+204036	20.629(71)	20.540(25)	20.255(27)	20.026(31)	19.702(91)	—	0.080(3)
OT J231142.8+204036	21.407(147)	21.244(54)	21.017(58)	20.874(75)	20.214(150)	—	0.071(3)
OT J231308.1+233702	21.055(91)	20.385(23)	19.523(18)	19.087(17)	18.809(43)	0.0692 <sup>†</sup>	0.290(69)
OT J231308.1+233702	21.498(115)	20.434(21)	19.505(15)	19.083(14)	18.844(38)	0.0692 <sup>†</sup>	0.117(21)
OT J231552.3+271037	20.587(104)	20.735(37)	20.121(33)	19.269(24)	18.625(46)	—	0.164(20)
OT J231552.3+271037	20.898(98)	20.651(26)	20.035(25)	19.168(19)	18.550(41)	—	0.155(41)
OT J232551.5−014024	18.476(17)	18.853(9)	18.210(8)	17.944(8)	17.716(18)	—	0.166(5)
OT J232619.4+282650	20.878(63)	20.893(27)	20.543(27)	20.582(40)	20.186(112)	—	0.072(4)
OT J232619.4+282650	20.928(118)	20.933(39)	20.595(44)	20.392(47)	20.167(140)	—	0.096(6)
OT J232619.4+282650	21.139(85)	21.074(32)	20.820(39)	20.580(43)	20.537(154)	—	0.105(7)
OT J233938.7−053305	20.851(101)	18.996(10)	18.606(10)	18.251(10)	18.235(31)	—	0.105(41)
OT J234440.5−001206	20.110(71)	20.308(30)	20.075(38)	19.977(45)	19.345(83)	0.0745 <sup>†</sup>	0.073(3)
OT J234440.5−001206	20.152(47)	20.358(23)	20.172(26)	20.099(33)	19.682(90)	0.0745 <sup>†</sup>	0.070(2)
OT J234440.5−001206	20.190(48)	20.374(22)	20.141(26)	20.062(31)	19.644(95)	0.0745 <sup>†</sup>	0.072(2)
OT J234440.5−001206	20.283(72)	20.401(39)	20.253(34)	20.182(38)	19.609(83)	0.0745 <sup>†</sup>	0.069(2)
OT J234440.5−001206	20.308(55)	20.498(28)	20.374(30)	20.263(39)	19.609(92)	0.0745 <sup>†</sup>	0.070(2)
OT J234440.5−001206	20.352(58)	20.317(26)	20.268(35)	20.180(43)	19.573(106)	0.0745 <sup>†</sup>	0.070(2)
OT J234440.5−001206	20.414(55)	20.524(23)	20.413(30)	20.221(32)	19.574(66)	0.0745 <sup>†</sup>	0.076(2)
OT J234440.5−001206	20.469(55)	20.518(24)	20.377(27)	20.188(31)	19.696(73)	0.0745 <sup>†</sup>	0.079(3)
OT J234440.5−001206	20.496(75)	20.474(28)	20.470(41)	20.324(48)	19.572(99)	0.0745 <sup>†</sup>	0.074(3)
OT J234440.5−001206	20.510(64)	20.519(28)	20.370(31)	20.182(38)	19.537(85)	0.0745 <sup>†</sup>	0.079(2)
OT J234440.5−001206	20.545(78)	20.423(31)	20.452(51)	20.318(54)	20.058(157)	0.0745 <sup>†</sup>	0.079(5)
OT J234440.5−001206	20.570(71)	20.531(30)	20.440(38)	20.235(45)	19.661(109)	0.0745 <sup>†</sup>	0.079(3)
OT J234440.5−001206	20.609(89)	20.639(43)	20.407(49)	20.206(53)	19.618(126)	0.0745 <sup>†</sup>	0.089(5)
OT J234440.5−001206	20.697(67)	20.637(31)	20.430(33)	20.237(40)	19.724(103)	0.0745 <sup>†</sup>	0.088(4)
OT J234440.5−001206	20.771(68)	20.677(27)	20.525(30)	20.363(35)	19.744(82)	0.0745 <sup>†</sup>	0.080(3)
OT J234440.5−001206	20.815(97)	20.618(31)	20.521(38)	20.358(46)	19.823(113)	0.0745 <sup>†</sup>	0.080(3)
OT J234440.5−001206	21.043(77)	20.804(28)	20.750(38)	20.480(44)	19.897(102)	0.0745 <sup>†</sup>	0.090(5)
OT J234440.5−001206	21.073(81)	20.737(27)	20.604(34)	20.478(42)	19.766(90)	0.0745 <sup>†</sup>	0.091(9)
OT J234440.5−001206	21.232(97)	21.087(36)	21.060(46)	20.743(50)	20.016(108)	0.0745 <sup>†</sup>	0.089(5)
OT J234440.5−001206	21.243(95)	20.981(31)	20.885(39)	20.719(50)	20.133(113)	0.0745 <sup>†</sup>	0.083(5)
OT J234440.5−001206	21.283(171)	21.034(57)	21.001(81)	20.580(71)	19.908(150)	0.0745 <sup>†</sup>	0.113(11)
OT J234440.5−001206	21.363(119)	21.056(36)	20.903(44)	20.655(52)	19.984(121)	0.0745 <sup>†</sup>	0.101(8)
ROTSE3 J004626+410714	24.885(881)	24.950(611)	22.995(265)	21.413(95)	20.814(212)	—	—
ROTSE3 J004626+410714	25.682(510)	24.117(382)	22.537(159)	21.506(90)	20.895(198)	—	—
ROTSE3 J031031+431115	20.293(41)	20.514(21)	20.289(22)	20.113(25)	19.977(76)	—	0.072(3)
ROTSE3 J100932.2−020155	20.498(64)	20.490(28)	20.690(47)	21.043(82)	21.068(377)	—	0.052(7)
ROTSE3 J100932.2−020155	20.540(106)	20.568(47)	20.875(74)	21.026(99)	21.679(778)	—	0.055(12)
ROTSE3 J100932.2−020155	20.606(62)	20.553(25)	20.824(42)	20.912(70)	21.297(416)	—	0.065(6)
ROTSE3 J113709+513451	21.101(90)	20.674(26)	20.079(23)	19.949(30)	19.742(97)	—	0.685(134)

\*Orbital period estimated with neural network.

†Determined from superhump period.

‡Dwarf novae proposed by Wils et al. (2010).

**Table 3.** List of dwarf novae (continued)

Object	$u$	$g$	$r$	$i$	$z$	$P_{\text{orb}}$	$P_{\text{est}}^*$
ROTSE3 J154041.5–002703.2	21.057(78)	21.057(35)	20.556(34)	20.276(37)	19.752(91)	–	0.129(10)
ROTSE3 J154041.5–002703.2	21.320(94)	21.356(44)	20.976(47)	20.391(42)	19.891(107)	–	0.144(8)
ROTSE3 J154041.5–002703.2	21.924(201)	21.824(70)	21.602(87)	20.997(79)	20.317(145)	–	0.136(13)
ROTSE3 J212313–021446.6	22.145(223)	22.117(78)	21.926(95)	22.488(232)	22.126(551)	–	–
ROTSE3 J214850–020622.2	23.102(433)	22.407(91)	22.293(124)	22.234(173)	21.334(296)	–	–
ROTSE3 J221519.8–003257.2	20.735(83)	20.980(37)	20.859(41)	20.713(51)	20.338(131)	–	0.074(3)
ROTSE3 J221519.8–003257.2	20.916(118)	21.192(69)	20.881(56)	20.796(68)	20.335(147)	–	0.071(3)
ROTSE3 J221519.8–003257.2	20.919(106)	21.039(43)	20.807(53)	20.620(51)	20.120(125)	–	0.077(3)
ROTSE3 J221519.8–003257.2	20.973(113)	21.069(43)	20.897(58)	20.667(62)	20.025(145)	–	0.078(4)
ROTSE3 J221519.8–003257.2	21.167(94)	21.131(35)	21.022(48)	20.813(58)	20.477(162)	–	0.083(4)
ROTSE3 J221519.8–003257.2	21.182(137)	21.395(87)	21.186(72)	21.071(83)	20.827(195)	–	0.073(4)
ROTSE3 J221519.8–003257.2	21.187(106)	21.366(48)	20.991(51)	20.786(65)	20.294(160)	–	0.085(5)
ROTSE3 J221519.8–003257.2	21.187(115)	21.185(63)	20.932(53)	20.855(74)	20.662(268)	–	0.080(5)
ROTSE3 J221519.8–003257.2	21.211(117)	21.238(47)	20.960(58)	20.727(65)	20.379(171)	–	0.090(5)
ROTSE3 J221519.8–003257.2	21.242(108)	21.341(44)	21.095(50)	20.896(64)	20.400(148)	–	0.078(4)
ROTSE3 J221519.8–003257.2	21.288(267)	21.286(141)	21.291(114)	20.943(98)	20.526(191)	–	0.098(12)
ROTSE3 J221519.8–003257.2	21.329(166)	21.182(59)	20.950(88)	20.948(123)	21.388(620)	–	0.075(15)
ROTSE3 J221519.8–003257.2	21.342(112)	21.455(51)	21.173(55)	20.985(63)	20.311(158)	–	0.078(4)
ROTSE3 J221519.8–003257.2	21.394(117)	21.679(59)	21.381(61)	21.237(75)	20.698(179)	–	0.074(3)
ROTSE3 J221519.8–003257.2	21.511(212)	21.348(84)	21.385(104)	21.274(128)	20.486(269)	–	0.078(7)
ROTSE3 J221519.8–003257.2	21.688(129)	21.598(50)	21.547(67)	21.407(80)	20.838(187)	–	0.073(4)
RX J1715.6+6856	18.305(15)	18.633(8)	18.409(9)	18.389(10)	18.305(26)	0.0683	0.070(1)
RX J1831.7+6511	16.975(8)	17.037(4)	16.846(4)	16.661(5)	16.377(8)	0.167	0.086(2)
RX J1831.7+6511	17.056(9)	17.208(4)	16.948(4)	16.701(5)	16.469(9)	0.167	0.100(1)
SDSS J003941.06+005427.5	20.237(50)	20.357(22)	20.561(36)	20.759(67)	20.597(205)	0.0635	0.062(4)
SDSS J003941.06+005427.5	20.278(44)	20.402(20)	20.571(29)	20.926(61)	20.697(175)	0.0635	0.057(7)
SDSS J003941.06+005427.5	20.291(61)	20.356(27)	20.488(38)	20.693(67)	20.929(296)	0.0635	0.057(3)
SDSS J003941.06+005427.5	20.291(64)	20.422(28)	20.410(38)	20.677(70)	20.610(243)	0.0635	0.055(2)
SDSS J003941.06+005427.5	20.317(53)	20.397(22)	20.601(44)	20.694(62)	20.735(194)	0.0635	0.065(3)
SDSS J003941.06+005427.5	20.331(51)	20.519(23)	20.580(37)	20.803(75)	21.235(400)	0.0635	0.055(4)
SDSS J003941.06+005427.5	20.419(53)	20.467(23)	20.646(36)	21.074(76)	20.960(250)	0.0635	0.052(8)
SDSS J003941.06+005427.5	20.455(135)	20.413(58)	20.406(60)	20.793(100)	20.648(223)	0.0635	0.054(4)
SDSS J003941.06+005427.5	20.462(53)	20.500(22)	20.745(37)	20.919(71)	20.600(193)	0.0635	0.065(4)
SDSS J003941.06+005427.5	20.503(62)	20.415(24)	20.594(38)	20.911(80)	20.632(221)	0.0635	0.055(4)
SDSS J003941.06+005427.5	20.511(52)	20.498(22)	20.706(32)	20.876(53)	21.315(266)	0.0635	0.060(4)
SDSS J003941.06+005427.5	20.523(63)	20.554(27)	20.691(40)	21.046(81)	20.783(241)	0.0635	0.055(6)
SDSS J003941.06+005427.5	20.590(77)	20.561(29)	20.698(39)	21.113(93)	20.945(292)	0.0635	0.051(6)
SDSS J003941.06+005427.5	20.792(71)	20.652(26)	20.878(49)	21.271(101)	21.053(265)	0.0635	0.053(6)
SDSS J004335.14–003729.8	19.929(37)	19.752(14)	19.794(19)	19.977(28)	19.946(91)	0.0572	0.056(1)
SDSS J004335.14–003729.8	19.983(44)	19.801(16)	19.920(22)	20.013(31)	19.706(89)	0.0572	0.059(1)
SDSS J004335.14–003729.8	19.983(47)	19.812(17)	19.855(20)	19.919(28)	19.861(99)	0.0572	0.064(2)
SDSS J004335.14–003729.8	20.024(54)	19.799(19)	19.821(22)	19.826(29)	19.851(95)	0.0572	0.074(2)
SDSS J004335.14–003729.8	20.044(45)	19.798(15)	19.804(19)	19.950(28)	19.711(82)	0.0572	0.058(1)
SDSS J004335.14–003729.8	20.054(46)	19.836(16)	19.847(23)	19.930(34)	19.654(95)	0.0572	0.061(1)
SDSS J004335.14–003729.8	20.056(67)	19.927(27)	19.887(28)	19.988(40)	19.862(132)	0.0572	0.063(2)
SDSS J004335.14–003729.8	20.084(56)	19.782(18)	19.825(23)	19.973(34)	19.882(119)	0.0572	0.059(2)
SDSS J004335.14–003729.8	20.103(44)	19.830(15)	19.840(20)	20.036(29)	19.960(91)	0.0572	0.057(1)
SDSS J004335.14–003729.8	20.107(44)	19.813(16)	19.905(21)	19.966(31)	19.819(105)	0.0572	0.062(2)
SDSS J004335.14–003729.8	20.113(46)	19.835(16)	19.868(21)	19.941(29)	19.822(98)	0.0572	0.063(2)
SDSS J004335.14–003729.8	20.113(55)	19.847(17)	19.845(22)	19.939(31)	19.980(108)	0.0572	0.066(2)
SDSS J004335.14–003729.8	20.126(55)	19.843(19)	19.865(25)	19.863(35)	19.804(106)	0.0572	0.073(3)
SDSS J004335.14–003729.8	20.127(43)	19.916(16)	19.940(20)	20.087(30)	20.099(99)	0.0572	0.059(2)
SDSS J004335.14–003729.8	20.135(55)	19.731(18)	19.820(24)	19.891(33)	19.750(101)	0.0572	0.063(2)
SDSS J004335.14–003729.8	20.139(47)	19.814(16)	19.789(19)	19.953(28)	19.794(97)	0.0572	0.063(2)
SDSS J004335.14–003729.8	20.165(46)	19.939(17)	19.900(21)	20.049(30)	19.830(86)	0.0572	0.061(1)
SDSS J004335.14–003729.8	20.193(45)	19.943(17)	19.872(19)	20.060(29)	20.002(87)	0.0572	0.064(2)

\*Orbital period estimated with neural network.

†Determined from superhump period.

‡Dwarf novae proposed by Wils et al. (2010).

**Table 3.** List of dwarf novae (continued)

Object	<i>u</i>	<i>g</i>	<i>r</i>	<i>i</i>	<i>z</i>	$P_{\text{orb}}$	$P_{\text{est}}^*$
SDSS J004335.14−003729.8	20.265(63)	19.898(19)	19.853(25)	19.954(35)	20.108(138)	0.0572	0.077(4)
SDSS J004335.14−003729.8	20.269(59)	19.860(19)	19.940(26)	20.032(43)	19.930(147)	0.0572	0.063(2)
SDSS J004335.14−003729.8	20.276(61)	19.925(19)	19.903(28)	20.020(41)	20.050(159)	0.0572	0.069(3)
SDSS J012940.05+384210.4	19.680(27)	19.786(14)	20.002(20)	20.179(34)	20.075(112)	0.0435 <sup>†</sup>	0.061(6)
SDSS J033449.86−071047.8	17.569(11)	17.862(6)	17.693(6)	17.577(7)	17.518(19)	0.0724 <sup>‡</sup>	0.078(1)
SDSS J033710.91−065059.4	19.621(33)	19.558(13)	19.724(19)	19.969(33)	20.099(146)	—	0.055(2)
SDSS J053659.12+002215.1	19.248(27)	18.804(9)	18.953(12)	19.084(16)	19.308(75)	—	0.053(3)
SDSS J053659.12+002215.1	19.262(27)	18.841(9)	18.945(11)	19.100(14)	19.348(56)	—	0.052(3)
SDSS J053659.12+002215.1	19.287(22)	18.851(8)	18.961(11)	19.107(15)	19.297(60)	—	0.052(3)
SDSS J053659.12+002215.1	19.291(26)	18.828(9)	18.965(11)	19.086(15)	19.229(53)	—	0.054(3)
SDSS J053659.12+002215.1	19.306(26)	18.849(9)	18.957(11)	19.195(14)	19.294(43)	—	0.049(6)
SDSS J053659.12+002215.1	19.326(31)	18.776(9)	18.928(13)	19.037(19)	19.177(98)	—	0.055(3)
SDSS J074355.56+183834.8	20.116(43)	20.089(18)	19.299(13)	18.799(12)	18.643(38)	—	0.268(54)
SDSS J074355.56+183834.8	20.362(48)	19.785(15)	18.460(8)	17.771(7)	17.598(15)	—	—
SDSS J074531.92+453829.6	18.809(20)	19.041(9)	18.914(11)	18.994(15)	18.940(50)	0.0528	0.062(1)
SDSS J074640.62+173412.8	19.492(30)	19.767(13)	19.635(17)	19.520(19)	19.430(62)	0.0649 <sup>†</sup>	0.078(2)
SDSS J074640.62+173412.8	19.999(37)	19.807(16)	19.524(16)	19.396(19)	19.301(59)	0.0649 <sup>†</sup>	0.133(6)
SDSS J075059.97+141150.1	18.914(22)	19.104(11)	18.779(12)	18.698(14)	18.553(38)	0.0932	0.093(3)
SDSS J075059.97+141150.1	19.202(25)	19.094(10)	18.982(11)	18.790(13)	18.585(36)	0.0932	0.097(2)
SDSS J075507.70+143547.6	18.074(13)	18.186(7)	18.234(8)	18.408(11)	18.406(30)	0.0589	0.058(1)
SDSS J075507.70+143547.6	18.084(13)	18.209(7)	18.209(8)	18.390(10)	18.336(24)	0.0589	0.057(1)
SDSS J075507.70+143547.6	18.106(13)	18.186(7)	18.208(8)	18.420(10)	18.400(30)	0.0589	0.056(1)
SDSS J075507.70+143547.6	18.108(13)	18.198(6)	18.279(8)	18.457(10)	18.459(32)	0.0589	0.058(1)
SDSS J075939.79+191417.3	18.038(13)	17.834(5)	17.627(6)	17.605(7)	17.593(17)	0.1309	0.104(2)
SDSS J075939.79+191417.3	18.318(14)	18.096(7)	17.800(6)	17.804(8)	17.791(17)	0.1309	0.138(4)
SDSS J075939.79+191417.3	18.347(16)	17.945(6)	17.790(6)	17.701(7)	17.682(16)	0.1309	0.127(6)
SDSS J075939.79+191417.3	18.649(17)	18.177(6)	18.463(8)	18.302(9)	18.087(23)	0.1309	0.089(2)
SDSS J080142.37+210345.8	18.335(15)	18.708(8)	18.409(8)	18.339(9)	18.406(27)	—	0.078(2)
SDSS J080142.37+210345.8	18.399(15)	18.840(8)	18.659(9)	18.535(10)	18.457(28)	—	0.075(2)
SDSS J080142.37+210345.8	18.883(21)	19.021(10)	18.821(11)	18.724(13)	18.643(42)	—	0.080(2)
SDSS J080303.90+251627.0	19.209(25)	19.577(14)	19.247(14)	18.973(16)	18.781(43)	0.071	0.105(3)
SDSS J080303.90+251627.0	19.454(25)	19.591(12)	19.394(14)	19.247(16)	18.893(41)	0.071	0.080(2)
SDSS J080434.20+510349.2	18.026(13)	17.843(5)	17.867(7)	18.018(8)	18.081(25)	0.0590	0.058(1)
SDSS J080534.49+072029.1	19.952(44)	18.503(8)	17.807(6)	17.532(7)	17.393(14)	0.2297	0.171(10)
SDSS J080534.49+072029.1	20.123(35)	18.561(8)	17.809(6)	17.537(7)	17.365(12)	0.2297	0.231(12)
SDSS J080534.49+072029.1	20.199(44)	18.659(8)	17.909(7)	17.650(7)	17.458(13)	0.2297	0.233(11)
SDSS J080846.19+313106.0	18.748(18)	18.807(9)	18.386(8)	17.909(8)	17.564(15)	0.2059	0.167(8)
SDSS J080846.19+313106.0	19.121(22)	19.430(12)	18.748(9)	18.166(9)	17.737(15)	0.2059	0.206(5)
SDSS J081207.63+131824.4	19.030(25)	19.203(10)	18.914(11)	18.835(14)	18.667(39)	0.0752 <sup>†</sup>	0.088(2)
SDSS J081207.63+131824.4	19.217(24)	19.266(11)	19.162(12)	19.034(15)	18.667(34)	0.0752 <sup>†</sup>	0.076(2)
SDSS J082457.15+073702.4	22.271(335)	22.131(122)	21.675(141)	21.860(281)	21.168(577)	—	—
SDSS J083754.64+564506.7	19.621(32)	18.985(9)	18.985(12)	19.079(17)	19.123(61)	—	0.076(3)
SDSS J083931.35+282824.0	20.014(37)	20.226(20)	20.174(25)	20.053(31)	19.521(64)	0.0760 <sup>†</sup>	0.072(2)
SDSS J083931.35+282824.0	20.641(62)	20.443(25)	20.481(33)	20.507(53)	20.027(102)	0.0760 <sup>†</sup>	0.062(2)
SDSS J083931.35+282824.0	20.553(62)	20.481(35)	20.232(28)	20.103(37)	19.615(86)	0.0760 <sup>†</sup>	0.087(4)
SDSS J084026.16+220446.6	19.834(40)	19.593(15)	19.525(16)	19.185(16)	18.333(26)	—	0.093(6)
SDSS J084026.16+220446.6	20.157(50)	19.894(16)	20.114(25)	20.133(35)	20.009(123)	—	0.068(3)
SDSS J084400.10+023919.3	17.907(11)	18.441(7)	17.746(6)	17.478(6)	17.296(14)	0.207	0.177(6)
SDSS J084400.10+023919.3	18.215(13)	18.335(7)	17.941(6)	17.571(6)	17.298(14)	0.207	0.148(4)
SDSS J084400.10+023919.3	18.664(17)	18.906(10)	18.455(9)	18.006(8)	17.566(19)	0.207	0.143(5)
SDSS J085623.00+310834.0	20.168(41)	19.967(17)	19.953(20)	20.196(34)	20.257(115)	—	0.055(1)
SDSS J085623.00+310834.0	20.251(46)	19.950(18)	19.967(21)	20.259(35)	20.465(154)	—	0.053(2)
SDSS J085623.00+310834.0	20.322(48)	20.028(16)	20.067(23)	20.286(34)	20.321(102)	—	0.055(1)
SDSS J085623.00+310834.0	20.375(52)	20.052(17)	20.011(20)	20.315(40)	20.464(162)	—	0.058(4)
SDSS J090016.56+430118.2	18.691(19)	18.876(9)	18.194(7)	17.507(6)	17.018(12)	0.2094	0.194(19)
SDSS J090103.93+480911.1	19.168(23)	19.237(11)	19.107(12)	19.006(14)	18.889(41)	0.0779	0.083(2)

\*Orbital period estimated with neural network.

<sup>†</sup>Determined from superhump period.<sup>‡</sup>Dwarf novae proposed by Wils et al. (2010).



**Table 3.** List of dwarf novae (continued)

Object	<i>u</i>	<i>g</i>	<i>r</i>	<i>i</i>	<i>z</i>	$P_{\text{orb}}$	$P_{\text{est}}^*$
SDSS J090350.73+330036.1	18.850(18)	18.829(8)	18.792(10)	18.879(12)	18.619(31)	0.0591	0.060(1)
SDSS J090403.48+035501.2	19.482(30)	19.218(12)	19.258(16)	19.411(24)	19.439(85)	0.0597	0.058(1)
SDSS J090403.48+035501.2	19.497(28)	19.304(12)	19.352(14)	19.509(22)	19.388(66)	0.0597	0.055(1)
SDSS J090403.48+035501.2	19.627(34)	19.335(12)	19.416(16)	19.513(25)	19.412(71)	0.0597	0.059(1)
SDSS J090452.09+440255.4	19.623(33)	19.381(13)	19.478(17)	19.693(28)	19.774(93)	–	0.054(1)
SDSS J090628.25+052656.9	18.824(18)	18.761(9)	18.452(8)	18.096(8)	17.829(16)	–	0.143(4)
SDSS J090628.25+052656.9	19.321(25)	19.415(12)	18.833(11)	18.403(11)	18.096(25)	–	0.223(11)
SDSS J091001.63+164820.0	18.474(16)	18.832(9)	18.542(9)	18.538(11)	18.333(24)	–	0.069(2)
SDSS J091001.63+164820.0	18.687(21)	18.781(9)	18.578(10)	18.466(12)	18.085(25)	–	0.076(2)
SDSS J091001.63+164820.0	18.714(20)	18.967(9)	18.698(10)	18.518(11)	18.203(23)	–	0.085(2)
SDSS J091001.63+164820.0	18.872(21)	19.252(11)	18.975(11)	18.797(13)	18.494(28)	–	0.081(1)
SDSS J091127.36+084140.7	19.662(32)	19.729(14)	19.167(13)	18.674(12)	18.287(30)	0.2054	0.199(9)
SDSS J091945.11+085710.1	18.358(15)	18.191(6)	18.246(8)	18.423(10)	18.539(37)	0.0565	0.056(1)
SDSS J092219.55+421256.7	19.836(30)	19.882(14)	20.088(21)	20.103(29)	19.779(74)	–	0.069(2)
SDSS J092229.26+330743.6	17.838(11)	18.439(7)	18.237(7)	18.041(8)	17.979(18)	–	0.086(4)
SDSS J092229.26+330743.6	17.927(12)	18.590(8)	18.385(8)	18.263(10)	18.049(25)	–	0.076(1)
SDSS J092229.26+330743.6	18.134(12)	18.435(7)	18.485(8)	18.444(10)	18.169(24)	–	0.072(1)
SDSS J093249.57+472523.0	17.973(12)	17.768(5)	17.798(6)	17.910(8)	17.840(20)	0.0663	0.060(1)
SDSS J094002.56+274942.0	19.678(34)	19.096(10)	18.315(8)	17.920(8)	17.615(18)	–	–
SDSS J094325.90+520128.8	17.747(11)	18.320(7)	18.368(8)	18.152(10)	17.916(21)	–	0.087(2)
SDSS J094325.90+520128.8	17.747(15)	18.304(12)	18.465(25)	18.085(13)	17.899(42)	–	0.096(14)
SDSS J094325.90+520128.8	17.776(12)	17.977(6)	17.991(7)	17.932(8)	17.716(18)	–	0.073(1)
SDSS J094325.90+520128.8	18.119(15)	18.749(8)	18.474(10)	18.320(11)	18.286(33)	–	0.082(3)
SDSS J094558.24+292253.2	19.155(24)	19.064(10)	19.144(12)	19.537(24)	19.553(74)	–	0.048(4)
SDSS J095135.21+602939.6	19.871(37)	19.996(18)	19.946(21)	20.155(35)	19.997(110)	–	0.056(1)
SDSS J095135.21+602939.6	20.039(44)	19.956(18)	19.960(22)	20.117(35)	19.951(105)	–	0.057(1)
SDSS J100515.39+191108.0	18.086(14)	18.173(6)	18.246(7)	18.120(8)	17.825(20)	0.0752 <sup>†</sup>	0.078(1)
SDSS J100658.40+233724.4	18.455(16)	18.311(7)	17.931(7)	17.517(6)	17.139(12)	0.1859	0.180(10)
SDSS J100658.40+233724.4	18.951(21)	18.691(8)	18.212(8)	17.595(7)	17.124(13)	0.1859	0.204(9)
SDSS J101037.05+024915.0	20.155(39)	20.701(27)	20.232(26)	20.671(56)	20.614(194)	–	0.082(12)
SDSS J101037.05+024915.0	20.371(52)	20.755(33)	20.327(32)	20.708(67)	20.451(187)	–	0.091(16)
SDSS J101037.05+024915.0	21.509(134)	21.990(89)	21.325(75)	21.883(184)	21.860(553)	–	–
SDSS J101323.64+455858.9	18.469(16)	18.818(9)	18.882(11)	18.701(13)	18.418(28)	–	0.086(2)
SDSS J102517.94+430221.2	20.032(38)	19.938(16)	19.854(19)	20.298(35)	20.206(109)	–	0.058(5)
SDSS J102517.94+430221.2	20.043(40)	19.964(16)	19.840(20)	20.219(37)	20.343(147)	–	0.059(4)
SDSS J103147.99+085224.3	18.802(18)	18.795(8)	18.756(10)	18.559(11)	18.290(29)	–	0.088(2)
SDSS J103533.02+055158.3	19.114(22)	18.786(9)	18.809(10)	18.970(13)	19.135(43)	0.0570	0.061(1)
SDSS J110014.72+131552.1	18.315(13)	18.648(8)	18.778(10)	18.546(11)	18.373(29)	0.0657 <sup>†</sup>	0.091(3)
SDSS J110014.72+131552.1	18.623(18)	19.041(11)	18.840(12)	18.830(16)	18.569(39)	0.0657 <sup>†</sup>	0.066(1)
SDSS J110706.76+340526.8	19.604(30)	19.467(12)	18.827(10)	18.614(12)	18.179(23)	–	0.566(106)
SDSS J113215.50+624900.4	17.926(12)	18.422(7)	18.164(7)	18.212(10)	18.175(31)	–	0.066(1)
SDSS J113215.50+624900.4	17.987(12)	18.390(7)	18.367(8)	18.180(9)	18.203(28)	–	0.090(5)
SDSS J113215.50+624900.4	17.997(12)	18.472(7)	18.385(8)	18.334(10)	18.247(28)	–	0.072(1)
SDSS J113215.50+624900.4	18.155(13)	18.497(8)	18.336(8)	18.260(10)	18.344(35)	–	0.081(1)
SDSS J113551.09+532246.2	20.739(64)	20.798(31)	20.711(35)	20.361(36)	20.009(104)	–	0.112(6)
SDSS J114628.80+675909.7	18.266(15)	18.607(8)	18.329(12)	18.459(12)	18.459(32)	0.0617 <sup>†</sup>	0.066(2)
SDSS J114628.80+675909.7	18.469(16)	18.753(8)	18.846(11)	18.662(12)	18.713(40)	0.0617 <sup>†</sup>	0.091(4)
SDSS J115207.00+404947.8	19.206(27)	19.247(11)	19.154(12)	19.115(16)	19.004(44)	0.0677	0.075(2)
SDSS J120231.01+450349.1	19.931(36)	19.946(14)	19.899(18)	20.092(26)	19.912(86)	–	0.056(1)
SDSS J121607.03+052013.9	20.204(56)	20.015(18)	19.914(23)	20.186(41)	20.599(250)	0.0686	0.061(7)
SDSS J121607.03+052013.9	20.377(48)	20.138(18)	19.998(20)	20.273(32)	20.276(125)	0.0686	0.070(4)
SDSS J122740.83+513925.0	19.109(23)	19.067(10)	19.055(11)	19.056(14)	18.707(31)	0.0630	0.064(1)
SDSS J123813.73–033933.0	17.889(11)	17.782(5)	17.801(6)	17.952(8)	18.030(24)	0.0559	0.059(1)
SDSS J124058.03–015919.2	19.474(27)	19.556(13)	19.790(19)	20.013(35)	20.123(134)	0.0259	0.057(4)
SDSS J124058.03–015919.2	19.530(35)	19.545(13)	19.749(18)	19.918(28)	20.127(112)	0.0259	0.059(2)
SDSS J124417.89+300401.0	19.380(30)	19.571(12)	19.494(15)	19.490(20)	19.080(49)	–	0.065(1)

\*Orbital period estimated with neural network.

†Determined from superhump period.

‡Dwarf novae proposed by Wils et al. (2010).

**Table 3.** List of dwarf novae (continued)

Object	<i>u</i>	<i>g</i>	<i>r</i>	<i>i</i>	<i>z</i>	$P_{\text{orb}}$	$P_{\text{est}}^*$
SDSS J124426.26+613514.6	18.513(17)	18.753(9)	18.733(10)	18.569(12)	18.365(31)	0.0992	0.084(1)
SDSS J124426.26+613514.6	18.740(18)	18.718(8)	18.843(11)	18.773(13)	18.431(29)	0.0992	0.072(2)
SDSS J124819.36+072049.4	21.663(141)	21.326(46)	21.401(70)	21.385(89)	21.285(330)	–	0.073(7)
SDSS J124819.36+072049.4	21.786(208)	21.371(59)	21.533(94)	21.329(116)	21.611(545)	–	0.098(17)
SDSS J125023.85+665525.5	18.727(18)	18.651(8)	18.653(10)	18.739(13)	18.627(39)	0.0587	0.061(1)
SDSS J125834.77+663551.6	20.026(41)	20.566(25)	20.234(29)	20.482(50)	20.100(132)	–	0.065(6)
SDSS J130514.73+582856.3	19.094(22)	19.283(11)	19.272(14)	19.117(17)	19.037(52)	–	0.087(2)
SDSS J133941.11+484727.5	17.861(11)	17.678(5)	17.774(6)	17.958(8)	18.099(26)	0.0573	0.057(1)
SDSS J140429.37+172359.4	17.113(9)	17.495(5)	17.360(6)	17.382(7)	17.265(13)	–	0.065(1)
SDSS J142955.86+414516.8	17.377(9)	17.695(5)	17.825(6)	17.807(7)	17.723(17)	0.059	0.071(2)
SDSS J143317.78+101123.3	18.520(16)	18.554(8)	18.442(8)	18.541(10)	18.524(30)	0.0542	0.063(2)
SDSS J143544.02+233638.7	18.284(15)	18.200(6)	18.247(8)	18.481(10)	18.646(37)	0.054	0.054(1)
SDSS J143544.02+233638.7	18.392(17)	18.285(6)	18.368(8)	18.573(11)	18.736(42)	0.054	0.055(1)
SDSS J145003.12+584501.9	20.518(51)	20.630(24)	20.457(30)	20.788(55)	20.727(187)	–	0.060(4)
SDSS J145003.12+584501.9	20.912(83)	20.742(31)	20.694(43)	21.075(99)	21.021(304)	–	0.056(5)
SDSS J145758.21+514807.9	19.112(23)	19.158(10)	19.252(16)	19.391(23)	19.305(81)	0.0541	0.060(1)
SDSS J145758.21+514807.9	19.174(23)	19.159(11)	19.224(13)	19.368(22)	19.403(84)	0.0541	0.059(1)
SDSS J145758.21+514807.9	19.398(28)	19.536(12)	19.496(15)	19.619(21)	19.564(63)	0.0541	0.060(1)
SDSS J150137.22+550123.4	19.650(33)	19.386(12)	19.349(15)	19.607(28)	19.542(83)	0.0568	0.059(2)
SDSS J150240.98+333423.9	17.804(10)	17.496(5)	17.554(6)	17.617(7)	17.513(13)	0.0589	0.064(1)
SDSS J150240.98+333423.9	17.833(11)	17.575(5)	17.662(6)	17.778(7)	17.632(17)	0.0589	0.058(1)
SDSS J150722.30+523039.8	18.479(17)	18.311(7)	18.451(8)	18.596(11)	18.436(28)	0.0463	0.056(1)
SDSS J151413.72+454911.9	20.030(43)	19.675(14)	19.674(17)	19.833(24)	19.995(106)	–	0.064(3)
SDSS J152212.20+080340.9	18.270(14)	18.379(7)	18.443(8)	18.439(10)	18.293(23)	–	0.068(1)
SDSS J152212.20+080340.9	18.418(16)	18.981(9)	18.952(11)	18.920(14)	18.512(32)	–	0.075(4)
SDSS J152419.33+220920.0	19.032(24)	19.055(9)	18.896(10)	18.806(12)	18.503(35)	0.0653	0.073(2)
SDSS J152717.96+543724.9	20.006(38)	20.140(18)	20.193(26)	20.258(39)	20.137(141)	–	0.064(2)
SDSS J152717.96+543724.9	20.025(36)	20.286(19)	20.240(25)	20.275(36)	20.145(118)	–	0.065(2)
SDSS J152717.96+543724.9	20.077(51)	20.296(23)	20.320(27)	20.380(36)	20.171(113)	–	0.064(2)
SDSS J152857.86+034911.7	19.078(24)	19.506(14)	19.354(15)	19.171(19)	19.094(55)	–	0.082(3)
SDSS J153015.04+094946.3	18.385(17)	18.867(9)	18.470(9)	18.473(11)	18.515(34)	–	0.075(3)
SDSS J153015.04+094946.3	18.387(16)	18.516(8)	18.608(9)	18.475(11)	18.397(33)	–	0.082(2)
SDSS J153634.42+332851.9	18.976(23)	19.209(10)	18.944(11)	18.763(12)	18.594(35)	–	0.093(2)
SDSS J153817.35+512338.0	18.294(14)	18.547(7)	18.866(10)	19.008(13)	18.799(40)	0.0647	0.067(9)
SDSS J154453.60+255348.8	16.430(7)	16.579(4)	16.140(5)	15.972(5)	15.663(7)	0.2513	0.116(3)
SDSS J154453.60+255348.8	17.019(8)	17.175(5)	16.530(5)	16.211(5)	16.018(7)	0.2513	0.260(9)
SDSS J155037.27+405440.0	18.195(16)	18.542(8)	18.311(8)	18.240(9)	18.391(34)	–	0.086(3)
SDSS J155037.27+405440.0	17.844(12)	18.413(7)	18.036(7)	18.052(8)	18.007(21)	–	0.071(2)
SDSS J155531.99–001055.0	18.901(22)	19.052(12)	19.000(12)	18.883(14)	18.563(35)	0.0789	0.073(1)
SDSS J155531.99–001055.0	19.072(20)	19.322(11)	19.102(12)	18.933(16)	18.811(45)	0.0789	0.077(1)
SDSS J155644.24–000950.2	18.176(15)	18.246(7)	17.997(7)	17.903(8)	17.512(15)	0.0800	0.066(1)
SDSS J155644.24–000950.2	18.274(13)	18.010(6)	17.891(6)	17.665(7)	17.287(15)	0.0800	0.080(1)
SDSS J155644.24–000950.2	18.412(17)	18.285(8)	18.105(8)	17.902(8)	17.481(16)	0.0800	0.075(1)
SDSS J155656.92+352336.6	19.181(25)	18.923(9)	18.856(10)	18.827(13)	18.746(42)	0.0892	0.082(2)
SDSS J155644.24–000950.2	18.265(14)	18.006(8)	17.889(8)	17.663(9)	17.285(16)	0.0800	0.080(1)
SDSS J155720.75+180720.2	18.108(14)	18.683(8)	18.477(9)	18.324(10)	18.234(26)	0.088	0.078(3)
SDSS J155720.75+180720.2	18.282(15)	18.644(7)	18.667(9)	18.324(9)	18.186(25)	0.088	0.109(5)
SDSS J160111.53+091712.7	19.988(40)	20.122(20)	20.114(24)	20.245(36)	19.752(72)	–	0.059(3)
SDSS J160111.53+091712.7	20.226(42)	20.603(26)	20.183(24)	20.259(39)	20.136(134)	–	0.078(4)
SDSS J160419.02+161548.5	18.685(20)	19.082(10)	18.822(10)	18.747(11)	18.728(39)	–	0.076(1)
SDSS J160501.35+203056.9	19.169(27)	19.361(11)	19.396(14)	19.509(22)	19.556(73)	0.0567	0.060(2)
SDSS J160501.35+203056.9	19.775(35)	19.883(15)	19.893(20)	19.960(30)	20.175(140)	0.0567	0.065(2)
SDSS J160501.35+203056.9	19.807(34)	19.891(15)	19.936(19)	20.040(28)	20.135(101)	0.0567	0.061(1)
SDSS J160501.35+203056.9	19.856(42)	19.926(16)	19.926(20)	20.083(35)	20.130(123)	0.0567	0.058(1)
SDSS J161030.35+445901.7	19.868(38)	19.753(15)	19.752(20)	20.184(41)	20.119(129)	–	0.050(4)
SDSS J161332.56–000331.0	18.568(15)	18.600(8)	17.940(7)	17.468(7)	17.174(13)	–	0.203(12)

\*Orbital period estimated with neural network.

†Determined from superhump period.

‡Dwarf novae proposed by Wils et al. (2010).

**Table 3.** List of dwarf novae (continued)

Object	<i>u</i>	<i>g</i>	<i>r</i>	<i>i</i>	<i>z</i>	$P_{\text{orb}}$	$P_{\text{est}}^*$
SDSS J161909.10+135145.5	18.897(20)	18.494(8)	17.800(6)	17.429(6)	17.174(12)	—	0.498(111)
SDSS J162212.45+341147.3	19.234(24)	19.168(10)	18.648(9)	18.295(10)	18.033(25)	—	0.266(13)
SDSS J162212.45+341147.3	19.241(26)	19.119(10)	18.684(9)	18.337(9)	18.042(20)	—	0.219(16)
SDSS J162212.45+341147.3	19.245(27)	19.116(10)	18.694(10)	18.335(10)	18.010(20)	—	0.210(16)
SDSS J162718.39+120435.0	20.122(46)	20.225(18)	19.786(19)	19.604(24)	19.062(49)	0.1041 <sup>†</sup>	0.109(6)
SDSS J162830.89+240259.1	19.854(39)	19.737(16)	19.775(18)	19.670(23)	19.367(61)	—	0.073(2)
SDSS J162830.89+240259.1	19.949(33)	19.780(14)	19.706(16)	19.739(21)	19.525(62)	—	0.063(1)
SDSS J162830.89+240259.1	20.137(41)	19.998(16)	19.827(17)	19.663(20)	19.463(55)	—	0.092(3)
SDSS J163722.21−001957.1	20.185(83)	20.536(41)	20.453(50)	20.207(67)	20.071(257)	0.0674	0.084(5)
SDSS J164248.52+134751.4	18.482(18)	18.651(8)	18.529(9)	18.437(10)	18.217(30)	0.0789	0.071(1)
SDSS J165244.84+333925.4	20.733(58)	20.854(28)	20.766(31)	20.720(40)	20.426(116)	—	0.070(2)
SDSS J165359.06+201010.4	18.457(16)	18.562(8)	18.310(8)	18.136(9)	18.094(23)	0.0635 <sup>†</sup>	0.094(2)
SDSS J165359.06+201010.4	18.463(14)	18.656(8)	18.418(8)	18.255(9)	18.170(24)	0.0635 <sup>†</sup>	0.085(1)
SDSS J165658.13+212139.3	17.994(12)	18.487(7)	18.276(7)	18.180(8)	18.036(22)	0.0631	0.072(1)
SDSS J165658.13+212139.3	18.510(15)	18.913(9)	18.708(9)	18.638(11)	18.389(28)	0.0631	0.069(1)
SDSS J165837.70+184727.4	20.518(57)	20.074(17)	20.116(22)	20.087(30)	19.657(76)	0.0681	0.063(2)
SDSS J165837.70+184727.4	20.528(58)	20.189(17)	20.236(27)	20.126(35)	19.797(81)	0.0681	0.072(3)
SDSS J170213.26+322954.1	18.162(13)	17.908(6)	17.808(6)	17.398(6)	16.989(11)	0.1001	0.128(7)
SDSS J170324.09+320953.2	18.237(13)	18.138(6)	17.595(5)	17.215(5)	16.859(10)	—	0.276(14)
SDSS J170542.54+313240.8	19.768(31)	19.668(12)	19.210(12)	18.753(11)	18.496(26)	—	0.209(18)
SDSS J171145.08+301320.0	20.284(41)	20.016(16)	19.985(20)	19.950(26)	19.787(89)	0.0558	0.072(2)
SDSS J171145.08+301320.0	20.429(47)	20.186(18)	20.123(21)	20.153(29)	20.171(106)	0.0558	0.072(3)
SDSS J171145.08+301320.0	20.441(48)	20.205(18)	20.165(20)	20.258(31)	20.317(100)	0.0558	0.065(2)
SDSS J204448.92−045928.8	17.213(9)	16.941(5)	16.185(5)	15.926(5)	15.676(6)	1.68	0.647(160)
SDSS J204448.92−045928.8	17.321(10)	16.844(5)	16.254(5)	15.980(5)	15.699(7)	1.68	0.614(119)
SDSS J204720.76+000007.7	19.201(25)	19.448(12)	19.373(15)	19.204(18)	19.187(69)	—	0.080(3)
SDSS J204720.76+000007.7	19.236(26)	19.351(11)	19.199(13)	19.195(15)	19.177(54)	—	0.067(1)
SDSS J204720.76+000007.7	19.485(30)	20.078(17)	19.866(23)	19.620(22)	19.743(88)	—	0.090(9)
SDSS J204720.76+000007.7	19.953(41)	20.270(20)	20.199(25)	20.068(30)	19.684(91)	—	0.075(2)
SDSS J204720.76+000007.7	20.035(42)	20.300(20)	20.130(22)	20.173(30)	19.749(91)	—	0.061(2)
SDSS J204720.76+000007.7	20.074(44)	20.286(21)	20.156(29)	20.019(35)	19.843(134)	—	0.075(2)
SDSS J204720.76+000007.7	20.134(59)	20.422(29)	20.088(32)	19.901(41)	19.813(187)	—	0.086(4)
SDSS J204720.76+000007.7	20.223(47)	20.314(20)	20.200(24)	20.128(30)	20.177(138)	—	0.073(3)
SDSS J204720.76+000007.7	20.319(55)	20.495(28)	20.362(30)	20.263(41)	20.044(150)	—	0.072(2)
SDSS J204720.76+000007.7	20.406(62)	20.677(35)	20.534(43)	20.483(60)	20.287(225)	—	0.068(3)
SDSS J204739.40+000840.3	23.154(715)	22.213(131)	21.997(153)	21.569(150)	21.322(512)	—	0.181(65)
SDSS J204817.85−061044.8	19.214(27)	19.340(12)	19.238(13)	19.205(16)	18.917(48)	0.0606	0.066(1)
SDSS J205914.87−061220.5	18.179(15)	18.354(7)	18.386(8)	18.178(9)	17.979(24)	0.0747	0.088(1)
SDSS J210014.12+004446.0	17.979(13)	17.961(6)	18.060(7)	18.057(9)	18.024(26)	0.0840 <sup>†</sup>	0.068(1)
SDSS J210014.12+004446.0	18.071(12)	18.047(6)	18.060(7)	17.959(8)	17.893(19)	0.0840 <sup>†</sup>	0.077(1)
SDSS J210014.12+004446.0	18.182(14)	17.828(6)	17.765(6)	17.743(8)	17.682(20)	0.0840 <sup>†</sup>	0.073(1)
SDSS J210014.12+004446.0	18.212(15)	18.041(6)	17.932(7)	17.859(7)	17.756(17)	0.0840 <sup>†</sup>	0.076(1)
SDSS J210014.12+004446.0	18.296(16)	18.380(7)	18.498(9)	18.375(10)	18.105(23)	0.0840 <sup>†</sup>	0.077(1)
SDSS J210014.12+004446.0	18.343(16)	18.366(7)	18.335(9)	18.264(13)	18.124(32)	0.0840 <sup>†</sup>	0.072(1)
SDSS J210014.12+004446.0	18.383(16)	18.453(7)	18.146(7)	18.020(9)	17.938(22)	0.0840 <sup>†</sup>	0.092(2)
SDSS J210014.12+004446.0	18.383(16)	18.574(8)	18.509(10)	18.350(14)	18.160(34)	0.0840 <sup>†</sup>	0.079(1)
SDSS J210014.12+004446.0	18.394(25)	18.407(12)	18.324(11)	18.233(12)	18.132(27)	0.0840 <sup>†</sup>	0.075(1)
SDSS J210014.12+004446.0	18.454(18)	18.630(8)	18.440(8)	18.309(10)	18.209(26)	0.0840 <sup>†</sup>	0.079(1)
SDSS J210014.12+004446.0	18.531(16)	18.731(8)	18.634(9)	18.546(11)	18.386(28)	0.0840 <sup>†</sup>	0.072(1)
SDSS J210014.12+004446.0	18.572(19)	18.714(11)	18.653(11)	18.539(12)	18.401(32)	0.0840 <sup>†</sup>	0.076(1)
SDSS J210014.12+004446.0	18.642(18)	18.808(9)	18.681(10)	18.563(12)	18.449(34)	0.0840 <sup>†</sup>	0.076(1)
SDSS J210449.94+010545.8	19.905(69)	19.974(35)	19.934(34)	19.916(42)	19.945(119)	—	0.065(2)
SDSS J210449.94+010545.8	19.962(51)	19.968(22)	19.676(20)	19.480(25)	19.283(75)	—	0.086(3)
SDSS J210449.94+010545.8	20.165(56)	20.137(22)	19.857(24)	19.703(34)	19.468(90)	—	0.081(3)
SDSS J210449.94+010545.8	20.176(50)	20.242(20)	20.747(60)	20.274(47)	19.846(109)	—	—
SDSS J210449.94+010545.8	20.214(76)	20.215(31)	20.019(36)	19.904(45)	19.705(127)	—	0.073(3)

\*Orbital period estimated with neural network.

<sup>†</sup>Determined from superhump period.<sup>‡</sup>Dwarf novae proposed by Wils et al. (2010).

**Table 3.** List of dwarf novae (continued)

Object	<i>u</i>	<i>g</i>	<i>r</i>	<i>i</i>	<i>z</i>	$P_{\text{orb}}$	$P_{\text{est}}^*$
SDSS J210449.94+010545.8	20.259(46)	20.304(19)	19.997(22)	19.869(29)	19.608(86)	–	0.075(3)
SDSS J210449.94+010545.8	20.395(62)	20.299(24)	20.116(32)	19.899(37)	19.556(91)	–	0.080(3)
SDSS J210449.94+010545.8	20.628(183)	20.965(100)	20.734(83)	20.593(90)	20.368(199)	–	0.074(5)
SDSS J210449.94+010545.8	20.717(70)	20.824(30)	20.787(42)	20.605(56)	20.483(175)	–	0.078(4)
SDSS J210449.94+010545.8	20.875(185)	20.654(53)	20.617(53)	20.394(65)	19.981(156)	–	0.080(5)
SDSS J210449.94+010545.8	20.884(78)	21.020(35)	20.743(44)	20.745(68)	20.451(160)	–	0.064(2)
SDSS J210449.94+010545.8	21.079(115)	21.061(43)	20.856(54)	20.730(73)	20.329(179)	–	0.073(4)
SDSS J210449.94+010545.8	21.272(173)	21.086(52)	20.852(73)	20.782(114)	20.436(299)	–	0.076(6)
SDSS J211605.43+113407.5	21.757(171)	21.689(68)	21.479(78)	21.907(181)	22.712(846)	–	–
SDSS J211605.43+113407.5	22.312(332)	21.747(68)	21.847(101)	22.316(240)	21.609(455)	–	0.075(21)
SDSS J211605.43+113407.5	22.459(272)	21.873(75)	21.942(114)	22.023(175)	21.680(438)	–	0.075(12)
SDSS J211605.43+113407.5	22.718(588)	21.677(73)	21.671(122)	21.711(211)	21.172(361)	–	–
SDSS J214354.60+124458.0	16.905(8)	16.176(4)	16.127(4)	16.145(4)	16.102(7)	–	0.124(3)
SDSS J220553.98+115553.7	20.119(38)	20.029(16)	20.065(19)	20.192(27)	20.219(96)	0.0575	0.058(1)
SDSS J220553.98+115553.7	20.237(57)	20.030(21)	20.164(30)	20.365(48)	20.525(199)	0.0575	0.055(2)
SDSS J220553.98+115553.7	20.338(50)	20.068(18)	20.090(22)	20.246(33)	20.178(113)	0.0575	0.054(1)
SDSS J223252.35+140353.0	22.022(167)	22.163(77)	21.493(62)	20.843(61)	20.199(136)	–	0.196(21)
SDSS J223252.35+140353.0	22.301(174)	22.377(88)	21.588(62)	20.790(49)	20.324(110)	–	0.178(56)
SDSS J223439.93+004127.2	17.488(10)	17.666(5)	17.469(6)	17.350(6)	17.184(12)	0.0884	0.075(1)
SDSS J223439.93+004127.2	17.570(11)	17.723(5)	17.489(6)	17.335(7)	17.186(15)	0.0884	0.081(1)
SDSS J223439.93+004127.2	17.623(10)	17.739(5)	17.685(6)	17.544(7)	17.265(13)	0.0884	0.075(1)
SDSS J223439.93+004127.2	17.675(10)	18.014(6)	17.739(6)	17.524(7)	17.313(13)	0.0884	0.083(1)
SDSS J223439.93+004127.2	17.738(11)	18.020(6)	17.869(7)	17.732(8)	17.374(14)	0.0884	0.073(1)
SDSS J223439.93+004127.2	17.756(11)	17.921(6)	17.850(6)	17.664(7)	17.473(14)	0.0884	0.082(1)
SDSS J223439.93+004127.2	17.809(11)	17.747(6)	17.846(7)	17.690(7)	17.323(14)	0.0884	0.078(2)
SDSS J223439.93+004127.2	17.829(15)	17.928(8)	17.701(7)	17.503(7)	17.478(15)	0.0884	0.095(2)
SDSS J223439.93+004127.2	17.832(11)	18.095(6)	17.917(6)	17.773(8)	17.458(18)	0.0884	0.073(1)
SDSS J223439.93+004127.2	17.874(12)	18.203(7)	17.810(6)	17.528(7)	17.421(18)	0.0884	0.105(4)
SDSS J223439.93+004127.2	17.953(11)	18.047(6)	17.776(6)	17.652(7)	17.502(15)	0.0884	0.081(2)
SDSS J223439.93+004127.2	18.167(14)	18.305(8)	18.220(8)	17.995(8)	17.654(17)	0.0884	0.083(1)
SDSS J223439.93+004127.2	18.215(14)	18.331(7)	18.264(8)	18.102(9)	17.865(21)	0.0884	0.079(1)
SDSS J223439.93+004127.2	18.302(15)	18.483(8)	18.082(7)	18.017(9)	17.941(29)	0.0884	0.087(3)
SDSS J223439.93+004127.2	18.317(16)	18.423(7)	18.095(7)	18.006(8)	17.703(17)	0.0884	0.077(2)
SDSS J223439.93+004127.2	18.451(15)	18.606(8)	18.530(9)	18.281(10)	18.005(19)	0.0884	0.088(2)
SDSS J223439.93+004127.2	18.465(16)	18.713(8)	18.416(8)	18.314(10)	18.051(22)	0.0884	0.072(1)
SDSS J225831.18–094931.7	15.019(4)	15.102(3)	15.099(3)	14.995(3)	14.980(4)	0.0830 <sup>†</sup>	0.081(1)
SDSS J225831.18–094931.7	15.224(4)	15.587(3)	15.405(4)	15.455(4)	15.237(5)	0.0830 <sup>†</sup>	0.062(1)
SDSS J233325.92+152222.2	18.163(12)	18.521(7)	18.321(8)	18.336(10)	18.375(27)	0.0577	0.065(1)
SDSS J233325.92+152222.2	18.370(15)	18.745(9)	18.401(8)	18.428(11)	18.438(30)	0.0577	0.068(2)
SDSS J233325.92+152222.2	18.654(17)	18.761(8)	18.848(10)	18.792(12)	18.702(31)	0.0577	0.072(1)
SDSSp J081321.91+452809.4	18.192(13)	18.259(7)	17.629(6)	17.189(6)	16.889(12)	0.289	0.256(9)
SDSSp J081321.91+452809.4	18.572(18)	18.517(8)	17.719(6)	17.271(6)	17.020(12)	0.289	0.361(52)
SDSSp J081610.84+453010.2	19.675(29)	20.056(17)	19.527(15)	19.051(14)	18.566(31)	–	0.133(6)
SDSSp J082409.73+493124.4	19.266(25)	19.576(14)	19.443(17)	19.264(20)	18.996(51)	0.0677 <sup>‡</sup>	0.081(2)
SDSSp J082409.73+493124.4	19.616(34)	19.887(20)	19.698(22)	19.531(28)	19.282(76)	0.0677 <sup>‡</sup>	0.082(2)
SDSSp J082409.73+493124.4	19.896(54)	20.138(28)	19.781(29)	19.637(35)	19.558(115)	0.0677 <sup>‡</sup>	0.103(4)
SDSSp J083845.23+491055.5	19.201(21)	19.578(13)	19.374(15)	19.353(19)	19.083(46)	0.0696 <sup>‡</sup>	0.066(1)
SDSSp J083845.23+491055.5	19.371(27)	19.846(15)	19.658(16)	19.751(25)	19.417(75)	0.0696 <sup>‡</sup>	0.061(2)
SDSSp J083845.23+491055.5	19.542(32)	19.705(16)	19.594(21)	19.608(27)	19.262(61)	0.0696 <sup>‡</sup>	0.063(1)
SDSSp J172601.96+543230.7	20.221(41)	20.531(22)	20.513(29)	20.554(48)	20.671(184)	–	0.065(2)
SDSSp J173008.38+624754.7	16.008(5)	15.886(3)	16.150(3)	16.274(4)	16.260(8)	0.0770 <sup>‡</sup>	0.063(2)
SDSSp J173008.38+624754.7	16.279(6)	16.318(4)	16.118(4)	16.172(5)	16.093(7)	0.0770 <sup>‡</sup>	0.072(2)
SDSSp J230351.64+010651.0	17.218(9)	17.644(5)	17.254(5)	17.107(5)	16.909(12)	0.0767	0.082(1)
SDSSp J230351.64+010651.0	17.405(10)	17.907(6)	17.574(6)	17.359(7)	17.225(14)	0.0767	0.087(2)
SDSSp J230351.64+010651.0	17.414(10)	17.668(5)	17.670(6)	17.476(6)	17.005(11)	0.0767	0.081(2)
SDSSp J230351.64+010651.0	17.425(10)	17.973(6)	17.770(6)	17.572(7)	17.201(15)	0.0767	0.080(1)

\*Orbital period estimated with neural network.

<sup>†</sup>Determined from superhump period.<sup>‡</sup>Dwarf novae proposed by Wils et al. (2010).



**Table 3.** List of dwarf novae (continued)

Object	<i>u</i>	<i>g</i>	<i>r</i>	<i>i</i>	<i>z</i>	$P_{\text{orb}}$	$P_{\text{est}}^*$
SDSSp J230351.64+010651.0	17.433(10)	18.106(6)	17.497(5)	17.379(6)	17.187(14)	0.0767	0.092(2)
SDSSp J230351.64+010651.0	17.441(10)	17.975(6)	17.668(6)	17.458(7)	17.315(16)	0.0767	0.084(2)
SDSSp J230351.64+010651.0	17.464(10)	18.028(6)	17.636(6)	17.393(6)	17.232(14)	0.0767	0.090(2)
SDSSp J230351.64+010651.0	17.512(10)	17.863(6)	17.802(6)	17.575(7)	17.197(14)	0.0767	0.085(2)
SDSSp J230351.64+010651.0	17.521(10)	17.917(6)	17.652(6)	17.447(6)	17.061(12)	0.0767	0.078(1)
SDSSp J230351.64+010651.0	17.556(10)	17.928(6)	17.610(6)	17.459(6)	17.254(14)	0.0767	0.080(1)
SDSSp J230351.64+010651.0	17.615(11)	17.972(6)	17.762(6)	17.516(7)	17.271(14)	0.0767	0.088(1)
SDSSp J230351.64+010651.0	17.647(12)	17.938(6)	17.704(7)	17.531(7)	17.171(14)	0.0767	0.077(1)
SDSSp J230351.64+010651.0	17.671(11)	17.887(6)	17.633(6)	17.391(6)	17.097(12)	0.0767	0.091(1)
SDSSp J230351.64+010651.0	17.722(12)	17.853(6)	17.781(6)	17.589(7)	17.225(12)	0.0767	0.080(1)
SDSSp J230351.64+010651.0	17.746(11)	18.106(6)	17.683(6)	17.465(6)	17.256(14)	0.0767	0.099(1)
SDSSp J230351.64+010651.0	17.816(12)	18.176(6)	17.948(7)	17.727(7)	17.462(17)	0.0767	0.085(1)
SDSSp J230351.64+010651.0	17.828(11)	18.267(7)	18.007(7)	17.754(7)	17.561(14)	0.0767	0.090(2)
SDSSp J230351.64+010651.0	17.847(12)	18.151(6)	17.596(6)	17.425(6)	17.230(14)	0.0767	0.137(3)
SDSSp J230351.64+010651.0	17.856(12)	18.154(6)	17.869(6)	17.746(7)	17.412(15)	0.0767	0.074(1)
SDSSp J230351.64+010651.0	17.886(13)	18.018(6)	17.897(7)	17.791(8)	17.466(16)	0.0767	0.072(1)
SDSSp J230351.64+010651.0	17.935(16)	18.346(10)	17.986(8)	17.748(8)	17.522(18)	0.0767	0.091(2)
SDSSp J230351.64+010651.0	18.000(13)	18.167(6)	17.888(6)	17.755(7)	17.323(16)	0.0767	0.077(2)
SDSSp J230351.64+010651.0	18.068(16)	18.300(7)	17.872(7)	17.753(8)	17.506(19)	0.0767	0.098(3)
SDSSp J230351.64+010651.0	18.250(16)	18.568(8)	18.216(9)	18.027(10)	17.743(24)	0.0767	0.087(2)
SDSSp J230351.64+010651.0	18.681(19)	19.037(10)	18.784(11)	18.710(16)	18.420(44)	0.0767	0.069(1)
SEKBO J140454.00−102702.14	20.015(45)	19.733(15)	19.859(21)	19.874(33)	19.578(77)	—	0.062(2)
SN 1964O	20.785(78)	21.069(37)	20.967(51)	21.212(104)	20.753(201)	—	0.061(5)
SDSS J013645.81−193949.1 <sup>‡</sup>	20.397(77)	20.288(23)	20.229(29)	20.068(41)	19.644(109)	—	0.082(3)
SDSS J015237.83−172019.3 <sup>‡</sup>	21.272(152)	21.040(47)	21.092(68)	20.928(81)	20.351(188)	—	0.082(5)
SDSS J015237.83−172019.3 <sup>‡</sup>	21.463(152)	21.397(54)	21.443(74)	21.293(92)	21.013(257)	—	0.083(7)
SDSS J032015.29+441059.3 <sup>‡</sup>	18.455(19)	18.768(8)	18.447(9)	18.211(9)	18.050(23)	—	0.082(2)
SDSS J064911.48+102322.1 <sup>‡</sup>	19.610(35)	19.253(11)	18.988(12)	18.903(14)	18.898(41)	—	0.136(6)
SDSS J073208.11+413008.7 <sup>‡</sup>	20.399(56)	20.869(36)	20.712(46)	20.259(46)	20.049(147)	0.0771 <sup>†</sup>	0.128(10)
SDSS J073208.11+413008.7 <sup>‡</sup>	20.427(50)	20.755(28)	20.446(30)	20.230(37)	19.834(97)	0.0771 <sup>†</sup>	0.089(4)
SDSS J073758.55+205544.5 <sup>‡</sup>	20.100(41)	19.984(18)	20.032(23)	20.278(44)	20.001(111)	—	0.053(2)
SDSS J074500.58+332859.6 <sup>‡</sup>	22.517(258)	22.185(82)	22.209(126)	21.719(120)	21.202(262)	—	0.138(18)
SDSS J074500.58+332859.6 <sup>‡</sup>	23.070(395)	22.235(97)	22.289(141)	21.691(126)	21.239(301)	—	0.170(41)
SDSS J074859.55+312512.6 <sup>‡</sup>	17.762(10)	17.768(5)	17.813(6)	17.864(8)	17.927(21)	—	0.067(1)
SDSS J075107.50+300628.4 <sup>‡</sup>	19.468(33)	20.213(27)	19.832(24)	19.804(29)	19.683(91)	—	0.066(2)
SDSS J075107.50+300628.4 <sup>‡</sup>	19.554(31)	19.777(15)	19.817(19)	19.835(23)	19.774(68)	—	0.067(1)
SDSS J075117.00+100016.2 <sup>‡</sup>	17.884(12)	18.488(7)	18.367(8)	18.393(9)	18.334(25)	—	0.066(3)
SDSS J075117.00+100016.2 <sup>‡</sup>	18.168(13)	18.429(7)	18.566(9)	18.541(11)	18.309(24)	—	0.073(1)
SDSS J075713.81+222253.0 <sup>‡</sup>	21.011(77)	21.298(42)	21.199(51)	21.095(66)	21.424(349)	—	0.079(8)
SDSS J080033.86+192416.5 <sup>‡</sup>	19.533(30)	19.732(15)	19.632(17)	19.649(22)	19.477(73)	—	0.065(1)
SDSS J080033.86+192416.5 <sup>‡</sup>	19.918(35)	20.127(17)	20.040(21)	19.960(28)	19.687(69)	—	0.071(2)
SDSS J080033.86+192416.5 <sup>‡</sup>	20.016(45)	20.205(23)	20.093(29)	20.029(33)	19.914(113)	—	0.074(2)
SDSS J080306.99+284855.8 <sup>‡</sup>	20.217(53)	20.475(25)	20.387(33)	20.302(43)	19.956(108)	0.0727 <sup>†</sup>	0.071(2)
SDSS J081030.45+091111.7 <sup>‡</sup>	22.871(410)	22.778(125)	22.841(188)	22.367(195)	22.117(436)	—	0.138(32)
SDSS J081408.42+090759.1 <sup>‡</sup>	20.582(49)	20.692(24)	20.475(27)	19.962(25)	19.415(49)	—	0.131(7)
SDSS J081408.42+090759.1 <sup>‡</sup>	20.679(59)	20.631(24)	20.437(28)	20.041(28)	19.457(59)	—	0.112(6)
SDSS J081408.42+090759.1 <sup>‡</sup>	20.680(64)	20.704(32)	20.405(31)	20.016(35)	19.656(87)	—	0.138(7)
SDSS J081408.42+090759.1 <sup>‡</sup>	20.889(75)	20.755(27)	20.586(38)	20.119(34)	19.468(57)	—	0.122(7)
SDSS J081529.89+171152.5 <sup>‡</sup>	22.117(168)	21.849(56)	21.968(96)	21.844(135)	21.743(465)	—	0.081(10)
SDSS J082648.28−000037.7 <sup>‡</sup>	20.638(54)	21.020(35)	20.835(37)	20.831(51)	20.607(178)	—	0.065(2)
SDSS J082648.28−000037.7 <sup>‡</sup>	21.259(84)	21.172(37)	21.154(55)	21.240(96)	22.300(830)	—	—
SDSS J083132.41+031420.7 <sup>‡</sup>	21.023(92)	21.175(44)	21.352(74)	21.177(96)	20.679(222)	—	0.085(7)
SDSS J083132.41+031420.7 <sup>‡</sup>	21.500(129)	21.518(66)	21.709(100)	21.846(180)	21.271(365)	—	0.070(8)
SDSS J083508.99+600643.9 <sup>‡</sup>	21.830(164)	21.625(60)	21.362(64)	21.262(79)	21.448(335)	—	0.123(20)
SDSS J084011.95+244709.8 <sup>‡</sup>	20.520(49)	20.579(24)	20.810(36)	21.105(61)	20.246(97)	—	0.073(15)
SDSS J084011.95+244709.8 <sup>‡</sup>	20.882(75)	21.007(32)	21.192(48)	21.361(76)	20.844(154)	—	0.066(6)

\*Orbital period estimated with neural network.

†Determined from superhump period.

‡Dwarf novae proposed by Wils et al. (2010).

**Table 3.** List of dwarf novae (continued)

Object	<i>u</i>	<i>g</i>	<i>r</i>	<i>i</i>	<i>z</i>	$P_{\text{orb}}$	$P_{\text{est}}^*$
SDSS J084108.10+102536.2 <sup>‡</sup>	19.818(34)	20.247(18)	20.132(21)	20.015(25)	20.047(95)	—	0.076(4)
SDSS J084108.10+102536.2 <sup>‡</sup>	20.621(93)	21.027(43)	20.808(57)	20.869(78)	21.109(376)	—	0.064(4)
SDSS J084108.10+102536.2 <sup>‡</sup>	20.818(124)	20.822(48)	20.806(80)	20.943(112)	21.158(574)	—	0.060(6)
SDSS J091242.18+620940.1 <sup>‡</sup>	18.729(19)	18.818(8)	18.729(10)	18.442(10)	17.856(21)	—	0.087(2)
SDSS J091741.29+073647.4 <sup>‡</sup>	21.804(142)	21.520(52)	21.396(69)	21.501(117)	21.152(304)	—	0.081(9)
SDSS J091741.29+073647.4 <sup>‡</sup>	21.854(149)	21.435(50)	21.449(83)	21.706(141)	21.096(307)	—	0.074(12)
SDSS J092620.42+034542.3 <sup>‡</sup>	19.455(29)	19.827(15)	19.609(16)	19.619(20)	19.563(64)	—	0.067(1)
SDSS J092620.42+034542.3 <sup>‡</sup>	19.677(31)	19.901(15)	19.809(18)	19.794(25)	19.848(99)	—	0.071(2)
SDSS J093946.03+065209.4 <sup>‡</sup>	22.050(204)	22.484(118)	22.042(128)	22.297(237)	21.212(231)	—	—
SDSS J093946.03+065209.4 <sup>‡</sup>	22.311(377)	22.317(124)	21.974(154)	21.912(263)	21.454(598)	—	0.140(49)
SDSS J100243.11−024635.9 <sup>‡</sup>	20.944(87)	21.240(48)	20.811(46)	20.875(77)	20.393(182)	—	0.088(9)
SDSS J100243.11−024635.9 <sup>‡</sup>	20.995(163)	21.024(65)	20.830(78)	20.784(101)	20.268(206)	—	0.075(5)
SDSS J100243.11−024635.9 <sup>‡</sup>	21.161(132)	21.371(64)	21.515(105)	21.190(106)	20.481(214)	—	0.096(9)
SDSS J100516.61+694136.5 <sup>‡</sup>	19.854(40)	19.423(12)	18.945(11)	18.638(11)	18.278(26)	—	0.357(26)
SDSS J105333.76+285033.6 <sup>‡</sup>	20.212(39)	20.193(17)	19.809(17)	19.631(24)	19.459(67)	—	0.157(8)
SDSS J112003.40+663632.4 <sup>‡</sup>	20.815(113)	20.945(54)	20.843(127)	20.590(73)	20.385(235)	0.0684 <sup>†</sup>	0.105(9)
SDSS J124328.27−055431.0 <sup>‡</sup>	23.194(573)	22.696(147)	22.558(173)	22.290(196)	21.787(505)	—	0.167(62)
SDSS J124602.02−202302.4 <sup>‡</sup>	18.363(19)	18.535(8)	18.406(9)	18.354(11)	18.270(30)	—	0.071(1)
SDSS J124719.03+013842.6 <sup>‡</sup>	20.577(66)	20.777(37)	21.048(57)	21.100(95)	21.100(369)	—	0.069(6)
SDSS J124719.03+013842.6 <sup>‡</sup>	20.616(72)	20.696(32)	20.909(47)	21.058(76)	21.063(318)	—	0.062(4)
SDSS J124719.03+013842.6 <sup>‡</sup>	20.619(53)	20.768(25)	20.920(36)	21.092(51)	20.711(149)	—	0.062(4)
SDSS J132040.96−030016.7 <sup>‡</sup>	26.249(436)	25.605(628)	21.672(106)	21.670(153)	21.130(359)	—	—
SDSS J132715.28+425932.8 <sup>‡</sup>	20.987(71)	20.805(25)	20.511(28)	20.350(33)	20.219(93)	—	0.153(11)
SDSS J141029.09+330706.2 <sup>‡</sup>	22.422(344)	21.738(88)	21.692(124)	21.443(144)	22.387(969)	—	—
SDSS J142953.56+073231.2 <sup>‡</sup>	21.001(90)	21.208(45)	20.809(42)	20.324(36)	19.804(74)	—	0.144(8)
SDSS J142953.56+073231.2 <sup>‡</sup>	21.374(156)	21.150(53)	20.945(58)	20.315(58)	19.773(131)	—	0.158(13)
SDSS J142953.56+073231.2 <sup>‡</sup>	21.390(117)	21.175(39)	20.882(46)	20.437(50)	20.163(143)	—	0.174(19)
SDSS J151109.79+574100.3 <sup>‡</sup>	20.898(68)	21.239(35)	21.176(49)	21.055(66)	20.866(239)	—	0.078(5)
SDSS J151109.79+574100.3 <sup>‡</sup>	21.106(85)	21.514(51)	21.299(65)	20.962(74)	20.877(287)	—	0.113(12)
SDSS J151109.79+574100.3 <sup>‡</sup>	21.239(86)	21.361(39)	21.069(42)	20.894(49)	20.486(153)	—	0.102(7)
SDSS J152124.38+112551.9 <sup>‡</sup>	22.091(158)	21.615(51)	21.683(71)	21.763(130)	21.777(520)	—	0.070(8)
SDSS J153457.24+505616.8 <sup>‡</sup>	21.933(196)	22.023(89)	21.807(113)	21.750(156)	21.187(348)	—	0.086(10)
SDSS J154817.56+153221.2 <sup>‡</sup>	21.565(140)	21.640(50)	21.408(66)	21.137(83)	21.231(341)	—	0.120(13)
SDSS J154817.56+153221.2 <sup>‡</sup>	21.587(127)	21.825(58)	21.744(67)	21.895(114)	21.763(342)	—	0.062(4)
SDSS J154817.56+153221.2 <sup>‡</sup>	22.306(232)	22.304(96)	22.236(123)	21.853(144)	22.903(622)	—	—
SDSS J155030.38−001417.3 <sup>‡</sup>	21.900(141)	22.013(72)	21.606(76)	21.031(63)	20.770(182)	—	0.164(16)
SDSS J155030.38−001417.3 <sup>‡</sup>	21.996(155)	21.857(63)	21.571(82)	20.936(71)	20.444(161)	—	0.158(12)
SDSS J155540.19+364643.1 <sup>‡</sup>	20.466(53)	20.809(27)	20.960(40)	20.766(45)	20.492(127)	—	0.086(4)
SDSS J161027.61+090738.4 <sup>‡</sup>	20.084(48)	20.082(19)	20.061(23)	20.234(36)	20.183(110)	0.0570	0.056(1)
SDSS J161027.61+090738.4 <sup>‡</sup>	20.171(47)	20.103(18)	20.054(22)	20.254(39)	20.001(126)	0.0570	0.056(2)
SDSS J161442.43+080407.9 <sup>‡</sup>	21.098(102)	20.940(43)	20.887(47)	20.700(54)	20.506(161)	—	0.090(6)
SDSS J161442.43+080407.9 <sup>‡</sup>	21.481(139)	21.248(40)	21.419(63)	20.946(52)	21.349(314)	—	0.155(23)
SDSS J162520.29+120308.7 <sup>‡</sup>	18.122(13)	18.527(8)	18.406(8)	18.210(9)	17.719(16)	0.0920 <sup>†</sup>	0.080(2)
SDSS J162520.29+120308.7 <sup>‡</sup>	18.416(16)	18.481(7)	18.407(8)	18.245(9)	17.684(15)	0.0920 <sup>†</sup>	0.073(1)
SDSS J162558.18+364200.6 <sup>‡</sup>	21.501(101)	21.684(48)	21.595(69)	21.548(99)	21.901(415)	—	0.077(9)
SDSS J164705.07+193335.0 <sup>‡</sup>	21.936(148)	21.980(69)	21.845(87)	21.704(114)	21.674(400)	—	0.083(9)
SDSS J164705.07+193335.0 <sup>‡</sup>	22.318(200)	21.977(62)	21.856(81)	21.862(137)	21.293(331)	—	0.079(10)
SDSS J170145.85+332339.5 <sup>‡</sup>	21.208(96)	21.582(54)	21.392(67)	21.320(93)	21.729(495)	—	0.077(9)
SDSS J170145.85+332339.5 <sup>‡</sup>	21.697(120)	21.818(66)	21.981(123)	22.198(226)	21.539(446)	—	0.072(11)
SDSS J170810.31+445450.7 <sup>‡</sup>	20.569(55)	20.734(25)	20.736(30)	20.933(45)	20.626(149)	—	0.057(3)
SDSS J170810.31+445450.7 <sup>‡</sup>	20.643(59)	20.784(23)	20.740(29)	20.911(48)	20.680(158)	—	0.058(2)
SDSS J170810.31+445450.7 <sup>‡</sup>	20.813(74)	20.832(29)	20.803(41)	20.847(61)	20.851(276)	—	0.066(3)
SDSS J171202.95+275411.0 <sup>‡</sup>	21.025(74)	21.417(40)	20.930(39)	20.673(42)	20.289(128)	—	0.108(6)
SDSS J171202.95+275411.0 <sup>‡</sup>	21.277(135)	21.417(59)	20.966(54)	20.522(61)	20.603(210)	—	0.178(27)
SDSS J174839.77+502420.3 <sup>‡</sup>	23.480(827)	22.309(131)	22.946(305)	23.805(843)	24.157(482)	—	—
SDSS J191616.53+385810.6 <sup>‡</sup>	17.947(13)	17.664(5)	17.486(5)	17.472(7)	17.413(14)	—	0.073(1)

\*Orbital period estimated with neural network.

†Determined from superhump period.

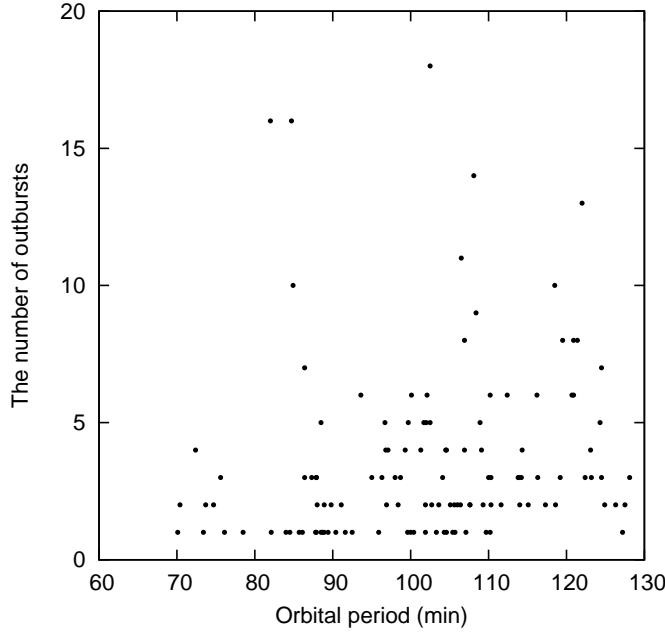
**Table 3.** List of dwarf novae (continued)

Object	$u$	$g$	$r$	$i$	$z$	$P_{\text{orb}}$	$P_{\text{est}}^*$
SDSS J205931.86−070516.6 <sup>‡</sup>	20.077(46)	20.198(22)	20.178(26)	19.973(30)	20.134(118)	—	0.095(8)
SDSS J205931.86−070516.6 <sup>‡</sup>	20.854(100)	20.755(30)	21.026(50)	21.237(87)	21.556(458)	—	0.056(7)
SDSS J223854.51+053606.8 <sup>‡</sup>	21.441(159)	21.432(57)	21.339(92)	21.314(136)	20.988(336)	—	0.070(5)
SDSS J223854.51+053606.8 <sup>‡</sup>	21.536(141)	21.396(55)	21.243(65)	21.299(96)	20.603(220)	—	0.068(5)
SDSS J223854.51+053606.8 <sup>‡</sup>	21.553(118)	21.548(47)	21.520(56)	21.531(84)	20.847(181)	—	0.066(4)

\*Orbital period estimated with neural network.

†Determined from superhump period.

‡Dwarf novae proposed by Wils et al. (2010).

**Fig. 5.** The number of outbursts of the CRTS-SDSS sample. The abscissa denotes the orbital period in min.

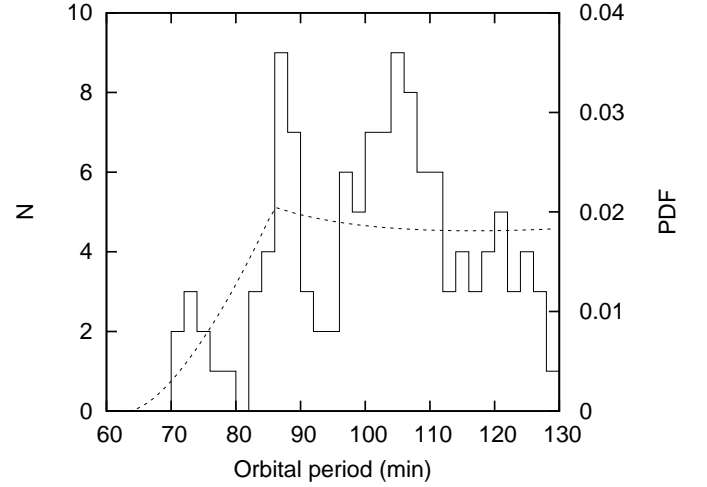
CRTS-SDSS sample has a different  $P_{\text{orb}}$  distribution from the samples in Uemura et al. (2010). Their  $P_{\text{orb}}$  distribution apparently has a peak at  $P_{\text{orb}} \sim 86$  min. In the CRTS-SDSS sample, the distribution is rather flat in a region of  $P_{\text{orb}} \gtrsim 86$  min. The relatively flat distribution may be partly due to a smearing effect of the  $P_{\text{orb}}$  distribution resulting from errors in estimating  $P_{\text{est}}$ . As shown in table 5, some of  $P_{\text{est}}$  have large uncertainties, which imply that the real distribution was significantly smeared out.

We estimated the intrinsic  $P_{\text{orb}}$  distribution using the CRTS-SDSS sample. The intrinsic  $P_{\text{orb}}$  distribution is described in the model is as follows:

$$I(p) = \begin{cases} p^{-\alpha} e^{-\alpha/p/A_I} & (p \geq 1) \\ 0 & (p < 1) \end{cases} \quad (3)$$

$$p = P_{\text{orb}} - P_{\text{min}} + 1 \text{ (min)}, \quad (4)$$

where  $\alpha$  is a parameter for the profile of the  $P_{\text{orb}}$  distribution,  $P_{\text{min}}$  the minimum  $P_{\text{orb}}$ , and  $A_I$  the normal-

**Fig. 6.** Distribution of  $P_{\text{est}}$  of the CRTS-SDSS sample. The dashed line indicates the probability density function (PDF) of the best model derived from our analysis (for details see the text).

ization factor. A larger  $\alpha$  yields a distribution with a stronger spike near  $P_{\text{min}}$ . The distribution is flat in the case of  $\alpha = 0$ . Using the same model as in Uemura et al. (2010) and adopting the derived  $n = 2.0$  for the dependence of the detection probability on  $P_{\text{orb}}$ , we calculated the posterior probability distribution of  $\alpha$  and  $P_{\text{min}}$  from the CRTS-SDSS sample. The medians and 68.3% confidence intervals were derived from the estimated posterior distribution, which are listed in table 6. The table also includes the results in Uemura et al. (2010). The model for the observed distribution is indicated by the dashed line in figure 6. The intrinsic  $P_{\text{orb}}$  distribution, which is obtained from the parameters, is depicted in figure 7. As can be seen in this figure, a period spike feature appears just above  $P_{\text{min}}$ . It is consistent with the results in Uemura et al. (2010).

On the other hand, the parameter  $\alpha$  is significantly smaller than those in Uemura et al. (2010), as shown in table 6. As a result, the spike feature is less prominent. As mentioned above, the samples used in Uemura et al. (2010) have a peak at  $P_{\text{orb}} \sim 86$  min in their  $P_{\text{orb}}$  distribution. Such a profile tends to give a higher  $\alpha$  in our

**Table 4.** Estimated extinction neural network classification

Object	$g$	$d$ (pc)	type*	$A_V$	$P_{\text{orb}}$	ultrashort <sup>†</sup>	short <sup>‡</sup>	long <sup>§</sup>
RX And	14.082(4)	149	2	0.079	0.2099	–	–	–
BV And	16.366(4)	779	3	0.533	–	0.462(55)	0.316(47)	0.222(100)
FN And	18.719(8)	356	3	0.144	–	0.000(0)	0.983(17)	0.017(17)
IZ And	19.621(13)	1099	3	0.226	–	0.000(0)	0.905(136)	0.095(136)
LL And	20.073(17)	550	1	0.133	0.0551	0.755(126)	0.234(125)	0.011(19)
LL And	20.152(21)	550	1	0.133	0.0551	0.876(199)	0.124(199)	0.001(2)
LT And	19.505(11)	559	5	0.173	–	0.030(16)	0.905(85)	0.065(77)
V402 And	20.390(20)	1100	1	0.220	0.0618 <sup>  </sup>	0.178(107)	0.609(276)	0.214(302)
UU Aql	16.851(5)	175	2	0.212	0.1635	0.000(0)	0.060(28)	0.940(28)
KX Aql	18.381(7)	320	1	0.674	0.0604	0.138(35)	0.862(35)	0.000(0)
V725 Aql	18.914(9)	500	1	0.517	0.0945 <sup>  </sup>	0.001(0)	0.999(0)	0.000(0)
V1047 Aql	18.275(7)	721	6	0.763	–	0.024(10)	0.976(10)	0.001(0)
VY Aqr	16.949(4)	97	1	0.195	0.0631	0.015(1)	0.985(1)	0.000(0)
VZ Aqr	17.605(5)	285	2	0.129	0.1606	0.000(0)	0.000(0)	1.000(0)
VZ Aqr	17.967(6)	285	2	0.129	0.1606	0.000(0)	0.005(2)	0.995(2)
VZ Aqr	17.953(6)	285	2	0.129	0.1606	0.000(0)	0.001(1)	0.999(1)
EG Aqr	19.102(11)	320	1	0.104	0.0763 <sup>  </sup>	0.000(0)	0.998(4)	0.002(4)
BG Ari	20.280(21)	700	1	0.238	0.0822 <sup>  </sup>	0.000(0)	0.831(193)	0.169(193)
V496 Aur	21.452(46)	1106	2	0.192	0.0597 <sup>  </sup>	0.035(98)	0.492(395)	0.473(416)
V496 Aur	21.724(76)	1106	2	0.192	0.0597 <sup>  </sup>	0.022(75)	0.719(398)	0.259(400)
V496 Aur	21.451(45)	1106	2	0.192	0.0597 <sup>  </sup>	0.013(86)	0.761(395)	0.226(391)
V496 Aur	21.820(71)	1106	2	0.192	0.0597 <sup>  </sup>	0.011(45)	0.858(305)	0.131(300)
TT Boo	19.322(11)	400	1	0.046	0.0755 <sup>  </sup>	0.006(2)	0.988(13)	0.005(13)
UZ Boo	19.704(14)	240	1	0.085	0.0604 <sup>  </sup>	0.862(86)	0.138(86)	0.000(2)
V391 Cam	16.346(5)	250	1	0.352	0.0562	0.794(20)	0.206(20)	0.000(0)
AM Cas	15.281(3)	231	2	0.910	0.1652	0.451(18)	0.514(13)	0.035(7)
KZ Cas	18.719(10)	745	3	0.946	–	0.000(0)	0.188(64)	0.812(64)
KZ Cas	19.153(11)	745	3	0.946	–	0.000(0)	0.033(38)	0.967(38)
LM Cas	19.472(13)	790	3	0.963	–	0.735(104)	0.265(104)	0.000(0)
V630 Cas	17.099(4)	1987	2	0.722	2.5639	0.000(0)	0.000(0)	1.000(0)
WW Cet	14.678(3)	89	2	0.058	0.1758	0.000(0)	0.001(0)	0.999(0)
EN Cet	20.168(25)	800	1	0.072	0.0593	0.373(230)	0.464(273)	0.163(280)
EN Cet	20.575(30)	800	1	0.072	0.0593	0.077(77)	0.920(77)	0.002(11)
EN Cet	20.690(34)	800	1	0.072	0.0593	0.044(64)	0.812(283)	0.143(283)
EN Cet	20.689(28)	800	1	0.072	0.0593	0.093(122)	0.901(131)	0.006(27)
EN Cet	20.698(29)	800	1	0.072	0.0593	0.070(72)	0.920(89)	0.010(60)
EN Cet	20.672(29)	800	1	0.072	0.0593	0.396(243)	0.573(244)	0.031(122)
EN Cet	20.684(28)	800	1	0.072	0.0593	0.290(226)	0.584(276)	0.126(270)
EN Cet	20.623(31)	800	1	0.072	0.0593	0.360(222)	0.573(239)	0.067(211)
EN Cet	20.775(31)	800	1	0.072	0.0593	0.240(199)	0.752(205)	0.008(27)
EN Cet	20.627(31)	800	1	0.072	0.0593	0.440(229)	0.523(239)	0.038(71)
EN Cet	20.733(27)	800	1	0.072	0.0593	0.297(202)	0.641(239)	0.061(122)
EN Cet	20.735(26)	800	1	0.072	0.0593	0.430(225)	0.511(238)	0.059(185)
EN Cet	20.813(28)	800	1	0.072	0.0593	0.461(252)	0.495(269)	0.044(125)
FI Cet	21.554(55)	550	3	0.086	–	0.361(367)	0.472(362)	0.167(307)
GS Cet	19.943(19)	826	5	0.079	–	0.877(199)	0.123(199)	0.000(0)
GS Cet	20.118(21)	826	5	0.079	–	0.740(333)	0.258(334)	0.002(10)
GS Cet	20.319(26)	826	5	0.079	–	0.493(404)	0.506(404)	0.001(3)
GS Cet	20.287(24)	826	5	0.079	–	0.838(149)	0.151(124)	0.011(100)

\*Method of distance estimation. 1: from Patterson (2011) and other references (see text),

2: determined from  $P_{\text{orb}}$  and maximum magnitude, 3: from estimated  $P_{\text{orb}}$  and maximum magnitude,

4: from  $P_{\text{orb}}$  and minimum magnitude, 5: from estimated  $P_{\text{orb}}$  and minimum magnitude

6: assuming maximum  $M_V = 4.95$ .

<sup>†</sup> $P_{\text{orb}} < 0.06$  (d).

<sup>‡</sup> $0.06 \leq P_{\text{orb}} < 0.10$  (d).

<sup>§</sup> $P_{\text{orb}} \geq 0.10$  (d).

<sup>||</sup>Determined from superhump period.

#Dwarf novae proposed by Wils et al. (2010).



**Table 4.** Estimated extinction and neural network classification (continued)

Object	$g$	$d$ (pc)	type*	$A_V$	$P_{\text{orb}}$	ultrashort <sup>†</sup>	short <sup>‡</sup>	long <sup>§</sup>
GS Cet	20.410(21)	826	5	0.079	—	0.184(294)	0.814(297)	0.002(13)
GS Cet	20.471(23)	826	5	0.079	—	0.811(150)	0.189(151)	0.001(2)
GS Cet	20.358(23)	826	5	0.079	—	0.099(227)	0.890(253)	0.011(44)
GS Cet	20.381(19)	826	5	0.079	—	0.861(95)	0.138(96)	0.001(4)
GS Cet	20.446(23)	826	5	0.079	—	0.235(351)	0.765(351)	0.000(0)
GS Cet	20.338(20)	826	5	0.079	—	0.861(181)	0.139(181)	0.000(2)
GS Cet	20.395(23)	826	5	0.079	—	0.772(189)	0.223(189)	0.005(18)
GS Cet	20.427(22)	826	5	0.079	—	0.439(315)	0.540(328)	0.021(60)
GS Cet	20.381(20)	826	5	0.079	—	0.413(355)	0.580(359)	0.007(52)
GS Cet	20.508(26)	826	5	0.079	—	0.304(341)	0.681(353)	0.015(70)
GS Cet	20.455(53)	826	5	0.079	—	0.004(10)	0.996(10)	0.000(0)
GY Cet	18.294(7)	300	1	0.097	0.0566	0.878(28)	0.122(28)	0.000(0)
GY Cet	18.296(7)	300	1	0.097	0.0566	0.809(41)	0.191(41)	0.000(0)
GZ Cet	18.710(9)	160	1	0.088	0.0553	0.000(0)	0.002(3)	0.998(3)
HP Cet	19.858(16)	6575	2	0.070	0.0667	0.469(211)	0.531(211)	0.000(1)
EU CMa	21.069(42)	1343	3	1.039	—	0.000(0)	0.307(332)	0.693(332)
AK Cnc	18.797(8)	360	1	0.096	0.0651	0.011(2)	0.984(5)	0.005(4)
AR Cnc	18.520(7)	1593	2	0.067	0.2146	0.000(0)	0.572(180)	0.428(180)
CC Cnc	15.873(3)	550	1	0.131	0.0735	0.235(24)	0.765(24)	0.000(0)
CC Cnc	16.769(4)	550	1	0.131	0.0735	0.015(3)	0.767(80)	0.218(79)
DE Cnc	18.465(7)	1165	3	0.098	—	0.000(0)	0.010(8)	0.990(8)
DE Cnc	18.458(7)	1165	3	0.098	—	0.000(0)	0.001(1)	0.999(1)
EG Cnc	18.839(9)	330	1	0.138	0.0600	0.956(17)	0.044(17)	0.000(0)
GY Cnc	16.029(4)	379	2	0.118	0.1754	0.000(0)	0.096(34)	0.904(34)
GZ Cnc	14.736(3)	320	1	0.111	0.0882	—	—	—
HH Cnc	19.158(10)	855	3	0.070	—	0.000(0)	0.000(0)	1.000(0)
FU Com	18.847(8)	1490	5	0.070	—	0.000(0)	0.998(1)	0.002(1)
GO Com	17.936(6)	500	1	0.029	0.0615 <sup>  </sup>	0.104(17)	0.894(18)	0.002(3)
GP Com	15.908(4)	75	1	0.044	0.0323	0.968(4)	0.032(4)	0.000(0)
GP Com	15.919(4)	75	1	0.044	0.0323	0.985(1)	0.015(1)	0.000(0)
IM Com	17.721(5)	1009	5	0.112	—	0.000(0)	1.000(0)	0.000(0)
IM Com	17.776(6)	1009	5	0.112	—	0.000(0)	0.999(1)	0.001(1)
IR Com	18.317(7)	250	1	0.125	0.0870	0.000(0)	0.997(1)	0.003(1)
MT Com	19.125(10)	360	1	0.025	0.0829	0.910(33)	0.089(33)	0.002(2)
VW CrB	19.636(16)	600	1	0.116	0.0706 <sup>  </sup>	0.091(49)	0.656(284)	0.253(293)
VW CrB	19.887(15)	600	1	0.116	0.0706 <sup>  </sup>	0.004(2)	0.983(76)	0.013(76)
V516 Cyg	14.416(3)	567	2	0.511	0.1712	—	—	—
V1081 Cyg	17.749(10)	633	6	0.545	—	—	—	—
V1089 Cyg	18.587(8)	1113	3	1.539	—	0.000(0)	0.000(0)	1.000(0)
V1153 Cyg	18.781(10)	1217	6	1.021	—	0.000(0)	0.991(43)	0.009(43)
V1251 Cyg	20.474(28)	330	1	0.477	0.0743	0.001(1)	0.930(212)	0.069(212)
V1363 Cyg	17.861(6)	321	6	0.520	—	0.000(0)	0.000(0)	1.000(0)
V1449 Cyg	19.049(19)	867	6	0.858	—	0.140(304)	0.000(1)	0.860(304)
HO Del	18.892(9)	425	2	0.192	0.0627	0.109(31)	0.891(31)	0.000(0)
AB Dra	15.530(4)	173	2	0.161	0.152	0.007(1)	0.401(89)	0.592(91)
DM Dra	20.296(23)	750	1	0.057	0.0733 <sup>  </sup>	0.003(2)	0.931(105)	0.067(105)
DM Dra	20.325(22)	750	1	0.057	0.0733 <sup>  </sup>	0.044(33)	0.849(224)	0.106(230)
DO Dra	15.557(4)	121	2	0.027	0.1654	0.000(0)	0.001(1)	0.999(1)
AQ Eri	17.411(5)	300	1	0.185	0.0609	0.162(15)	0.835(15)	0.003(2)
BF Eri	14.599(3)	782	2	0.200	0.2709	0.000(0)	0.128(37)	0.872(37)

\*Method of distance estimation. 1: from Patterson (2011) and other references (see text),  
 2: determined from  $P_{\text{orb}}$  and maximum magnitude, 3: from estimated  $P_{\text{orb}}$  and maximum magnitude,  
 4: from  $P_{\text{orb}}$  and minimum magnitude, 5: from estimated  $P_{\text{orb}}$  and minimum magnitude  
 6: assuming maximum  $M_V = 4.95$ .

<sup>†</sup>  $P_{\text{orb}} < 0.06$  (d).

<sup>‡</sup>  $0.06 \leq P_{\text{orb}} < 0.10$  (d).

<sup>§</sup>  $P_{\text{orb}} \geq 0.10$  (d).

<sup>||</sup> Determined from superhump period.

<sup>#</sup> Dwarf novae proposed by Wils et al. (2010).

**Table 4.** Estimated extinction and neural network classification (continued)

Object	$g$	$d$ (pc)	type*	$A_V$	$P_{\text{orb}}$	ultrashort <sup>†</sup>	short <sup>‡</sup>	long <sup>§</sup>
LT Eri	17.748(5)	858	2	0.305	0.1702	0.000(0)	0.011(9)	0.989(9)
HQ Gem	20.386(21)	3543	3	1.619	—	0.000(0)	0.000(1)	1.000(1)
IR Gem	15.996(5)	320	1	0.178	0.0684	0.025(3)	0.974(3)	0.001(0)
KZ Gem	18.666(8)	1677	3	0.291	—	0.000(0)	0.998(1)	0.002(1)
AH Her	—	237	2	0.105	0.2581	—	—	—
AH Her	14.975(10)	237	2	0.105	0.2581	0.000(0)	0.317(42)	0.683(42)
V478 Her	17.741(6)	4244	2	0.241	0.6290	0.000(0)	0.016(15)	0.984(15)
V544 Her	19.744(15)	1176	3	0.207	—	0.000(0)	0.000(0)	1.000(0)
V589 Her	18.305(7)	500	1	0.174	—	0.011(2)	0.973(17)	0.016(16)
V589 Her	18.631(8)	500	1	0.174	—	0.000(0)	0.575(97)	0.425(97)
V589 Her	19.105(10)	500	1	0.174	—	0.002(1)	0.997(2)	0.001(1)
V592 Her	21.459(53)	390	1	0.127	0.0558 <sup>  </sup>	0.183(241)	0.695(324)	0.122(277)
V592 Her	21.421(36)	390	1	0.127	0.0558 <sup>  </sup>	0.608(318)	0.338(311)	0.054(166)
V592 Her	21.301(35)	390	1	0.127	0.0558 <sup>  </sup>	0.582(318)	0.393(318)	0.025(98)
V610 Her	21.222(39)	1881	3	0.170	—	0.000(0)	0.080(194)	0.920(194)
V610 Her	21.421(57)	1881	3	0.170	—	0.001(1)	0.244(335)	0.755(336)
V610 Her	21.582(79)	1881	3	0.170	—	0.000(0)	0.316(403)	0.684(403)
V611 Her	20.584(22)	1017	3	0.191	—	0.005(5)	0.995(6)	0.000(2)
V611 Her	20.659(25)	1017	3	0.191	—	0.034(53)	0.964(56)	0.001(10)
V660 Her	19.696(15)	700	1	0.340	0.0782 <sup>  </sup>	0.006(2)	0.990(14)	0.004(13)
V844 Her	17.193(5)	310	1	0.027	0.0546	0.057(7)	0.853(57)	0.089(56)
V844 Her	17.742(5)	310	1	0.027	0.0546	0.295(43)	0.701(46)	0.004(5)
V849 Her	15.002(3)	776	3	0.240	—	0.981(2)	0.017(1)	0.002(0)
V849 Her	15.210(4)	776	3	0.240	—	0.967(2)	0.031(1)	0.002(1)
CT Hya	18.733(9)	650	1	0.106	0.0646 <sup>  </sup>	0.050(17)	0.846(110)	0.104(107)
CT Hya	18.774(8)	650	1	0.106	0.0646 <sup>  </sup>	0.171(64)	0.827(67)	0.002(6)
X Leo	15.832(3)	197	2	0.061	0.1644	0.000(0)	0.088(24)	0.912(24)
X Leo	16.337(3)	197	2	0.061	0.1644	0.000(0)	0.028(7)	0.972(7)
RZ Leo	18.716(9)	250	1	0.078	0.0760	0.000(0)	0.989(7)	0.011(7)
DO Leo	17.970(6)	2313	2	0.094	0.2345	0.000(0)	0.000(0)	1.000(0)
HM Leo	18.320(7)	467	2	0.140	0.1868	0.000(0)	0.000(0)	1.000(0)
SS LMi	21.556(107)	1400	1	0.062	0.0566	0.051(197)	0.019(111)	0.929(232)
SS LMi	22.150(96)	1400	1	0.062	0.0566	0.137(285)	0.616(442)	0.247(418)
SX LMi	16.740(4)	400	1	0.102	0.0672	0.043(5)	0.956(5)	0.001(0)
CW Mon	15.913(4)	243	2	0.493	0.1766	0.000(0)	0.034(4)	0.966(4)
V982 Oph	20.251(20)	1530	3	0.489	—	0.000(0)	0.001(3)	0.999(3)
V1032 Oph	17.647(5)	926	2	0.925	0.0811	0.429(25)	0.514(23)	0.057(23)
V2335 Oph	22.507(124)	995	3	0.520	—	0.000(0)	0.017(84)	0.983(84)
BI Ori	16.290(4)	512	2	0.275	0.1915	0.080(8)	0.678(51)	0.242(57)
BI Ori	16.596(3)	512	2	0.275	0.1915	0.024(2)	0.690(73)	0.287(75)
BI Ori	16.705(4)	512	2	0.275	0.1915	0.001(0)	0.380(58)	0.619(58)
BI Ori	16.689(4)	512	2	0.275	0.1915	0.013(2)	0.600(73)	0.387(75)
BI Ori	16.725(4)	512	2	0.275	0.1915	0.024(4)	0.484(77)	0.492(80)
BI Ori	17.098(4)	512	2	0.275	0.1915	0.000(0)	0.000(0)	1.000(0)
GR Ori	22.405(144)	187	6	0.197	—	0.000(0)	0.144(305)	0.856(305)
GR Ori	22.358(136)	187	6	0.197	—	0.000(0)	0.077(240)	0.923(240)
HX Peg	—	486	2	0.151	0.2008	—	—	—
IP Peg	15.287(4)	286	2	0.108	0.1582	0.000(0)	0.000(0)	1.000(0)
V367 Peg	17.348(5)	1560	2	0.250	0.1619	0.008(4)	0.186(109)	0.805(114)
V369 Peg	18.762(10)	1180	2	0.310	0.0827 <sup>  </sup>	0.000(0)	0.738(114)	0.262(114)

\*Method of distance estimation. 1: from Patterson (2011) and other references (see text),

2: determined from  $P_{\text{orb}}$  and maximum magnitude, 3: from estimated  $P_{\text{orb}}$  and maximum magnitude,4: from  $P_{\text{orb}}$  and minimum magnitude, 5: from estimated  $P_{\text{orb}}$  and minimum magnitude6: assuming maximum  $M_V = 4.95$ .<sup>†</sup> $P_{\text{orb}} < 0.06$  (d).<sup>‡</sup> $0.06 \leq P_{\text{orb}} < 0.10$  (d).<sup>§</sup> $P_{\text{orb}} \geq 0.10$  (d).<sup>||</sup>Determined from superhump period.<sup>#</sup>Dwarf novae proposed by Wils et al. (2010).

**Table 4.** Estimated extinction and neural network classification (continued)

Object	$g$	$d$ (pc)	type*	$A_V$	$P_{\text{orb}}$	ultrashort <sup>†</sup>	short <sup>‡</sup>	long <sup>§</sup>
V405 Peg	16.100(3)	1251	2	0.637	0.1776	0.000(0)	0.042(13)	0.958(13)
V405 Peg	16.792(5)	1251	2	0.637	0.1776	–	–	–
FO Per	16.859(4)	271	2	0.119	0.1719	0.000(0)	0.198(59)	0.802(59)
GK Per	–	455	1	0.645	1.9968	–	–	–
KT Per	15.316(3)	207	2	0.343	0.1627	0.000(0)	0.000(0)	1.000(0)
QY Per	20.313(21)	550	1	0.382	0.0760 <sup>  </sup>	0.014(11)	0.705(308)	0.282(310)
V336 Per	19.703(15)	1286	3	0.555	–	0.000(0)	0.000(0)	1.000(0)
V336 Per	20.021(15)	1286	3	0.555	–	0.000(0)	0.000(0)	1.000(0)
V336 Per	19.996(18)	1286	3	0.555	–	0.000(0)	0.000(0)	1.000(0)
V372 Per	21.629(53)	1336	3	0.365	–	0.000(0)	0.006(34)	0.994(34)
TY Psc	17.167(5)	240	1	0.151	0.0683	0.020(5)	0.979(6)	0.001(1)
TY Psc	17.078(4)	240	1	0.151	0.0683	0.114(15)	0.886(16)	0.001(1)
XY Psc	20.943(38)	347	3	0.087	–	0.225(229)	0.515(344)	0.259(389)
XY Psc	21.130(33)	347	3	0.087	–	0.304(230)	0.556(270)	0.140(244)
XY Psc	21.136(35)	347	3	0.087	–	0.044(68)	0.807(312)	0.149(316)
AS Psc	22.015(113)	1910	6	0.145	–	0.300(428)	0.258(407)	0.442(463)
AY Psc	16.590(4)	1449	2	0.192	0.2173	0.000(0)	0.000(0)	1.000(0)
EI Psc	16.331(4)	230	1	0.216	0.0446	0.000(0)	0.161(66)	0.839(66)
GV Psc	20.409(21)	1142	2	0.135	0.0904 <sup>  </sup>	0.001(0)	0.819(272)	0.180(272)
GV Psc	20.508(27)	1142	2	0.135	0.0904 <sup>  </sup>	0.000(0)	0.883(111)	0.117(111)
X Ser	17.298(5)	3122	2	0.600	1.478	0.004(2)	0.198(59)	0.798(61)
RY Ser	16.091(3)	719	2	1.192	0.3009	0.000(0)	0.001(0)	0.999(0)
RY Ser	16.598(4)	719	2	1.192	0.3009	0.000(0)	0.000(0)	1.000(0)
QW Ser	17.805(6)	380	1	0.107	0.0745	0.028(4)	0.971(4)	0.001(1)
QZ Ser	16.275(3)	380	1	0.157	0.0832	0.000(0)	0.399(60)	0.601(60)
QZ Ser	16.291(4)	380	1	0.157	0.0832	0.000(0)	0.372(60)	0.628(60)
QZ Ser	16.302(4)	380	1	0.157	0.0832	0.000(0)	0.406(57)	0.594(57)
QZ Ser	16.304(4)	380	1	0.157	0.0832	0.000(0)	0.356(75)	0.644(75)
V386 Ser	19.049(10)	420	1	0.368	0.0559	0.989(5)	0.011(5)	0.000(0)
V386 Ser	19.012(10)	420	1	0.368	0.0559	0.928(26)	0.072(26)	0.000(0)
V386 Ser	19.024(12)	420	1	0.368	0.0559	0.959(21)	0.039(20)	0.002(2)
VZ Sex	16.762(4)	396	2	0.134	0.1487	0.000(0)	0.000(0)	1.000(0)
TX Tri	17.490(5)	2105	3	0.171	–	0.000(0)	0.000(0)	1.000(0)
UW Tri	22.370(107)	800	1	0.303	0.0533	0.101(254)	0.754(376)	0.146(322)
UZ Tri	19.525(13)	1312	3	0.204	–	0.000(0)	0.971(65)	0.029(65)
SW UMa	16.866(4)	164	1	0.080	0.0568	0.557(26)	0.443(26)	0.000(0)
SW UMa	16.862(4)	164	1	0.080	0.0568	0.394(33)	0.606(34)	0.000(0)
BC UMa	18.514(7)	260	1	0.073	0.0626	0.212(35)	0.787(35)	0.000(1)
BZ UMa	15.877(3)	228	1	0.122	0.0680	0.029(2)	0.971(2)	0.000(0)
BZ UMa	16.371(3)	228	1	0.122	0.0680	0.002(1)	0.998(1)	0.000(0)
BZ UMa	16.468(4)	228	1	0.122	0.0680	0.296(47)	0.704(47)	0.000(0)
CY UMa	17.768(5)	300	1	0.042	0.0696	0.008(1)	0.811(39)	0.181(40)
DI UMa	17.912(6)	800	1	0.050	0.0546	0.334(35)	0.587(26)	0.079(21)
DV UMa	19.372(11)	380	1	0.029	0.0859	0.000(0)	0.988(6)	0.012(6)
EL UMa	20.274(19)	539	2	0.053	0.0594	0.964(37)	0.036(37)	0.000(0)
ER UMa	15.415(3)	350	1	0.032	0.0637	0.069(13)	0.749(38)	0.182(33)
IY UMa	17.537(5)	170	1	0.024	0.0739	0.223(38)	0.765(39)	0.011(3)
IY UMa	17.561(5)	170	1	0.024	0.0739	0.061(8)	0.931(8)	0.007(2)
IY UMa	17.637(5)	170	1	0.024	0.0739	0.034(5)	0.946(6)	0.020(6)
KS UMa	17.354(4)	360	1	0.023	0.0680	0.039(6)	0.960(7)	0.001(0)

\*Method of distance estimation. 1: from Patterson (2011) and other references (see text),  
 2: determined from  $P_{\text{orb}}$  and maximum magnitude, 3: from estimated  $P_{\text{orb}}$  and maximum magnitude,  
 4: from  $P_{\text{orb}}$  and minimum magnitude, 5: from estimated  $P_{\text{orb}}$  and minimum magnitude  
 6: assuming maximum  $M_V = 4.95$ .

<sup>†</sup>  $P_{\text{orb}} < 0.06$  (d).

<sup>‡</sup>  $0.06 \leq P_{\text{orb}} < 0.10$  (d).

<sup>§</sup>  $P_{\text{orb}} \geq 0.10$  (d).

<sup>||</sup> Determined from superhump period.

<sup>#</sup> Dwarf novae proposed by Wils et al. (2010).

**Table 4.** Estimated extinction and neural network classification (continued)

Object	$g$	$d$ (pc)	type*	$A_V$	$P_{\text{orb}}$	ultrashort <sup>†</sup>	short <sup>‡</sup>	long <sup>§</sup>
KS UMa	17.418(5)	360	1	0.023	0.0680	0.008(3)	0.990(3)	0.002(1)
HV Vir	19.181(11)	300	1	0.103	0.0571	0.802(62)	0.196(62)	0.002(3)
OU Vir	18.564(7)	550	1	0.124	0.0727	0.344(40)	0.622(46)	0.034(21)
QZ Vir	14.864(3)	101	1	0.042	0.0588	0.147(7)	0.842(10)	0.011(5)
VW Vul	15.772(3)	430	2	0.395	0.1687	0.001(0)	0.197(23)	0.802(23)
1502+09	18.995(9)	426	5	0.104	—	0.038(16)	0.962(16)	0.000(0)
1502+09	19.111(10)	426	5	0.104	—	0.031(15)	0.969(15)	0.000(0)
1H1025+220	17.402(5)	1579	3	0.081	—	0.010(3)	0.195(86)	0.795(89)
1RXS J003828.7+250920	18.741(8)	755	3	0.109	—	0.001(0)	0.998(2)	0.002(2)
1RXS J003828.7+250920	18.849(8)	755	3	0.109	—	0.000(0)	0.999(1)	0.001(1)
1RXS J012750.5+380830	17.177(4)	181	5	0.093	—	0.609(30)	0.390(30)	0.000(0)
1RXS J171456.2+585130	15.021(3)	612	4	0.094	0.8380	—	—	—
2QZ J112555.7–001639	19.601(18)	514	5	0.092	—	0.804(122)	0.196(122)	0.000(0)
2QZ J112555.7–001639	19.555(16)	514	5	0.092	—	0.715(122)	0.284(122)	0.000(1)
2QZ J112555.7–001639	19.511(13)	514	5	0.092	—	—	—	—
2QZ J121005.3–025543	20.866(32)	941	5	0.088	—	0.920(215)	0.027(90)	0.053(202)
2QZ J130441.7+010330	20.187(19)	704	5	0.078	—	0.281(150)	0.718(150)	0.001(4)
2QZ J130441.7+010330	20.690(27)	704	5	0.078	—	0.341(241)	0.643(240)	0.016(43)
2QZ J142701.6–012310	19.985(17)	833	3	0.139	—	0.657(233)	0.343(234)	0.000(1)
ASAS J224349+0809.5	19.549(14)	370	1	0.306	0.0678 <sup>  </sup>	0.012(6)	0.988(6)	0.000(0)
ASAS J224349+0809.5	19.707(15)	370	1	0.306	0.0678 <sup>  </sup>	0.025(9)	0.975(9)	0.000(0)
FSV J1722+2723	19.950(16)	900	5	0.135	—	0.014(9)	0.984(9)	0.002(1)
FSV J1722+2723	20.664(32)	900	5	0.135	—	0.007(6)	0.991(7)	0.002(4)
FSV J1722+2723	20.599(23)	900	5	0.135	—	0.067(50)	0.922(49)	0.011(16)
FSV J1722+2723	20.902(28)	900	5	0.135	—	0.004(3)	0.995(4)	0.001(1)
GD 552	16.398(4)	105	1	0.248	0.0713	0.246(94)	0.754(94)	0.000(0)
GSC 847.1021	15.138(3)	446	3	0.108	—	0.000(0)	0.567(34)	0.433(34)
GUVV J090904.4+091714.4	21.447(57)	1971	3	0.320	—	0.001(1)	0.939(146)	0.061(146)
GUVV J090904.4+091714.4	22.360(91)	1971	3	0.320	—	0.000(0)	0.723(367)	0.277(367)
GUVV J090904.4+091714.4	22.467(110)	1971	3	0.320	—	0.000(0)	0.421(412)	0.579(412)
HS 1016+3412	18.391(7)	864	2	0.064	0.0794	0.014(2)	0.985(2)	0.001(0)
HS 1055+0939	15.876(3)	833	2	0.090	0.3763	0.000(0)	0.029(16)	0.971(16)
HS 1340+1524	17.316(5)	590	2	0.091	0.0644	0.195(20)	0.797(19)	0.008(3)
HS 1340+1524	17.960(6)	590	2	0.091	0.0644	0.000(0)	0.941(33)	0.059(33)
HS 2205+0201	17.224(5)	1043	2	0.141	0.208	0.000(0)	0.035(16)	0.965(16)
HS 2219+1824	17.524(5)	260	1	0.131	0.0599	0.118(16)	0.881(16)	0.000(0)
HS 2219+1824	17.555(5)	260	1	0.131	0.0599	0.144(17)	0.855(17)	0.000(0)
MASTER J013241.20+343809.1	21.483(79)	3511	6	0.123	—	0.053(184)	0.390(467)	0.557(488)
MASTER J071948.9+405332	21.831(97)	1852	3	0.207	—	0.042(146)	0.722(393)	0.236(390)
MASTER J071948.9+405332	21.739(47)	1852	3	0.207	—	0.204(284)	0.399(332)	0.397(404)
NSV 02026	17.549(5)	545	3	0.829	—	0.095(12)	0.866(14)	0.039(8)
NSV 04394	21.853(102)	501	6	0.051	—	0.375(458)	0.140(306)	0.485(468)
NSV 04838	18.617(8)	1000	1	0.048	0.0679 <sup>  </sup>	0.049(11)	0.932(11)	0.019(11)
NSV 04838	18.851(9)	1000	1	0.048	0.0679 <sup>  </sup>	0.052(13)	0.911(15)	0.037(14)
NSV 05031	19.232(11)	667	3	0.188	—	0.002(1)	0.998(1)	0.000(0)
NSV 05285	19.623(15)	659	2	0.088	0.0847 <sup>  </sup>	0.007(4)	0.993(4)	0.001(1)
NSV 14652	17.918(6)	1100	1	0.659	0.0788 <sup>  </sup>	0.144(18)	0.853(20)	0.004(2)
NSV 14652	18.545(7)	1100	1	0.659	0.0788 <sup>  </sup>	0.046(9)	0.950(8)	0.004(2)
NSV 14681	20.179(18)	491	3	0.454	—	0.003(1)	0.868(203)	0.129(202)
NSV 18230	20.141(22)	1224	3	0.042	—	0.035(28)	0.965(28)	0.000(0)

\*Method of distance estimation. 1: from Patterson (2011) and other references (see text),

2: determined from  $P_{\text{orb}}$  and maximum magnitude, 3: from estimated  $P_{\text{orb}}$  and maximum magnitude,4: from  $P_{\text{orb}}$  and minimum magnitude, 5: from estimated  $P_{\text{orb}}$  and minimum magnitude6: assuming maximum  $M_V = 4.95$ .<sup>†</sup> $P_{\text{orb}} < 0.06$  (d).<sup>‡</sup> $0.06 \leq P_{\text{orb}} < 0.10$  (d).<sup>§</sup> $P_{\text{orb}} \geq 0.10$  (d).<sup>||</sup>Determined from superhump period.<sup>#</sup>Dwarf novae proposed by Wils et al. (2010).



**Table 4.** Estimated extinction and neural network classification (continued)

Object	$g$	$d$ (pc)	type*	$A_V$	$P_{\text{orb}}$	ultrashort <sup>†</sup>	short <sup>‡</sup>	long <sup>§</sup>
NSV 18230	20.429(22)	1224	3	0.042	—	0.015(18)	0.963(93)	0.022(94)
NSV 19466	18.290(7)	1748	3	0.097	—	0.123(29)	0.876(30)	0.001(1)
NSV 19466	17.686(6)	1748	3	0.097	—	0.024(4)	0.974(4)	0.003(1)
NSV 20657	21.200(38)	1414	3	0.070	—	0.178(226)	0.667(310)	0.155(288)
OT J000024.7+332543	20.760(31)	1149	3	0.159	—	0.010(12)	0.953(113)	0.037(109)
OT J000130.5+050624	20.967(34)	1106	3	0.113	—	0.000(0)	0.331(393)	0.669(393)
OT J000659.6+192818	21.231(56)	3082	3	0.143	—	0.030(54)	0.940(127)	0.030(116)
OT J000659.6+192818	21.363(53)	3082	3	0.143	—	0.007(35)	0.596(402)	0.397(407)
OT J001158.3+315544	21.869(65)	2413	3	0.172	—	0.031(80)	0.705(346)	0.264(357)
OT J001340.0+332124	21.911(69)	3330	3	0.141	—	0.069(184)	0.226(358)	0.705(419)
OT J001340.0+332124	22.021(95)	3330	3	0.141	—	0.002(16)	0.013(100)	0.985(102)
OT J001538.3+263657	17.894(6)	406	3	0.106	—	0.000(0)	0.916(22)	0.084(22)
OT J001538.3+263657	17.802(6)	406	3	0.106	—	0.020(3)	0.980(3)	0.000(0)
OT J002500.2+073349	19.677(13)	2075	3	0.073	—	0.000(0)	0.164(171)	0.836(171)
OT J002500.2+073349	19.989(22)	2075	3	0.073	—	0.000(0)	0.002(5)	0.998(5)
OT J002500.2+073349	20.218(20)	2075	3	0.073	—	0.000(0)	0.000(0)	1.000(0)
OT J002656.6+284933	21.592(49)	1579	3	0.121	—	0.000(0)	0.174(286)	0.826(286)
OT J003203.6+314510	19.070(10)	926	3	0.187	—	0.001(0)	0.987(14)	0.012(14)
OT J003304.0+380106	20.437(29)	1019	3	0.192	—	0.005(5)	0.972(93)	0.023(92)
OT J003304.0+380106	20.726(31)	1019	3	0.192	—	0.058(74)	0.875(147)	0.068(116)
OT J003500.0+273620	21.118(42)	3797	6	0.153	—	0.000(0)	0.103(261)	0.897(261)
OT J004500.3+222708	20.447(29)	722	3	0.107	—	0.004(5)	0.988(56)	0.008(56)
OT J004518.4+185350	21.049(54)	4970	3	0.168	—	0.000(0)	0.295(423)	0.705(423)
OT J004606.7+052100	21.596(101)	6217	6	0.082	—	0.000(0)	0.281(415)	0.719(415)
OT J004807.2+264621	21.703(100)	3322	3	0.158	—	0.223(329)	0.770(331)	0.007(34)
OT J004807.2+264621	21.571(58)	3322	3	0.158	—	0.071(178)	0.878(251)	0.052(196)
OT J004902.0+074726	21.520(59)	3770	3	0.254	—	0.297(409)	0.567(453)	0.137(331)
OT J005152.9+204017	19.059(11)	2102	3	0.102	—	0.000(0)	0.000(0)	1.000(0)
OT J005824.6+283304	19.217(10)	502	3	0.206	—	0.066(54)	0.934(54)	0.000(0)
OT J010329.0+331822	17.982(6)	2280	3	0.202	—	0.697(64)	0.303(64)	0.000(0)
OT J010411.6−031341	19.516(13)	2806	3	0.097	—	0.000(0)	0.998(1)	0.002(1)
OT J010522.2+110253	20.712(23)	912	3	0.137	—	0.002(3)	0.310(300)	0.688(302)
OT J010522.2+110253	20.850(33)	912	3	0.137	—	0.002(2)	0.925(199)	0.073(200)
OT J010522.2+110253	20.914(34)	912	3	0.137	—	0.005(8)	0.652(388)	0.343(390)
OT J010550.1+190317	19.644(16)	1464	3	0.129	—	0.900(90)	0.100(90)	0.000(0)
OT J011134.5+275922	22.292(169)	7148	6	0.179	—	0.000(0)	0.236(416)	0.764(416)
OT J011516.5+245530	20.933(29)	3220	3	0.236	—	0.056(50)	0.931(64)	0.013(33)
OT J011516.5+245530	21.076(42)	3220	3	0.236	—	0.166(165)	0.823(184)	0.012(99)
OT J011516.5+245530	21.240(35)	3220	3	0.236	—	0.203(204)	0.725(251)	0.072(158)
OT J011543.2+333724	20.558(31)	1455	3	0.222	—	0.002(3)	0.957(184)	0.041(185)
OT J011613.8+092216	19.131(11)	1501	3	0.143	—	0.010(5)	0.494(233)	0.496(236)
OT J012059.6+325545	20.088(18)	355	2	0.142	0.0572	0.230(368)	0.770(368)	0.000(0)
OT J014150.4+090822	20.061(21)	663	2	0.212	0.0610 <sup>  </sup>	0.428(205)	0.562(203)	0.010(17)
OT J020056.0+195727	19.280(15)	4950	3	0.291	—	0.011(25)	0.989(25)	0.000(0)
OT J021110.2+171624	19.405(12)	700	1	0.342	0.0789 <sup>  </sup>	0.020(9)	0.969(48)	0.011(46)
OT J021308.0+184416	20.798(29)	2586	3	0.452	—	0.000(0)	0.000(0)	1.000(0)
OT J023211.7+303636	20.825(28)	2345	3	0.329	—	0.000(0)	0.015(38)	0.985(38)
OT J025615.0+191611	23.895(343)	906	6	2.765	—	0.123(289)	0.873(291)	0.004(29)
OT J032651.7+011513	22.746(198)	2768	6	0.339	—	0.000(0)	0.011(68)	0.989(68)
OT J032651.7+011513	22.251(105)	2768	6	0.339	—	0.000(0)	0.031(140)	0.969(140)

\*Method of distance estimation. 1: from Patterson (2011) and other references (see text),  
 2: determined from  $P_{\text{orb}}$  and maximum magnitude, 3: from estimated  $P_{\text{orb}}$  and maximum magnitude,  
 4: from  $P_{\text{orb}}$  and minimum magnitude, 5: from estimated  $P_{\text{orb}}$  and minimum magnitude  
 6: assuming maximum  $M_V = 4.95$ .

<sup>†</sup> $P_{\text{orb}} < 0.06$  (d).

<sup>‡</sup> $0.06 \leq P_{\text{orb}} < 0.10$  (d).

<sup>§</sup> $P_{\text{orb}} \geq 0.10$  (d).

<sup>||</sup>Determined from superhump period.

<sup>#</sup>Dwarf novae proposed by Wils et al. (2010).

**Table 4.** Estimated extinction and neural network classification (continued)

Object	$g$	$d$ (pc)	type*	$A_V$	$P_{\text{orb}}$	ultrashort <sup>†</sup>	short <sup>‡</sup>	long <sup>§</sup>
OT J032651.7+011513	22.091(122)	2768	6	0.339	–	0.000(0)	0.039(161)	0.961(161)
OT J032651.7+011513	22.407(123)	2768	6	0.339	–	0.000(0)	0.003(23)	0.997(23)
OT J032651.7+011513	22.350(95)	2768	6	0.339	–	0.000(0)	0.025(113)	0.975(113)
OT J032651.7+011513	22.397(126)	2768	6	0.339	–	0.000(0)	0.010(82)	0.990(82)
OT J032651.7+011513	22.495(108)	2768	6	0.339	–	0.000(0)	0.022(109)	0.978(109)
OT J032651.7+011513	22.235(98)	2768	6	0.339	–	0.000(0)	0.030(125)	0.970(125)
OT J032651.7+011513	22.486(98)	2768	6	0.339	–	0.000(0)	0.006(42)	0.994(42)
OT J032651.7+011513	22.335(103)	2768	6	0.339	–	0.000(0)	0.004(17)	0.996(17)
OT J032651.7+011513	22.365(138)	2768	6	0.339	–	0.000(0)	0.036(155)	0.964(155)
OT J032651.7+011513	22.545(113)	2768	6	0.339	–	0.000(0)	0.019(82)	0.981(82)
OT J032651.7+011513	22.419(101)	2768	6	0.339	–	0.000(0)	0.002(15)	0.998(15)
OT J032651.7+011513	22.459(116)	2768	6	0.339	–	0.000(0)	0.008(77)	0.992(77)
OT J032651.7+011513	22.387(128)	2768	6	0.339	–	0.000(0)	0.039(162)	0.961(162)
OT J032651.7+011513	22.664(137)	2768	6	0.339	–	0.000(0)	0.110(278)	0.890(278)
OT J032651.7+011513	22.418(133)	2768	6	0.339	–	0.000(0)	0.027(145)	0.973(145)
OT J032651.7+011513	22.549(122)	2768	6	0.339	–	0.000(0)	0.009(66)	0.991(66)
OT J032651.7+011513	22.517(115)	2768	6	0.339	–	0.000(0)	0.030(117)	0.970(117)
OT J032651.7+011513	22.669(115)	2768	6	0.339	–	0.000(0)	0.007(38)	0.993(38)
OT J032651.7+011513	22.559(115)	2768	6	0.339	–	0.000(0)	0.000(1)	1.000(1)
OT J032651.7+011513	22.471(103)	2768	6	0.339	–	0.000(0)	0.001(3)	0.999(3)
OT J032651.7+011513	22.580(130)	2768	6	0.339	–	0.000(0)	0.007(74)	0.993(74)
OT J032651.7+011513	22.336(100)	2768	6	0.339	–	0.000(0)	0.000(0)	1.000(0)
OT J032651.7+011513	22.270(97)	2768	6	0.339	–	0.000(0)	0.000(0)	1.000(0)
OT J032839.9–010240	20.714(30)	592	3	0.350	–	0.173(168)	0.810(170)	0.016(57)
OT J032839.9–010240	20.759(29)	592	3	0.350	–	0.745(231)	0.255(230)	0.000(1)
OT J032839.9–010240	20.830(28)	592	3	0.350	–	0.620(313)	0.380(313)	0.000(2)
OT J032839.9–010240	20.785(28)	592	3	0.350	–	0.660(207)	0.340(207)	0.000(0)
OT J032839.9–010240	21.074(75)	592	3	0.350	–	0.383(306)	0.584(307)	0.033(162)
OT J032839.9–010240	21.033(48)	592	3	0.350	–	0.448(342)	0.523(334)	0.030(141)
OT J032839.9–010240	21.205(55)	592	3	0.350	–	0.413(283)	0.587(283)	0.000(2)
OT J032839.9–010240	21.134(36)	592	3	0.350	–	0.364(223)	0.636(222)	0.000(2)
OT J032839.9–010240	21.060(34)	592	3	0.350	–	0.266(220)	0.714(221)	0.020(64)
OT J032839.9–010240	21.199(49)	592	3	0.350	–	0.589(290)	0.394(280)	0.017(121)
OT J032839.9–010240	21.111(37)	592	3	0.350	–	0.392(393)	0.602(389)	0.006(23)
OT J032839.9–010240	21.328(46)	592	3	0.350	–	0.441(369)	0.552(363)	0.007(28)
OT J032839.9–010240	21.321(58)	592	3	0.350	–	0.343(300)	0.642(302)	0.015(101)
OT J032839.9–010240	21.220(64)	592	3	0.350	–	0.478(355)	0.443(335)	0.079(225)
OT J032839.9–010240	21.391(42)	592	3	0.350	–	0.430(349)	0.511(330)	0.059(189)
OT J032839.9–010240	21.518(49)	592	3	0.350	–	0.188(295)	0.649(348)	0.163(309)
OT J032839.9–010240	21.563(67)	592	3	0.350	–	0.363(335)	0.600(336)	0.037(141)
OT J032839.9–010240	21.550(67)	592	3	0.350	–	0.188(312)	0.512(388)	0.299(384)
OT J032839.9–010240	21.396(47)	592	3	0.350	–	0.491(450)	0.491(452)	0.018(122)
OT J032839.9–010240	21.305(56)	592	3	0.350	–	0.548(462)	0.053(161)	0.399(474)
OT J032839.9–010240	21.662(83)	592	3	0.350	–	0.020(74)	0.767(370)	0.213(370)
OT J032839.9–010240	21.507(51)	592	3	0.350	–	0.374(398)	0.487(396)	0.138(319)
OT J032839.9–010240	21.634(63)	592	3	0.350	–	0.478(427)	0.445(412)	0.076(230)
OT J032839.9–010240	21.544(64)	592	3	0.350	–	0.294(313)	0.590(335)	0.116(247)
OT J032839.9–010240	21.507(47)	592	3	0.350	–	0.568(283)	0.393(276)	0.039(166)
OT J032839.9–010240	21.598(64)	592	3	0.350	–	0.184(237)	0.610(318)	0.207(322)
OT J032839.9–010240	21.536(65)	592	3	0.350	–	0.764(361)	0.156(288)	0.080(267)

\*Method of distance estimation. 1: from Patterson (2011) and other references (see text),

2: determined from  $P_{\text{orb}}$  and maximum magnitude, 3: from estimated  $P_{\text{orb}}$  and maximum magnitude,4: from  $P_{\text{orb}}$  and minimum magnitude, 5: from estimated  $P_{\text{orb}}$  and minimum magnitude6: assuming maximum  $M_V = 4.95$ .†  $P_{\text{orb}} < 0.06$  (d).‡  $0.06 \leq P_{\text{orb}} < 0.10$  (d).§  $P_{\text{orb}} \geq 0.10$  (d).

|| Determined from superhump period.

# Dwarf novae proposed by Wils et al. (2010).

**Table 4.** Estimated extinction and neural network classification (continued)

Object	$g$	$d$ (pc)	type*	$A_V$	$P_{\text{orb}}$	ultrashort <sup>†</sup>	short <sup>‡</sup>	long <sup>§</sup>
OT J032839.9–010240	21.774(82)	592	3	0.350	–	0.141(292)	0.842(305)	0.016(85)
OT J032839.9–010240	21.525(60)	592	3	0.350	–	0.292(385)	0.683(400)	0.025(145)
OT J032839.9–010240	21.584(55)	592	3	0.350	–	0.035(162)	0.546(468)	0.418(471)
OT J032839.9–010240	21.448(50)	592	3	0.350	–	0.381(398)	0.265(368)	0.354(431)
OT J032902.0+060047	21.625(64)	1789	3	1.130	–	0.001(3)	0.521(449)	0.479(450)
OT J032902.0+060047	21.274(42)	1789	3	1.130	–	0.011(19)	0.553(360)	0.436(365)
OT J032902.0+060047	22.037(72)	1789	3	1.130	–	0.001(3)	0.277(383)	0.723(384)
OT J033104.4+172540	19.862(15)	1272	3	0.438	–	0.000(0)	0.010(14)	0.990(14)
OT J035003.4+370052	18.938(9)	2242	3	1.011	–	0.992(2)	0.008(2)	0.000(0)
OT J035003.4+370052	19.297(11)	2242	3	1.011	–	0.968(14)	0.031(14)	0.001(0)
OT J040659.8+005244	17.844(5)	500	1	1.167	0.0774 <sup>  </sup>	0.045(6)	0.955(6)	0.000(0)
OT J040659.8+005244	18.584(7)	500	1	1.167	0.0774 <sup>  </sup>	0.001(0)	0.999(0)	0.000(0)
OT J040659.8+005244	18.386(7)	500	1	1.167	0.0774 <sup>  </sup>	0.042(6)	0.958(6)	0.000(0)
OT J041636.9+292806	22.252(89)	555	3	1.870	–	0.001(2)	0.962(161)	0.037(161)
OT J041734.6–061357	22.732(243)	4819	6	0.135	–	0.000(0)	1.000(0)	0.000(0)
OT J042142.1+340329	22.427(96)	2102	3	1.031	–	0.001(3)	0.722(363)	0.277(364)
OT J042229.3+161430	21.958(80)	632	3	1.733	–	0.023(51)	0.557(411)	0.421(424)
OT J042434.2+001419	23.098(196)	1470	6	0.314	–	0.188(368)	0.033(164)	0.779(400)
OT J043020.0+095318	20.377(20)	698	3	1.342	–	0.000(0)	0.165(166)	0.834(166)
OT J043517.8+002941	21.124(40)	2659	3	0.240	–	0.424(306)	0.469(306)	0.106(236)
OT J043517.8+002941	21.744(67)	2659	3	0.240	–	0.116(253)	0.743(337)	0.141(285)
OT J043517.8+002941	21.957(65)	2659	3	0.240	–	0.891(284)	0.078(239)	0.031(168)
OT J043546.9+090837	21.827(52)	823	3	0.829	–	0.038(69)	0.894(213)	0.068(205)
OT J043742.1+003048	20.368(23)	2227	3	0.204	–	0.020(17)	0.944(132)	0.036(135)
OT J043829.1+004016	19.218(12)	1838	3	0.203	–	0.021(9)	0.965(11)	0.014(9)
OT J043829.1+004016	19.080(11)	1838	3	0.203	–	0.403(130)	0.584(138)	0.014(28)
OT J043829.1+004016	19.226(11)	1838	3	0.203	–	0.083(47)	0.730(133)	0.187(164)
OT J043829.1+004016	19.540(12)	1838	3	0.203	–	0.000(0)	0.069(168)	0.931(168)
OT J043829.1+004016	19.489(13)	1838	3	0.203	–	0.178(53)	0.814(55)	0.009(6)
OT J043829.1+004016	19.375(12)	1838	3	0.203	–	0.090(39)	0.815(137)	0.095(124)
OT J043829.1+004016	19.306(11)	1838	3	0.203	–	0.145(61)	0.840(88)	0.015(48)
OT J043829.1+004016	19.571(14)	1838	3	0.203	–	0.185(84)	0.807(89)	0.008(11)
OT J043829.1+004016	19.677(14)	1838	3	0.203	–	0.081(35)	0.908(37)	0.011(7)
OT J043829.1+004016	19.618(14)	1838	3	0.203	–	0.003(4)	0.912(133)	0.085(133)
OT J043829.1+004016	19.492(12)	1838	3	0.203	–	0.055(23)	0.909(83)	0.036(75)
OT J043829.1+004016	19.639(13)	1838	3	0.203	–	0.070(37)	0.927(40)	0.003(7)
OT J043829.1+004016	19.714(16)	1838	3	0.203	–	0.007(14)	0.707(310)	0.286(313)
OT J044216.0–002334	21.927(76)	1884	2	0.136	0.0743 <sup>  </sup>	0.001(2)	0.237(389)	0.762(389)
OT J044216.0–002334	22.266(115)	1884	2	0.136	0.0743 <sup>  </sup>	0.012(39)	0.589(424)	0.400(426)
OT J044216.0–002334	21.931(70)	1884	2	0.136	0.0743 <sup>  </sup>	0.092(229)	0.680(406)	0.228(386)
OT J051419.9+011121	19.799(15)	928	3	0.386	–	0.002(3)	0.833(204)	0.165(205)
OT J051419.9+011121	19.844(20)	928	3	0.386	–	0.041(38)	0.951(48)	0.008(21)
OT J051419.9+011121	20.214(21)	928	3	0.386	–	0.008(7)	0.992(7)	0.001(1)
OT J051419.9+011121	20.509(22)	928	3	0.386	–	0.043(36)	0.954(38)	0.003(5)
OT J052033.9–000530	19.566(13)	3950	3	0.440	–	0.000(0)	0.000(1)	1.000(1)
OT J052033.9–000530	20.195(24)	3950	3	0.440	–	0.000(0)	0.000(0)	1.000(0)
OT J052033.9–000530	20.561(24)	3950	3	0.440	–	0.000(0)	0.000(1)	1.000(1)
OT J052033.9–000530	20.473(24)	3950	3	0.440	–	0.000(0)	0.000(0)	1.000(0)
OT J052033.9–000530	20.553(30)	3950	3	0.440	–	0.000(0)	0.000(0)	1.000(0)
OT J052033.9–000530	20.521(21)	3950	3	0.440	–	0.000(0)	0.000(0)	1.000(0)

\*Method of distance estimation. 1: from Patterson (2011) and other references (see text),  
2: determined from  $P_{\text{orb}}$  and maximum magnitude, 3: from estimated  $P_{\text{orb}}$  and maximum magnitude,  
4: from  $P_{\text{orb}}$  and minimum magnitude, 5: from estimated  $P_{\text{orb}}$  and minimum magnitude  
6: assuming maximum  $M_V = 4.95$ .

<sup>†</sup> $P_{\text{orb}} < 0.06$  (d).

<sup>‡</sup> $0.06 \leq P_{\text{orb}} < 0.10$  (d).

<sup>§</sup> $P_{\text{orb}} \geq 0.10$  (d).

<sup>||</sup>Determined from superhump period.

<sup>#</sup>Dwarf novae proposed by Wils et al. (2010).

**Table 4.** Estimated extinction and neural network classification (continued)

Object	$g$	$d$ (pc)	type*	$A_V$	$P_{\text{orb}}$	ultrashort <sup>†</sup>	short <sup>‡</sup>	long <sup>§</sup>
OT J055730.1+001514	22.920(137)	1377	6	2.156	—	0.001(4)	0.652(457)	0.347(457)
OT J055842.8+000626	20.329(20)	714	3	1.721	—	0.000(0)	0.001(3)	0.999(3)
OT J055842.8+000626	19.803(15)	714	3	1.721	—	0.000(0)	0.000(0)	1.000(0)
OT J055842.8+000626	20.434(22)	714	3	1.721	—	0.000(0)	0.001(9)	0.999(9)
OT J055842.8+000626	20.732(29)	714	3	1.721	—	0.000(0)	0.000(0)	1.000(0)
OT J073055.5+425636	22.761(150)	1185	6	0.182	—	0.536(456)	0.251(394)	0.213(374)
OT J073339.3+212201	20.447(27)	2068	6	0.172	—	0.000(0)	0.000(0)	1.000(0)
OT J073559.9+220132	20.198(22)	5754	3	0.152	—	0.728(191)	0.245(183)	0.027(56)
OT J073758.5+205545	19.984(18)	1146	3	0.154	—	0.944(55)	0.056(55)	0.000(0)
OT J073921.2+222454	22.698(136)	3356	3	0.102	—	0.010(86)	0.766(392)	0.225(388)
OT J074222.5+172807	19.942(15)	3532	3	0.127	—	0.136(84)	0.854(103)	0.011(40)
OT J074222.5+172807	19.861(17)	3532	3	0.127	—	0.027(29)	0.184(184)	0.789(205)
OT J074222.5+172807	19.897(18)	3532	3	0.127	—	0.001(3)	0.023(93)	0.976(96)
OT J074222.5+172807	20.227(19)	3532	3	0.127	—	0.014(13)	0.293(314)	0.693(323)
OT J074419.7+325448	20.763(24)	2225	3	0.156	—	0.829(190)	0.170(190)	0.001(1)
OT J074419.7+325448	21.310(46)	2225	3	0.156	—	0.647(423)	0.350(422)	0.003(22)
OT J074419.7+325448	21.441(48)	2225	3	0.156	—	0.900(176)	0.099(175)	0.001(7)
OT J074419.7+325448	21.460(61)	2225	3	0.156	—	0.340(371)	0.637(378)	0.023(98)
OT J074727.6+065050	19.402(13)	350	1	0.059	0.0594 <sup>  </sup>	0.932(86)	0.068(86)	0.000(0)
OT J074820.0+245759	22.523(134)	3509	3	0.180	—	0.245(382)	0.728(389)	0.026(130)
OT J074820.0+245759	22.366(128)	3509	3	0.180	—	0.898(284)	0.009(62)	0.093(271)
OT J074820.0+245759	22.514(114)	3509	3	0.180	—	0.005(25)	0.529(441)	0.466(444)
OT J074928.0+190452	20.794(33)	1929	3	0.168	—	0.008(11)	0.989(19)	0.003(16)
OT J074928.0+190452	21.115(42)	1929	3	0.168	—	0.008(12)	0.992(12)	0.000(0)
OT J074928.0+190452	20.748(31)	1929	3	0.168	—	0.049(71)	0.722(300)	0.229(303)
OT J075332.0+375801	21.289(46)	1958	3	0.162	—	0.056(65)	0.919(141)	0.025(128)
OT J075332.0+375801	21.191(45)	1958	3	0.162	—	0.000(0)	0.581(420)	0.419(420)
OT J075332.0+375801	21.333(46)	1958	3	0.162	—	0.093(168)	0.842(237)	0.065(188)
OT J075414.5+313216	19.651(14)	565	2	0.165	0.0615 <sup>  </sup>	0.697(88)	0.302(89)	0.001(6)
OT J075414.5+313216	20.018(20)	565	2	0.165	0.0615 <sup>  </sup>	0.649(247)	0.312(238)	0.038(85)
OT J075648.0+305805	21.077(46)	1646	3	0.186	—	0.421(338)	0.576(338)	0.003(11)
OT J075648.0+305805	20.859(33)	1646	3	0.186	—	0.313(246)	0.460(282)	0.228(286)
OT J080428.4+363104	22.113(70)	4809	3	0.175	—	0.000(0)	0.223(335)	0.777(335)
OT J080428.4+363104	22.948(175)	4809	3	0.175	—	0.000(0)	0.225(384)	0.775(384)
OT J080714.2+113812	20.537(24)	540	1	0.064	0.0596 <sup>  </sup>	0.998(3)	0.001(3)	0.000(0)
OT J080714.2+113812	20.909(28)	540	1	0.064	0.0596 <sup>  </sup>	0.904(143)	0.091(132)	0.005(43)
OT J080729.7+153442	22.483(95)	2636	3	0.090	—	0.009(45)	0.672(420)	0.319(424)
OT J080729.7+153442	22.367(119)	2636	3	0.090	—	0.000(0)	0.406(440)	0.594(441)
OT J080729.7+153442	22.628(202)	2636	3	0.090	—	0.029(153)	0.605(474)	0.365(471)
OT J080853.7+355053	19.656(13)	1423	3	0.151	—	0.082(42)	0.855(105)	0.064(86)
OT J081030.6+002429	21.358(46)	2596	3	0.112	—	0.000(0)	0.626(347)	0.374(347)
OT J081414.9+080450	21.337(48)	4942	3	0.073	—	0.000(2)	0.250(369)	0.750(369)
OT J081414.9+080450	21.700(57)	4942	3	0.073	—	0.002(3)	0.573(397)	0.425(398)
OT J081414.9+080450	22.232(100)	4942	3	0.073	—	0.000(0)	0.622(415)	0.378(415)
OT J081418.9–005022	18.567(7)	689	2	0.120	0.0741 <sup>  </sup>	0.002(0)	0.924(68)	0.074(68)
OT J081418.9–005022	18.921(9)	689	2	0.120	0.0741 <sup>  </sup>	0.016(6)	0.984(6)	0.000(0)
OT J081418.9–005022	19.116(10)	689	2	0.120	0.0741 <sup>  </sup>	0.009(3)	0.971(29)	0.020(27)
OT J081418.9–005022	19.101(10)	689	2	0.120	0.0741 <sup>  </sup>	0.009(4)	0.990(6)	0.001(2)
OT J081418.9–005022	19.193(11)	689	2	0.120	0.0741 <sup>  </sup>	0.037(12)	0.963(12)	0.000(0)
OT J081712.3+055208	21.387(55)	7044	3	0.082	—	0.000(0)	0.000(1)	1.000(1)

\*Method of distance estimation. 1: from Patterson (2011) and other references (see text),

2: determined from  $P_{\text{orb}}$  and maximum magnitude, 3: from estimated  $P_{\text{orb}}$  and maximum magnitude,4: from  $P_{\text{orb}}$  and minimum magnitude, 5: from estimated  $P_{\text{orb}}$  and minimum magnitude6: assuming maximum  $M_V = 4.95$ .<sup>†</sup> $P_{\text{orb}} < 0.06$  (d).<sup>‡</sup> $0.06 \leq P_{\text{orb}} < 0.10$  (d).<sup>§</sup> $P_{\text{orb}} \geq 0.10$  (d).<sup>||</sup>Determined from superhump period.

#Dwarf novae proposed by Wils et al. (2010).



**Table 4.** Estimated extinction and neural network classification (continued)

Object	$g$	$d$ (pc)	type*	$A_V$	$P_{\text{orb}}$	ultrashort <sup>†</sup>	short <sup>‡</sup>	long <sup>§</sup>
OT J081712.3+055208	21.462(60)	7044	3	0.082	—	0.000(0)	0.287(419)	0.713(419)
OT J081936.1+191540	20.364(24)	4275	3	0.162	—	0.000(0)	0.338(409)	0.662(409)
OT J081936.1+191540	20.479(24)	4275	3	0.162	—	0.000(0)	0.902(236)	0.098(236)
OT J082019.4+474732	21.361(50)	2322	3	0.139	—	0.200(223)	0.763(250)	0.037(152)
OT J082123.7+454135	19.472(12)	2214	3	0.141	—	0.000(0)	0.004(11)	0.996(11)
OT J082123.7+454135	19.923(19)	2214	3	0.141	—	0.000(0)	0.815(115)	0.184(115)
OT J082123.7+454135	19.987(20)	2214	3	0.141	—	0.001(1)	0.952(78)	0.047(78)
OT J082123.7+454135	19.891(18)	2214	3	0.141	—	0.001(1)	0.941(146)	0.058(146)
OT J082123.7+454135	20.090(20)	2214	3	0.141	—	0.001(0)	0.399(282)	0.601(282)
OT J082123.7+454135	20.605(27)	2214	3	0.141	—	0.000(0)	0.637(236)	0.363(236)
OT J082603.7+113821	20.630(26)	874	3	0.117	—	0.017(18)	0.979(27)	0.004(22)
OT J082603.7+113821	20.459(23)	874	3	0.117	—	0.018(19)	0.816(201)	0.166(200)
OT J082603.7+113821	20.687(30)	874	3	0.117	—	0.001(2)	0.538(376)	0.461(376)
OT J082654.7−000733	19.460(13)	1683	3	0.159	—	0.041(38)	0.473(248)	0.485(259)
OT J082654.7−000733	19.523(12)	1683	3	0.159	—	0.754(64)	0.246(64)	0.000(0)
OT J082821.8+105344	22.291(111)	1712	3	0.143	—	0.163(314)	0.651(420)	0.187(368)
OT J082908.4+482639	21.433(63)	1464	6	0.122	—	0.081(239)	0.907(254)	0.012(84)
OT J084041.5+000520	20.590(23)	1088	3	0.127	—	0.825(211)	0.175(211)	0.000(1)
OT J084041.5+000520	20.793(28)	1088	3	0.127	—	0.753(237)	0.247(237)	0.000(0)
OT J084041.5+000520	20.777(29)	1088	3	0.127	—	0.622(279)	0.377(279)	0.002(9)
OT J084127.4+210053	20.498(26)	1232	3	0.125	—	0.002(1)	0.832(290)	0.166(290)
OT J084127.4+210053	20.610(25)	1232	3	0.125	—	0.000(0)	0.728(377)	0.272(377)
OT J084358.1+425037	19.913(16)	1134	3	0.103	—	0.004(3)	0.989(19)	0.006(18)
OT J084413.7−012807	20.349(25)	2569	3	0.112	—	0.198(172)	0.761(190)	0.041(79)
OT J084413.7−012807	20.112(18)	2569	3	0.112	—	0.536(208)	0.373(205)	0.091(176)
OT J084413.7−012807	20.522(26)	2569	3	0.112	—	0.972(78)	0.028(78)	0.000(1)
OT J084555.1+033930	20.592(22)	450	1	0.115	0.0591 <sup>  </sup>	0.959(103)	0.041(103)	0.000(0)
OT J084555.1+033930	20.885(36)	450	1	0.115	0.0591 <sup>  </sup>	0.658(330)	0.342(329)	0.001(4)
OT J084555.1+033930	20.810(52)	450	1	0.115	0.0591 <sup>  </sup>	0.363(411)	0.534(432)	0.102(294)
OT J085113.4+344449	20.108(21)	514	3	0.105	—	0.004(4)	0.899(117)	0.097(116)
OT J085113.4+344449	20.445(21)	514	3	0.105	—	0.000(0)	0.751(201)	0.249(201)
OT J085409.4+201339	20.910(30)	2289	3	0.089	—	0.000(1)	0.886(253)	0.113(253)
OT J085603.8+322109	19.638(13)	1417	3	0.090	—	0.416(161)	0.580(163)	0.004(9)
OT J085822.9−003729	21.710(57)	2889	3	0.112	—	0.003(13)	0.358(431)	0.639(433)
OT J085822.9−003729	22.343(158)	2889	3	0.112	—	0.014(69)	0.389(438)	0.598(449)
OT J085822.9−003729	22.785(211)	2889	3	0.112	—	0.016(115)	0.132(318)	0.851(335)
OT J090016.7+343928	20.467(24)	4784	3	0.090	—	0.000(0)	0.001(4)	0.999(4)
OT J090016.7+343928	20.615(24)	4784	3	0.090	—	0.000(0)	0.035(141)	0.965(141)
OT J090239.7+052501	23.161(177)	1285	2	0.145	0.0565	0.036(151)	0.147(313)	0.818(350)
OT J090516.1+120451	19.796(17)	1428	3	0.062	—	0.070(39)	0.929(39)	0.001(1)
OT J090516.1+120451	19.754(14)	1428	3	0.062	—	0.047(26)	0.923(45)	0.030(32)
OT J090852.2+071640	20.130(19)	2266	3	0.163	—	0.388(202)	0.330(196)	0.282(315)
OT J090852.2+071640	20.987(36)	2266	3	0.163	—	0.019(32)	0.649(364)	0.332(370)
OT J091453.6+113402	20.971(33)	1162	3	0.100	—	0.611(329)	0.357(323)	0.033(132)
OT J091453.6+113402	20.962(39)	1162	3	0.100	—	0.456(340)	0.406(331)	0.137(278)
OT J091534.9+081356	22.802(162)	3219	3	0.136	—	0.075(221)	0.797(352)	0.128(299)
OT J091534.9+081356	23.028(169)	3219	3	0.136	—	0.051(193)	0.144(319)	0.805(382)
OT J091634.6+130358	21.453(61)	4224	3	0.079	—	0.008(26)	0.988(28)	0.004(12)
OT J091634.6+130358	21.894(76)	4224	3	0.079	—	0.063(160)	0.840(286)	0.097(254)
OT J091634.6+130358	21.834(87)	4224	3	0.079	—	0.111(270)	0.779(360)	0.110(283)

\*Method of distance estimation. 1: from Patterson (2011) and other references (see text),

2: determined from  $P_{\text{orb}}$  and maximum magnitude, 3: from estimated  $P_{\text{orb}}$  and maximum magnitude,4: from  $P_{\text{orb}}$  and minimum magnitude, 5: from estimated  $P_{\text{orb}}$  and minimum magnitude6: assuming maximum  $M_V = 4.95$ .<sup>†</sup> $P_{\text{orb}} < 0.06$  (d).<sup>‡</sup> $0.06 \leq P_{\text{orb}} < 0.10$  (d).<sup>§</sup> $P_{\text{orb}} \geq 0.10$  (d).<sup>||</sup>Determined from superhump period.<sup>#</sup>Dwarf novae proposed by Wils et al. (2010).

**Table 4.** Estimated extinction and neural network classification (continued)

Object	$g$	$d$ (pc)	type*	$A_V$	$P_{\text{orb}}$	ultrashort <sup>†</sup>	short <sup>‡</sup>	long <sup>§</sup>
OT J092839.3+005944	21.236(136)	2474	3	0.232	—	0.020(86)	0.381(408)	0.599(425)
OT J092839.3+005944	21.775(76)	2474	3	0.232	—	0.011(65)	0.752(360)	0.237(360)
OT J092839.3+005944	21.800(79)	2474	3	0.232	—	0.000(0)	0.562(396)	0.438(396)
OT J092839.3+005944	21.901(71)	2474	3	0.232	—	0.000(1)	0.572(410)	0.428(410)
OT J101035.5+140239	17.196(4)	6408	3	0.140	—	0.000(0)	1.000(0)	0.000(0)
OT J101035.5+140239	18.051(6)	6408	3	0.140	—	0.000(0)	1.000(0)	0.000(0)
OT J103704.6+100224	23.421(274)	3921	6	0.083	—	0.012(90)	0.429(473)	0.558(476)
OT J103704.6+100224	22.857(180)	3921	6	0.083	—	0.000(0)	0.342(444)	0.658(444)
OT J101545.9+033312	20.168(19)	904	3	0.091	—	0.093(83)	0.906(83)	0.001(2)
OT J102146.4+234926	20.725(26)	700	1	0.071	0.0554 <sup>  </sup>	0.457(331)	0.305(244)	0.238(375)
OT J102616.0+192045	20.126(18)	859	2	0.081	0.0800 <sup>  </sup>	0.004(2)	0.852(229)	0.144(229)
OT J102637.0+475426	19.929(17)	733	2	0.030	0.0663 <sup>  </sup>	0.522(147)	0.423(164)	0.054(154)
OT J102637.0+475426	20.127(23)	733	2	0.030	0.0663 <sup>  </sup>	0.709(187)	0.291(187)	0.000(3)
OT J102937.7+414046	22.269(86)	1970	3	0.036	—	0.522(442)	0.046(171)	0.432(448)
OT J102937.7+414046	22.401(100)	1970	3	0.036	—	0.217(361)	0.653(434)	0.130(318)
OT J102937.7+414046	22.137(89)	1970	3	0.036	—	0.046(159)	0.945(168)	0.009(62)
OT J103317.3+072119	19.893(16)	638	3	0.077	—	0.058(25)	0.938(32)	0.004(14)
OT J103738.7+124250	21.903(77)	2747	3	0.085	—	0.014(44)	0.306(370)	0.679(380)
OT J103738.7+124250	22.064(130)	2747	3	0.085	—	0.006(33)	0.373(426)	0.621(430)
OT J104411.4+211307	19.347(11)	278	2	0.084	0.0591	0.697(72)	0.303(72)	0.000(0)
OT J105550.1+095621	19.153(11)	919	3	0.085	—	0.000(0)	0.000(0)	1.000(0)
OT J105835.1+054706	20.299(24)	832	3	0.088	—	0.279(198)	0.716(202)	0.005(10)
OT J105835.1+054706	20.401(23)	832	3	0.088	—	0.041(30)	0.933(68)	0.026(61)
OT J112112.0−130843	19.851(18)	3339	3	0.201	—	0.000(0)	0.043(106)	0.957(106)
OT J112253.3−111037	20.438(21)	542	2	0.155	0.0472 <sup>  </sup>	0.789(106)	0.205(102)	0.006(32)
OT J112332.0+431718	19.912(16)	1234	3	0.067	—	0.024(12)	0.974(12)	0.002(2)
OT J112509.7+231036	20.988(36)	1930	3	0.058	—	0.746(285)	0.254(285)	0.000(0)
OT J112509.7+231036	20.964(34)	1930	3	0.058	—	0.148(190)	0.557(312)	0.295(326)
OT J112634.0−100210	18.809(9)	1477	3	0.137	—	0.003(2)	0.400(246)	0.597(247)
OT J115330.2+315836	20.113(18)	3253	3	0.072	—	0.002(3)	0.955(149)	0.043(149)
OT J122756.8+622935	21.572(55)	8428	3	0.058	—	0.000(0)	0.008(77)	0.992(77)
OT J122756.8+622935	21.813(69)	8428	3	0.058	—	0.000(0)	0.309(417)	0.691(417)
OT J122756.8+622935	21.811(74)	8428	3	0.058	—	0.000(0)	0.089(268)	0.911(268)
OT J123833.7+031854	21.560(65)	3916	6	0.086	—	0.000(3)	0.769(390)	0.231(390)
OT J124027.4−150558	21.021(39)	4606	3	0.154	—	0.004(8)	0.390(369)	0.606(373)
OT J124417.9+300401	19.571(12)	871	3	0.054	—	0.042(21)	0.958(21)	0.000(0)
OT J124819.4+072050	21.326(46)	1968	3	0.097	—	0.269(287)	0.454(349)	0.277(369)
OT J124819.4+072050	21.371(59)	1968	3	0.097	—	0.033(123)	0.675(418)	0.292(414)
OT J130030.3+115101	19.783(16)	480	1	0.086	0.0627 <sup>  </sup>	0.365(175)	0.634(176)	0.001(1)
OT J132536.0+210037	—	2274	6	0.066	—	—	—	—
OT J134052.1+151341	18.623(8)	926	3	0.103	—	0.000(0)	0.954(20)	0.046(20)
OT J134052.1+151341	18.731(8)	926	3	0.103	—	0.000(0)	0.103(80)	0.897(80)
OT J135219.0+280917	20.669(26)	8008	3	0.045	—	0.000(0)	0.000(0)	1.000(0)
OT J135336.0−022043	21.711(72)	8757	3	0.149	—	0.000(0)	0.001(9)	0.999(9)
OT J135716.8−093239	22.761(157)	1671	6	0.135	—	0.000(0)	0.052(196)	0.948(196)
OT J141002.2−124809	19.160(11)	1131	3	0.239	—	0.869(66)	0.130(66)	0.001(4)
OT J141712.0−180328	20.616(28)	826	3	0.280	—	0.000(0)	0.989(80)	0.010(81)
OT J142548.1+151502	21.802(61)	3058	3	0.068	—	0.000(1)	0.201(324)	0.799(325)
OT J144011.0+494734	21.161(51)	1127	2	0.075	0.0631 <sup>  </sup>	0.057(192)	0.921(237)	0.022(136)
OT J144316.5−010222	22.185(88)	1963	3	0.140	—	0.065(154)	0.918(178)	0.017(102)

\*Method of distance estimation. 1: from Patterson (2011) and other references (see text),

2: determined from  $P_{\text{orb}}$  and maximum magnitude, 3: from estimated  $P_{\text{orb}}$  and maximum magnitude,4: from  $P_{\text{orb}}$  and minimum magnitude, 5: from estimated  $P_{\text{orb}}$  and minimum magnitude6: assuming maximum  $M_V = 4.95$ .<sup>†</sup> $P_{\text{orb}} < 0.06$  (d).<sup>‡</sup> $0.06 \leq P_{\text{orb}} < 0.10$  (d).<sup>§</sup> $P_{\text{orb}} \geq 0.10$  (d).<sup>||</sup>Determined from superhump period.<sup>#</sup>Dwarf novae proposed by Wils et al. (2010).

**Table 4.** Estimated extinction and neural network classification (continued)

Object	$g$	$d$ (pc)	type*	$A_V$	$P_{\text{orb}}$	ultrashort <sup>†</sup>	short <sup>‡</sup>	long <sup>§</sup>
OT J144316.5–010222	22.417(106)	1963	3	0.140	–	0.190(328)	0.469(441)	0.341(441)
OT J144316.5–010222	22.236(87)	1963	3	0.140	–	0.008(29)	0.830(278)	0.162(278)
OT J145502.2+143815	20.117(21)	1435	3	0.119	–	0.000(0)	0.004(9)	0.996(9)
OT J145502.2+143815	20.485(22)	1435	3	0.119	–	0.000(0)	0.007(46)	0.993(46)
OT J145502.2+143815	20.282(23)	1435	3	0.119	–	0.000(0)	0.001(6)	0.999(6)
OT J145921.8+354806	21.544(39)	1110	2	0.040	0.0822 <sup>  </sup>	0.000(0)	0.165(304)	0.835(304)
OT J151020.7+182303	21.424(43)	11218	3	0.093	–	0.000(0)	0.003(17)	0.997(17)
OT J151037.4+084104	19.120(10)	4213	3	0.119	–	0.830(164)	0.170(164)	0.000(0)
OT J152037.9+040948	22.495(143)	1349	3	0.155	–	0.003(18)	0.957(159)	0.040(159)
OT J152501.8–013021	22.679(138)	1888	6	0.470	–	0.570(462)	0.069(243)	0.361(451)
OT J153150.8+152447	23.130(157)	6277	3	0.119	–	0.007(46)	0.345(439)	0.648(442)
OT J153317.6+273428	21.932(76)	5582	6	0.116	–	0.000(0)	0.526(484)	0.474(484)
OT J153645.2–142543	22.879(150)	1634	3	0.525	–	0.090(246)	0.614(451)	0.296(438)
OT J154354.1–143745	21.404(51)	2425	3	0.463	–	0.038(78)	0.939(134)	0.023(114)
OT J154428.1+335725	22.108(90)	2963	6	0.091	–	0.054(187)	0.234(402)	0.712(436)
OT J154544.9+442830	20.943(26)	934	2	0.062	0.0747 <sup>  </sup>	0.013(13)	0.952(136)	0.036(134)
OT J155325.7+114437	22.646(142)	3019	6	0.151	–	0.074(230)	0.691(441)	0.235(406)
OT J155325.7+114437	23.235(186)	3019	6	0.151	–	0.025(132)	0.657(445)	0.318(442)
OT J155430.6+365043	21.608(59)	2171	3	0.062	–	0.206(349)	0.785(358)	0.010(88)
OT J155430.6+365043	21.703(80)	2171	3	0.062	–	0.048(142)	0.877(266)	0.075(237)
OT J155748.0+070543	22.813(149)	4603	6	0.135	–	0.475(450)	0.101(268)	0.424(452)
OT J155748.0+070543	22.740(202)	4603	6	0.135	–	0.377(442)	0.255(412)	0.368(448)
OT J160204.8+031632	22.653(178)	2407	3	0.448	–	0.245(385)	0.318(414)	0.438(447)
OT J160204.8+031632	23.223(200)	2407	3	0.448	–	0.003(15)	0.412(457)	0.585(459)
OT J160232.2+161733	21.905(63)	4042	6	0.117	–	0.053(167)	0.308(403)	0.638(435)
OT J160524.1+060816	22.839(150)	4389	3	0.175	–	0.000(1)	0.789(375)	0.211(375)
OT J160524.1+060816	22.678(181)	4389	3	0.175	–	0.000(0)	0.592(468)	0.408(468)
OT J160844.8+220610	21.048(32)	2423	3	0.309	–	0.059(84)	0.908(107)	0.034(66)
OT J160844.8+220610	20.890(91)	2423	3	0.309	–	0.481(360)	0.402(335)	0.118(285)
OT J160844.8+220610	21.638(45)	2423	3	0.309	–	0.000(0)	0.450(421)	0.550(421)
OT J162012.0+115257	22.211(83)	5990	3	0.175	–	0.090(240)	0.786(370)	0.124(315)
OT J162235.7+035247	22.240(125)	1670	3	0.183	–	0.000(0)	0.042(158)	0.958(158)
OT J162605.7+225044	22.681(98)	4444	3	0.165	–	0.000(1)	0.631(420)	0.369(421)
OT J162605.7+225044	22.998(166)	4444	3	0.165	–	0.000(1)	0.281(431)	0.718(431)
OT J162656.8–002549	22.610(146)	3892	3	0.277	–	0.000(0)	0.753(385)	0.247(385)
OT J162806.2+065316	20.544(27)	541	2	0.195	0.0671 <sup>  </sup>	0.192(142)	0.803(144)	0.005(15)
OT J162806.2+065316	20.649(26)	541	2	0.195	0.0671 <sup>  </sup>	0.090(75)	0.826(214)	0.084(218)
OT J162619.8–125557	21.601(61)	1235	3	1.139	–	0.135(157)	0.801(219)	0.064(177)
OT J163120.9+103134	19.061(10)	560	1	0.275	0.0624 <sup>  </sup>	0.432(96)	0.568(96)	0.000(0)
OT J163239.3+351108	22.697(118)	3599	6	0.069	–	0.467(461)	0.013(93)	0.521(466)
OT J163311.3–011132	21.356(43)	2637	3	0.414	–	0.174(199)	0.818(204)	0.008(71)
OT J163942.7+122414	19.481(12)	1458	3	0.156	–	0.024(8)	0.597(169)	0.379(171)
OT J163942.7+122414	20.457(25)	1458	3	0.156	–	0.025(21)	0.966(41)	0.009(29)
OT J164146.8+121026	21.333(48)	2186	3	0.142	–	0.000(1)	0.802(255)	0.197(255)
OT J164146.8+121026	21.363(43)	2186	3	0.142	–	0.000(0)	0.622(368)	0.378(368)
OT J164146.8+121026	21.488(46)	2186	3	0.142	–	0.002(5)	0.378(399)	0.619(401)
OT J164624.8+180808	22.351(84)	2936	6	0.311	–	0.003(16)	0.089(249)	0.909(257)
OT J164748.0+433845	21.650(80)	5211	3	0.046	–	0.590(456)	0.353(441)	0.058(220)
OT J164748.0+433845	21.535(46)	5211	3	0.046	–	0.974(91)	0.026(91)	0.000(2)
OT J164950.4+035835	18.548(12)	524	3	0.289	–	0.329(81)	0.602(143)	0.069(111)

\*Method of distance estimation. 1: from Patterson (2011) and other references (see text),

2: determined from  $P_{\text{orb}}$  and maximum magnitude, 3: from estimated  $P_{\text{orb}}$  and maximum magnitude,4: from  $P_{\text{orb}}$  and minimum magnitude, 5: from estimated  $P_{\text{orb}}$  and minimum magnitude6: assuming maximum  $M_V = 4.95$ .<sup>†</sup> $P_{\text{orb}} < 0.06$  (d).<sup>‡</sup> $0.06 \leq P_{\text{orb}} < 0.10$  (d).<sup>§</sup> $P_{\text{orb}} \geq 0.10$  (d).<sup>||</sup>Determined from superhump period.<sup>#</sup>Dwarf novae proposed by Wils et al. (2010).

**Table 4.** Estimated extinction and neural network classification (continued)

Object	$g$	$d$ (pc)	type*	$A_V$	$P_{\text{orb}}$	ultrashort <sup>†</sup>	short <sup>‡</sup>	long <sup>§</sup>
OT J165002.8+435616	22.758(164)	4749	3	0.056	—	0.000(1)	0.521(447)	0.479(447)
OT J165002.8+435616	22.376(113)	4749	3	0.056	—	0.028(131)	0.749(396)	0.223(388)
OT J165002.8+435616	22.855(161)	4749	3	0.056	—	0.050(186)	0.368(443)	0.582(464)
OT J170115.8−024159	22.977(203)	2061	6	1.080	—	0.022(138)	0.687(443)	0.291(436)
OT J170151.6+132131	21.317(76)	4327	3	0.248	—	0.000(0)	0.100(262)	0.900(262)
OT J170606.1+255153	21.479(66)	1768	3	0.112	—	0.048(94)	0.836(257)	0.116(258)
OT J170609.7+143452	18.231(7)	642	3	0.458	—	0.009(2)	0.991(2)	0.000(0)
OT J170609.7+143452	18.453(8)	642	3	0.458	—	0.018(6)	0.982(6)	0.000(0)
OT J170702.5+165339	21.593(51)	1771	3	0.297	—	0.001(2)	0.989(45)	0.010(45)
OT J171223.1+362516	20.885(32)	3036	3	0.128	—	0.000(0)	0.000(0)	1.000(0)
OT J171223.1+362516	20.770(33)	3036	3	0.128	—	0.000(0)	0.000(0)	1.000(0)
OT J171223.1+362516	20.533(29)	3036	3	0.128	—	0.000(0)	0.000(0)	1.000(0)
OT J171223.1+362516	20.652(33)	3036	3	0.128	—	0.000(0)	0.000(0)	1.000(0)
OT J172515.5+073249	20.656(30)	735	6	0.320	—	0.105(277)	0.894(277)	0.000(0)
OT J173307.9+300635	22.535(106)	2245	3	0.173	—	0.000(0)	0.381(438)	0.619(438)
OT J175901.1+395551	22.030(98)	4126	3	0.160	—	0.041(174)	0.337(446)	0.622(461)
OT J182142.8+212154	20.260(21)	726	2	0.441	0.0794 <sup>  </sup>	0.003(2)	0.922(148)	0.075(148)
OT J202857.1−061803	20.606(30)	1237	3	0.170	—	0.415(234)	0.570(238)	0.015(90)
OT J204001.4−144909	20.563(25)	3256	3	0.129	—	0.179(137)	0.788(153)	0.033(56)
OT J204739.4+000840	22.213(131)	3461	3	0.316	—	0.000(0)	0.412(456)	0.588(456)
OT J210034.4+055436	22.113(72)	1544	3	0.285	—	0.044(129)	0.757(370)	0.198(365)
OT J210034.4+055436	22.248(90)	1544	3	0.285	—	0.009(41)	0.492(449)	0.498(456)
OT J210043.9−005212	21.301(65)	3216	3	0.283	—	0.000(0)	0.175(291)	0.825(291)
OT J210043.9−005212	21.613(51)	3216	3	0.283	—	0.000(1)	0.946(117)	0.054(118)
OT J210043.9−005212	21.461(60)	3216	3	0.283	—	0.001(2)	0.601(403)	0.398(403)
OT J210043.9−005212	21.183(52)	3216	3	0.283	—	0.018(30)	0.691(374)	0.291(382)
OT J210043.9−005212	21.466(57)	3216	3	0.283	—	0.006(42)	0.604(397)	0.390(400)
OT J210043.9−005212	21.596(93)	3216	3	0.283	—	0.002(11)	0.656(401)	0.342(402)
OT J210043.9−005212	21.536(65)	3216	3	0.283	—	0.002(6)	0.397(437)	0.601(439)
OT J210043.9−005212	21.344(67)	3216	3	0.283	—	0.002(7)	0.309(392)	0.689(394)
OT J210043.9−005212	22.237(498)	3216	3	0.283	—	0.024(110)	0.457(456)	0.519(454)
OT J210043.9−005212	21.525(59)	3216	3	0.283	—	0.001(2)	0.263(377)	0.736(378)
OT J210043.9−005212	21.662(93)	3216	3	0.283	—	0.005(32)	0.558(474)	0.437(477)
OT J210043.9−005212	21.506(102)	3216	3	0.283	—	0.040(141)	0.399(445)	0.561(466)
OT J210043.9−005212	22.284(317)	3216	3	0.283	—	0.000(0)	0.336(422)	0.664(422)
OT J210205.7+025834	21.483(47)	1477	3	0.278	—	0.000(0)	0.147(293)	0.853(293)
OT J210650.6+110250	20.242(21)	1280	3	0.354	—	0.094(91)	0.906(91)	0.000(0)
OT J210650.6+110250	20.501(25)	1280	3	0.354	—	0.012(12)	0.988(12)	0.000(0)
OT J210704.5+014416	23.890(267)	3287	6	0.366	—	0.396(447)	0.536(455)	0.068(205)
OT J210846.4−035031	17.881(6)	1050	3	0.337	—	0.003(1)	0.741(164)	0.256(164)
OT J210846.4−035031	18.615(9)	1050	3	0.337	—	0.000(0)	0.000(0)	1.000(0)
OT J210954.1+163052	19.521(12)	1237	3	0.412	—	0.074(29)	0.926(29)	0.000(0)
OT J211550.9−000716	22.533(169)	3279	3	0.233	—	0.065(212)	0.667(419)	0.268(398)
OT J211550.9−000716	22.973(200)	3279	3	0.233	—	0.532(473)	0.406(465)	0.063(203)
OT J211550.9−000716	22.873(397)	3279	3	0.233	—	0.000(0)	0.845(327)	0.155(327)
OT J211550.9−000716	22.664(121)	3279	3	0.233	—	0.141(300)	0.797(337)	0.061(200)
OT J211550.9−000716	23.277(221)	3279	3	0.233	—	0.000(0)	0.733(401)	0.267(401)
OT J211550.9−000716	22.938(226)	3279	3	0.233	—	0.034(138)	0.376(435)	0.591(450)
OT J211550.9−000716	22.245(110)	3279	3	0.233	—	0.021(118)	0.504(477)	0.475(480)
OT J211550.9−000716	22.424(119)	3279	3	0.233	—	0.001(5)	0.054(207)	0.945(209)

\*Method of distance estimation. 1: from Patterson (2011) and other references (see text),

2: determined from  $P_{\text{orb}}$  and maximum magnitude, 3: from estimated  $P_{\text{orb}}$  and maximum magnitude,4: from  $P_{\text{orb}}$  and minimum magnitude, 5: from estimated  $P_{\text{orb}}$  and minimum magnitude6: assuming maximum  $M_V = 4.95$ .<sup>†</sup> $P_{\text{orb}} < 0.06$  (d).<sup>‡</sup> $0.06 \leq P_{\text{orb}} < 0.10$  (d).<sup>§</sup> $P_{\text{orb}} \geq 0.10$  (d).<sup>||</sup>Determined from superhump period.<sup>#</sup>Dwarf novae proposed by Wils et al. (2010).



**Table 4.** Estimated extinction and neural network classification (continued)

Object	$g$	$d$ (pc)	type*	$A_V$	$P_{\text{orb}}$	ultrashort <sup>†</sup>	short <sup>‡</sup>	long <sup>§</sup>
OT J211550.9–000716	22.795(566)	3279	3	0.233	–	0.002(18)	0.588(481)	0.410(482)
OT J211550.9–000716	23.313(183)	3279	3	0.233	–	0.004(43)	0.099(284)	0.897(293)
OT J211550.9–000716	23.120(198)	3279	3	0.233	–	0.001(6)	0.172(360)	0.828(361)
OT J212025.1+194157	21.819(64)	1578	6	0.259	–	0.029(123)	0.949(183)	0.022(135)
OT J212555.1–032406	21.977(88)	2928	6	0.217	–	0.438(472)	0.022(139)	0.539(474)
OT J212555.1–032406	22.000(179)	2928	6	0.217	–	0.554(472)	0.101(289)	0.345(446)
OT J212633.3+085459	20.757(26)	2077	3	0.182	–	0.018(31)	0.945(73)	0.037(69)
OT J213122.4–003937	20.894(74)	991	2	0.152	0.0629 <sup>  </sup>	0.351(422)	0.520(444)	0.130(313)
OT J213122.4–003937	21.550(48)	991	2	0.152	0.0629 <sup>  </sup>	0.461(427)	0.533(427)	0.005(28)
OT J213122.4–003937	21.210(49)	991	2	0.152	0.0629 <sup>  </sup>	0.198(317)	0.629(412)	0.173(324)
OT J213122.4–003937	21.492(61)	991	2	0.152	0.0629 <sup>  </sup>	0.391(443)	0.368(440)	0.241(415)
OT J213122.4–003937	21.380(49)	991	2	0.152	0.0629 <sup>  </sup>	0.784(330)	0.135(239)	0.081(251)
OT J213122.4–003937	21.605(54)	991	2	0.152	0.0629 <sup>  </sup>	0.306(372)	0.645(389)	0.049(192)
OT J213122.4–003937	21.481(71)	991	2	0.152	0.0629 <sup>  </sup>	0.440(409)	0.163(276)	0.397(447)
OT J213122.4–003937	21.398(42)	991	2	0.152	0.0629 <sup>  </sup>	0.002(7)	0.431(437)	0.567(439)
OT J213122.4–003937	21.489(55)	991	2	0.152	0.0629 <sup>  </sup>	0.145(274)	0.378(409)	0.477(470)
OT J213122.4–003937	21.526(60)	991	2	0.152	0.0629 <sup>  </sup>	0.322(378)	0.599(409)	0.078(224)
OT J213122.4–003937	21.472(48)	991	2	0.152	0.0629 <sup>  </sup>	0.288(420)	0.054(205)	0.658(451)
OT J213122.4–003937	21.382(74)	991	2	0.152	0.0629 <sup>  </sup>	0.174(345)	0.175(360)	0.651(463)
OT J213432.3–012040	23.255(215)	3736	6	0.188	–	0.204(377)	0.459(476)	0.337(456)
OT J213309.4+155004	22.075(91)	1429	3	0.338	–	0.000(0)	0.168(320)	0.831(320)
OT J213701.8+071446	19.017(9)	330	1	0.081	0.0950 <sup>  </sup>	0.000(0)	0.649(168)	0.351(168)
OT J213829.5–001742	23.531(362)	7527	6	0.167	–	0.000(0)	0.706(425)	0.294(425)
OT J213937.6–023913	20.138(26)	648	3	0.155	–	0.005(7)	0.982(27)	0.013(21)
OT J213937.6–023913	20.010(19)	648	3	0.155	–	0.005(3)	0.903(144)	0.092(145)
OT J213937.6–023913	20.069(19)	648	3	0.155	–	0.001(1)	0.691(265)	0.309(265)
OT J214426.4+222024	17.644(5)	2647	3	0.364	–	0.000(0)	0.999(0)	0.001(0)
OT J214639.9+092119	21.829(71)	3047	3	0.227	–	0.155(290)	0.754(368)	0.091(274)
OT J214804.4+080951	20.957(30)	2317	3	0.229	–	0.014(22)	0.981(24)	0.005(11)
OT J214842.5–000723	22.776(150)	1146	3	0.416	–	0.041(148)	0.631(418)	0.329(420)
OT J214842.5–000723	22.854(158)	1146	3	0.416	–	0.156(319)	0.302(406)	0.542(466)
OT J214842.5–000723	22.722(182)	1146	3	0.416	–	0.302(402)	0.399(439)	0.299(431)
OT J214842.5–000723	23.050(192)	1146	3	0.416	–	0.489(455)	0.318(425)	0.193(374)
OT J214842.5–000723	22.546(153)	1146	3	0.416	–	0.479(456)	0.086(267)	0.435(460)
OT J214842.5–000723	22.899(160)	1146	3	0.416	–	0.008(50)	0.758(392)	0.234(389)
OT J214842.5–000723	22.760(154)	1146	3	0.416	–	0.207(365)	0.114(284)	0.680(443)
OT J214842.5–000723	22.677(120)	1146	3	0.416	–	0.400(447)	0.147(317)	0.453(464)
OT J214842.5–000723	23.006(205)	1146	3	0.416	–	0.011(83)	0.728(420)	0.261(419)
OT J214842.5–000723	22.853(162)	1146	3	0.416	–	0.061(230)	0.007(64)	0.932(247)
OT J214959.9+124529	21.928(80)	1409	3	0.293	–	0.182(321)	0.631(417)	0.187(357)
OT J215344.7+123524	21.494(98)	3844	3	0.338	–	0.000(1)	0.322(423)	0.678(423)
OT J215344.7+123524	22.107(92)	3844	3	0.338	–	0.000(0)	0.595(430)	0.405(430)
OT J215344.7+123524	21.924(122)	3844	3	0.338	–	0.000(0)	0.036(167)	0.964(167)
OT J215630.5–031957	22.142(125)	2082	3	0.267	–	0.279(384)	0.633(426)	0.089(267)
OT J215630.5–031957	22.169(111)	2082	3	0.267	–	0.130(288)	0.359(414)	0.511(463)
OT J215636.3+193242	18.783(9)	2060	3	0.275	–	0.007(3)	0.981(9)	0.012(8)
OT J215636.3+193242	19.339(12)	2060	3	0.275	–	0.005(1)	0.994(2)	0.001(2)
OT J215636.3+193242	19.553(13)	2060	3	0.275	–	0.000(0)	0.050(74)	0.950(74)
OT J215815.3+094709	17.478(5)	388	2	0.170	0.0750 <sup>  </sup>	0.081(11)	0.919(11)	0.000(0)
OT J220031.2+033431	18.664(8)	1643	3	0.165	–	0.001(1)	0.233(71)	0.765(71)

\*Method of distance estimation. 1: from Patterson (2011) and other references (see text),

2: determined from  $P_{\text{orb}}$  and maximum magnitude, 3: from estimated  $P_{\text{orb}}$  and maximum magnitude,4: from  $P_{\text{orb}}$  and minimum magnitude, 5: from estimated  $P_{\text{orb}}$  and minimum magnitude6: assuming maximum  $M_V = 4.95$ .<sup>†</sup>  $P_{\text{orb}} < 0.06$  (d).<sup>‡</sup>  $0.06 \leq P_{\text{orb}} < 0.10$  (d).<sup>§</sup>  $P_{\text{orb}} \geq 0.10$  (d).<sup>||</sup> Determined from superhump period.

# Dwarf novae proposed by Wils et al. (2010).

**Table 4.** Estimated extinction and neural network classification (continued)

Object	$g$	$d$ (pc)	type*	$A_V$	$P_{\text{orb}}$	ultrashort <sup>†</sup>	short <sup>‡</sup>	long <sup>§</sup>
OT J220449.7+054852	20.035(19)	886	3	0.233	—	0.001(0)	0.720(295)	0.279(295)
OT J220449.7+054852	20.940(32)	886	3	0.233	—	0.000(0)	0.033(85)	0.967(85)
OT J221128.7−030516	19.555(13)	1229	3	0.305	—	0.224(74)	0.776(74)	0.000(0)
OT J221128.7−030516	19.718(17)	1229	3	0.305	—	0.108(61)	0.890(65)	0.002(10)
OT J221128.7−030516	19.864(17)	1229	3	0.305	—	0.124(82)	0.875(83)	0.001(2)
OT J221128.7−030516	20.177(24)	1229	3	0.305	—	0.010(9)	0.985(31)	0.005(31)
OT J221128.7−030516	20.597(25)	1229	3	0.305	—	0.441(254)	0.559(254)	0.000(0)
OT J221232.0+160140	19.112(10)	956	3	0.185	—	0.002(1)	0.659(248)	0.339(249)
OT J221232.0+160140	19.247(11)	956	3	0.185	—	0.002(1)	0.860(158)	0.138(158)
OT J221344.0+173252	19.261(11)	1343	3	0.141	—	0.051(33)	0.949(35)	0.001(3)
OT J222002.3+113825	20.653(26)	4328	3	0.241	—	0.000(0)	0.009(22)	0.991(22)
OT J222002.3+113825	21.372(40)	4328	3	0.241	—	0.000(0)	0.004(16)	0.996(16)
OT J222548.1+252511	20.196(21)	2042	3	0.186	—	0.000(0)	0.002(6)	0.998(6)
OT J222724.5+284404	18.563(8)	739	3	0.224	—	0.000(0)	0.736(139)	0.264(139)
OT J222824.1+134944	22.345(81)	934	3	0.227	—	0.602(412)	0.270(354)	0.127(293)
OT J222824.1+134944	22.310(101)	934	3	0.227	—	0.185(340)	0.463(462)	0.352(469)
OT J222853.7+295115	23.489(194)	1463	6	0.223	—	0.000(0)	0.545(464)	0.455(464)
OT J223018.8+292849	22.481(127)	2769	6	0.238	—	0.166(342)	0.267(421)	0.567(477)
OT J223058.3+210147	20.788(37)	1732	3	0.141	—	0.315(295)	0.592(320)	0.093(259)
OT J223136.0+180747	21.663(56)	3155	3	0.218	—	0.176(266)	0.810(271)	0.014(84)
OT J223235.4+304105	22.473(99)	2560	3	0.275	—	0.041(152)	0.653(402)	0.307(401)
OT J223418.5−035530	20.502(25)	987	2	0.138	0.0884 <sup>  </sup>	0.000(0)	0.622(344)	0.377(344)
OT J223606.3+050517	22.304(94)	2291	3	0.377	—	0.610(404)	0.298(364)	0.092(262)
OT J223909.8+250331	19.158(10)	2337	3	0.161	—	0.039(24)	0.326(189)	0.636(209)
OT J223958.2+231837	22.167(131)	3843	3	0.140	—	0.093(233)	0.418(435)	0.489(465)
OT J223958.2+231837	22.144(64)	3843	3	0.140	—	0.000(2)	0.935(233)	0.065(232)
OT J223958.4+342306	22.395(87)	5541	6	0.232	—	0.009(50)	0.038(177)	0.953(193)
OT J224253.4+172538	20.439(25)	1851	3	0.148	—	0.013(14)	0.761(334)	0.226(336)
OT J224505.4+011547	21.463(68)	1945	3	0.271	—	0.518(402)	0.455(395)	0.028(148)
OT J224505.4+011547	21.502(62)	1945	3	0.271	—	0.526(409)	0.426(405)	0.048(169)
OT J224505.4+011547	21.553(57)	1945	3	0.271	—	0.599(336)	0.389(326)	0.012(63)
OT J224753.9+235522	21.188(68)	902	3	0.370	—	0.014(69)	0.549(419)	0.437(427)
OT J224753.9+235522	21.500(52)	902	3	0.370	—	0.300(309)	0.530(334)	0.171(320)
OT J224814.5+331224	19.625(13)	2658	3	0.331	—	0.000(0)	0.022(37)	0.978(37)
OT J224814.5+331224	20.938(28)	2658	3	0.331	—	0.229(200)	0.613(278)	0.157(255)
OT J224823.7−092059	21.128(48)	1304	3	0.132	—	0.140(179)	0.704(298)	0.157(282)
OT J225749.6−082228	20.181(30)	335	3	0.116	—	0.020(117)	0.979(119)	0.000(2)
OT J225749.6−082228	20.137(21)	335	3	0.116	—	0.401(355)	0.398(356)	0.201(369)
OT J230115.4+224111	22.109(104)	1594	6	0.737	—	0.008(53)	0.698(429)	0.294(428)
OT J230131.1+040417	21.951(69)	6169	6	0.199	—	0.000(0)	0.266(408)	0.734(408)
OT J230425.8+062546	20.962(34)	466	2	0.206	0.0653 <sup>  </sup>	0.008(27)	0.388(430)	0.604(433)
OT J230425.8+062546	21.090(34)	466	2	0.206	0.0653 <sup>  </sup>	0.539(422)	0.201(287)	0.260(404)
OT J230711.3+294011	21.496(40)	2833	6	0.189	—	0.000(0)	0.000(0)	1.000(0)
OT J231110.9+013003	21.620(61)	1384	6	0.144	—	0.110(257)	0.107(261)	0.783(371)
OT J231142.8+204036	20.540(25)	839	3	0.597	—	0.026(24)	0.859(208)	0.114(207)
OT J231142.8+204036	21.244(54)	839	3	0.597	—	0.115(147)	0.845(210)	0.041(168)
OT J231308.1+233702	20.385(23)	354	2	0.430	0.0692 <sup>  </sup>	0.000(0)	0.000(1)	1.000(1)
OT J231308.1+233702	20.434(21)	354	2	0.430	0.0692 <sup>  </sup>	0.000(0)	0.816(300)	0.184(300)
OT J231552.3+271037	20.735(37)	1863	3	0.292	—	0.000(0)	0.002(7)	0.998(7)
OT J231552.3+271037	20.651(26)	1863	3	0.292	—	0.000(0)	0.000(0)	1.000(0)

\*Method of distance estimation. 1: from Patterson (2011) and other references (see text),

2: determined from  $P_{\text{orb}}$  and maximum magnitude, 3: from estimated  $P_{\text{orb}}$  and maximum magnitude,4: from  $P_{\text{orb}}$  and minimum magnitude, 5: from estimated  $P_{\text{orb}}$  and minimum magnitude6: assuming maximum  $M_V = 4.95$ .<sup>†</sup> $P_{\text{orb}} < 0.06$  (d).<sup>‡</sup> $0.06 \leq P_{\text{orb}} < 0.10$  (d).<sup>§</sup> $P_{\text{orb}} \geq 0.10$  (d).<sup>||</sup>Determined from superhump period.<sup>#</sup>Dwarf novae proposed by Wils et al. (2010).

**Table 4.** Estimated extinction and neural network classification (continued)

Object	$g$	$d$ (pc)	type*	$A_V$	$P_{\text{orb}}$	ultrashort <sup>†</sup>	short <sup>‡</sup>	long <sup>§</sup>
OT J232551.5–014024	18.853(9)	1226	3	0.196	–	0.000(0)	0.000(0)	1.000(0)
OT J232619.4+282650	20.893(27)	1720	3	0.369	–	0.006(12)	0.833(277)	0.161(280)
OT J232619.4+282650	20.933(39)	1720	3	0.369	–	0.012(21)	0.703(323)	0.285(325)
OT J232619.4+282650	21.074(32)	1720	3	0.369	–	0.018(21)	0.491(301)	0.491(307)
OT J233938.7–053305	18.996(10)	4296	3	0.110	–	0.000(0)	0.004(7)	0.996(7)
OT J234440.5–001206	20.308(30)	600	2	0.122	0.0745 <sup>  </sup>	0.005(7)	0.970(117)	0.025(118)
OT J234440.5–001206	20.358(23)	600	2	0.122	0.0745 <sup>  </sup>	0.012(9)	0.988(10)	0.000(1)
OT J234440.5–001206	20.374(22)	600	2	0.122	0.0745 <sup>  </sup>	0.007(6)	0.988(32)	0.005(30)
OT J234440.5–001206	20.401(39)	600	2	0.122	0.0745 <sup>  </sup>	0.021(23)	0.979(23)	0.000(1)
OT J234440.5–001206	20.498(28)	600	2	0.122	0.0745 <sup>  </sup>	0.013(16)	0.986(16)	0.000(1)
OT J234440.5–001206	20.317(26)	600	2	0.122	0.0745 <sup>  </sup>	0.059(72)	0.932(80)	0.009(19)
OT J234440.5–001206	20.524(23)	600	2	0.122	0.0745 <sup>  </sup>	0.003(4)	0.995(6)	0.002(3)
OT J234440.5–001206	20.518(24)	600	2	0.122	0.0745 <sup>  </sup>	0.004(4)	0.995(6)	0.002(4)
OT J234440.5–001206	20.474(28)	600	2	0.122	0.0745 <sup>  </sup>	0.033(55)	0.920(146)	0.047(126)
OT J234440.5–001206	20.519(28)	600	2	0.122	0.0745 <sup>  </sup>	0.005(5)	0.982(38)	0.013(37)
OT J234440.5–001206	20.423(31)	600	2	0.122	0.0745 <sup>  </sup>	0.065(111)	0.681(363)	0.254(379)
OT J234440.5–001206	20.531(30)	600	2	0.122	0.0745 <sup>  </sup>	0.007(8)	0.958(110)	0.035(108)
OT J234440.5–001206	20.639(43)	600	2	0.122	0.0745 <sup>  </sup>	0.002(3)	0.861(266)	0.138(266)
OT J234440.5–001206	20.637(31)	600	2	0.122	0.0745 <sup>  </sup>	0.003(3)	0.936(143)	0.062(143)
OT J234440.5–001206	20.677(27)	600	2	0.122	0.0745 <sup>  </sup>	0.010(9)	0.908(161)	0.082(160)
OT J234440.5–001206	20.618(31)	600	2	0.122	0.0745 <sup>  </sup>	0.016(18)	0.824(226)	0.160(226)
OT J234440.5–001206	20.804(28)	600	2	0.122	0.0745 <sup>  </sup>	0.003(4)	0.668(306)	0.329(306)
OT J234440.5–001206	20.737(27)	600	2	0.122	0.0745 <sup>  </sup>	0.008(14)	0.192(241)	0.801(247)
OT J234440.5–001206	21.087(36)	600	2	0.122	0.0745 <sup>  </sup>	0.001(3)	0.697(288)	0.302(288)
OT J234440.5–001206	20.981(31)	600	2	0.122	0.0745 <sup>  </sup>	0.016(19)	0.559(346)	0.426(350)
OT J234440.5–001206	21.034(57)	600	2	0.122	0.0745 <sup>  </sup>	0.000(1)	0.294(359)	0.706(359)
OT J234440.5–001206	21.056(36)	600	2	0.122	0.0745 <sup>  </sup>	0.002(5)	0.323(326)	0.675(327)
ROTSE3 J004626+410714	24.950(611)	1121	6	0.203	–	0.000(0)	0.051(202)	0.949(202)
ROTSE3 J004626+410714	24.117(382)	1121	6	0.203	–	0.000(0)	0.000(2)	1.000(2)
ROTSE3 J031031+431115	20.514(21)	1239	3	0.694	–	0.115(66)	0.884(66)	0.001(1)
ROTSE3 J100932.2–020155	20.490(28)	570	3	0.147	–	0.926(223)	0.074(223)	0.000(0)
ROTSE3 J100932.2–020155	20.568(47)	570	3	0.147	–	0.505(440)	0.495(441)	0.001(3)
ROTSE3 J100932.2–020155	20.553(25)	570	3	0.147	–	0.468(397)	0.528(400)	0.004(23)
ROTSE3 J113709+513451	20.674(26)	10498	3	0.049	–	0.000(0)	0.020(104)	0.980(104)
ROTSE3 J154041.5–002703.2	21.057(35)	1026	3	0.354	–	0.000(0)	0.311(379)	0.689(379)
ROTSE3 J154041.5–002703.2	21.356(44)	1026	3	0.354	–	0.000(0)	0.212(327)	0.788(327)
ROTSE3 J154041.5–002703.2	21.824(70)	1026	3	0.354	–	0.000(0)	0.340(388)	0.660(388)
ROTSE3 J212313–021446.6	22.117(78)	1879	3	0.196	–	0.330(409)	0.319(418)	0.350(442)
ROTSE3 J214850–020622.2	22.407(91)	2146	6	0.192	–	0.014(67)	0.116(267)	0.870(293)
ROTSE3 J221519.8–003257.2	20.980(37)	1757	3	0.317	–	0.034(53)	0.961(55)	0.005(17)
ROTSE3 J221519.8–003257.2	21.192(69)	1757	3	0.317	–	0.007(12)	0.953(153)	0.041(154)
ROTSE3 J221519.8–003257.2	21.039(43)	1757	3	0.317	–	0.004(5)	0.943(178)	0.052(179)
ROTSE3 J221519.8–003257.2	21.069(43)	1757	3	0.317	–	0.007(21)	0.966(115)	0.027(114)
ROTSE3 J221519.8–003257.2	21.131(35)	1757	3	0.317	–	0.030(43)	0.758(318)	0.212(323)
ROTSE3 J221519.8–003257.2	21.395(87)	1757	3	0.317	–	0.057(93)	0.895(162)	0.048(145)
ROTSE3 J221519.8–003257.2	21.366(48)	1757	3	0.317	–	0.001(2)	0.884(246)	0.115(246)
ROTSE3 J221519.8–003257.2	21.185(63)	1757	3	0.317	–	0.111(174)	0.797(266)	0.091(230)
ROTSE3 J221519.8–003257.2	21.238(47)	1757	3	0.317	–	0.006(10)	0.783(321)	0.212(321)
ROTSE3 J221519.8–003257.2	21.341(44)	1757	3	0.317	–	0.005(6)	0.960(145)	0.035(146)
ROTSE3 J221519.8–003257.2	21.286(141)	1757	3	0.317	–	0.007(19)	0.602(434)	0.392(438)

\*Method of distance estimation. 1: from Patterson (2011) and other references (see text),

2: determined from  $P_{\text{orb}}$  and maximum magnitude, 3: from estimated  $P_{\text{orb}}$  and maximum magnitude,4: from  $P_{\text{orb}}$  and minimum magnitude, 5: from estimated  $P_{\text{orb}}$  and minimum magnitude6: assuming maximum  $M_V = 4.95$ .<sup>†</sup> $P_{\text{orb}} < 0.06$  (d).<sup>‡</sup> $0.06 \leq P_{\text{orb}} < 0.10$  (d).<sup>§</sup> $P_{\text{orb}} \geq 0.10$  (d).<sup>||</sup>Determined from superhump period.

**Table 4.** Estimated extinction and neural network classification (continued)

Object	$g$	$d$ (pc)	type*	$A_V$	$P_{\text{orb}}$	ultrashort <sup>†</sup>	short <sup>‡</sup>	long <sup>§</sup>
ROTSE3 J221519.8–003257.2	21.182(59)	1757	3	0.317	–	0.092(189)	0.723(371)	0.185(348)
ROTSE3 J221519.8–003257.2	21.455(51)	1757	3	0.317	–	0.003(5)	0.862(289)	0.135(290)
ROTSE3 J221519.8–003257.2	21.679(59)	1757	3	0.317	–	0.012(45)	0.937(180)	0.051(176)
ROTSE3 J221519.8–003257.2	21.348(84)	1757	3	0.317	–	0.168(273)	0.554(390)	0.278(380)
ROTSE3 J221519.8–003257.2	21.598(50)	1757	3	0.317	–	0.083(138)	0.850(223)	0.067(187)
RX J1715.6+6856	18.633(8)	1235	2	0.112	0.0683	0.157(30)	0.840(30)	0.004(3)
RX J1831.7+6511	17.037(4)	661	2	0.149	0.167	0.008(1)	0.973(14)	0.018(13)
RX J1831.7+6511	17.208(4)	661	2	0.149	0.167	0.004(0)	0.593(86)	0.403(86)
SDSS J003941.06+005427.5	20.357(22)	843	4	0.068	0.0635	0.870(140)	0.130(140)	0.000(1)
SDSS J003941.06+005427.5	20.402(20)	843	4	0.068	0.0635	0.988(15)	0.012(15)	0.000(0)
SDSS J003941.06+005427.5	20.356(27)	843	4	0.068	0.0635	0.848(232)	0.152(232)	0.000(0)
SDSS J003941.06+005427.5	20.422(28)	843	4	0.068	0.0635	0.898(149)	0.094(126)	0.008(71)
SDSS J003941.06+005427.5	20.397(22)	843	4	0.068	0.0635	0.758(233)	0.234(233)	0.008(17)
SDSS J003941.06+005427.5	20.519(23)	843	4	0.068	0.0635	0.609(416)	0.391(416)	0.000(0)
SDSS J003941.06+005427.5	20.467(23)	843	4	0.068	0.0635	0.995(19)	0.005(19)	0.000(0)
SDSS J003941.06+005427.5	20.413(58)	843	4	0.068	0.0635	0.792(329)	0.167(284)	0.041(186)
SDSS J003941.06+005427.5	20.500(22)	843	4	0.068	0.0635	0.806(187)	0.191(186)	0.003(23)
SDSS J003941.06+005427.5	20.415(24)	843	4	0.068	0.0635	0.976(41)	0.024(41)	0.000(0)
SDSS J003941.06+005427.5	20.498(22)	843	4	0.068	0.0635	0.609(397)	0.390(397)	0.000(2)
SDSS J003941.06+005427.5	20.554(27)	843	4	0.068	0.0635	0.986(23)	0.014(23)	0.000(0)
SDSS J003941.06+005427.5	20.561(29)	843	4	0.068	0.0635	0.969(129)	0.031(129)	0.000(0)
SDSS J003941.06+005427.5	20.652(26)	843	4	0.068	0.0635	0.990(55)	0.010(55)	0.000(0)
SDSS J004335.14–003729.8	19.752(14)	500	1	0.058	0.0572	0.878(46)	0.122(46)	0.000(1)
SDSS J004335.14–003729.8	19.801(16)	500	1	0.058	0.0572	0.623(161)	0.376(161)	0.000(1)
SDSS J004335.14–003729.8	19.812(17)	500	1	0.058	0.0572	0.621(141)	0.342(143)	0.036(97)
SDSS J004335.14–003729.8	19.799(19)	500	1	0.058	0.0572	0.379(192)	0.348(204)	0.273(276)
SDSS J004335.14–003729.8	19.798(15)	500	1	0.058	0.0572	0.782(114)	0.217(114)	0.000(0)
SDSS J004335.14–003729.8	19.836(16)	500	1	0.058	0.0572	0.577(195)	0.421(195)	0.002(3)
SDSS J004335.14–003729.8	19.927(27)	500	1	0.058	0.0572	0.567(175)	0.427(175)	0.006(19)
SDSS J004335.14–003729.8	19.782(18)	500	1	0.058	0.0572	0.780(109)	0.219(109)	0.001(4)
SDSS J004335.14–003729.8	19.830(15)	500	1	0.058	0.0572	0.840(77)	0.160(77)	0.000(0)
SDSS J004335.14–003729.8	19.813(16)	500	1	0.058	0.0572	0.560(129)	0.414(133)	0.027(89)
SDSS J004335.14–003729.8	19.835(16)	500	1	0.058	0.0572	0.595(118)	0.392(116)	0.012(68)
SDSS J004335.14–003729.8	19.847(17)	500	1	0.058	0.0572	0.599(146)	0.381(149)	0.020(56)
SDSS J004335.14–003729.8	19.843(19)	500	1	0.058	0.0572	0.325(164)	0.430(222)	0.245(317)
SDSS J004335.14–003729.8	19.916(16)	500	1	0.058	0.0572	0.826(76)	0.173(76)	0.001(3)
SDSS J004335.14–003729.8	19.731(18)	500	1	0.058	0.0572	0.543(155)	0.445(153)	0.013(43)
SDSS J004335.14–003729.8	19.814(16)	500	1	0.058	0.0572	0.734(128)	0.265(129)	0.001(1)
SDSS J004335.14–003729.8	19.939(17)	500	1	0.058	0.0572	0.707(128)	0.293(127)	0.001(4)
SDSS J004335.14–003729.8	19.943(17)	500	1	0.058	0.0572	0.584(160)	0.416(160)	0.000(1)
SDSS J004335.14–003729.8	19.898(19)	500	1	0.058	0.0572	0.225(199)	0.772(201)	0.002(10)
SDSS J004335.14–003729.8	19.860(19)	500	1	0.058	0.0572	0.604(199)	0.383(192)	0.013(72)
SDSS J004335.14–003729.8	19.925(19)	500	1	0.058	0.0572	0.407(238)	0.590(240)	0.002(10)
SDSS J012940.05+384210.4	19.786(14)	603	2	0.199	0.0435 <sup>  </sup>	0.915(79)	0.085(79)	0.000(0)
SDSS J033449.86–071047.8	17.862(6)	850	1	0.161	0.0724 <sup>  </sup>	0.070(11)	0.910(11)	0.019(4)
SDSS J033710.91–065059.4	19.558(13)	2508	3	0.143	–	0.985(14)	0.015(14)	0.000(0)
SDSS J053659.12+002215.1	18.804(9)	274	5	0.777	–	0.981(35)	0.019(35)	0.000(0)
SDSS J053659.12+002215.1	18.841(9)	274	5	0.777	–	0.988(19)	0.012(19)	0.000(0)
SDSS J053659.12+002215.1	18.851(8)	274	5	0.777	–	0.993(8)	0.007(8)	0.000(0)
SDSS J053659.12+002215.1	18.828(9)	274	5	0.777	–	0.994(7)	0.006(7)	0.000(0)

\*Method of distance estimation. 1: from Patterson (2011) and other references (see text),

2: determined from  $P_{\text{orb}}$  and maximum magnitude, 3: from estimated  $P_{\text{orb}}$  and maximum magnitude,4: from  $P_{\text{orb}}$  and minimum magnitude, 5: from estimated  $P_{\text{orb}}$  and minimum magnitude6: assuming maximum  $M_V = 4.95$ .<sup>†</sup> $P_{\text{orb}} < 0.06$  (d).<sup>‡</sup> $0.06 \leq P_{\text{orb}} < 0.10$  (d).<sup>§</sup> $P_{\text{orb}} \geq 0.10$  (d).<sup>||</sup>Determined from superhump period.<sup>#</sup>Dwarf novae proposed by Wils et al. (2010).



**Table 4.** Estimated extinction and neural network classification (continued)

Object	$g$	$d$ (pc)	type*	$A_V$	$P_{\text{orb}}$	ultrashort <sup>†</sup>	short <sup>‡</sup>	long <sup>§</sup>
SDSS J053659.12+002215.1	18.849(9)	274	5	0.777	–	0.999(0)	0.001(0)	0.000(0)
SDSS J053659.12+002215.1	18.776(9)	274	5	0.777	–	0.977(70)	0.023(70)	0.000(0)
SDSS J074355.56+183834.8	20.089(18)	1095	5	0.120	–	0.000(0)	0.000(0)	1.000(0)
SDSS J074355.56+183834.8	19.785(15)	1095	5	0.120	–	0.000(0)	0.000(0)	1.000(0)
SDSS J074531.92+453829.6	19.041(9)	300	1	0.154	0.0528	0.619(125)	0.381(125)	0.000(0)
SDSS J074640.62+173412.8	19.767(13)	1062	2	0.116	0.0649 <sup>  </sup>	0.065(31)	0.903(39)	0.032(25)
SDSS J074640.62+173412.8	19.807(16)	1062	2	0.116	0.0649 <sup>  </sup>	0.001(1)	0.115(158)	0.884(159)
SDSS J075059.97+141150.1	19.104(11)	350	1	0.081	0.0932	0.002(3)	0.695(241)	0.303(241)
SDSS J075059.97+141150.1	19.094(10)	350	1	0.081	0.0932	0.009(6)	0.429(293)	0.562(297)
SDSS J075507.70+143547.6	18.186(7)	230	1	0.061	0.0589	0.912(33)	0.088(33)	0.000(0)
SDSS J075507.70+143547.6	18.209(7)	230	1	0.061	0.0589	0.822(35)	0.178(35)	0.000(0)
SDSS J075507.70+143547.6	18.186(7)	230	1	0.061	0.0589	0.904(25)	0.096(25)	0.000(0)
SDSS J075507.70+143547.6	18.198(6)	230	1	0.061	0.0589	0.922(30)	0.077(30)	0.000(0)
SDSS J075939.79+191417.3	17.834(5)	321	4	0.082	0.1309	0.054(16)	0.569(141)	0.376(141)
SDSS J075939.79+191417.3	18.096(7)	321	4	0.082	0.1309	0.000(0)	0.024(15)	0.976(15)
SDSS J075939.79+191417.3	17.945(6)	321	4	0.082	0.1309	0.028(6)	0.542(159)	0.430(161)
SDSS J075939.79+191417.3	18.177(6)	321	4	0.082	0.1309	0.016(12)	0.118(100)	0.866(112)
SDSS J080142.37+210345.8	18.708(8)	1970	3	0.173	–	0.068(14)	0.929(14)	0.003(1)
SDSS J080142.37+210345.8	18.840(8)	1970	3	0.173	–	0.035(10)	0.963(10)	0.002(1)
SDSS J080142.37+210345.8	19.021(10)	1970	3	0.173	–	0.126(35)	0.772(69)	0.102(65)
SDSS J080303.90+251627.0	19.577(14)	692	2	0.089	0.071	0.001(0)	0.823(76)	0.176(76)
SDSS J080303.90+251627.0	19.591(12)	692	2	0.089	0.071	0.004(2)	0.994(5)	0.001(4)
SDSS J080434.20+510349.2	17.843(5)	240	1	0.126	0.0590	0.927(15)	0.072(15)	0.000(0)
SDSS J080534.49+072029.1	18.503(8)	540	4	0.072	0.2297	0.000(0)	0.290(171)	0.710(171)
SDSS J080534.49+072029.1	18.561(8)	540	4	0.072	0.2297	0.000(0)	0.023(15)	0.977(15)
SDSS J080534.49+072029.1	18.659(8)	540	4	0.072	0.2297	0.000(0)	0.031(24)	0.969(24)
SDSS J080846.19+313106.0	18.807(9)	946	2	0.138	0.2059	0.000(0)	0.003(1)	0.997(1)
SDSS J080846.19+313106.0	19.430(12)	946	2	0.138	0.2059	0.000(0)	0.000(0)	1.000(0)
SDSS J081207.63+131824.4	19.203(10)	530	1	0.071	0.0752 <sup>  </sup>	0.008(7)	0.912(110)	0.080(107)
SDSS J081207.63+131824.4	19.266(11)	530	1	0.071	0.0752 <sup>  </sup>	0.008(2)	0.991(6)	0.001(5)
SDSS J082457.15+073702.4	22.131(122)	2950	6	0.101	–	0.023(134)	0.250(395)	0.727(407)
SDSS J083754.64+564506.7	18.985(9)	417	5	0.180	–	0.038(51)	0.962(51)	0.000(0)
SDSS J083931.35+282824.0	20.226(20)	540	2	0.162	0.0760 <sup>  </sup>	0.007(6)	0.993(6)	0.000(0)
SDSS J083931.35+282824.0	20.443(25)	540	2	0.162	0.0760 <sup>  </sup>	0.450(253)	0.543(253)	0.007(22)
SDSS J083931.35+282824.0	20.481(35)	540	2	0.162	0.0760 <sup>  </sup>	0.005(7)	0.895(206)	0.100(207)
SDSS J084026.16+220446.6	19.593(15)	1826	3	0.130	–	0.000(0)	0.183(121)	0.817(121)
SDSS J084026.16+220446.6	19.894(16)	1826	3	0.130	–	0.575(196)	0.316(194)	0.109(214)
SDSS J084400.10+023919.3	18.441(7)	833	2	0.124	0.207	0.000(0)	0.000(0)	1.000(0)
SDSS J084400.10+023919.3	18.335(7)	833	2	0.124	0.207	0.000(0)	0.022(7)	0.978(7)
SDSS J084400.10+023919.3	18.906(10)	833	2	0.124	0.207	0.000(0)	0.208(131)	0.792(131)
SDSS J085623.00+310834.0	19.967(17)	647	5	0.087	–	0.903(55)	0.097(55)	0.000(0)
SDSS J085623.00+310834.0	19.950(18)	647	5	0.087	–	0.641(292)	0.359(292)	0.000(0)
SDSS J085623.00+310834.0	20.028(16)	647	5	0.087	–	0.868(102)	0.132(102)	0.000(0)
SDSS J085623.00+310834.0	20.052(17)	647	5	0.087	–	0.460(299)	0.539(299)	0.000(0)
SDSS J090016.56+430118.2	18.876(9)	1491	2	0.075	0.2094	0.000(0)	0.000(0)	1.000(0)
SDSS J090103.93+480911.1	19.237(11)	450	1	0.077	0.0779	0.077(25)	0.694(185)	0.228(191)
SDSS J090350.73+330036.1	18.829(8)	257	1	0.064	0.0591	0.360(69)	0.640(69)	0.000(0)
SDSS J090403.48+035501.2	19.218(12)	300	1	0.102	0.0597	0.845(56)	0.155(57)	0.001(1)
SDSS J090403.48+035501.2	19.304(12)	300	1	0.102	0.0597	0.830(58)	0.170(58)	0.000(0)
SDSS J090403.48+035501.2	19.335(12)	300	1	0.102	0.0597	0.722(80)	0.276(80)	0.001(4)

\*Method of distance estimation. 1: from Patterson (2011) and other references (see text),

2: determined from  $P_{\text{orb}}$  and maximum magnitude, 3: from estimated  $P_{\text{orb}}$  and maximum magnitude,4: from  $P_{\text{orb}}$  and minimum magnitude, 5: from estimated  $P_{\text{orb}}$  and minimum magnitude6: assuming maximum  $M_V = 4.95$ .<sup>†</sup> $P_{\text{orb}} < 0.06$  (d).<sup>‡</sup> $0.06 \leq P_{\text{orb}} < 0.10$  (d).<sup>§</sup> $P_{\text{orb}} \geq 0.10$  (d).<sup>||</sup>Determined from superhump period.

#Dwarf novae proposed by Wils et al. (2010).

**Table 4.** Estimated extinction and neural network classification (continued)

Object	$g$	$d$ (pc)	type*	$A_V$	$P_{\text{orb}}$	ultrashort <sup>†</sup>	short <sup>‡</sup>	long <sup>§</sup>
SDSS J090452.09+440255.4	19.381(13)	498	5	0.051	—	0.920(62)	0.080(62)	0.000(0)
SDSS J090628.25+052656.9	18.761(9)	1448	3	0.148	—	0.000(0)	0.017(13)	0.983(13)
SDSS J090628.25+052656.9	19.415(12)	1448	3	0.148	—	0.000(0)	0.000(0)	1.000(0)
SDSS J091001.63+164820.0	18.832(9)	434	5	0.106	—	0.010(7)	0.989(7)	0.000(0)
SDSS J091001.63+164820.0	18.781(9)	434	5	0.106	—	0.006(1)	0.994(1)	0.000(0)
SDSS J091001.63+164820.0	18.967(9)	434	5	0.106	—	0.002(1)	0.995(4)	0.002(3)
SDSS J091001.63+164820.0	19.252(11)	434	5	0.106	—	0.003(1)	0.994(6)	0.003(5)
SDSS J091127.36+084140.7	19.729(14)	1385	2	0.208	0.2054	0.000(0)	0.000(0)	1.000(0)
SDSS J091945.11+085710.1	18.191(6)	270	1	0.134	0.0565	0.966(8)	0.033(8)	0.000(0)
SDSS J092219.55+421256.7	19.882(14)	653	5	0.055	—	0.207(101)	0.793(102)	0.001(3)
SDSS J092229.26+330743.6	18.439(7)	335	5	0.051	—	0.003(1)	0.997(1)	0.000(0)
SDSS J092229.26+330743.6	18.590(8)	335	5	0.051	—	0.008(2)	0.991(2)	0.000(0)
SDSS J092229.26+330743.6	18.435(7)	335	5	0.051	—	0.055(18)	0.945(18)	0.000(0)
SDSS J093249.57+472523.0	17.768(5)	834	2	0.051	0.0663	0.676(28)	0.323(28)	0.000(0)
SDSS J094002.56+274942.0	19.096(10)	1377	3	0.059	—	0.000(0)	0.000(0)	1.000(0)
SDSS J094325.90+520128.8	18.320(7)	1408	3	0.030	—	0.003(1)	0.995(1)	0.002(1)
SDSS J094325.90+520128.8	18.304(12)	1408	3	0.030	—	0.000(0)	0.997(2)	0.003(1)
SDSS J094325.90+520128.8	17.977(6)	1408	3	0.030	—	0.073(16)	0.924(18)	0.003(4)
SDSS J094325.90+520128.8	18.749(8)	1408	3	0.030	—	0.004(1)	0.995(1)	0.000(0)
SDSS J094558.24+292253.2	19.064(10)	418	5	0.073	—	0.994(2)	0.006(2)	0.000(0)
SDSS J095135.21+602939.6	19.996(18)	658	5	0.058	—	0.746(120)	0.254(120)	0.000(0)
SDSS J095135.21+602939.6	19.956(18)	658	5	0.058	—	0.747(135)	0.252(135)	0.000(1)
SDSS J100515.39+191108.0	18.173(6)	280	2	0.083	0.0752 <sup>  </sup>	0.029(8)	0.963(16)	0.008(10)
SDSS J100658.40+233724.4	18.311(7)	1366	2	0.103	0.1859	0.000(0)	0.009(7)	0.991(7)
SDSS J100658.40+233724.4	18.691(8)	1366	2	0.103	0.1859	0.000(0)	0.000(0)	1.000(0)
SDSS J101037.05+024915.0	20.701(27)	908	5	0.099	—	0.001(2)	0.985(56)	0.014(55)
SDSS J101037.05+024915.0	20.755(33)	908	5	0.099	—	0.001(1)	0.918(182)	0.081(182)
SDSS J101037.05+024915.0	21.990(89)	908	5	0.099	—	0.112(245)	0.725(373)	0.163(321)
SDSS J101323.64+455858.9	18.818(9)	419	5	0.026	—	0.011(3)	0.966(19)	0.023(19)
SDSS J102517.94+430221.2	19.938(16)	637	5	0.030	—	0.353(295)	0.513(270)	0.134(244)
SDSS J102517.94+430221.2	19.964(16)	637	5	0.030	—	0.235(278)	0.745(277)	0.020(93)
SDSS J103147.99+085224.3	18.795(8)	1056	3	0.083	—	0.010(3)	0.731(239)	0.259(241)
SDSS J103533.02+055158.3	18.786(9)	220	1	0.080	0.0570	0.665(118)	0.335(118)	0.000(0)
SDSS J110014.72+131552.1	18.648(8)	631	2	0.054	0.0657 <sup>  </sup>	0.008(3)	0.915(22)	0.077(22)
SDSS J110014.72+131552.1	19.041(11)	631	2	0.054	0.0657 <sup>  </sup>	0.022(13)	0.978(13)	0.000(0)
SDSS J110706.76+340526.8	19.467(12)	1539	5	0.062	—	0.000(0)	0.000(0)	1.000(0)
SDSS J113215.50+624900.4	18.422(7)	354	5	0.031	—	0.109(32)	0.890(32)	0.001(0)
SDSS J113215.50+624900.4	18.390(7)	354	5	0.031	—	0.007(2)	0.988(4)	0.005(2)
SDSS J113215.50+624900.4	18.472(7)	354	5	0.031	—	0.090(17)	0.909(17)	0.001(0)
SDSS J113215.50+624900.4	18.497(8)	354	5	0.031	—	0.075(20)	0.916(21)	0.009(4)
SDSS J113551.09+532246.2	20.798(31)	1007	3	0.032	—	0.000(0)	0.425(422)	0.575(422)
SDSS J114628.80+675909.7	18.607(8)	865	2	0.040	0.0617 <sup>  </sup>	0.033(41)	0.946(48)	0.021(35)
SDSS J114628.80+675909.7	18.753(8)	865	2	0.040	0.0617 <sup>  </sup>	0.016(7)	0.963(17)	0.021(13)
SDSS J115207.00+404947.8	19.247(11)	430	1	0.062	0.0677	0.188(61)	0.747(126)	0.065(108)
SDSS J120231.01+450349.1	19.946(14)	406	3	0.047	—	0.728(89)	0.272(89)	0.000(0)
SDSS J121607.03+052013.9	20.015(18)	400	1	0.071	0.0686	0.223(281)	0.776(281)	0.001(5)
SDSS J121607.03+052013.9	20.138(18)	400	1	0.071	0.0686	0.119(180)	0.790(247)	0.091(222)
SDSS J122740.83+513925.0	19.067(10)	380	1	0.054	0.0630	0.112(32)	0.888(32)	0.000(0)
SDSS J123813.73-033933.0	17.782(5)	140	1	0.072	0.0559	0.932(15)	0.068(15)	0.001(0)
SDSS J124058.03-015919.2	19.556(13)	379	2	0.087	0.0259	0.978(24)	0.022(24)	0.000(0)

\*Method of distance estimation. 1: from Patterson (2011) and other references (see text),

2: determined from  $P_{\text{orb}}$  and maximum magnitude, 3: from estimated  $P_{\text{orb}}$  and maximum magnitude,4: from  $P_{\text{orb}}$  and minimum magnitude, 5: from estimated  $P_{\text{orb}}$  and minimum magnitude6: assuming maximum  $M_V = 4.95$ .<sup>†</sup> $P_{\text{orb}} < 0.06$  (d).<sup>‡</sup> $0.06 \leq P_{\text{orb}} < 0.10$  (d).<sup>§</sup> $P_{\text{orb}} \geq 0.10$  (d).<sup>||</sup>Determined from superhump period.<sup>#</sup>Dwarf novae proposed by Wils et al. (2010).

**Table 4.** Estimated extinction and neural network classification (continued)

Object	$g$	$d$ (pc)	type*	$A_V$	$P_{\text{orb}}$	ultrashort <sup>†</sup>	short <sup>‡</sup>	long <sup>§</sup>
SDSS J124058.03−015919.2	19.545(13)	379	2	0.087	0.0259	0.962(78)	0.038(78)	0.000(0)
SDSS J124417.89+300401.0	19.571(12)	871	3	0.054	—	0.040(21)	0.960(21)	0.000(0)
SDSS J124426.26+613514.6	18.753(9)	3067	2	0.050	0.0992	0.024(7)	0.867(68)	0.110(68)
SDSS J124426.26+613514.6	18.718(8)	3067	2	0.050	0.0992	0.043(10)	0.956(10)	0.001(1)
SDSS J124819.36+072049.4	21.326(46)	1887	3	0.097	—	0.321(316)	0.462(349)	0.217(339)
SDSS J124819.36+072049.4	21.371(59)	1887	3	0.097	—	0.053(152)	0.684(403)	0.264(391)
SDSS J125023.85+665525.5	18.651(8)	320	1	0.050	0.0587	0.534(67)	0.465(68)	0.000(1)
SDSS J125834.77+663551.6	20.566(25)	881	5	0.053	—	0.000(2)	0.993(19)	0.007(19)
SDSS J130514.73+582856.3	19.283(11)	2370	3	0.025	—	0.035(19)	0.665(110)	0.300(117)
SDSS J133941.11+484727.5	17.678(5)	180	1	0.021	0.0573	0.950(7)	0.050(7)	0.000(0)
SDSS J140429.37+172359.4	17.495(5)	562	3	0.099	—	0.256(27)	0.744(27)	0.000(0)
SDSS J142955.86+414516.8	17.695(5)	2978	2	0.037	0.059	0.328(34)	0.666(33)	0.005(1)
SDSS J143317.78+101123.3	18.554(8)	250	1	0.088	0.0542	0.675(79)	0.323(80)	0.001(3)
SDSS J143544.02+233638.7	18.200(6)	3564	2	0.112	0.054	0.986(3)	0.014(3)	0.000(0)
SDSS J143544.02+233638.7	18.285(6)	3564	2	0.112	0.054	0.983(5)	0.017(5)	0.000(0)
SDSS J145003.12+584501.9	20.630(24)	921	5	0.036	—	0.230(310)	0.711(311)	0.059(165)
SDSS J145003.12+584501.9	20.742(31)	921	5	0.036	—	0.445(406)	0.359(381)	0.196(360)
SDSS J145758.21+514807.9	19.158(10)	360	1	0.083	0.0541	0.784(128)	0.216(128)	0.000(1)
SDSS J145758.21+514807.9	19.159(11)	360	1	0.083	0.0541	0.909(74)	0.089(74)	0.001(3)
SDSS J145758.21+514807.9	19.536(12)	360	1	0.083	0.0541	0.704(145)	0.296(146)	0.000(1)
SDSS J150137.22+550123.4	19.386(12)	330	1	0.037	0.0568	0.796(111)	0.203(111)	0.000(1)
SDSS J150240.98+333423.9	17.496(5)	170	1	0.038	0.0589	0.491(24)	0.508(23)	0.001(1)
SDSS J150240.98+333423.9	17.575(5)	170	1	0.038	0.0589	0.698(32)	0.302(32)	0.000(0)
SDSS J150722.30+523039.8	18.311(7)	230	1	0.052	0.0463	0.789(34)	0.211(34)	0.000(0)
SDSS J151413.72+454911.9	19.675(14)	350	1	0.080	—	0.463(243)	0.537(243)	0.000(0)
SDSS J152212.20+080340.9	18.379(7)	1087	3	0.110	—	0.371(66)	0.625(69)	0.004(4)
SDSS J152212.20+080340.9	18.981(9)	1087	3	0.110	—	0.010(3)	0.990(3)	0.000(0)
SDSS J152419.33+220920.0	19.055(9)	420	1	0.166	0.0653	0.024(8)	0.975(9)	0.001(2)
SDSS J152717.96+543724.9	20.140(18)	777	5	0.047	—	0.509(213)	0.483(216)	0.008(17)
SDSS J152717.96+543724.9	20.286(19)	777	5	0.047	—	0.276(171)	0.719(172)	0.004(9)
SDSS J152717.96+543724.9	20.296(23)	777	5	0.047	—	0.327(198)	0.672(199)	0.001(3)
SDSS J152857.86+034911.7	19.506(14)	1581	3	0.166	—	0.011(5)	0.986(6)	0.003(2)
SDSS J153015.04+094946.3	18.867(9)	874	3	0.129	—	0.002(2)	0.829(141)	0.169(142)
SDSS J153015.04+094946.3	18.516(8)	874	3	0.129	—	0.101(27)	0.666(54)	0.233(60)
SDSS J153634.42+332851.9	19.209(10)	1013	3	0.105	—	0.010(3)	0.820(109)	0.170(109)
SDSS J153817.35+512338.0	18.547(7)	340	4	0.044	0.0647	0.643(86)	0.357(86)	0.000(0)
SDSS J154453.60+255348.8	16.579(4)	230	4	0.160	0.2513	0.000(0)	0.236(84)	0.764(84)
SDSS J154453.60+255348.8	17.175(5)	230	4	0.160	0.2513	0.000(0)	0.000(0)	1.000(0)
SDSS J155037.27+405440.0	18.542(8)	355	5	0.048	—	0.056(14)	0.940(16)	0.004(3)
SDSS J155037.27+405440.0	18.413(7)	355	5	0.048	—	0.001(1)	0.910(73)	0.089(74)
SDSS J155531.99−001055.0	19.052(12)	439	4	0.383	0.0789	0.059(26)	0.940(27)	0.001(2)
SDSS J155531.99−001055.0	19.322(11)	439	4	0.383	0.0789	0.056(22)	0.935(21)	0.009(4)
SDSS J155644.24−000950.2	18.246(7)	340	1	0.453	0.0800	0.027(4)	0.973(4)	0.000(0)
SDSS J155644.24−000950.2	18.010(6)	340	1	0.453	0.0800	0.017(2)	0.969(16)	0.015(15)
SDSS J155644.24−000950.2	18.285(8)	340	1	0.453	0.0800	0.010(2)	0.989(2)	0.001(0)
SDSS J155656.92+352336.6	18.923(9)	2036	2	0.070	0.0892	0.217(53)	0.663(160)	0.121(160)
SDSS J155644.24−000950.2	18.006(8)	340	1	0.453	0.0800	0.016(2)	0.967(21)	0.017(20)
SDSS J155720.75+180720.2	18.683(8)	368	4	0.119	0.088	0.009(3)	0.991(3)	0.000(0)
SDSS J155720.75+180720.2	18.644(7)	368	4	0.119	0.088	0.001(0)	0.965(17)	0.035(17)
SDSS J160111.53+091712.7	20.122(20)	872	5	0.131	—	0.559(201)	0.441(201)	0.000(0)

\*Method of distance estimation. 1: from Patterson (2011) and other references (see text),

2: determined from  $P_{\text{orb}}$  and maximum magnitude, 3: from estimated  $P_{\text{orb}}$  and maximum magnitude,4: from  $P_{\text{orb}}$  and minimum magnitude, 5: from estimated  $P_{\text{orb}}$  and minimum magnitude6: assuming maximum  $M_V = 4.95$ .<sup>†</sup> $P_{\text{orb}} < 0.06$  (d).<sup>‡</sup> $0.06 \leq P_{\text{orb}} < 0.10$  (d).<sup>§</sup> $P_{\text{orb}} \geq 0.10$  (d).<sup>||</sup>Determined from superhump period.<sup>#</sup>Dwarf novae proposed by Wils et al. (2010).

**Table 4.** Estimated extinction and neural network classification (continued)

Object	$g$	$d$ (pc)	type*	$A_V$	$P_{\text{orb}}$	ultrashort <sup>†</sup>	short <sup>‡</sup>	long <sup>§</sup>
SDSS J160111.53+091712.7	20.603(26)	872	5	0.131	–	0.000(1)	0.571(395)	0.429(395)
SDSS J160419.02+161548.5	19.082(10)	1592	3	0.119	–	0.063(13)	0.933(14)	0.004(2)
SDSS J160501.35+203056.9	19.361(11)	199	2	0.191	0.0567	0.896(54)	0.104(54)	0.000(0)
SDSS J160501.35+203056.9	19.883(15)	199	2	0.191	0.0567	0.756(167)	0.243(167)	0.002(5)
SDSS J160501.35+203056.9	19.891(15)	199	2	0.191	0.0567	0.907(74)	0.092(74)	0.001(1)
SDSS J160501.35+203056.9	19.926(16)	199	2	0.191	0.0567	0.916(81)	0.083(81)	0.000(0)
SDSS J161030.35+445901.7	19.753(15)	585	5	0.049	–	0.966(74)	0.032(62)	0.002(17)
SDSS J161332.56–000331.0	18.600(8)	845	3	0.448	–	0.000(0)	0.000(0)	1.000(0)
SDSS J161909.10+135145.5	18.494(8)	3124	3	0.207	–	0.000(0)	0.000(0)	1.000(0)
SDSS J162212.45+341147.3	19.168(10)	683	5	0.064	–	0.000(0)	0.000(0)	1.000(0)
SDSS J162212.45+341147.3	19.119(10)	683	5	0.064	–	0.000(0)	0.000(0)	1.000(0)
SDSS J162212.45+341147.3	19.116(10)	683	5	0.064	–	0.000(0)	0.000(0)	1.000(0)
SDSS J162718.39+120435.0	20.225(18)	799	2	0.205	0.1041 <sup>  </sup>	0.000(0)	0.304(306)	0.696(306)
SDSS J162830.89+240259.1	19.737(16)	837	3	0.195	–	0.075(42)	0.882(129)	0.043(111)
SDSS J162830.89+240259.1	19.780(14)	837	3	0.195	–	0.392(103)	0.606(105)	0.001(9)
SDSS J162830.89+240259.1	19.998(16)	837	3	0.195	–	0.024(13)	0.592(320)	0.384(328)
SDSS J163722.21–001957.1	20.536(41)	1100	1	0.394	0.0674	0.013(36)	0.979(45)	0.007(27)
SDSS J164248.52+134751.4	18.651(8)	913	2	0.242	0.0789	0.094(31)	0.899(37)	0.006(9)
SDSS J165244.84+333925.4	20.854(28)	4377	3	0.080	–	0.066(65)	0.907(136)	0.027(118)
SDSS J165359.06+201010.4	18.562(8)	723	2	0.241	0.0635 <sup>  </sup>	0.037(8)	0.670(68)	0.294(71)
SDSS J165359.06+201010.4	18.656(8)	723	2	0.241	0.0635 <sup>  </sup>	0.045(9)	0.863(26)	0.093(27)
SDSS J165658.13+212139.3	18.487(7)	2037	2	0.190	0.0631	0.044(8)	0.956(8)	0.000(0)
SDSS J165658.13+212139.3	18.913(9)	2037	2	0.190	0.0631	0.035(12)	0.965(12)	0.000(0)
SDSS J165837.70+184727.4	20.074(17)	640	1	0.260	0.0681	0.429(187)	0.521(201)	0.050(72)
SDSS J165837.70+184727.4	20.189(17)	640	1	0.260	0.0681	0.116(99)	0.762(241)	0.121(254)
SDSS J170213.26+322954.1	17.908(6)	440	1	0.070	0.1001	0.000(0)	0.034(25)	0.966(25)
SDSS J170324.09+320953.2	18.138(6)	1143	3	0.090	–	0.000(0)	0.000(0)	1.000(0)
SDSS J170542.54+313240.8	19.668(12)	2789	3	0.118	–	0.000(0)	0.000(0)	1.000(0)
SDSS J171145.08+301320.0	20.016(16)	693	4	0.145	0.0558	0.214(104)	0.619(252)	0.167(284)
SDSS J171145.08+301320.0	20.186(18)	693	4	0.145	0.0558	0.546(131)	0.393(139)	0.062(126)
SDSS J171145.08+301320.0	20.205(18)	693	4	0.145	0.0558	0.752(106)	0.242(106)	0.006(12)
SDSS J204448.92–045928.8	16.941(5)	5035	2	0.174	1.68	0.000(0)	0.000(0)	1.000(0)
SDSS J204448.92–045928.8	16.844(5)	5035	2	0.174	1.68	0.000(0)	0.000(0)	1.000(0)
SDSS J204720.76+000007.7	19.448(12)	470	5	0.299	–	0.051(27)	0.941(28)	0.008(6)
SDSS J204720.76+000007.7	19.351(11)	470	5	0.299	–	0.594(93)	0.400(92)	0.007(5)
SDSS J204720.76+000007.7	20.078(17)	470	5	0.299	–	0.001(1)	0.999(1)	0.000(0)
SDSS J204720.76+000007.7	20.270(20)	470	5	0.299	–	0.022(22)	0.977(23)	0.001(2)
SDSS J204720.76+000007.7	20.300(20)	470	5	0.299	–	0.120(70)	0.880(70)	0.000(0)
SDSS J204720.76+000007.7	20.286(21)	470	5	0.299	–	0.078(66)	0.903(69)	0.019(24)
SDSS J204720.76+000007.7	20.422(29)	470	5	0.299	–	0.015(17)	0.964(42)	0.021(38)
SDSS J204720.76+000007.7	20.314(20)	470	5	0.299	–	0.311(157)	0.656(161)	0.033(45)
SDSS J204720.76+000007.7	20.495(28)	470	5	0.299	–	0.121(112)	0.860(121)	0.019(44)
SDSS J204720.76+000007.7	20.677(35)	470	5	0.299	–	0.182(183)	0.816(183)	0.002(6)
SDSS J204739.40+000840.3	22.213(131)	3537	3	0.316	–	0.000(1)	0.465(459)	0.535(460)
SDSS J204817.85–061044.8	19.340(12)	762	2	0.207	0.0606	0.072(27)	0.928(28)	0.000(0)
SDSS J205914.87–061220.5	18.354(7)	938	2	0.154	0.0747	0.021(5)	0.716(68)	0.264(71)
SDSS J210014.12+004446.0	17.961(6)	769	2	0.249	0.0840 <sup>  </sup>	0.769(40)	0.204(34)	0.027(13)
SDSS J210014.12+004446.0	18.047(6)	769	2	0.249	0.0840 <sup>  </sup>	0.256(48)	0.414(41)	0.330(77)
SDSS J210014.12+004446.0	17.828(6)	769	2	0.249	0.0840 <sup>  </sup>	0.455(35)	0.494(63)	0.051(49)
SDSS J210014.12+004446.0	18.041(6)	769	2	0.249	0.0840 <sup>  </sup>	0.282(36)	0.541(100)	0.177(112)

\*Method of distance estimation. 1: from Patterson (2011) and other references (see text),

2: determined from  $P_{\text{orb}}$  and maximum magnitude, 3: from estimated  $P_{\text{orb}}$  and maximum magnitude,4: from  $P_{\text{orb}}$  and minimum magnitude, 5: from estimated  $P_{\text{orb}}$  and minimum magnitude6: assuming maximum  $M_V = 4.95$ .<sup>†</sup> $P_{\text{orb}} < 0.06$  (d).<sup>‡</sup> $0.06 \leq P_{\text{orb}} < 0.10$  (d).<sup>§</sup> $P_{\text{orb}} \geq 0.10$  (d).<sup>||</sup>Determined from superhump period.

#Dwarf novae proposed by Wils et al. (2010).



**Table 4.** Estimated extinction and neural network classification (continued)

Object	$g$	$d$ (pc)	type*	$A_V$	$P_{\text{orb}}$	ultrashort <sup>†</sup>	short <sup>‡</sup>	long <sup>§</sup>
SDSS J210014.12+004446.0	18.380(7)	769	2	0.249	0.0840 <sup>  </sup>	0.108(26)	0.872(41)	0.020(22)
SDSS J210014.12+004446.0	18.366(7)	769	2	0.249	0.0840 <sup>  </sup>	0.295(68)	0.639(95)	0.066(63)
SDSS J210014.12+004446.0	18.453(7)	769	2	0.249	0.0840 <sup>  </sup>	0.046(10)	0.638(95)	0.315(98)
SDSS J210014.12+004446.0	18.574(8)	769	2	0.249	0.0840 <sup>  </sup>	0.058(15)	0.885(32)	0.056(33)
SDSS J210014.12+004446.0	18.407(12)	769	2	0.249	0.0840 <sup>  </sup>	0.242(52)	0.594(85)	0.164(105)
SDSS J210014.12+004446.0	18.630(8)	769	2	0.249	0.0840 <sup>  </sup>	0.093(18)	0.844(24)	0.063(23)
SDSS J210014.12+004446.0	18.731(8)	769	2	0.249	0.0840 <sup>  </sup>	0.165(33)	0.824(33)	0.011(8)
SDSS J210014.12+004446.0	18.714(11)	769	2	0.249	0.0840 <sup>  </sup>	0.152(33)	0.794(41)	0.053(25)
SDSS J210014.12+004446.0	18.808(9)	769	2	0.249	0.0840 <sup>  </sup>	0.128(33)	0.821(31)	0.050(24)
SDSS J210449.94+010545.8	19.974(35)	1202	3	0.421	—	0.623(201)	0.373(199)	0.004(9)
SDSS J210449.94+010545.8	19.968(22)	1202	3	0.421	—	0.036(20)	0.755(190)	0.209(190)
SDSS J210449.94+010545.8	20.137(22)	1202	3	0.421	—	0.056(49)	0.847(165)	0.097(152)
SDSS J210449.94+010545.8	20.242(20)	1202	3	0.421	—	0.001(2)	0.518(269)	0.481(269)
SDSS J210449.94+010545.8	20.215(31)	1202	3	0.421	—	0.140(135)	0.779(194)	0.081(151)
SDSS J210449.94+010545.8	20.304(19)	1202	3	0.421	—	0.040(36)	0.942(73)	0.018(50)
SDSS J210449.94+010545.8	20.299(24)	1202	3	0.421	—	0.018(13)	0.772(303)	0.210(306)
SDSS J210449.94+010545.8	20.965(100)	1202	3	0.421	—	0.058(118)	0.924(132)	0.018(57)
SDSS J210449.94+010545.8	20.824(30)	1202	3	0.421	—	0.087(117)	0.862(148)	0.051(113)
SDSS J210449.94+010545.8	20.654(53)	1202	3	0.421	—	0.047(75)	0.735(340)	0.218(354)
SDSS J210449.94+010545.8	21.020(35)	1202	3	0.421	—	0.160(173)	0.837(174)	0.003(10)
SDSS J210449.94+010545.8	21.061(43)	1202	3	0.421	—	0.067(85)	0.860(201)	0.073(195)
SDSS J210449.94+010545.8	21.086(52)	1202	3	0.421	—	0.164(221)	0.639(339)	0.197(336)
SDSS J211605.43+113407.5	21.689(68)	940	3	0.236	—	0.109(279)	0.754(408)	0.137(335)
SDSS J211605.43+113407.5	21.747(68)	940	3	0.236	—	0.484(455)	0.174(356)	0.342(446)
SDSS J211605.43+113407.5	21.873(75)	940	3	0.236	—	0.330(404)	0.350(412)	0.320(425)
SDSS J211605.43+113407.5	21.677(73)	940	3	0.236	—	0.060(205)	0.337(444)	0.603(466)
SDSS J214354.60+124458.0	16.176(4)	81	5	0.107	—	0.002(0)	0.998(0)	0.000(0)
SDSS J220553.98+115553.7	20.029(16)	650	1	0.297	0.0575	0.951(46)	0.049(46)	0.001(2)
SDSS J220553.98+115553.7	20.030(21)	650	1	0.297	0.0575	0.914(212)	0.086(212)	0.000(0)
SDSS J220553.98+115553.7	20.068(18)	650	1	0.297	0.0575	0.927(38)	0.073(38)	0.000(1)
SDSS J223252.35+140353.0	22.163(77)	6160	3	0.196	—	0.000(0)	0.018(92)	0.982(92)
SDSS J223252.35+140353.0	22.377(88)	6160	3	0.196	—	0.000(0)	0.000(0)	1.000(0)
SDSS J223439.93+004127.2	17.666(5)	771	2	0.274	0.0884	0.094(10)	0.885(14)	0.021(10)
SDSS J223439.93+004127.2	17.723(5)	771	2	0.274	0.0884	0.057(8)	0.863(27)	0.080(28)
SDSS J223439.93+004127.2	17.739(5)	771	2	0.274	0.0884	0.049(8)	0.945(15)	0.007(8)
SDSS J223439.93+004127.2	18.014(6)	771	2	0.274	0.0884	0.010(1)	0.975(3)	0.015(4)
SDSS J223439.93+004127.2	18.020(6)	771	2	0.274	0.0884	0.011(2)	0.989(2)	0.000(0)
SDSS J223439.93+004127.2	17.921(6)	771	2	0.274	0.0884	0.043(6)	0.854(23)	0.103(26)
SDSS J223439.93+004127.2	17.747(6)	771	2	0.274	0.0884	0.030(5)	0.967(8)	0.002(3)
SDSS J223439.93+004127.2	17.928(8)	771	2	0.274	0.0884	0.029(5)	0.719(59)	0.252(59)
SDSS J223439.93+004127.2	18.095(6)	771	2	0.274	0.0884	0.015(4)	0.984(4)	0.000(0)
SDSS J223439.93+004127.2	18.203(7)	771	2	0.274	0.0884	0.002(0)	0.958(17)	0.041(16)
SDSS J223439.93+004127.2	18.047(6)	771	2	0.274	0.0884	0.073(9)	0.865(40)	0.062(35)
SDSS J223439.93+004127.2	18.305(8)	771	2	0.274	0.0884	0.010(2)	0.970(22)	0.021(20)
SDSS J223439.93+004127.2	18.331(7)	771	2	0.274	0.0884	0.055(10)	0.893(46)	0.052(43)
SDSS J223439.93+004127.2	18.483(8)	771	2	0.274	0.0884	0.002(3)	0.412(193)	0.586(195)
SDSS J223439.93+004127.2	18.423(7)	771	2	0.274	0.0884	0.004(2)	0.996(2)	0.000(0)
SDSS J223439.93+004127.2	18.606(8)	771	2	0.274	0.0884	0.011(2)	0.793(80)	0.196(82)
SDSS J223439.93+004127.2	18.713(8)	771	2	0.274	0.0884	0.019(7)	0.981(8)	0.000(1)
SDSS J225831.18−094931.7	15.102(3)	410	1	0.124	0.0830 <sup>  </sup>	0.148(11)	0.549(15)	0.303(18)

\*Method of distance estimation. 1: from Patterson (2011) and other references (see text),

2: determined from  $P_{\text{orb}}$  and maximum magnitude, 3: from estimated  $P_{\text{orb}}$  and maximum magnitude,4: from  $P_{\text{orb}}$  and minimum magnitude, 5: from estimated  $P_{\text{orb}}$  and minimum magnitude6: assuming maximum  $M_V = 4.95$ .<sup>†</sup> $P_{\text{orb}} < 0.06$  (d).<sup>‡</sup> $0.06 \leq P_{\text{orb}} < 0.10$  (d).<sup>§</sup> $P_{\text{orb}} \geq 0.10$  (d).<sup>||</sup>Determined from superhump period.<sup>#</sup>Dwarf novae proposed by Wils et al. (2010).

**Table 4.** Estimated extinction and neural network classification (continued)

Object	$g$	$d$ (pc)	type*	$A_V$	$P_{\text{orb}}$	ultrashort <sup>†</sup>	short <sup>‡</sup>	long <sup>§</sup>
SDSS J225831.18−094931.7	15.587(3)	410	1	0.124	0.0830 <sup>  </sup>	0.086(5)	0.914(5)	0.000(0)
SDSS J233325.92+152222.2	18.521(7)	355	4	0.206	0.0577	0.411(55)	0.588(55)	0.000(0)
SDSS J233325.92+152222.2	18.745(9)	355	4	0.206	0.0577	0.069(35)	0.922(31)	0.010(9)
SDSS J233325.92+152222.2	18.761(8)	355	4	0.206	0.0577	0.429(65)	0.532(60)	0.039(19)
SDSSp J081321.91+452809.4	18.259(7)	1933	2	0.159	0.289	0.000(0)	0.000(0)	1.000(0)
SDSSp J081321.91+452809.4	18.517(8)	1933	2	0.159	0.289	0.000(0)	0.000(0)	1.000(0)
SDSSp J081610.84+453010.2	20.056(17)	1454	3	0.195	—	0.000(0)	0.334(258)	0.666(258)
SDSSp J082409.73+493124.4	19.576(14)	1100	1	0.119	0.0677 <sup>  </sup>	0.010(5)	0.963(36)	0.027(34)
SDSSp J082409.73+493124.4	19.887(20)	1100	1	0.119	0.0677 <sup>  </sup>	0.011(8)	0.950(69)	0.039(68)
SDSSp J082409.73+493124.4	20.138(28)	1100	1	0.119	0.0677 <sup>  </sup>	0.004(5)	0.540(338)	0.456(340)
SDSSp J083845.23+491055.5	19.578(13)	1100	1	0.138	0.0696 <sup>  </sup>	0.030(17)	0.970(17)	0.000(0)
SDSSp J083845.23+491055.5	19.846(15)	1100	1	0.138	0.0696 <sup>  </sup>	0.075(42)	0.925(42)	0.000(0)
SDSSp J083845.23+491055.5	19.705(16)	1100	1	0.138	0.0696 <sup>  </sup>	0.087(47)	0.913(47)	0.000(0)
SDSSp J172601.96+543230.7	20.531(22)	823	5	0.107	—	0.473(235)	0.526(235)	0.001(1)
SDSSp J173008.38+624754.7	15.886(3)	450	1	0.083	0.0770 <sup>  </sup>	0.945(5)	0.054(5)	0.001(0)
SDSSp J173008.38+624754.7	16.318(4)	450	1	0.083	0.0770 <sup>  </sup>	0.142(30)	0.856(31)	0.001(1)
SDSSp J230351.64+010651.0	17.644(5)	564	2	0.172	0.0767	0.002(1)	0.981(6)	0.017(7)
SDSSp J230351.64+010651.0	17.907(6)	564	2	0.172	0.0767	0.003(1)	0.994(1)	0.003(1)
SDSSp J230351.64+010651.0	17.668(5)	564	2	0.172	0.0767	0.002(0)	0.998(0)	0.000(0)
SDSSp J230351.64+010651.0	17.973(6)	564	2	0.172	0.0767	0.002(0)	0.998(0)	0.000(0)
SDSSp J230351.64+010651.0	18.106(6)	564	2	0.172	0.0767	0.000(0)	0.063(27)	0.937(27)
SDSSp J230351.64+010651.0	17.975(6)	564	2	0.172	0.0767	0.003(1)	0.995(1)	0.002(0)
SDSSp J230351.64+010651.0	18.028(6)	564	2	0.172	0.0767	0.001(0)	0.997(1)	0.002(1)
SDSSp J230351.64+010651.0	17.863(6)	564	2	0.172	0.0767	0.004(1)	0.993(3)	0.003(3)
SDSSp J230351.64+010651.0	17.917(6)	564	2	0.172	0.0767	0.001(0)	0.999(0)	0.000(0)
SDSSp J230351.64+010651.0	17.928(6)	564	2	0.172	0.0767	0.010(2)	0.982(4)	0.007(3)
SDSSp J230351.64+010651.0	17.972(6)	564	2	0.172	0.0767	0.004(1)	0.956(11)	0.040(11)
SDSSp J230351.64+010651.0	17.938(6)	564	2	0.172	0.0767	0.003(1)	0.997(1)	0.000(0)
SDSSp J230351.64+010651.0	17.887(6)	564	2	0.172	0.0767	0.004(0)	0.942(38)	0.054(38)
SDSSp J230351.64+010651.0	17.853(6)	564	2	0.172	0.0767	0.006(1)	0.992(3)	0.002(2)
SDSSp J230351.64+010651.0	18.106(6)	564	2	0.172	0.0767	0.000(0)	0.711(87)	0.288(87)
SDSSp J230351.64+010651.0	18.176(6)	564	2	0.172	0.0767	0.006(1)	0.976(7)	0.018(7)
SDSSp J230351.64+010651.0	18.267(7)	564	2	0.172	0.0767	0.003(0)	0.984(3)	0.013(3)
SDSSp J230351.64+010651.0	18.151(6)	564	2	0.172	0.0767	0.000(0)	0.001(1)	0.999(1)
SDSSp J230351.64+010651.0	18.154(6)	564	2	0.172	0.0767	0.003(1)	0.997(1)	0.000(0)
SDSSp J230351.64+010651.0	18.018(6)	564	2	0.172	0.0767	0.016(3)	0.984(3)	0.000(0)
SDSSp J230351.64+010651.0	18.346(10)	564	2	0.172	0.0767	0.002(0)	0.970(11)	0.028(11)
SDSSp J230351.64+010651.0	18.167(6)	564	2	0.172	0.0767	0.002(0)	0.998(0)	0.000(0)
SDSSp J230351.64+010651.0	18.300(7)	564	2	0.172	0.0767	0.000(0)	0.508(195)	0.492(195)
SDSSp J230351.64+010651.0	18.568(8)	564	2	0.172	0.0767	0.002(1)	0.991(7)	0.007(7)
SDSSp J230351.64+010651.0	19.037(10)	564	2	0.172	0.0767	0.014(8)	0.986(8)	0.000(0)
SEKBO J140454.00−102702.14	19.733(15)	812	3	0.193	—	0.476(163)	0.521(163)	0.003(4)
SN 1964O	21.069(37)	849	3	0.045	—	0.435(324)	0.495(313)	0.070(228)
SDSS J013645.81−193949.1 <sup>#</sup>	20.288(23)	1526	3	0.040	—	0.013(18)	0.900(199)	0.087(200)
SDSS J015237.83−172019.3 <sup>#</sup>	21.040(47)	1446	3	0.064	—	0.046(115)	0.482(383)	0.473(397)
SDSS J015237.83−172019.3 <sup>#</sup>	21.397(54)	1446	3	0.064	—	0.060(130)	0.620(378)	0.319(384)
SDSS J032015.29+441059.3 <sup>#</sup>	18.768(8)	662	3	0.457	—	0.012(3)	0.984(4)	0.004(2)
SDSS J064911.48+102322.1 <sup>#</sup>	19.253(11)	219	5	0.191	—	0.004(4)	0.238(170)	0.758(171)
SDSS J073208.11+413008.7 <sup>#</sup>	20.869(36)	121	4	0.071	0.0771 <sup>  </sup>	0.000(0)	0.903(136)	0.097(136)
SDSS J073208.11+413008.7 <sup>#</sup>	20.755(28)	121	4	0.071	0.0771 <sup>  </sup>	0.001(1)	0.950(138)	0.049(138)

\*Method of distance estimation. 1: from Patterson (2011) and other references (see text),

2: determined from  $P_{\text{orb}}$  and maximum magnitude, 3: from estimated  $P_{\text{orb}}$  and maximum magnitude,4: from  $P_{\text{orb}}$  and minimum magnitude, 5: from estimated  $P_{\text{orb}}$  and minimum magnitude6: assuming maximum  $M_V = 4.95$ .<sup>†</sup> $P_{\text{orb}} < 0.06$  (d).<sup>‡</sup> $0.06 \leq P_{\text{orb}} < 0.10$  (d).<sup>§</sup> $P_{\text{orb}} \geq 0.10$  (d).<sup>||</sup>Determined from superhump period.<sup>#</sup>Dwarf novae proposed by Wils et al. (2010).

**Table 4.** Estimated extinction and neural network classification (continued)

Object	$g$	$d$ (pc)	type*	$A_V$	$P_{\text{orb}}$	ultrashort <sup>†</sup>	short <sup>‡</sup>	long <sup>§</sup>
SDSS J073758.55+205544.5 <sup>#</sup>	19.984(18)	195	5	0.075	—	0.941(61)	0.059(61)	0.000(0)
SDSS J074500.58+332859.6 <sup>#</sup>	22.185(82)	510	5	0.132	—	0.000(1)	0.189(332)	0.810(332)
SDSS J074500.58+332859.6 <sup>#</sup>	22.235(97)	510	5	0.132	—	0.000(0)	0.121(304)	0.879(304)
SDSS J074859.55+312512.6 <sup>#</sup>	17.768(5)	97	5	0.070	—	0.804(25)	0.162(17)	0.034(13)
SDSS J075107.50+300628.4 <sup>#</sup>	20.213(27)	866	3	0.161	—	0.008(8)	0.992(8)	0.000(1)
SDSS J075107.50+300628.4 <sup>#</sup>	19.777(15)	866	3	0.161	—	0.554(128)	0.443(128)	0.003(4)
SDSS J075117.00+100016.2 <sup>#</sup>	18.488(7)	692	3	0.058	—	0.193(38)	0.807(38)	0.000(0)
SDSS J075117.00+100016.2 <sup>#</sup>	18.429(7)	692	3	0.058	—	0.139(38)	0.860(39)	0.001(1)
SDSS J075713.81+222253.0 <sup>#</sup>	21.298(42)	2759	3	0.190	—	0.055(102)	0.936(114)	0.009(56)
SDSS J080033.86+192416.5 <sup>#</sup>	19.732(15)	1714	3	0.129	—	0.212(125)	0.787(126)	0.001(2)
SDSS J080033.86+192416.5 <sup>#</sup>	20.127(17)	1714	3	0.129	—	0.041(30)	0.948(57)	0.011(42)
SDSS J080033.86+192416.5 <sup>#</sup>	20.205(23)	1714	3	0.129	—	0.161(112)	0.790(120)	0.049(62)
SDSS J080306.99+284855.8 <sup>#</sup>	20.475(25)	1086	2	0.221	0.0727 <sup>  </sup>	0.037(38)	0.960(39)	0.003(9)
SDSS J081030.45+091111.7 <sup>#</sup>	22.778(125)	9735	3	0.070	—	0.003(16)	0.443(457)	0.554(460)
SDSS J081408.42+090759.1 <sup>#</sup>	20.692(24)	778	3	0.074	—	0.000(0)	0.343(390)	0.657(390)
SDSS J081408.42+090759.1 <sup>#</sup>	20.631(24)	778	3	0.074	—	0.000(0)	0.841(206)	0.159(206)
SDSS J081408.42+090759.1 <sup>#</sup>	20.704(32)	778	3	0.074	—	0.000(0)	0.309(377)	0.691(377)
SDSS J081408.42+090759.1 <sup>#</sup>	20.755(27)	778	3	0.074	—	0.000(0)	0.536(271)	0.464(271)
SDSS J081529.89+171152.5 <sup>#</sup>	21.849(56)	2419	3	0.147	—	0.198(305)	0.451(386)	0.351(410)
SDSS J082648.28−000037.7 <sup>#</sup>	21.020(35)	1317	3	0.158	—	0.104(122)	0.895(122)	0.001(2)
SDSS J082648.28−000037.7 <sup>#</sup>	21.172(37)	1317	3	0.158	—	0.109(259)	0.881(276)	0.011(96)
SDSS J083132.41+031420.7 <sup>#</sup>	21.175(44)	2308	3	0.099	—	0.026(50)	0.809(291)	0.165(297)
SDSS J083132.41+031420.7 <sup>#</sup>	21.518(66)	2308	3	0.099	—	0.630(372)	0.315(354)	0.055(180)
SDSS J083508.99+600643.9 <sup>#</sup>	21.625(60)	4495	3	0.148	—	0.021(65)	0.580(415)	0.399(420)
SDSS J084011.95+244709.8 <sup>#</sup>	20.579(24)	6342	3	0.109	—	0.984(33)	0.016(33)	0.000(0)
SDSS J084011.95+244709.8 <sup>#</sup>	21.007(32)	6342	3	0.109	—	0.673(289)	0.326(289)	0.000(1)
SDSS J084108.10+102536.2 <sup>#</sup>	20.247(18)	1030	3	0.166	—	0.034(27)	0.965(27)	0.001(2)
SDSS J084108.10+102536.2 <sup>#</sup>	21.027(43)	1030	3	0.166	—	0.216(235)	0.772(238)	0.011(77)
SDSS J084108.10+102536.2 <sup>#</sup>	20.822(48)	1030	3	0.166	—	0.442(384)	0.543(387)	0.015(82)
SDSS J091242.18+620940.1 <sup>#</sup>	18.818(8)	708	3	0.139	—	0.000(0)	0.999(0)	0.001(0)
SDSS J091741.29+073647.4 <sup>#</sup>	21.520(52)	3841	3	0.110	—	0.169(245)	0.355(363)	0.476(453)
SDSS J091741.29+073647.4 <sup>#</sup>	21.435(50)	3841	3	0.110	—	0.394(411)	0.078(183)	0.528(459)
SDSS J092620.42+034542.3 <sup>#</sup>	19.827(15)	2164	3	0.102	—	0.196(75)	0.803(75)	0.002(2)
SDSS J092620.42+034542.3 <sup>#</sup>	19.901(15)	2164	3	0.102	—	0.333(140)	0.654(136)	0.014(19)
SDSS J093946.03+065209.4 <sup>#</sup>	22.484(118)	2921	6	0.122	—	0.035(151)	0.278(397)	0.686(412)
SDSS J093946.03+065209.4 <sup>#</sup>	22.317(124)	2921	6	0.122	—	0.007(43)	0.410(449)	0.583(456)
SDSS J100243.11−024635.9 <sup>#</sup>	21.240(48)	1624	3	0.155	—	0.000(0)	0.521(377)	0.479(377)
SDSS J100243.11−024635.9 <sup>#</sup>	21.024(65)	1624	3	0.155	—	0.046(106)	0.628(408)	0.325(426)
SDSS J100243.11−024635.9 <sup>#</sup>	21.371(64)	1624	3	0.155	—	0.007(28)	0.845(299)	0.148(300)
SDSS J100516.61+694136.5 <sup>#</sup>	19.423(12)	7958	3	0.154	—	0.000(0)	0.000(0)	1.000(0)
SDSS J105333.76+285033.6 <sup>#</sup>	20.193(17)	3159	3	0.066	—	0.000(0)	0.016(80)	0.984(80)
SDSS J112003.40+663632.4 <sup>#</sup>	20.945(54)	92	4	0.016	0.0684 <sup>  </sup>	0.003(7)	0.559(393)	0.438(394)
SDSS J124328.27−055431.0 <sup>#</sup>	22.696(147)	7838	6	0.079	—	0.004(21)	0.301(427)	0.695(432)
SDSS J124602.02−202302.4 <sup>#</sup>	18.535(8)	1046	3	0.197	—	0.279(49)	0.701(48)	0.020(11)
SDSS J124719.03+013842.6 <sup>#</sup>	20.777(37)	2809	3	0.064	—	0.514(342)	0.480(341)	0.006(24)
SDSS J124719.03+013842.6 <sup>#</sup>	20.696(32)	2809	3	0.064	—	0.764(270)	0.233(266)	0.003(20)
SDSS J124719.03+013842.6 <sup>#</sup>	20.768(25)	2809	3	0.064	—	0.661(220)	0.339(220)	0.000(0)
SDSS J132040.96−030016.7 <sup>#</sup>	25.605(628)	7386	6	0.108	—	0.000(0)	0.282(405)	0.718(405)
SDSS J132715.28+425932.8 <sup>#</sup>	20.805(25)	4393	3	0.041	—	0.000(0)	0.073(163)	0.926(163)
SDSS J141029.09+330706.2 <sup>#</sup>	21.738(88)	9045	6	0.068	—	0.003(28)	0.859(337)	0.137(337)

\*Method of distance estimation. 1: from Patterson (2011) and other references (see text),

2: determined from  $P_{\text{orb}}$  and maximum magnitude, 3: from estimated  $P_{\text{orb}}$  and maximum magnitude,4: from  $P_{\text{orb}}$  and minimum magnitude, 5: from estimated  $P_{\text{orb}}$  and minimum magnitude6: assuming maximum  $M_V = 4.95$ .<sup>†</sup> $P_{\text{orb}} < 0.06$  (d).<sup>‡</sup> $0.06 \leq P_{\text{orb}} < 0.10$  (d).<sup>§</sup> $P_{\text{orb}} \geq 0.10$  (d).<sup>||</sup>Determined from superhump period.

**Table 4.** Estimated extinction and neural network classification (continued)

Object	$g$	$d$ (pc)	type*	$A_V$	$P_{\text{orb}}$	ultrashort <sup>†</sup>	short <sup>‡</sup>	long <sup>§</sup>
SDSS J142953.56+073231.2 <sup>#</sup>	21.208(45)	204	5	0.073	—	0.000(0)	0.429(374)	0.571(374)
SDSS J142953.56+073231.2 <sup>#</sup>	21.150(53)	204	5	0.073	—	0.000(0)	0.055(155)	0.945(155)
SDSS J142953.56+073231.2 <sup>#</sup>	21.175(39)	204	5	0.073	—	0.000(0)	0.041(134)	0.959(134)
SDSS J151109.79+574100.3 <sup>#</sup>	21.239(35)	2788	3	0.048	—	0.040(64)	0.935(90)	0.025(71)
SDSS J151109.79+574100.3 <sup>#</sup>	21.514(51)	2788	3	0.048	—	0.001(2)	0.916(168)	0.084(168)
SDSS J151109.79+574100.3 <sup>#</sup>	21.361(39)	2788	3	0.048	—	0.001(1)	0.722(373)	0.278(373)
SDSS J152124.38+112551.9 <sup>#</sup>	21.615(51)	505	5	0.118	—	0.274(352)	0.469(424)	0.257(384)
SDSS J153457.24+505616.8 <sup>#</sup>	22.023(89)	2366	3	0.064	—	0.012(43)	0.560(440)	0.428(447)
SDSS J154817.56+153221.2 <sup>#</sup>	21.640(50)	1822	3	0.112	—	0.002(5)	0.621(404)	0.377(405)
SDSS J154817.56+153221.2 <sup>#</sup>	21.825(58)	1822	3	0.112	—	0.513(347)	0.458(333)	0.029(135)
SDSS J154817.56+153221.2 <sup>#</sup>	22.304(96)	1822	3	0.112	—	0.002(15)	0.937(217)	0.062(217)
SDSS J155030.38−001417.3 <sup>#</sup>	22.013(72)	2814	3	0.272	—	0.000(0)	0.173(294)	0.827(294)
SDSS J155030.38−001417.3 <sup>#</sup>	21.857(63)	2814	3	0.272	—	0.000(0)	0.095(244)	0.905(244)
SDSS J155540.19+364643.1 <sup>#</sup>	20.809(27)	1824	3	0.062	—	0.015(20)	0.949(68)	0.036(67)
SDSS J161027.61+090738.4 <sup>#</sup>	20.082(19)	650	1	0.135	0.0570	0.861(85)	0.139(85)	0.000(2)
SDSS J161027.61+090738.4 <sup>#</sup>	20.103(18)	650	1	0.135	0.0570	0.846(112)	0.154(112)	0.000(0)
SDSS J161442.43+080407.9 <sup>#</sup>	20.940(43)	2151	3	0.193	—	0.038(64)	0.511(412)	0.452(435)
SDSS J161442.43+080407.9 <sup>#</sup>	21.248(40)	2151	3	0.193	—	0.000(0)	0.622(431)	0.378(431)
SDSS J162520.29+120308.7 <sup>#</sup>	18.527(8)	375	2	0.261	0.0920 <sup>  </sup>	0.001(0)	0.999(0)	0.000(0)
SDSS J162520.29+120308.7 <sup>#</sup>	18.481(7)	375	2	0.261	0.0920 <sup>  </sup>	0.006(2)	0.994(2)	0.000(0)
SDSS J162558.18+364200.6 <sup>#</sup>	21.684(48)	2368	3	0.043	—	0.143(226)	0.835(244)	0.023(82)
SDSS J164705.07+193335.0 <sup>#</sup>	21.980(69)	1808	3	0.266	—	0.091(178)	0.759(298)	0.150(274)
SDSS J164705.07+193335.0 <sup>#</sup>	21.977(62)	1808	3	0.266	—	0.196(279)	0.383(368)	0.421(435)
SDSS J170145.85+332339.5 <sup>#</sup>	21.582(54)	4998	3	0.074	—	0.056(135)	0.936(141)	0.008(48)
SDSS J170145.85+332339.5 <sup>#</sup>	21.818(66)	4998	3	0.074	—	0.588(403)	0.328(375)	0.084(253)
SDSS J170810.31+445450.7 <sup>#</sup>	20.734(25)	526	3	0.090	—	0.737(183)	0.263(183)	0.000(0)
SDSS J170810.31+445450.7 <sup>#</sup>	20.784(23)	526	3	0.090	—	0.669(199)	0.331(199)	0.000(1)
SDSS J170810.31+445450.7 <sup>#</sup>	20.832(29)	526	3	0.090	—	0.434(264)	0.549(271)	0.017(53)
SDSS J171202.95+275411.0 <sup>#</sup>	21.417(40)	2984	3	0.144	—	0.000(0)	0.483(375)	0.517(375)
SDSS J171202.95+275411.0 <sup>#</sup>	21.417(59)	2984	3	0.144	—	0.000(0)	0.357(421)	0.643(421)
SDSS J174839.77+502420.3 <sup>#</sup>	22.309(131)	968	6	0.121	—	0.702(432)	0.284(429)	0.015(104)
SDSS J191616.53+385810.6 <sup>#</sup>	17.664(5)	971	3	0.365	—	0.553(31)	0.432(36)	0.016(10)
SDSS J205931.86−070516.6 <sup>#</sup>	20.198(22)	2436	3	0.225	—	0.028(36)	0.927(109)	0.045(97)
SDSS J205931.86−070516.6 <sup>#</sup>	20.755(30)	2436	3	0.225	—	0.738(385)	0.261(385)	0.001(5)
SDSS J223854.51+053606.8 <sup>#</sup>	21.432(57)	2330	3	0.327	—	0.276(319)	0.583(356)	0.141(289)
SDSS J223854.51+053606.8 <sup>#</sup>	21.396(55)	2330	3	0.327	—	0.272(279)	0.477(348)	0.251(383)
SDSS J223854.51+053606.8 <sup>#</sup>	21.548(47)	2330	3	0.327	—	0.367(302)	0.627(305)	0.006(30)

\*Method of distance estimation. 1: from Patterson (2011) and other references (see text),

2: determined from  $P_{\text{orb}}$  and maximum magnitude, 3: from estimated  $P_{\text{orb}}$  and maximum magnitude,4: from  $P_{\text{orb}}$  and minimum magnitude, 5: from estimated  $P_{\text{orb}}$  and minimum magnitude6: assuming maximum  $M_V = 4.95$ .<sup>†</sup> $P_{\text{orb}} < 0.06$  (d).<sup>‡</sup> $0.06 \leq P_{\text{orb}} < 0.10$  (d).<sup>§</sup> $P_{\text{orb}} \geq 0.10$  (d).<sup>||</sup>Determined from superhump period.<sup>#</sup>Dwarf novae proposed by Wils et al. (2010).



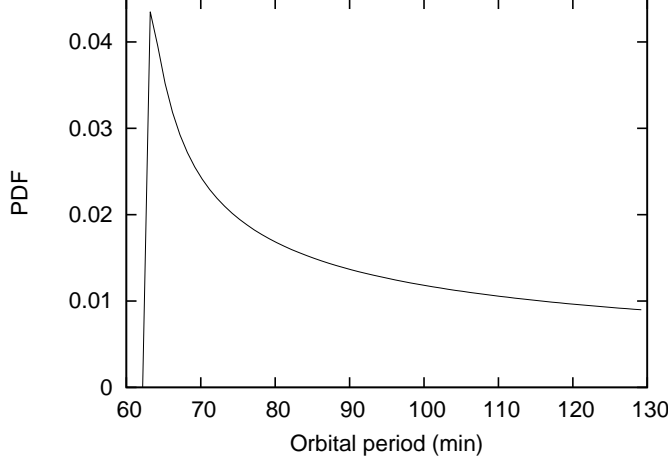


**Fig. 7.** Probability density function (PDF) of the intrinsic  $P_{\text{orb}}$  distribution of DNe estimated from the CRTS-SDSS sample.

model. The small  $\alpha$  for the CRTS-SDSS sample is probably due to the relatively flat distribution in a region of  $P_{\text{orb}} \gtrsim 86$  min; in other words, it is a potential smearing effect of the distribution in  $P_{\text{est}}$ . The parameter  $P_{\text{min}}$  is estimated to be smaller than those in Uemura et al. (2010). This parameter is highly dependent on the number of objects near  $P_{\text{min}}$ . In the CRTS-SDSS sample, there are larger number of objects in the region of  $P_{\text{orb}} = 70\text{--}80$ , compared to the samples in Uemura et al. (2010). This may also be due to the smearing effect and the period minimum determined from  $P_{\text{est}}$  could be shorter than the real  $P_{\text{min}}$ . The systematic trends of shortening of the  $P_{\text{min}}$  and smaller  $\alpha$  have been confirmed by artificially introducing “zitter” errors to the samples in Uemura et al. (2010). We thus could not find very convincing difference in the distribution of  $P_{\text{orb}}$  between CRTS-SDSS and past outburst-selected samples. Most objects with a short  $P_{\text{est}}$ , however, do not have a measured  $P_{\text{orb}}$  (either spectroscopically or photometrically), and there remains a possibility that these objects may be genuine ultrashort-period CVs. Characterizations of these objects by further observations are desired.

## 6. Conclusion

We investigated de-reddened SDSS colors of known dwarf novae, and found correlations between orbital periods and colors. The  $u - g$  color is a particularly good indicator for systems with the shortest orbital periods and can be used to distinguish WZ Sge-type candidates. We have also developed a method for estimating orbital periods of dwarf novae from SDSS colors in quiescence using an artificial neural network. For typical objects below the period gap with considerable photometric accuracy, we could estimate orbital periods to a  $1\sigma$  error of 22 %. The error in estimation is worse for longer period systems. We also developed a neural-network-based method for a categori-

**Table 5.** CRTS sources for the estimation of the intrinsic  $P_{\text{orb}}$  distribution.

$P_{\text{est}}^*$	error*	$N^\dagger$	Object
70.1	14.0	1	OT J004902.0+074726
70.4	7.2	2	OT J151037.4+084104
72.4	18.2	4:	OT J164748.0+433845
73.4	2.4	1	EL UMa
73.7	4.1	2	OT J073758.5+205545
74.7	4.1	2	OT J010550.1+190317
75.6	2.5	3	OT J035003.4+370052
76.1	3.0	1	OT J084555.1+033930
78.5	2.6	1	OT J104411.4+211307
82.0	2.1	16	OT J010329.0+331822
82.1	29.4	1	OT J230425.8+062546
84.0	15.0	1	OT J223606.3+050517
84.5	2.2	1	OT J112253.3−111037
84.7	22.8	16	OT J215630.5−031957
84.9	1.5	10:	OT J141002.2−124809
85.7	2.5	1	OT J005824.6+283304
86.1	4.5	1	OT J084041.5+000520
86.4	1.9	7:	OT J074419.7+325448
86.4	8.6	3	OT J223136.0+180747
87.3	20.3	3	OT J102937.7+414046
87.8	1.3	1	OT J032839.9−010240
87.9	3.4	1	OT J102637.0+475426
87.9	4.4	3	OT J075414.5+313216
87.9	4.6	3:	OT J163311.3−011132
88.0	4.0	2	OT J163120.9+103134
88.5	4.8	5:	OT J224505.4+011547
88.5	4.8	1	OT J102146.4+234926
88.7	45.3	1	OT J091453.6+113402
88.9	1.9	1	OT J130030.3+115101
88.9	1.9	2	OT J132536.0+210037
89.4	5.7	1	OT J222824.1+134944
89.8	9.0	2	OT J082654.7−000733
90.4	2.6	1	OT J202857.1−061803
91.1	13.0	2	OT J004807.2+264621
91.6	5.6	1	OT J223058.3+210147
92.5	2.2	1	OT J221128.7−030516
93.6	2.2	6	OT J085603.8+322109
95.0	1.7	3	OT J124417.9+300401
95.9	2.3	1	OT J014150.4+090822
96.3	4.5	3:	OT J084413.7−012807
96.7	0.1	5	ASAS J224349+0809.5
96.8	2.8	4	OT J162806.2+065316
96.9	23.3	2	OT J214639.9+092119
97.1	4.5	4:	OT J082019.4+474732
98.0	4.6	3:	OT J043517.8+002941
98.4	2.9	2	OT J101545.9+033312
98.7	2.9	3	OT J040659.8+005244
99.3	3.2	4:	OT J210954.1+163052
99.6	8.1	1	OT J020056.0+195727
99.7	4.8	5	OT J075648.0+305805
100.0	1.9	1:	OT J011516.5+245530
100.1	4.7	6:	OT J154354.1−143745
100.4	1.5	1:	OT J221344.0+173252
101.3	2.0	4	OT J164950.4+035835

\*Unit min.

$^\dagger$ Number of outbursts recorded by CRTS.

**Table 5.** CRTS sources for the estimation of the intrinsic  $P_{\text{orb}}$  distribution (continued).

$P_{\text{est}}^*$	error*	$N^\dagger$	Object
101.7	5.1	5	OT J162619.8–125557
101.9	2.8	2	OT J001538.3+263657
101.9	2.4	1	OT J215815.3+094709
102.0	35.4	5:	OT J162012.0+115257
102.1	3.8	6:	OT J224814.5+331224
102.5	3.3	5:	OT J204001.4–144909
102.5	1.2	18:	V1032 Oph
102.7	0.8	2	OT J170609.7+143452
103.3	5.2	1	OT J075332.0+375801
103.6	4.0	2	OT J105835.1+054706
104.1	66.9	3:	OT J091634.6+130358
104.3	3.3	1	OT J210650.6+110250
104.5	2.6	4	OT J103317.3+072119
104.6	19.9	1	OT J214959.9+124529
104.6	3.0	4	OT J004500.3+222708
105.1	9.1	2	OT J224753.9+235522
105.4	5.6	1	OT J074928.0+190452
105.6	1.9	2	OT J043829.1+004016
105.7	2.3	1	SDSS J152419.33+220920.0
106.0	5.9	2	OT J081418.9–005022
106.4	5.0	2	OT J043546.9+090837
106.5	41.1	11:	OT J090852.2+071640
106.9	6.2	4	OT J224823.7–092059
106.9	6.1	8	V844 Her
107.1	2.0	1	OT J051419.9+011121
107.6	3.7	2	OT J112509.7+231036
107.6	8.0	2	OT J082603.7+113821
108.1	2.1	14:	OT J080853.7+355053
108.4	1.7	9	QW Ser
108.9	8.1	5	OT J124819.4+072050
109.1	11.5	4	OT J160844.8+220610
109.3	2.5	2	OT J112332.0+431718
109.7	33.3	1	UW Tri
110.0	9.7	3	OT J231142.8+204036
110.2	4.1	1	OT J154544.9+442830
110.2	3.1	6	OT J003304.0+380106
110.3	31.6	2	OT J090516.1+120451
110.3	15.8	3	OT J144316.5–010222
111.6	1.5	2	HS 1016+3412
112.4	2.5	6	OT J021110.2+171624
113.8	2.9	3	SDSS J100515.39+191108.0
113.9	3.9	3	OT J011543.2+333724
114.0	2.6	2	TT Boo
114.2	5.4	3	OT J170702.5+165339
114.3	4.1	4:	OT J043742.1+003048
115.1	4.5	2:	OT J214804.4+080951
116.2	0.4	6	NSV04838
116.3	4.4	3	OT J000024.7+332543
117.3	29.5	2	OT J082821.8+105344
118.5	10.6	10	OT J163942.7+122414
118.6	3.9	2	OT J141712.0–180328
119.2	4.7	3:	OT J212633.3+085459
119.5	3.5	8	OT J084358.1+425037
120.7	12.7	6	OT J085113.4+344449

\*Unit min.

 $^\dagger$ Number of outbursts recorded by CRTS.**Table 5.** CRTS sources for the estimation of the intrinsic  $P_{\text{orb}}$  distribution (continued).

$P_{\text{est}}^*$	error*	$N^\dagger$	Object
120.9	27.1	8	OT J155430.6+365043
120.9	5.1	6	OT J213937.6–023913
121.4	4.2	8:	OT J224253.4+172538
122.0	9.2	13:	OT J232619.4+282650
122.4	4.0	3	OT J085409.4+201339
123.1	13.5	4	OT J001158.3+315544
123.2	11.8	3	OT J152037.9+040948
124.3	2.9	5	OT J000659.6+192818
124.5	3.3	3	EG Aqr
124.5	8.7	7	OT J041636.9+292806
124.9	35.7	2	OT J211550.9–000716
126.3	3.1	2:	OT J223909.8+250331
127.2	23.2	1	OT J214842.5–000723
127.5	10.3	2	OT J215636.3+193242
128.1	3.7	3	OT J102616.0+192045

\*Unit min.

 $^\dagger$ Number of outbursts recorded by CRTS.**Table 6.** Parameters estimated from the Bayesian analysis.

Sample	$\alpha$	$P_{\text{min}}$ (min)
CRTS-SDSS	$0.49^{+0.22}_{-0.24}$	$63.2^{+2.7}_{-3.8}$
ASAS*	$1.00^{+0.28}_{-0.30}$	$71.9^{+2.4}_{-3.8}$
all RKcat*	$0.98^{+0.16}_{-0.16}$	$72.5^{+1.3}_{-1.6}$

\*Uemura et al. (2010)

cal classification. This method has proven to be efficient in classifying objects into three categories (WZ Sge type, SU UMa type and SS Cyg/Z Cam type) and works for very faint objects to a limit of  $g=21$ . Using these methods, we investigated the distribution of orbital periods of dwarf novae from a modern transient survey (CRTS). We confirmed that the number of detected outbursts were smaller in systems with orbital periods shorter than 85 min. The estimated parent population was different from those of earlier outburst-selected samples investigated by Uemura et al. (2010), in that the present sample tends to give a flatter distribution toward the shortest period and a shorter estimate of the period minimum. Although it is likely this was a result of uncertainties resulting from neural-network analysis and photometric errors, it is necessary to confirm of the real nature of objects having the shortest estimated periods. We also provide estimated orbital periods, estimated classifications and supplementary information for known dwarf novae with quiescent SDSS photometry. We have also shown that there are a significant number of transients whose quiescent colors are inside the WD exclusion box of SDSS spectroscopic follow-up, and suggested that the fraction of shorttrst- $P_{\text{orb}}$  objects and period bouncers were significantly biased in the SDSS CVs.

**Note added in proof:**

The following objects have been named in Kazarovets et al. (2011) during the proofreading period: 2QZ J142701.6–012310 = V558 Vir, GSC 847.1021 = IU Leo, HS 1016+3412 = AC LMi, HS 1340+1524 = HW Boo, OT J074727.6+065050 = DY CMi, OT J080714.2+113812 = KK Cnc, OT J084555.1+033930 = V498 Hya, OT J102146.4+234926 = IK Leo, ROTSE3 J151453.6+020934.2 = V418 Ser, SDSS J005050.88+000912.6 = GS Cet, SDSS J013132.39–090122.3 = GY Cet, SDSS J040714.78–064425.1 = LT Eri, SDSS J074531.92+453829.6 = EQ Lyn, SDSS J080434.20+510349.2 = EZ Lyn, SDSS J084400.10+023919.3 = V495 Hya, SDSS J090103.93+480911.1 = PU UMa, SDSS J090452.09+440255.4 = FV Lyn, SDSS J123813.73–033933.0 = V406 Vir, SDSS J124426.26+613514.6 = V351 UMa, SDSS J125023.85+665525.5 = OV Dra, SDSS J133941.11+484727.5 = V355 UMa, SDSS J150240.98+333423.9 = NZ Boo, SDSS J151413.72+454911.9 = PP Boo, SDSS J155644.24–000950.2 = V493 Ser, SDSS J081321.91+452809.4 = FH Lyn, SDSS J082409.73+493124.4 = FV Lyn.

*V1047 Aql*

According to Rod Stubbings, the observation by Greg Bolt during the 2005 August outburst detected superhumps, and the superhump period was about 0.074 d. This result is consistent with our categorical classification.

This work was supported by the Grant-in-Aid for the Global COE Program “The Next Generation of Physics, Spun from Universality and Emergence” from the Ministry of Education, Culture, Sports, Science and Technology (MEXT) of Japan. This work was partly supported by the Grant-in-Aid for Young Scientists (B) No.11020523 (HM) from the MEXT of Japan. We are grateful to the Catalina Real-time Transient Survey team for making their real-time detection of transient objects available to the public. Funding for the SDSS has been provided by the Alfred P. Sloan Foundation, the Participating Institutions, the National Aeronautics and Space Administration, the National Science Foundation, the US Department of Energy, the Japanese MEXT and the Max Planck Society. The SDSS web site is <<http://www.sdss.org>>. Simbad’s VizieR service, the NASA Astrophysics Data System and the AAVSO VSX service have been important resources of information for this research. We are grateful to Elena Pavlenko for making historical materials of NSV 00895 available to us and to Tomohito Ohshima for helping us in astrometry of SX LMi. We are also grateful to many numbers of observers including the VSNET Collaboration, AAVSO, CVNET, BAA VSS alert and AVSON networks who have greatly contributed to the detections of outbursts of dwarf novae

and determinations of superhump or orbital periods.

**Appendix 1. Notes on Individual Objects**

In addition to statistics of dwarf novae, the neural network analysis has clarified a wealth of previously unknown properties of individual dwarf novae. We discuss on new findings of individual objects. We also present some negative results, or suggestible identifications on objects whose reality or identification have been ambiguous.

*FN And*

Our analysis favors an orbital period above the period gap. Our unpublished photometry during a long outburst in 1994 July did not detect superhumps. The object is likely an SS Cyg-type dwarf nova. The relatively rapid fading rate ( $1.2 \text{ mag d}^{-1}$ ) during the terminal stage of the outburst suggests a relatively short orbital period, consistent with the present analysis. The object appears to be similar to a short- $P_{\text{orb}}$  SS Cyg-type dwarf nova AR And (Szkody, Mattei 1984; Taylor, Thorstensen 1996).

*IZ And*

The current analysis is consistent with the lack of superhumps and the relatively slow fading rate (Kato 2001b).

*LL And*

Kato (2004) suggested that this object may have a massive secondary for its  $P_{\text{orb}}$ . The present analysis did not show a very strong contribution from the secondary, as has been observed in QZ Ser.

*PT And*

This object was originally considered to be a nova in M31 (Grubisich, Rosino 1958). Additional detections of the outbursts led to a classification of a possible dwarf nova (Sharov, Alksnis 1989). Alksnis, Zharova (2000) presented a finding chart and summary of past observations. The object underwent another outburst in 2010, and was confirmed to be a dwarf nova (T. Ohshima et al., in preparation). Although the SDSS image is present, there is no photometric entry. A visual inspection of the image suggests a 22 mag quiescent counterpart.

*V496 Aur*

Although the period was not meaningfully estimated with the neural-network analysis due to its faintness, the colors tend to be in the region of WZ Sge-type dwarf novae (subsection 3.1). There were five outbursts recorded by CRTS; the behavior is unlikely to be that of a WZ Sge-type dwarf nova. The object may be related to “borderline” WZ Sge-type dwarf novae.

*T Boo*

The existence of this object has long been debated (see e.g. Duerbeck 1987), and has also been suspected to be a dwarf nova. The candidates 5 in Downes, Szkody (1989) has a blue color (SDSS J141356.53+190328.6, classified as an F2-9 type according to Ringwald et al. 1996), while

candidate 2 is a red object. The invisibility of the candidate 2 on a  $U$  image of Downes, Szkody (1989) can be understood as being a result of a large  $u - g$  color index (type K5-M4 according to Ringwald et al. 1996. Candidates 1, 4, 8 and 9 are galaxies. The present result is consistent with Shara et al. (1990).

#### *LM Cas*

Liu, Hu (2000) suggested that the fainter component of a close pair is the CV. Our measurement of the fainter component is consistent with the dwarf-nova classification.

#### *GZ Cet*

The estimated orbital period represented a markedly large departure from the real period, which is expected for a dwarf nova with an unusually luminous secondary. Among samples with known  $P_{\text{orb}}$ , GZ Cet showed the widest deviation among dwarf novae below the period gap, and no systems with intermediate deviations were present in our sample. This suggests that such systems are relatively rare.

#### *EU CMa*

Our analysis favors an orbital period above the period gap. Our unpublished photometry during a long outburst in 2003 February did not detect superhumps. The object is likely to be an SS Cyg-type dwarf nova.

#### *DE Cnc*

This object was originally detected during the course of a search for flare stars (Götz 1977). The object was caught in outburst on 1977 February 21 at  $U=15.8$ . An examination of archival plates detected another outburst on 1931 January 11 at  $B=14.6$ . Other fainter outbursts were also suspected. Götz (1979) further studied the object and suggested it to be a dwarf nova. Munari, Zwitter (1998) observed the counterpart suggested by Downes et al. (1997) and obtained a featureless continuum resembling field G-K stars. Liu, Hu (2000) obtained a similar result. The present analysis has confirmed that the color is also unlikely that of a quiescent dwarf nova. Since the position marked on the finding chart in (Götz 1977) appears to be slightly south of the position suggested by Downes et al. (1997), the true quiescent counterpart may be fainter. An inspection of the SDSS image was unable to detect a promising quiescent counterpart.

#### *GZ Cnc*

The  $u - g$  and  $g - z$  colors for this objects are approximately consistent with those of WZ Sge-type dwarf novae. The neural-network analysis, however, distinguished this object from WZ Sge-type dwarf novae. A combination of color criteria and neural network would be helpful in identifying certain classes of objects.

#### *HH Cnc*

Our analysis favors an orbital period above the period gap. The result is consistent with the lack of superhumps

(Kato, Uemura 2001b), and our unpublished photometry during the 2003 January outburst. In the spectrum presented by Szkody et al. (2007), there was no evidence for the secondary.

#### *FU Com*

Although Downes et al. (2001) proposed the counterpart, citing Howell et al. (1990) as a reference, Howell et al. (1990) were unable to identify the variable object in their field. The proposed counterpart did not show a color resembling a CV (listed in table 3). After examining the position, we found a likely X-ray counterpart 1RXS J123054.8+270759, which has a likely blue optical counterpart SDSS J123053.11+270822.0,  $32''$  distant from the X-ray position. This object is a quasar ( $z=0.472$ , SDSS spectroscopy). Its classification appears to be consistent with the low-amplitude variation of FU Com reported in Luyten, Erickson (1965).

#### *FY Com*

Due to the lack of the finding chart, it is almost impossible to identify the object unambiguously. Although Downes et al. (2001) proposed the counterpart, this object is not particularly blue. A relatively blue object SDSS J124925.74+272511.9 ( $g = 21.0$ ) is present within the error of the original report, although its  $u - g$  color is unlikely for a CV.

#### *GP Com*

This is a helium CV permanently (as of now) in quiescence (Smak 1975; Tsugawa, Osaki 1997). It is included in this survey in order to examine the response of the neural network to quiescent helium dwarf novae.

#### *IM Com*

IM Com was discovered as an eruptive object by Začs (1982). The object exhibited a 0.7 mag brightening in 6 d in 1981 March (see figure 4 in Začs 1982) and already faded after 30 d. Although GCVS classified the object as a possible dwarf nova, the original author suggested either nova like (NL)-type variable or a dwarf nova. The identification in Downes et al. (2001) is correct [note that the chart in Začs (1982) was intentionally reversed]. Although Munari, Zwitter (1998) reported a featureless continuum resembling those of the field G-K stars, the SDSS  $g - r$  color is much bluer than in the assumed candidate for DE Cnc with a similar description. The large  $u - g = +1.0$ , however, is rare in CVs. The object should deserve further research.

#### *MT Com*

This object was proposed to be the optical counterpart of the EUV transient RE J1255+266 (Dahlem et al. 1995; Watson et al. 1996; Wheatley et al. 2000). Patterson et al. (2005) proposed a possible orbital period of 0.0829 d and suggested it a candidate period bouncer.



*V1081 Cyg*

Although the orbital period was not directly estimated due to a lack of the  $r$ -band data, we can obtain a period of 0.2–0.7 d assuming an  $r$  magnitude of 16.8–17.3. The object is likely a long- $P_{\text{orb}}$  dwarf nova. The result is consistent with a strong red continuum reported in Bruch, Schimpke (1992).

*V1089 Cyg*

Liu et al. (1999) reported a reddish continuum in the spectrum, although no clear signature of the secondary was detected. The present analysis is in agreement with the spectroscopic result.

*V1363 Cyg*

The object is renowned for its long-term variability, unlike most of other dwarf novae (Miller 1971; Pinto, Romano 1972). The object was classified either as a Z Cam-type dwarf nova (Kholopov et al. 1985) or as a VY Scl-type NL variable (Bruch, Schimpke 1992). Schimpke, Bruch (1990) also reported the presence of a secondary that is directly visible in the spectrum. This spectrum was apparently taken during its faint state. The object recently underwent major outbursts in 2007–2008 and 2011, superimposed on a gradually fading bright state lasting since 2005. The 2011 outburst was well observed, and was composed of a slow rise by  $\sim 3.5$  mag in 30 d, and a slow fade lasting more than 40 d. The overall behavior of the outburst resembled those of two famous long- $P_{\text{orb}}$  DNe, V630 Cas (Whitney 1973; Warner 1994; Orosz et al. 2001) and V1017 Sgr (Sekiguchi 1992). The present analysis strongly favors a long- $P_{\text{orb}}$  dwarf nova. The inferred period is close to the 0.4 d periodicity detected during the outburst (vsnet-alert 13326), although both values have large uncertainties. The unusual behavior of this object seems to be understood as if the system generally has low, highly variable mass-transfer rate, and the natural consequence of a long orbital period which de-stabilize the outer accretion disk due to the thermal disk instability.

*V1449 Cyg*

The color is unusually red. This may have been resulted from an unresolved companion due to the crowded field, or a contribution from a luminous secondary. The classification appears to be secure from the recorded light curve (Pinto, Romano 1972). This object has been confirmed to show  $H\alpha$  in emission (Drew et al. 2005).

*V1697 Cyg*

This is a faint red star in SDSS, and unlikely a CV.

*V1711 Cyg*

The suggested object (Downes et al. 2001) is not particularly blue, and it is less likely a CV. No photometric data were available.

*V2466 Cyg*

A very faint object is present in SDSS image. No photometric data were available.

*DO Dra*

Although this object is better understood to be an outbursting intermediate polar (Patterson et al. 1992; Patterson, Szkody 1993), we included this object in the current study because the accretion disk in this system is mostly in cold state, as in quiescent dwarf novae.

*HQ Gem*

This object has been confirmed to show  $H\alpha$  in emission (Drew et al. 2005).

*KZ Gem*

The classification appears to be secure from the multiple outbursts reported to VSNET (Kato et al. 2004). The brightest maximum reached a visual magnitudes of 14.0.

*MV Gem*

This variable was discovered by Hoffmeister (1968). Zwitter, Munari (1996) reported a mid-F dwarf spectrum, and it is not usually considered as a CV. An inspection of the SDSS image, the object is a close pair, and the fainter object ( $g=20.4$ ) has a color similar to CVs. The object (not included in the table) apparently needs to be examined. According to the observations by M. Iida, the object (in combined light) brightened more than 2 mag in 7 d.

*V610 Her*

The object listed ( $16^{\text{h}}43^{\text{m}}39^{\text{s}}.09$ ,  $+22^{\circ}31'25''.2$ ) is  $10^{\circ}5'$  distant from the nominal GCVS position, but has a more CV-like color. This degree of uncertainty in the original identification can be reconciled with the quality of the hand-written chart (Hoffmeister 1968; Kato 1999). The suggested counterpart in Downes, Shara (1993) was correct.

*DO Leo*

Although Kholopov et al. (1985), Downes et al. (2001) and Ritter, Kolb (2003) classified this object as NL, the object is actually an eclipsing Z Cam-type dwarf nova.<sup>10</sup> The SDSS observations were recorded during its quiescent state.

*HM Leo*

Outbursts fading more rapidly than what is expected from the orbital period have been reported (e.g. 0.9 mag  $\text{d}^{-1}$  for the 2009 March outburst). This object might be somewhat similar to DO Dra in its outburst characteristics.

*SS LMi*

The true position is  $10^{\text{h}}34^{\text{m}}05^{\text{s}}.85$ ,  $+31^{\circ}07'59''.6$ , correctly listed in Samus et al. (2011) but several catalogs

<sup>10</sup> cf. <http://nesssi.cacr.caltech.edu/catalina/20010514/105141150564100059p.html>.

including VizieR give incorrect coordinates. The color is consistent with the WZ Sge-type classification.

#### *SX LMi*

This object is a close double. Although the presence of a companion was already mentioned in Wagner et al. (1998), it was not perfectly clear whether Wagner et al. (1998) measured only the bright component in obtaining the quiescent light curve. The astrometry of our CCD image during the outburst in 1994 December favored a position close to the brighter component. The result has confirmed the unusually low outburst amplitude claimed by Nogami et al. (1997). It would be worth noting that the fainter component is also a blue object in SDSS, contrary to the suggestion in Wagner et al. (1998). Although the object underwent frequent outburst in the 1990's (Nogami et al. 1997; Kato 2001a), the frequency of outbursts (particularly superoutbursts) has remarkably reduced since 2007.

#### *V699 Oph*

This object is an an unresolved companion to a 16 mag star. These stars remained unresolved in SDSS, and we did not include this object in the sample.

#### *GR Ori*

The object was discovered as a possible nova in 1916 (Thiele 1916). It was recorded at a photographic magnitude of 11.5 on January 30 and gradually faded to 12.5 on February 7, and further faded to 13.0 on February 30. The object has long been considered as a distant nova (McLaughlin 1945; Duerbeck 1985), although there was a suggestion of a dwarf nova (Brun, Petit 1957). During a “reconnaissance program” of old suspected novae, Robertson et al. (2000) identified GR Ori as a 22.8 mag blue object. The present identification by the SDSS data has confirmed this identification. Although the result of neural-network analysis was inconclusive due to faintness of the object, the color (especially the  $u - g$  color) resembles those of WZ Sge-type dwarf novae. The relatively rapid decline, especially at the late epoch of the outburst, seems to strengthen this classification.

#### *V370 Peg*

This object is a transient object reported in Modjaz et al. (1998). The true quiescent counterpart is a blue object east to the cataloged object (red star in SDSS) in Samus et al. (2011). The blue object well matches the finding chart (object in outburst) available at <http://astro.berkeley.edu/bait/public.html/cv.gif>. The object is not in the SDSS photometric catalog. The object was again recorded in outburst in 2010 October (Eddy Muylaert, cf. vsnet-alert 12304), reaching a magnitude of 16.7 (unfiltered CCD). This outburst lasted at least for 9 d.

#### *GK Per*

The object was included because this old nova exhibits dwarf nova-type outbursts (e.g. Bianchini et al. 1986;

Cannizzo, Kenyon 1986).

#### *QY Per*

The object is a well-confirmed SU UMa-type dwarf nova with long outburst intervals for its  $P_{\text{orb}}$  (Kato et al. 2000; Kato et al. 2009). The variation of the superhump amplitudes was also unusual (Kato et al. 2012).

#### *V336 Per*

This object is renowned for its low outburst frequency (Busch et al. 1979) and was suspected to be a WZ Sge-type dwarf nova (Kato et al. 2001).<sup>11</sup> Liu, Hu (2000) also suggested the low mass-transfer rate from its spectroscopy and inferred a short  $P_{\text{orb}}$ . In 2009 August, a long-awaited outburst was reported (cf. vsnet-alert 11447). A lack of superhumps in time-series observations by Ian Miller, Jeremy Shears and David Boyd was remarkable (vsnet-alert 11452). The negative result for an SU UMa (or WZ Sge) type dwarf nova can be reconciled with the present neural-network analysis.

#### *V372 Per*

The object has a low outburst frequency (Romano, Minello 1976). Photometry during the state  $\sim 3$  mag above quiescence indicated a relatively red color (Romano, Minello 1976), which is in agreement with the present study.

#### *XY Psc*

The object was discovered as a candidate supernova near UGC 729 in 1972 (Rosino, Pigatto 1972a). Rosino, Pigatto (1972b) later suggested the object to be a dwarf nova with a large outburst amplitude. Although identification of the object remained ambiguous for a long time, Henden et al. (2001) identified a counterpart based on original discovery photographs. Kato et al. (2001) suggested that the object is a very likely candidate for a WZ Sge-type dwarf nova based on the lack of outbursts for a long time [note, however, there was a photographic record of an outburst on 1985 January 12 (vsnet-chat 432)<sup>12</sup>, which still needs to be confirmed]. The present neural-network analysis seems to strengthen the SU UMa-type nature of this object, although the color is not so striking as those of extreme WZ Sge-type dwarf novae.

#### *AH Psc*

This is a missing BD star, which has been suspected to be some kind of an eruptive object (cf. Duerbeck 1987). There is no good candidate in SDSS.

#### *AS Psc*

This object is a dwarf nova in the field of M33 (see Kato, Uemura 2001a for its history and references). Thorstensen (2002) further identified the quiescent counterpart. This object was also detected in SDSS to be a blue object. The

<sup>11</sup> See also the description <http://hea.iki.rssi.ru/~denis/CVmonitoring.html>.

<sup>12</sup> <http://www.kusastro.kyoto-u.ac.jp/vsnet/Mail/vsnet-chat/msg00432.html>

color seems to suggest a more usual SU UMa-type dwarf nova rather than an extreme WZ Sge-type dwarf nova (see also discussions in Kato, Uemura 2001a and Thorstensen 2002). There was another outburst detected by CRTS at a magnitude of 15.8 (unfiltered CCD) in 2008 January.<sup>13</sup>

#### *X Ser*

This object is an old nova showing dwarf nova-type outbursts similar to GK Per (Honeycutt et al. 1998; Honeycutt 2001). The most recent outburst was detected by CRTS in 2009 August and reached  $V=14.2$ . The fading stage of the outburst lasted for  $\sim 30$  d and bore a similarity with outbursts of GK Per and V630 Cas (see the note for V1363 Cyg for the references). The orbital parameters are also similar to those of GK Per and V630 Cas (Thorstensen, Taylor 2000).

#### *QZ Ser*

Samus et al. (2011) gives the position of the brighter component of a close pair. The true CV is the fainter component.

#### *XX Tau*

Although this is a classical nova, Schmidtobreick et al. (2005) recently reported that the spectrum of this nova is similar to those of dwarf novae, and suggested a low mass-transfer rate. We have confirmed the SDSS color similar to those of dwarf novae. Although it is not certain whether the present neural-network analysis applies to such a system, the color favors a system below the period gap. Rodríguez-Gil, Torres (2005) reported a possible photometric periodicity of 0.14 d. Further detailed research is certainly needed.

#### *TX Tri*

This object was discovered as a dwarf nova by (Kurochkin 1978). Richter (1979) independently detected this variable and suggested it to be a quasar based on its color. Further examination by Richter et al. (1981) indicated that the object is a dwarf nova. Based on the presence of HeII and CIII/NIH lines, the authors proposed that the object is similar to WZ Sge. Richter (1989) measured the cycle length of outbursts to be 90 d, while Kurochkin (1978) suggested a period of 70 d. The spectroscopic observation by Liu, Hu (2000) was taken during an outburst, and the contribution by the secondary was not detected. Our analysis seems to preclude the possibility of a WZ Sge-type object, and the object is likely a usual SS Cyg-type dwarf nova above the period gap.

#### *UZ Tri*

The object was detected in outburst only on two nights: 1980 November 1 (14.2 mag, photographic) and November 27 (15.5 mag). The object was invisible on 1980 September 7 and 1981 January 23 (Meinunger 1986). According to Meinunger (1986), there is a colorless star

and a galaxy on the Palomar Sky Survey at the location of UZ Tri, and either of them underwent an outburst. Downes et al. (2001) proposed that the former is the candidate quiescent counterpart. We provide SDSS data for the candidate object. The object appears to be slightly too red for a CV.

#### *NSV 00895*

The object was discovered by T. Hvan as a possible dwarf nova (Meshkova 1940). Kholopov (1953) studied this object and suggested that it may be a dwarf nova with a very long interval ( $> 1000$  d) of outbursts, or a nova. Kholopov (1953) presented a reliable finding chart and description in relation to the UGC 2172 (referred to as a nebula). The information is sufficient to search for a counterpart in SDSS. There was no promising candidate for a quiescent dwarf nova. Wenzel, Wicklein (1990) reported another positive measurement and its light curve. Wenzel, Wicklein (1990) concluded that it is not possible to determine whether NSV 00895 is a nova or a supernova. According to Trentham, Tully (2009), UGC 2172 is a dwarf irregular galaxy of the NGC 1023 group at a distance of 1 Mpc. The lack of a promising quiescent candidate and the proximity of the galaxy strongly favor a supernova of  $M_{\text{pg}} = -19$

#### *NSV 02853*

None of the objects around the star marked in Downes et al. (2001) show a CV-like color.

#### *NSV 04394*

The object was originally discovered by Wild (1972) and was suspected to be a dwarf nova or a supernova. There was no promising candidate according to Downes et al. (2001). There are two blue SDSS objects in this field: SDSS J090938.24+444633.2 ( $g = 21.9$ ),  $1''$  distant from the nominal position of NSV 04394 and SDSS J090939.78+444638.2 ( $g = 21.2$ )  $17''$  distant. We adopted the first candidate in the table. If this is indeed a dwarf nova, the amplitude strongly suggests a WZ Sge-type dwarf nova.

#### *NSV 04498*

This object was discovered by Luyten et al. (1968). Haefner et al. (1996) were unable to identify a variable object in the field. The blue object SDSS J092849.78+231114.2 ( $g=19.9$ ,  $68''$  distant from the reported approximate coordinates) might be a viable candidate.

#### *NSV 05031*

The coordinates are  $10^{\text{h}}57^{\text{m}}49^{\text{s}}81$ ,  $-21^{\circ}56'58''0$ . The object is identical with CTCV J1057-2156 (Augusteijn et al. 2010) whose orbital period is 1.68 hr. The existence of a past outburst and the quiescent spectrum suggest an SU UMa-type dwarf nova.

<sup>13</sup> <<http://nessi.cacr.caltech.edu/catalina/20010316/103161320074100046p.html>>

*NSV 05543*

This object was recorded by Rügemer (1933). Downes et al. (2001) selected a very blue object as the possible quiescent counterpart. The spectrum of this object (SDSS J121829.75+400522.3) in the SDSS archive is dominated by Balmer absorption lines (classified as A0 in the SDSS archive) and lacks emission lines. The identified object is unlikely to be a dwarf nova in quiescence; 33'' distant from this object, there is another relatively blue object (SDSS J121831.75+400546.1) with  $g=21.0$ . The  $u-g$  color, however, is atypical for a CV.

*NSV 09445*

There was no very promising candidate within the circle shown in Downes et al. (2001). The blue object (less likely related to NSV 09445) marked in Downes et al. (2001) (=SDSS J173930.43+210851.4,  $g=18.8$ ) has a blue color in SDSS. The likely association with a ROSAT source 1RXS J173930.9+210847 might suggest a QSO.

*NSV 14681*

The fainter component of a pair.

*NSV 18230*

This object (=KUV 09313+4052) was reported to be a likely dwarf nova (Noguchi et al. 1979). CRTS recorded additional two outbursts. The brightest outburst reached an unfiltered CCD magnitude of 16.9.

*NSV 18704 (SN 1985J), RS Psc*

Although both objects were discovered as supernovae, there are suspicions that they are possible foreground variables. Although both objects have SDSS images, the galaxies were too bright to search for possible candidate stellar images.

*NSV 19466*

The object is suspected to be either a dwarf nova or a VY Scl-type NL object (Szkody et al. 2003). The spectrum suggests a dwarf nova.

*1502+09*

This object was reported in Filippenko et al. (1985) which was caught in outburst during a spectroscopic survey. The quiescent spectra presented in Filippenko et al. (1985) and taken by SDSS, are sufficient to classify the object as a dwarf nova. Our neural-network analysis strongly favors a short orbital period and this object is a good candidate for an SU UMa-type dwarf nova. No further outburst has been recorded.

*2QZ J142701.6-012310, OT J204739.4+000840, SDSS J012940.05+384210.4, SDSS J124058.03-015919.2, SDSS J204739.40+000840.3*

These objects are helium dwarf novae.

*OT J162322.2+121334*

During this survey, we noticed that this object (=CSS080606:162322+121334, not included in tables) showed multiple deep fadings similar to VY Scl-type CVs (Warner 1995; Leach et al. 1999; Honeycutt, Kafka 2004). The object has a blue SDSS counterpart, and fortunately, there were its observations both in high and low states. Assuming that the color of VY Scl-type CVs in very low state is similar to dwarf novae, we estimated an estimated  $P_{\text{orb}}$  of 0.13(3) d using the present neural network. The estimated period is compatible with the expected  $P_{\text{orb}}$  for a VY Scl-type CV. The range of variability based on SDSS data is  $g=17.0-21.9$ . Further spectroscopic confirmation is desired.

*OT J170606.1+255153*

This is an anonymous object near UGC 10700 (Graham, Li 2003). The CV-type nature has been established (Filippenko, Chornock 2003). The SDSS counterpart suggests a large ( $\sim 6$  mag) outburst amplitude and the object is a good candidate for an SU UMa-type dwarf nova.

*OT J213806.6+261957*

This WZ Sge-type dwarf nova (Kato et al. 2010) is a companion to a brighter star. Although these stars are barely resolved in SDSS image, photometric data are given for the combined magnitude. We did not include this object in the sample.

*OT J215815.3+094709*

The detection of superhumps was reported in Kato et al. (2010). Prior to this CRTS discovery, two bright superoutbursts were recorded by ASAS-3 (2003 August,  $V=12.75$  and 2004 October,  $V=12.99$ ). The large amplitudes of superhumps reported in Kato et al. (2010) may have been somewhat anomalous (cf. Kato et al. 2012) considering that the 2010 observation was obtained when the object was much fainter (around 13.4 mag). The present neural-network analysis showed no particular anomaly.

*OT J220449.7+054852, ROTSE3 J004626+410714*

The blue component of a close pair is selected.

*OT J223958.2+231837*

The object was spectroscopically confirmed as a CV (CRTS page). The light curve is rather unusual for a typical dwarf nova.

*SDSS J075939.79+191417.3*

The object was classified either a dwarf nova or a polar (Szkody et al. 2006). We classified it a dwarf nova based on the general appearance of the spectrum. The object has recently been shown to be eclipsing (Drake et al. 2010). No outburst has been recorded.

*SDSS J204448.92-045928.8*

The long orbital period of 1.68(1) d was reported from a radial-velocity study (Peters, Thorstensen 2005). The



detection of a long-duration outburst (Wils 2009) also supports a long  $P_{\text{orb}}$ . The failure to reproduce the  $P_{\text{orb}}$  by the neural-network analysis is not very surprising since our method is insensitive for characterizing objects with  $P_{\text{orb}}$  longer than 1 d (another long- $P_{\text{orb}}$  system X Ser did not yield a meaningful value; in this case it may have been a result of the contribution from the luminous inner accretion disk). It is noteworthy that  $(V - J)$  color of this object is similar to that of another long- $P_{\text{orb}}$  system GK Per, and bluer than most of secondary-dominated SS Cyg-type dwarf novae. A neural-network analysis using categories provides better results for these systems: all objects have a high probability for the *long* category.

*SDSS J233325.92+152222.2*

The object is an intermediate polar with a long spin period (Southworth et al. 2007a). We included it in this sample because the object is not dominated by the disk and system resembles dwarf novae, as in EX Hya (Hellier et al. 1989; Hellier et al. 2000).

*SN 1964O*

The object was suspected to be a dwarf nova rather than a supernova in Downes et al. (1997). Although two candidates were listed in Downes et al. (2001), both stars are K stars. We identified a more likely counterpart (SDSS J150849.85+552807.6) between these two stars. The magnitudes listed in the table refers to this object. If this is the true quiescent counterpart, the amplitude of the 1964 outburst was at least 6 mag.

## Appendix 2. Names of Optical Transients

In the main text of this paper, we have used coordinated-based names for optical transients (OTs), as in the series of papers starting with Kato et al. (2009). This measure has been taken for two reasons: consistency of the names between this paper and a series of our ones (e.g. Kato et al. 2009), and the reader's convenience with unique identifications of the objects by coordinates (CRTS identifiers lack the accuracy in the right ascension for unique identifications). We list original IDs for CRTS (CSS, MLS and SSS objects) and references for other transients (table 7).

## References

Abbott, T. M. C., Shafter, A. W., Wood, J. H., Tomaney, A. B., & Haswell, C. A. 1990, *PASP*, 102, 558  
 Ak, T., Bilir, S., Ak, S., & Eker, Z. 2008, *New Astron.*, 13, 133  
 Ak, T., Bilir, S., Ak, S., & Retter, A. 2007, *New Astron.*, 12, 446  
 Ak, T., Retter, A., Liu, A., & Esenoglu, H. H. 2005, *Publ. Astron. Soc. Australia*, 22, 105  
 Alksnis, A., & Zharova, A. V. 2000, *IBVS*, 4909  
 Anderson, S. F., et al. 2008, *AJ*, 135, 2108  
 Araujo-Betancor, S., Gänsicke, B. T., Long, K. S., Beuermann, K., de Martino, D., Sion, E. M., & Szkody, P. 2005, *ApJ*, 622, 589

Augusteijn, T., Tappert, C., Dall, T., & Maza, J. 2010, *MNRAS*, 405, 621  
 Augusteijn, T., van der Hooft, F., de Jong, J. A., & van Paradijs, J. 1996, *A&A*, 311, 889  
 Augusteijn, T., van Kerkwijk, M. H., & van Paradijs, J. 1993, *A&A*, 267, L55  
 Aungwerojwit, A., et al. 2006, *A&A*, 455, 659  
 Bahcall, J. N., & Soneira, R. M. 1980, *ApJS*, 44, 73  
 Bailey, J. 1979, *MNRAS*, 189, 41P  
 Bianchini, A., Sabbadin, F., Favero, G. C., & Dalmeri, I. 1986, *A&A*, 160, 367  
 Bishop, C. M. 1995, *Neural Networks for Pattern Recognition* (Oxford University Press, Oxford)  
 Bruch, A. 1984, *A&AS*, 56, 441  
 Bruch, A., & Engel, A. 1994, *A&AS*, 104, 79  
 Bruch, A., & Schimpke, T. 1992, *A&AS*, 93, 419  
 Brun, A., & Petit, M. 1957, *Perem. Zvezdy*, 12, 18  
 Busch, H., Häussler, K., & Splittgerber, E. 1979, *Veröff. Sternw. Sonneberg*, 9, 125  
 Cannizzo, J. K., & Kenyon, S. J. 1986, *ApJL*, 309, L43  
 Christensen, E. J. 2006, *Cent. Bur. Electron. Telegrams*, 746  
 Collister, A. A., & Lahav, O. 2004, *PASP*, 116, 345  
 Copperwheat, C. M., Marsh, T. R., Dhillon, V. S., Littlefair, S. P., Hickman, R., Gänsicke, B. T., & Southworth, J. 2010, *MNRAS*, 402, 1824  
 Crampton, D., Fisher, W. A., & Cowley, A. P. 1986, *ApJ*, 300, 788  
 Dahlem, M., et al. 1995, *A&A*, 295, L13  
 Diaz, M. P., & Steiner, J. E. 1990, *A&A*, 238, 170  
 Dillon, M., et al. 2008, *MNRAS*, 386, 1568  
 Donalek, C., et al. 2008, *Astron. Telegram*, 1362  
 Downes, R., Webbink, R. F., & Shara, M. M. 1997, *PASP*, 109, 345  
 Downes, R. A., & Shara, M. M. 1993, *PASP*, 105, 127  
 Downes, R. A., & Szkody, P. 1989, *AJ*, 97, 1729  
 Downes, R. A., Webbink, R. F., Shara, M. M., Ritter, H., Kolb, U., & Duerbeck, H. W. 2001, *PASP*, 113, 764  
 Drake, A. J., et al. 2010, *ApJ*, submitted (arXiv astro-ph/1009.3048)  
 Drake, A. J., et al. 2009, *ApJ*, 696, 870  
 Drew, J. E., et al. 2005, *MNRAS*, 362, 753  
 Duerbeck, H. W. 1985, *Mitteil. der Astronom. Gesell. Hamburg*, 63, 190  
 Duerbeck, H. W. 1987, *Space Sci. Rev.*, 45, 1  
 Eisenstein, D. J., et al. 2011, *AJ*, 142, 72  
 Feline, W. J., Dhillon, V. S., Marsh, T. R., Watson, C. A., & Littlefair, S. P. 2005, *MNRAS*, 364, 1158  
 Filippenko, A. V., & Chornock, R. 2003, *IAU Circ.*, 8158  
 Filippenko, A. V., Sargent, W. L. W., & Hazard, C. 1985, *PASP*, 97, 41  
 Gänsicke, B. T., et al. 2009, *MNRAS*, 397, 2170  
 Götz, W. 1977, *Mitteil. Veränderl. Sterne*, 8, 33  
 Götz, W. 1979, *Mitteil. Veränderl. Sterne*, 8, 103  
 Graham, J., & Li, W. 2003, *IAU Circ.*, 8153  
 Green, R. F., Schmidt, M., & Liebert, J. 1986, *ApJS*, 61, 305  
 Grubissich, C., & Rosino, L. 1958, *Asiago Contr.*, 93, 1  
 Haefner, R., Fiedler, A., & Rau, S. 1996, *IBVS*, 4366  
 Hagen, H.-J., Groote, D., Engels, D., & Reimers, D. 1995, *A&AS*, 111, 195  
 Haswell, C. A., Patterson, J., Thorstensen, J. R., Hellier, C., & Skillman, D. R. 1997, *ApJ*, 476, 847  
 Hellier, C. 2001, *Cataclysmic Variable Stars: how and why they vary* (Berlin: Springer-Verlag)

**Table 7.** Identification list of optical transients

Object	ID or discoverer	Object	ID or discoverer
OT J000024.7+332543	CSS100910:000025+332543	OT J073921.2+222454	CSS080303:073921+222454
OT J000130.5+050624	CSS101127:000130+050624	OT J074222.5+172807	MLS110309:074223+172807
OT J000659.6+192818	CSS100602:000700+192818	OT J074419.7+325448	CSS091029:074420+325448
OT J001158.3+315544	CSS101111:001158+315544	OT J074727.6+065050	Itagaki (Yamaoka et al. 2008d)
OT J001340.0+332124	CSS101111:001340+332124	OT J074820.0+245759	CSS101115:074820+245759
OT J001538.3+263657	CSS090918:001538+263657	OT J074928.0+190452	MLS091117:074928+190452
OT J002500.2+073349	CSS081123:002500+073350	OT J075332.0+375801	CSS100407:075332+375801
OT J002656.6+284933	CSS101212:002657+284933	OT J075414.5+313216	CSS110414:075414+313216
OT J003203.6+314510	CSS091220:003204+314510	OT J075648.0+305805	CSS080406:075648+305805
OT J003304.0+380106	CSS110115:003304+380106	OT J080428.4+363104	CSS091116:080428+363104
OT J003500.0+273620	CSS081031:003500+273620	OT J080714.2+113812	Itagaki (Yamaoka et al. 2008d)
OT J004500.3+222708	CSS081102:004500+222708	OT J080729.7+153442	CSS090317:080730+153442
OT J004518.4+185350	CSS081024:004518+185349	OT J080853.7+355053	CSS080416:080854+355053
OT J004606.7+052100	CSS100911:004607+052060	OT J081030.6+002429	CSS100108:081031+002429
OT J004807.2+264621	CSS090925:004807+264621	OT J081414.9+080450	CSS080202:081415+080450
OT J004902.0+074726	CSS090204:004902+074726	OT J081418.9+005022	CSS080409:081419+005022
OT J005152.9+204017	CSS091026:005153+204017	OT J081712.3+055208	CSS091215:081712+055208
OT J005824.6+283304	CSS101009:005825+283304	OT J081936.1+191540	CSS100202:081936+191540
OT J010329.0+331822	CSS110116:010329+331822	OT J082019.4+474732	CSS091213:082019+474732
OT J010411.6+031341	CSS091009:010412+031341	OT J082123.7+454135	CSS090224:082124+454135
OT J010522.2+110253	CSS080921:010522+110253	OT J082603.7+113821	CSS110124:082604+113821
OT J010550.1+190317	CSS091016:010550+190317	OT J082654.7+000733	CSS080306:082655+000733
OT J011134.5+275922	CSS081024:011134+275922	OT J082821.8+105344	CSS071231:082822+105344
OT J011516.5+245530	CSS101008:011517+245530	OT J082908.4+482639	CSS091120:082908+482639
OT J011543.2+333724	CSS081205:011543+333724	OT J084041.5+000520	CSS090331:084041+000520
OT J011613.8+092216	MLS101127:011614+092216	OT J084127.4+210053	MLS110522:084127+210054
OT J012059.6+325545	Itagaki (vsnet-alert 12431)	OT J084358.1+425037	CSS080309:084358+425037
OT J014150.4+090822	MLS101213:014150+090822	OT J084413.7+012807	CSS090331:084414+012807
OT J020056.0+195727	CSS090117:020056+195727	OT J084555.1+033930	Itagaki (Yamaoka et al. 2008b)
OT J021110.2+171624	CSS080130:021110+171624	OT J085113.4+344449	CSS080401:085113+344449
OT J021308.0+184416	CSS101214:021308+184416	OT J085409.4+201339	CSS080506:085409+201339
OT J023211.7+303636	CSS101029:023212+303636	OT J085603.8+322109	CSS100508:085604+322109
OT J025615.0+191611	CSS090128:025615+191611	OT J085822.9+003729	CSS071112:085823+003729
OT J032651.7+011513	CSS100219:032652+011513	OT J090016.7+343928	CSS110512:090017+343928
OT J032839.9+010240	CSS101116:032840+010240	OT J090239.7+052501	CSS080304:090240+052501
OT J032902.0+060047	CSS101202:032902+060047	OT J090516.1+120451	CSS091022:090516+120451
OT J033104.4+172540	MLS100911:033104+172540	OT J090852.2+071640	CSS110125:090852+071640
OT J035003.4+370052	CSS100113:035003+370052	OT J091453.6+113402	CSS081107:091454+113402
OT J040659.8+005244	Itagaki (Yamaoka et al. 2008a)	OT J091534.9+081356	Donalek et al. (2008)
OT J041636.9+292806	CSS100317:041637+292806	OT J091634.6+130358	MLS100315:091635+130358
OT J041734.6+061357	CSS081202:041735+061357	OT J092839.3+005944	CSS110212:092839+005945
OT J042142.1+340329	CSS090403:042142+340328	OT J101035.5+140239	MLS110305:101036+140239
OT J042229.3+161430	CSS091024:042229+161430	OT J101545.9+033312	CSS090429:101546+033312
OT J042434.2+001419	CSS081030:042434+001419	OT J102146.4+234926	Christensen (2006)
OT J043020.0+095318	CSS080929:043020+095318	OT J102616.0+192045	Itagaki (Yamaoka, Itagaki 2009)
OT J043517.8+002941	CSS090219:043518+002941	OT J102637.0+475426	Itagaki (Yamaoka, Itagaki 2009)
OT J043546.9+090837	CSS091123:043547+090837	OT J102937.7+414046	CSS080305:102938+414046
OT J043742.1+003048	CSS081203:043742+003048	OT J103317.3+072119	CSS080208:103317+072119
OT J043829.1+004016	CSS100218:043829+004016	OT J103704.6+100224	MLS101214:103705+100224
OT J044216.0+002334	CSS071115:044216+002334	OT J103738.7+124250	CSS090516:103739+124250
OT J051419.9+011121	CSS091109:051420+011121	OT J104411.4+211307	CSS100217:104411+211307
OT J052033.9+000530	CSS080207:052034+000530	OT J105550.1+095621	CSS080130:105550+095621
OT J055730.1+001514	CSS080307:055730+001514	OT J105835.1+054706	CSS081025:105835+054706
OT J055842.8+000626	CSS100114:055843+000626	OT J112112.0+130843	CSS110301:112112+130842
OT J073055.5+425636	CSS090911:073056+425636	OT J112253.3+111037	CSS100603:112253+111037
OT J073339.3+212201	CSS091111:073339+212201	OT J112332.0+431718	CSS090602:112332+431717
OT J073559.9+220132	MLS110305:073600+220132	OT J112509.7+231036	CSS110226:112510+231036
OT J073758.5+205545	CSS110301:073759+205545	OT J112634.0+100210	CSS080227:112634+100210

**Table 7.** Identification list of optical transients (continued)

Object	ID or discoverer	Object	ID or discoverer
OT J115330.2+315836	CSS080201:115330+315836	OT J173307.9+300635	CSS090820:173308+300635
OT J122756.8+622935	CSS110503:122757+622934	OT J175901.1+395551	CSS100510:175901+395551
OT J123833.7+031854	CSS090615:123834+031854	OT J182142.8+212154	Itagaki (vsnet-alert 11952)
OT J124027.4−150558	CSS071218:124027−150558	OT J202857.1−061803	CSS110621:202857−061803
OT J124417.9+300401	CSS080427:124418+300401	OT J204001.4−144909	CSS101116:204001−144908
OT J124819.4+072050	CSS090516:124819+072050	OT J204739.4+000840	Anderson et al. (2008)
OT J130030.3+115101	CSS080702:130030+115101	OT J210034.4+055436	CSS101009:210034+055436
OT J132536.0+210037	CSS090102:132536+210037	OT J210043.9−005212	CSS090615:210044−005212
OT J134052.1+151341	CSS100531:134052+151341	OT J210205.7+025834	CSS091017:210206+025834
OT J135219.0+280917	CSS090705:135219+280917	OT J210650.6+110250	CSS090924:210651+110250
OT J135336.0−022043	CSS100405:135336−022043	OT J210704.5+014416	CSS090428:210705+014416
OT J135716.8−093239	CSS110208:135717−093238	OT J210846.4−035031	CSS110513:210846−035031
OT J141002.2−124809	CSS080502:141002−124809	OT J210954.1+163052	CSS100404:210954+163052
OT J141712.0−180328	CSS080425:141712−180328	OT J211550.9−000716	CSS090828:211551−000716
OT J142548.1+151502	CSS110628:142548+151502	OT J212025.1+194157	CSS090817:212025+194157
OT J144011.0+494734	CSS090530:144011+494734	OT J212555.1−032406	CSS080511:212555−032406
OT J144316.5−010222	CSS100115:144317−010222	OT J212633.3+085459	CSS100509:212633+085459
OT J145502.2+143815	CSS100407:145502+143815	OT J213122.4−003937	Itagaki (Yamaoka et al. 2008c)
OT J145921.8+354806	CSS110613:145922+354806	OT J213309.4+155004	CSS080404:213309+155004
OT J151020.7+182303	CSS080514:151021+182303	OT J213432.3−012040	CSS081120:213432−012040
OT J151037.4+084104	CSS110306:151037+084104	OT J213701.8+071446	Itagaki (vsnet-alert 10670)
OT J152037.9+040948	CSS110301:152038+040948	OT J213829.5−001742	CSS100524:213830−001742
OT J152501.8−013021	CSS100506:152502−013021	OT J213937.6−023913	CSS091119:213938−023913
OT J153150.8+152447	CSS080401:153151+152447	OT J214426.4+222024	CSS100520:214426+222024
OT J153317.6+273428	CSS110611:153318+273428	OT J214639.9+092119	CSS110613:214640+092119
OT J153645.2−142543	SSS110721:153645−142543	OT J214804.4+080951	CSS080505:214804+080951
OT J154354.1−143745	CSS100531:154354−143745	OT J214842.5−000723	CSS071116:214843−000723
OT J154428.1+335725	CSS090322:154428+335725	OT J214959.9+124529	CSS090722:215000+124529
OT J154544.9+442830	CSS110428:154545+442830	OT J215344.7+123524	CSS090526:215345+123524
OT J155325.7+114437	CSS080424:155326+114437	OT J215630.5−031957	CSS090728:215630−031956
OT J155430.6+365043	CSS081009:155431+365043	OT J215636.3+193242	CSS090622:215636+193242
OT J155748.0+070543	CSS100507:155748+070543	OT J215815.3+094709	CSS100615:215815+094709
OT J160204.8+031632	CSS080331:160205+031632	OT J220031.2+033431	CSS100624:220031+033431
OT J160232.2+161733	CSS080424:160232+161732	OT J220449.7+054852	CSS091019:220450+054852
OT J160524.1+060816	CSS080428:160524+060816	OT J221128.7−030516	CSS100519:221129−030516
OT J160844.8+220610	CSS080302:160845+220610	OT J221232.0+160140	CSS090911:221232+160140
OT J162012.0+115257	CSS080415:162012+115257	OT J221344.0+173252	CSS090917:221344+173252
OT J162235.7+035247	CSS090601:162236+035247	OT J222002.3+113825	CSS081230:222002+113825
OT J162605.7+225044	CSS080514:162606+225044	OT J222548.1+252511	CSS091027:222548+252511
OT J162619.8−125557	CSS090419:162620−125557	OT J222724.5+284404	CSS090531:222724+284404
OT J162656.8−002549	CSS080426:162657−002549	OT J222824.1+134944	CSS100615:222824+134944
OT J162806.2+065316	CSS110611:162806+065316	OT J222853.7+295115	CSS091110:222854+295114
OT J163120.9+103134	CSS080505:163121+103134	OT J223018.8+292849	CSS101010:223019+292849
OT J163239.3+351108	CSS110507:163239+351108	OT J223058.3+210147	CSS080501:223058+210147
OT J163311.3−011132	CSS100601:163311−011132	OT J223136.0+180747	CSS090911:223136+180747
OT J163942.7+122414	CSS080131:163943+122414	OT J223235.4+304105	CSS081107:223235+304105
OT J164146.8+121026	CSS080606:164147+121026	OT J223418.5−035530	CSS090910:223418−035530
OT J164624.8+180808	CSS100616:164625+180808	OT J223606.3+050517	CSS080611:223606+050517
OT J164748.0+433845	CSS100513:164748+433845	OT J223909.8+250331	CSS100521:223910+250331
OT J164950.4+035835	CSS100707:164950+035835	OT J223958.2+231837	CSS090826:223958+231837
OT J165002.8+435616	CSS090930:165003+435616	OT J223958.4+342306	CSS091016:223958+342305
OT J170115.8−024159	CSS090612:170116−024158	OT J224253.4+172538	CSS090622:224253+172538
OT J170151.6+132131	CSS110426:170152+132131	OT J224505.4+011547	CSS100624:224505+011547
OT J170606.1+255153	Filippenko, Chornock (2003)	OT J224753.9+235522	CSS100521:224754+235522
OT J170609.7+143452	CSS090205:170610+143452	OT J224814.5+331224	CSS091110:224814+331224
OT J170702.5+165339	CSS090818:170702+165339	OT J224823.7−092059	CSS081029:224824−092059
OT J171223.1+362516	CSS090516:171223+362516	OT J225749.6−082228	Itagaki (vsnet-outburst 10891)
OT J172515.5+073249	CSS100706:172516+073249	OT J230115.4+224111	CSS080923:230115+224111

**Table 7.** Identification list of optical transients (continued)

Object	ID or discoverer	Object	ID or discoverer
OT J230131.1+040417	CSS080907:230131+040417	OT J231552.3+271037	CSS100610:231552+271037
OT J230425.8+062546	Nishimura (Nakano et al. 2011)	OT J232551.5−014024	CSS091116:232551−014024
OT J230711.3+294011	CSS090926:230711+294010	OT J232619.4+282650	CSS080930:232619+282650
OT J231110.9+013003	Itagaki (vsnet-outburst 8239)	OT J233938.7−053305	MLS100902:233939−053305
OT J231142.8+204036	CSS091108:231143+204036	OT J234440.5−001206	MLS100904:234441−001206
OT J231308.1+233702	Itagaki (TCP J23130812+2337018)	—	—

- Hellier, C., Kemp, J., Naylor, T., Bateson, F. M., Jones, A., Overbeek, D., Stubbings, R., & Mukai, K. 2000, *MNRAS*, 313, 703
- Hellier, C., Mason, K. O., Smale, A. P., Corbet, R. H. D., O'Donoghue, D., Barrett, P. E., & Warner, B. 1989, *MNRAS*, 238, 1107
- Henden, A. A., Munari, U., & Sumner, B. 2001, *IBVS*, 5140
- Hessman, F. V., & Hopp, U. 1990, *A&A*, 228, 387
- Hoard, D. W., Wachter, S., Clark, L. L., & Bowers, T. P. 2002, *ApJ*, 565, 511
- Hoffmeister, C. 1968, *Astron. Nachr.*, 290, 277
- Honeycutt, R. K. 2001, *PASP*, 113, 473
- Honeycutt, R. K., & Kafka, S. 2004, *AJ*, 128, 1279
- Honeycutt, R. K., Robertson, J. W., & Turner, G. W. 1998, *AJ*, 115, 2527
- Horne, K., Wade, R. A., & Szkody, P. 1986, *MNRAS*, 219, 791
- Howell, S. B., Nelson, L. A., & Rappaport, S. 2001, *ApJ*, 550, 897
- Howell, S. B., Szkody, P., Kreidl, T. J., Mason, K. O., & Puchnarewicz, E. M. 1990, *PASP*, 102, 758
- Imada, A., et al. 2006, *PASJ*, 58, 143
- Ishioka, R., Sekiguchi, K., & Maehara, H. 2007, *PASJ*, 59, 929
- Kaitchuck, R. H. 1989, *PASP*, 101, 1129
- Kato, T. 1999, *IBVS*, 4790
- Kato, T. 2001a, *IBVS*, 5071
- Kato, T. 2001b, *IBVS*, 5102
- Kato, T. 2004, *PASJ*, 56, S135
- Kato, T., et al. 2009, *PASJ*, 61, S395
- Kato, T., et al. 2012, *PASJ*, 64, 21
- Kato, T., et al. 2010, *PASJ*, 62, 1525
- Kato, T., Sekine, Y., & Hirata, R. 2001, *PASJ*, 53, 1191
- Kato, T., & Uemura, M. 2001a, *IBVS*, 5158
- Kato, T., & Uemura, M. 2001b, *IBVS*, 5097
- Kato, T., Uemura, M., Ishioka, R., Nogami, D., Kunjaya, C., Baba, H., & Yamaoka, H. 2004, *PASJ*, 56, S1
- Kato, T., et al. 2003, *PASJ*, 55, 489
- Kato, T., et al. 2000, *IAU Circ.*, 7343
- Kazarovets, E. V., Samus, N. N., Durlevich, O. V., Kireeva, N. N., & Pastukhova, E. N. 2011, *IBVS*, 6008, 1
- Kholopov, P. N. 1953, *Perem. Zvezdy*, 9, 334
- Kholopov, P. N., et al. 1985, *General Catalogue of Variable Stars*, fourth edition (Moscow: Nauka Publishing House)
- Knigge, C., Baraffe, I., & Patterson, J. 2011, *ApJS*, 194, 28
- Kolb, U. 1993, *A&A*, 271, 149
- Kolb, U., & Baraffe, I. 1999, *MNRAS*, 309, 1034
- Kurochkin, N. E. 1978, *Astron. Tsirk.*, 1023, 4
- Leach, R., Hessman, F. V., King, A. R., Stehle, R., & Mattei, J. 1999, *MNRAS*, 305, 225
- Littlefair, S. P., Dhillon, V. S., Marsh, T. R., Gänsicke, B. T., Baraffe, I., & Watson, C. A. 2007, *MNRAS*, 381, 827
- Littlefair, S. P., Dhillon, V. S., Marsh, T. R., Gänsicke, B. T., Southworth, J., Baraffe, I., Watson, C. A., & Copperwheat, C. 2008, *MNRAS*, 388, 1582
- Liu, Wu., & Hu, J. Y. 2000, *ApJS*, 128, 387
- Liu, Wu., Hu, J. Y., Zhu, X. H., & Li, Z. Y. 1999, *ApJS*, 122, 243
- Luyten, W. J., Anderson, J. H., & Sandage, A. R. 1968, A search for faint blue stars. XLVIII. A field centered at 9:32+24. XLIX. A field centered at 12:34+30. (Univ. Minnesota, Minneapolis, Minnesota)
- Luyten, W. J., & Erickson, R. R. 1965, *PASP*, 77, 472
- Marsh, T. R. 1999, *MNRAS*, 304, 443
- McLaughlin, D. B. 1945, *AJ*, 51, 136
- Meinunger, L. 1986, *Mitteil. Veränderl. Sterne*, 11, 1
- Meshkova, T. S. 1940, *Perem. Zvezdy*, 5, 255
- Miller, W. J. 1971, *Ricerche Astronomiche*, 8, 167
- Modjaz, M., Halderson, E., Shefler, T., King, J. Y., Papenkova, M., Li, W. D., Treffers, R. R., & Filippenko, A. V. 1998, *IAU Circ.*, 7021
- Munari, U., & Zwitter, T. 1998, *A&AS*, 128, 277
- Nakano, S., Nishimura, H., Kadota, K., & Yusa, T. 2011, *Cent. Bur. Electron. Telegrams*, 2616
- Nogami, D., Masuda, S., & Kato, T. 1997, *PASP*, 109, 1114
- Noguchi, T., Mdehara, H., & Kondo, M. 1979, *PASJ*, 31, 425
- O'Donoghue, D., Chen, A., Marang, F., Mittaz, J. P. D., Winkler, H., & Warner, B. 1991, *MNRAS*, 250, 363
- Orosz, J. A., Thorstensen, J. R., & Honeycutt, R. K. 2001, *MNRAS*, 326, 1134
- Osaki, Y. 1989, *PASJ*, 41, 1005
- Paczyński, B., & Sienkiewicz, R. 1981, *ApJL*, 248, L27
- Paczyński, B., & Sienkiewicz, R. 1983, *ApJ*, 268, 825
- Patterson, J. 2011, *MNRAS*, 411, 2695
- Patterson, J., Schwartz, D. A., Pye, J. P., Blair, W. P., Williams, G. A., & Caillault, J.-P. 1992, *ApJ*, 392, 233
- Patterson, J., & Szkody, P. 1993, *PASP*, 105, 1116
- Patterson, J., Thorstensen, J. R., & Kemp, J. 2005, *PASP*, 117, 427
- Patterson, J., Thorstensen, J. R., & Knigge, C. 2008, *PASP*, 120, 510
- Peters, C. S., & Thorstensen, J. R. 2005, *PASP*, 117, 1386
- Pinto, G., & Romano, G. 1972, *Mem. Soc. Astron. Ital.*, 43, 135
- Pojmański, G. 2002, *Acta Astron.*, 52, 397
- Pretorius, M. L., Knigge, C., O'Donoghue, D., Henry, J. P., Gioia, I. M., & Mullis, C. R. 2007, *MNRAS*, 382, 1279
- Provençal, J. L., et al. 1997, *ApJ*, 480, 383
- Rappaport, S., Joss, P. C., & Verbunt, F. 1983, *ApJ*, 275, 713
- Rappaport, S., Joss, P. C., & Webbink, R. F. 1982, *ApJ*, 254, 616
- Renoizé, V., Baraffe, I., Kolb, U., & Ritter, H. 2002, *A&A*, 389, 485
- Richards, G. T., et al. 2002, *AJ*, 123, 2945



- Richter, G. A. 1979, *Mitteil. Veränderl. Sterne*, 8, 119
- Richter, G. A. 1989, *Mitteil. Veränderl. Sterne*, 12, 2
- Richter, G. R., Notni, P., Borngen, F., Afanasjev, V., Karachentsev, I. D., & Kopylov, A. 1981, *Astron. Nachr.*, 302, 211
- Ringwald, F. A. 1994, *MNRAS*, 270, 804
- Ringwald, F. A., Naylor, T., & Mukai, K. 1996, *MNRAS*, 281, 192
- Ringwald, F. A., & Velasco, K. 2011, *New Astron.*, in press (arXiv astro-ph/1107.4175)
- Ritter, H., & Kolb, U. 2003, *A&A*, 404, 301
- Robertson, J. W., Honeycutt, R. K., Hillwig, T., Jurcevic, J. S., & Henden, A. A. 2000, *AJ*, 119, 1365
- Rodríguez-Gil, P., Gänsicke, B. T., Hagen, H.-J., Marsh, T. R., Harlaftis, E. T., Kitsionas, S., & Engels, D. 2005, *A&A*, 431, 269
- Rodríguez-Gil, P., & Torres, M. A. P. 2005, *A&A*, 431, 289
- Roelofs, G. H. A., Groot, P. J., Benedict, G. F., McArthur, B. E., Steeghs, D., Morales-Rueda, L., Marsh, T. R., & Nelemans, G. 2007, *ApJ*, 666, 1174
- Roelofs, G. H. A., Groot, P. J., Marsh, T. R., Steeghs, D., Barros, S. C. C., & Nelemans, G. 2005, *MNRAS*, 361, 487
- Romano, G., & Minello, S. 1976, *IBVS*, 1140
- Rosino, L., & Pigatto, L. 1972a, *IAU Circ.*, 2453
- Rosino, L., & Pigatto, L. 1972b, *IAU Circ.*, 2464
- Rügemer, H. 1933, *Astron. Nachr.*, 248, 409
- Samus, N. N., V., Durlevich O., Kazarovets, E. V., Kireeva, N. N., Pastukhova, E. N., Zharova, A. V., & et al. 2011, *CDS B/gcvs*
- Schimpke, T., & Bruch, A. 1990, *Astronomische Gesellschaft Abstract Ser.*, 4, 24
- Schlegel, D. J., Finkbeiner, D. P., & Davis, M. 1998, *ApJ*, 500, 525
- Schmidtobreick, L., Tappert, C., Bianchini, A., & Mennickent, R. E. 2005, *A&A*, 432, 199
- Sekiguchi, K. 1992, *Nature*, 358, 563
- Shafter, A. W., & Harkness, R. P. 1986, *AJ*, 92, 658
- Shara, M. M., Potter, M., & Moffat, A. F. J. 1990, *AJ*, 100, 540
- Sharov, A. S., & Alksnis, A. K. 1989, *Soviet Astronomy Letters*, 15, 382
- Sheets, H. A., Thorstensen, J. R., Peters, C. J., Kapusta, A. B., & Taylor, C. J. 2007, *PASP*, 119, 494
- Skinner, J. N., Thorstensen, J. R., Armstrong, E., & Brady, S. 2011, *PASP*, 123, 259
- Slavin, A. J., O'Brien, T. J., & Dunlop, J. S. 1995, *MNRAS*, 276, 353
- Smak, J. 1975, *Acta Astron.*, 25, 227
- Solheim, J.-E. 2010, *PASP*, 122, 1133
- Southworth, J., Gänsicke, B. T., Marsh, T. R., de Martino, D., & Aungwerojwit, A. 2007a, *MNRAS*, 378, 635
- Southworth, J., Gänsicke, B. T., Marsh, T. R., de Martino, D., Hakala, P., Littlefair, S., Rodríguez-Gil, P., & Szkody, P. 2006, *MNRAS*, 373, 687
- Southworth, J., et al. 2008, *MNRAS*, 391, 591
- Southworth, J., Hickman, R. D. G., Marsh, T. R., Rebassa-Mansergas, A., Gänsicke, B. T., Copperwheat, C. M., & Rodríguez-Gil, P. 2009, *A&A*, 507, 929
- Southworth, J., Marsh, T. R., Gänsicke, B. T., Aungwerojwit, A., Hakala, P., de Martino, D., & Lehto, H. 2007b, *MNRAS*, 382, 1145
- Southworth, J., Marsh, T. R., Gänsicke, B. T., Steeghs, D., & Copperwheat, C. M. 2010, *A&A*, 524, A86
- Spitzer, L. 1978, *Physical Processes in the Interstellar Medium* (New York: Wiley)
- Sproats, L. N., Howell, S. B., & Mason, K. O. 1996, *MNRAS*, 282, 1211
- Stolz, B., & Schoembs, R. 1984, *A&A*, 132, 187
- Szkody, P. 1987, *ApJS*, 63, 685
- Szkody, P., et al. 2002, *AJ*, 123, 430
- Szkody, P., et al. 2009, *AJ*, 137, 4011
- Szkody, P., et al. 2003, *AJ*, 126, 1499
- Szkody, P., et al. 2006, *AJ*, 131, 973
- Szkody, P., et al. 2004, *AJ*, 128, 1882
- Szkody, P., et al. 2005, *AJ*, 129, 2386
- Szkody, P., et al. 2007, *AJ*, 134, 185
- Szkody, P., & Mattei, J. A. 1984, *PASP*, 96, 988
- Tappert, C., Wargau, W. F., Hanuschik, R. W., & Vogt, N. 1997, *A&A*, 327, 231
- Taylor, C. J., & Thorstensen, J. R. 1996, *PASP*, 108, 894
- Thiele, H. 1916, *Astron. Nachr.*, 202, 213
- Thorstensen, J. R. 2002, *IBVS*, 5266
- Thorstensen, J. R., Fenton, W. H., Patterson, J. O., Kemp, J., Halpern, J., & Baraffe, I. 2002, *PASP*, 114, 1117
- Thorstensen, J. R., Fenton, W. H., & Taylor, C. J. 2004, *PASP*, 116, 300
- Thorstensen, J. R., & Freed, I. W. 1985, *AJ*, 90, 2082
- Thorstensen, J. R., Peters, C. S., & Skinner, J. N. 2010, *PASP*, 122, 1285
- Thorstensen, J. R., & Ringwald, F. A. 1997, *PASP*, 109, 483
- Thorstensen, J. R., Schwarz, R., Schwöpe, A. D., Staude, A., Vogel, J., Krumpke, M., Kohnert, J., & Nebot Gómez-Morán, A. 2009, *PASP*, 121, 465
- Thorstensen, J. R., & Taylor, C. J. 2000, *MNRAS*, 312, 629
- Thorstensen, J. R., & Taylor, C. J. 2001, *MNRAS*, 326, 1235
- Thorstensen, J. R., Taylor, C. J., & Kemp, J. 1998, *PASP*, 110, 1405
- Trentham, N., & Tully, R. B. 2009, *MNRAS*, 398, 722
- Tsugawa, M., & Osaki, Y. 1997, *PASJ*, 49, 75
- Uemura, M., Kato, T., Nogami, D., & Ohsugi, T. 2010, *PASJ*, 62, 613
- Unda-Sanzana, E., et al. 2008, *MNRAS*, 388, 889
- Uthas, H. 2011, Ph. D. thesis, (arXiv astro-ph/1105.1164)
- Verbunt, F., & Zwaan, C. 1981, *A&A*, 100, L7
- Wagner, R. M., et al. 1998, *AJ*, 115, 787
- Warner, B. 1987, *MNRAS*, 227, 23
- Warner, B. 1994, *Ap&SS*, 222, 225
- Warner, B. 1995, *Cataclysmic Variable Stars* (Cambridge: Cambridge University Press)
- Watson, M. G., Marsh, T. R., Fender, R. P., Barstow, M. A., Still, M., Page, M., Dhillon, V. S., & Beardmore, A. P. 1996, *MNRAS*, 281, 1016
- Wenzel, W., & Wicklein, A. 1990, *Mitteil. Veränderl. Sterne*, 12, 76
- Wheatley, P. J., Burleigh, M. R., & Watson, M. G. 2000, *MNRAS*, 317, 343
- Whitney, B. S. 1973, *IBVS*, 797
- Wild, P. 1972, *IAU Circ.*, 2392
- Wils, P. 2009, *Perem. Zvezdy, Prilozh.*, 9, 19
- Wils, P. 2011, *J. American Assoc. Variable Star Obs.*, 39, 60
- Wils, P., Gänsicke, B. T., Drake, A. J., & Southworth, J. 2010, *MNRAS*, 402, 436
- Woudt, P. A., Warner, B., & Pretorius, M. L. 2004, *MNRAS*, 351, 1015
- Woudt, P. A., Warner, B., Pretorius, M. L., & Dale, D. 2005a, in *ASP Conf. Ser.* 330, *The Astrophysics of Cataclysmic*

- Variables and Related Objects, ed. J.-M. Hameury & J.-P. Lasota Vol. 330(. San Francisco: ASP), p. 325
- Woudt, P. A., Warner, B., & Spark, M. 2005b, MNRAS, 364, 107
- Wu, C., Holm, A. V., Panek, R. J., Raymond, J. C., Hartmann, L. W., & Swank, J. H. 1989, ApJ, 339, 443
- Yamaoka, H., & Itagaki, K. 2009, Cent. Bur. Electron. Telegrams, 1644
- Yamaoka, H., Itagaki, K., Kaneda, H., Jacques, C., Pimentel, E., Maehara, H., & Bolt, G. 2008a, Cent. Bur. Electron. Telegrams, 1463
- Yamaoka, H., Itagaki, K., Maehara, H., & Henden, A. 2008b, Cent. Bur. Electron. Telegrams, 1225
- Yamaoka, H., Itagaki, K., Miyashita, A., & Koff, R. A. 2008c, Cent. Bur. Electron. Telegrams, 1631
- Yamaoka, H., Itagaki, K., Naito, H., & Narusawa, S. 2008d, Cent. Bur. Electron. Telegrams, 1216
- York, D. G., et al. 2000, AJ, 120, 1579
- Začs, L. A. 1982, Nauchnye Informatsii, 57, 101
- Zharikov, S. V., Tovmassian, G. H., Napiwotzki, R., Michel, R., & Neustroev, V. 2006, A&A, 449, 645
- Zwitter, T., & Munari, U. 1996, A&AS, 117, 449